Energy-aware Wireless Multi-hop Networks

Javad Vazifehdan

Energy-aware Wireless Multi-hop Networks

PROEFSCHRIFT

ter verkrijging van de graad van doctor
aan de Technische Universiteit Delft,
op gezag van de Rector Magnificus prof. ir. K.C.A.M. Luyben,
voorzitter van het College voor Promoties
in het openbaar te verdedigen op donderdag 7 juli 2011 om 15.00 uur
door

Javad VAZIFEHDAN

Master of Science in Electrical Engineering,
University of Tehran, Tehran, Iran,
geboren te Ferdos, Iran.

Dit proefschrift is goedgekeurd door de promotor:

Prof. dr. ir. I.G.M.M Niemegeers

Samenstelling promotiecommissie:

Rector Magnificus	voorzitter
Prof. dr. ir. I.G.M.M. Niemegeers	Technische Universiteit Delft, promotor
Dr. R.V. Prasad	Technische Universiteit Delft, copromotor
Prof. dr. ir. N. Baken	Technische Universiteit Delft
Prof. dr. ir. S. Heemstra de Groot	Technische Universiteit Delft
Prof. dr. A. Liotta	Technische Universiteit Eindhoven
Prof. dr. ir. I. Moerman	Universiteit Gent
Prof. dr. N. Balakrishnan	Indian Institute of Science

Printed in The Netherlands

Author email: `jvazifehdan@yahoo.com`

to my parents

Preface

This research was funded by Dutch Research Delta (DRD)[1] and Trans-sector Research Academy for Complex Networks and Services (TRANS)[2]. DRD is a research corporation between Dutch universities, including the Delft University of Technology, TNO and the Royal Dutch KPN. TRANS was formed later as an academy of the Delft University of Technology in association with TNO, the Royal Dutch KPN and the Cor Wit Foundation. TRANS aims to spread the idea of "trans-sector innovation" and to bring many stakeholders together – both from the academic world and the corporate world. Trans-sector innovation is a new way of thinking, addressing, and resolving complex challenges that we face nowadays in each sector of our society (e.g., health, transport, education, communication, entertainment, energy, etc.). Some challenges are, for example, how to address the healthcare of each citizen and how to efficiently use the energy. The challenges are daunting. They have many facets and impact many sectors. They are usually inter-related; thus require a trans-sectoral way of addressing them.

Communication networks are "enabling technology" for trans-sector innovation. We are in the era where without the use of communication networks, no government, factory, bank, shop, and stock market can operate, neither goods nor passengers could be transported efficiently, and so on. They are substrates to connect different sectors of society and facilitate information flow between them. This, in turn, can help the society to efficiently solve the complex problems that it faces in different sectors.

In this research, we targeted design, analysis, and optimization of *personal networks* which are a novel type of communication network. A personal network is a network belonging to a person that links together diverse devices of a person in a self-organized and secure way. *Wireless multi-hop communication* is recognized as an enabler for self-organized communication in personal networks. A variety of services such as health-care and telepresence could be supported by personal networks. The main challenge, however, is to make these networks dependable. To

---

[1] www.dutchresearchdelta.nl
[2] www.trans-research.nl

this aim, we identified energy-efficiency as a key requirement for dependability of personal networks, because energy-efficiency can increase the lifetime of individual devices as well as the operational lifetime of the network as a whole. Thus, a service could be available for the user for a longer period of time. The work presented in this dissertation provides a platform for energy-efficient and energy-aware communication in personal types of wireless multi-hop networks. The proposed schemes, however, are generic and applicable to other types of wireless multi-hop networks such as wireless ad hoc and sensor networks.

Javad Vazifehdan
Delft, July 2011

Summary

Wireless networks have provided us a variety of services which facilitate communication between people beyond the physical boundaries. Mobile telephony, mobile Internet and high-definition video calls are examples of services supported by modern networks nowadays. Beyond this, enhancements in processing capabilities of electronic devices coupled with advances in wireless communication have resulted in the emergence of devices which have high processing and communication capabilities. Small devices that we carry or miniaturized devices embedded in our surroundings can execute sophisticated communication protocols. This allows them to form distributed networks in which nodes collaboratively offer services without the need for pre-established expensive infrastructures. Such networks are known as wireless multi-hop networks, where instead of powerful base stations, multi-hop communication connects all the devices that are outside the transmission range of each other. In wireless multi-hop networks, each device may act as a router which relays packets on behalf of other devices. Ad hoc communication between laptops in a conference hall, multi-hop communication between personal devices at home, and collaborative communication between sensors distributed over a large area are example scenarios of multi-hop communication in wireless networks.

This dissertation addresses the design of energy-aware wireless multi-hop networks, where energy is the key element in the design and analysis. Wireless multi-hop networks must be energy-aware for two reasons. First, devices in these networks often run on batteries. Thus, reducing energy consumption can save scarce battery energy of devices and extend the autonomy of systems that are composed of such devices. Second, vast deployment of these easy-to-establish networks can excessively increase energy consumption in the ICT sector. As a matter of fact, energy-efficient and energy-aware communication protocols and mechanisms not only extend the operational lifetime of devices but also reduce the environmental impacts of these networks. The novelty of this dissertation is the proposal of a suite of new protocols which together form a platform for energy-aware and energy-efficient communication in wireless multi-hop networks. The proposed platform scans different layers of the communication stack taking

into account cross-layer dependency between them from an energy-efficiency point of view. The energy efficiency across OSI Reference Architecture layers is addressed. Notably, from the physical layer (Layer 1) to the transport layer (Layer 4) is covered. For the physical layer, we propose cooperative signal transmission techniques based on the MIMO (Multi-Input Multi-Output) technology to reduce the transmission power of nodes without sacrificing link reliability. For the data link layer, we propose a network topology control algorithm which specifies a neighbor discovery policy to keep the transmission power of nodes as low as required for network connectivity. For the network layer, we propose routing schemes for finding the most energy-efficient routes between any two nodes of the network taking into account the impact of the transmission control of the transport layer. Furthermore, we enhance these routing schemes with the capability to balance the traffic according to the available battery energy of nodes. We also analyze the expected duration that two nodes in a wireless multi-hop network with a random topology can communicate with each other (from the transport layer point of view) through intermediate nodes between them. The proposed schemes in this dissertation together make the communication stack in wireless multi-hop networks more energy-efficient leading to *green* wireless multi-hop networks. This work is of a fundamental and theoretical nature supported by simulations. It should be continued by experimental studies using a testbed.

Contents

Chapter 1

Introduction

The need for communication has always been an important requirement for humans. Societies would not have been formed, if people were not been able to communicate with each other. Human beings need to communicate with each other to get across their thoughts and ideas and fulfill their many daily needs. Prosperous societies, we see nowadays, are the ones in which people have stronger and persistent empathetic relations (communication) with each other.

While the emergence of language facilitated communication between humans for centuries, modern communication networks started a new era allowing people to easily connect with each other beyond geographical boundaries. This new era of information networking laid the foundation for modern life giving us new ways of working and accessing information. On top of this, communication networks keep our economy and our society together. They provide a substrate to link together various sectors of our society and facilitate trans-sectoral information flow. This helps societies to solve complex challenges that it faces in different sectors in an efficient way [1].

Communication and information networks themselves have been subjected to major changes during the last two centuries. From the time that the telephone was invented, to the time that the first commercial digital mobile network was launched in the 90s and now that the forth generation of mobile networks supports high definition video streaming and 3D telepresence, human kind has witnessed a rapid and vast progress in this area. Many of these rapid developments have been in wireless networking. Nowadays, there are various wireless technologies with different specifications and capabilities (e.g., GSM, UMTS, WiMax, WiFi, UWB). They have provided pervasive services for users; from mobile telephony to short-range wireless communication between electronic devices and machine to machine-cognitive communication.

1.1 Wireless Multi-hop Networking

From a technological viewpoint, there are two distinct ways for networking of wireless devices: infrastructure networking and multi-hop networking. Infrastructure networking is now widely used in cellular networks for mobile telephony. Wireless devices outside of transmission range of each other are linked together through centralized base stations (see Figure 1.1). Wireless multi-hop networks, on the other hand, allow device-to-device communication even if devices are not within each others transmission range. In this architecture, wireless devices detect each other, establish local links between each other, and form a wireless network in a completely self-organized way without the need for expensive establishment of an infrastructure.

Multi-hop communication is a well-established method in packet-switched networking. It has enabled scalable expansion of the Internet, where information packets are routed between hosts hop-by-hop through intermediate routers (see Figure 1.2(a)). This architecture could be used in wireless networks on a smaller scale to provide local services, i.e., each wireless device can act as a router to forward information packets on behalf of other wireless devices (see Figure 1.2(b)). While infrastructure-based communication in cellular networks provides country-wide coverage for mobile users, wireless multi-hop networks can support variety of localized applications. We can highlight three application areas for these networks in the sequel.

1.1.1 Mobile Ad hoc Networks (MANETs)

In a MANET [2, 3], mobile devices, which may belong to different users, start communicating with each other in a multi-hop way (see Figure 1.3(a)). The network is formed between devices when users need to exchange information with each other. As soon as there is no such a need anymore, the network is dismantled or some users may leave the network. That is why these networks are called ad hoc. In general, devices could be mobile within the network area, but they remain connected to each other in a multi-hop ways. There are multiple scenarios where mobile ad hoc networking could effectively be deployed. For instance, laptops of participants in a conference center could form a MANET to exchange information wirelessly. Soldiers in a battle-field could exchange information about the ongoing battle between each other through a MANET formed between their radios. Cars in a highway could form a MANET to inform each other about an accident which has happened several miles ahead.
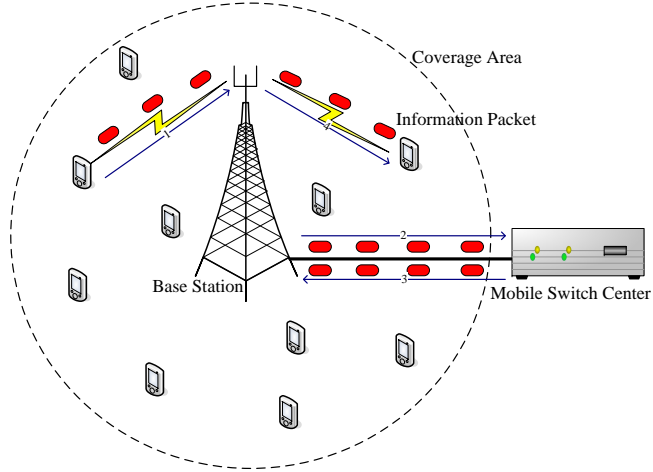
Figure 1.1 – Infrastructured wireless communication.
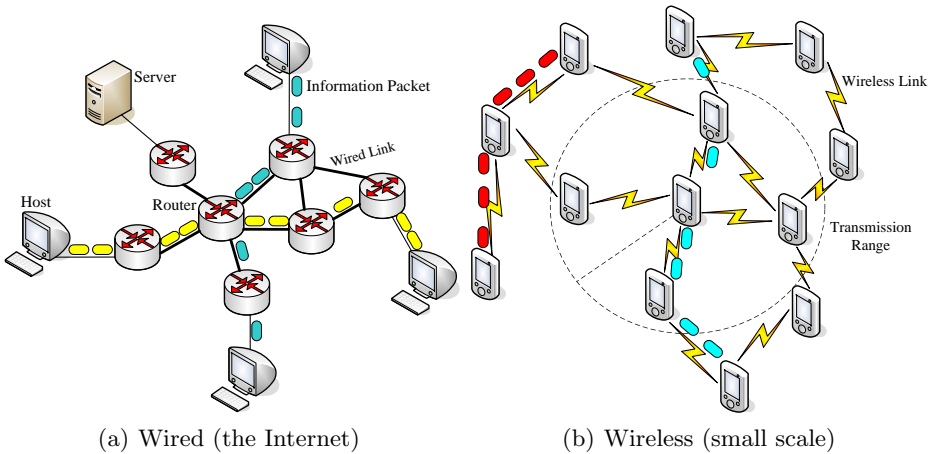
(a) Wired (the Internet)   (b) Wireless (small scale)

Figure 1.2 – Wired and wireless multi-hop communication.

(a) Mobile ad hoc network

(b) Wireless sensor network
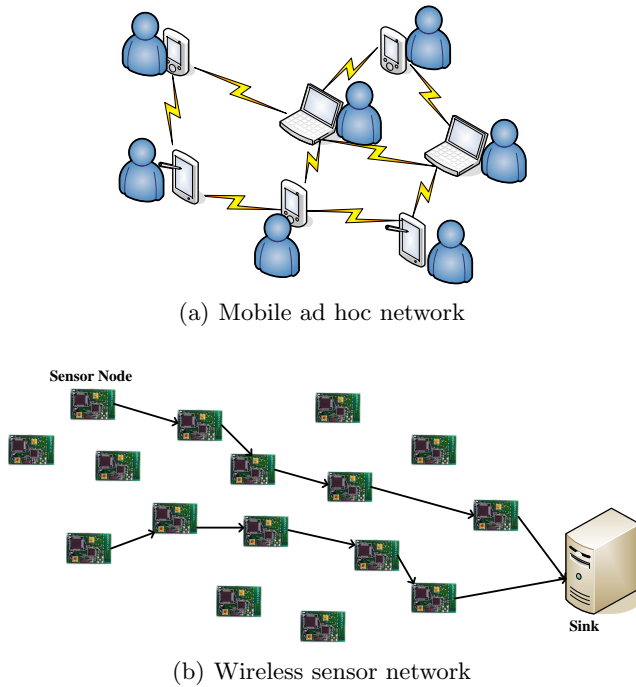
Figure 1.3 – Schematic of a mobile ah hoc network and a wireless sensor network; two application areas for multi-hop wireless communications.

1.1.2 Wireless Sensor Networks

Recent advances in micro-electronic systems has enabled manufacturing of small low-power devices, which have sensing, processing and communication capabilities altogether. This allows them to exchange with each other information they gather by sensing. Multi-hop communication is a well-accepted means for this purpose [4–6]. Sensor nodes can share data between each other and transfer it to a common sink in a multi-hop way (see Figure 1.3(b)). Disaster management is one of the scenarios where wireless sensor networks could be deployed. Nodes could detect survivors and collaboratively inform rescuers about the location of survivors. Monitoring large areas, such as jungles, large buildings, and oceans, are also the task of wireless sensor networks.

1.1.3 Wireless Personal Networks

With the proliferation of wireless technologies, users may use a multitude of devices with different capabilities ranging from smart phones, laptops, and digital cameras
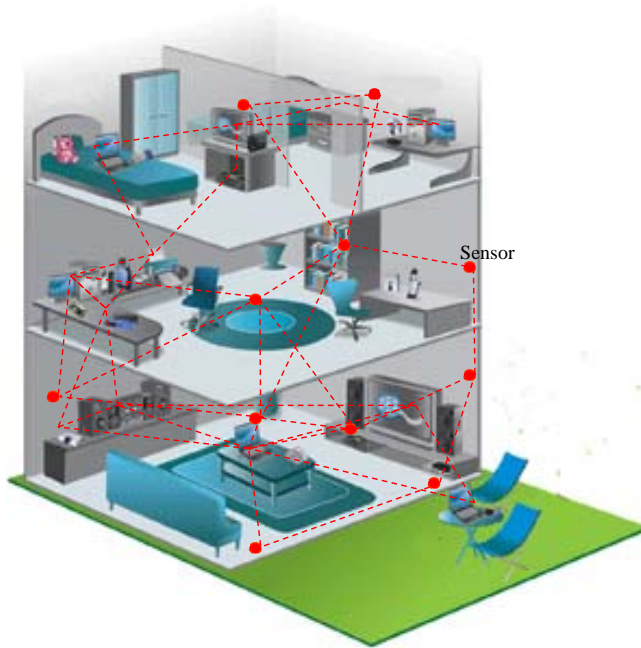
Figure 1.4 – Wireless multi-hop communication between personal devices at home.

to home entertainment systems, smart appliances, and sensors. Wireless personal networks – or simply personal networks [7, 8] - link together devices used by a person in a self-organized way (see Figure 1.4). Such a communication substrate can provide a distributed intelligence around a person to monitor his activities, learn about his preferences, and take an appropriate action based on the context. It is envisaged that personal networks will become a part of human lives in the near future supporting people with a variety of services which are not just communication. For example, a personal network can take care of the energy budget inside houses by reducing the energy consumption for heating and cooling using the context information (e.g., the presence of the user in his house).

1.2 Energy-awareness in Wireless Multi-hop Networks

Although easy and cost-effective deployment of wireless multi-hop networks can provide us many services, there is a potential threat. To keep wireless devices
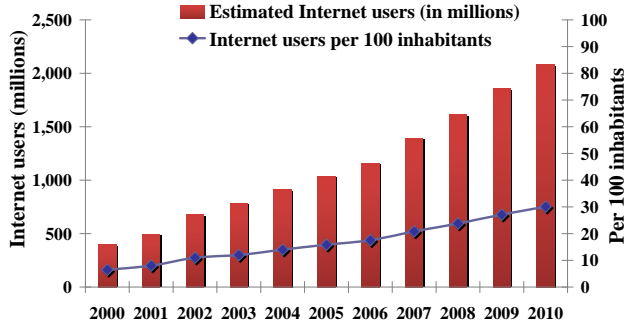
(a) Internet users
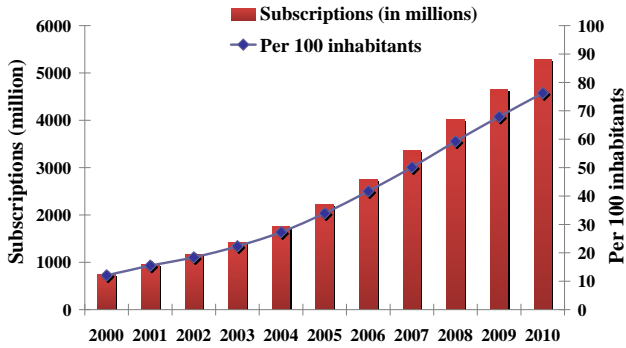
(b) Mobile subscribers

Figure 1.5 – The number of Internet users and mobile subscribers worldwide [source: International Telecommunication Union].

networked, they need to consume energy. On the other hand, vast deployment of multi-hop wireless networks in the near future will cause an explosion in the number of devices around the world. Consequently, energy consumption by these devices will increase tremendously.

Statistics of the International Telecommunication Union (ITU) show that there has been around two billion Internet users and five billion mobile subscribers in 2010 worldwide (see Figure 1.5). With increased penetration of ICT services in developing countries, the number of ICT users (and eventually devices) will increase in the near future even more. Furthermore, the emergence of other types of ICT services such as ambient intelligence [9] can increase the number of devices that exist per user around the world. It has been predicted by Wireless World Research Forum (WWRF) that in the near future there could be up to one thousand devices per user (person), everything from mobile phones to small sensors all communicating with

each other [10]. Nevertheless, even if we assume that there are four billion users in 2020 each of them has on the average ten devices communicating with each other in the form of a wireless multi-hop network, and we assume each device requires 100 [mWatt] of power for wireless communication, the total energy consumption for communication in one hour will be 14.4×10^{12} [J] globally. This is ten times more than the energy produced by a 400 MWatt power station (a medium size nuclear plant) in one hour. If the number of devices per user increases to 100 by 2030, the energy consumption for keeping these devices networked will be 100 times more than the energy generated by the 400 MWatt power station. We can imagine that reducing small amounts of energy consumption for networking of these devices can result in a huge gain in large scales. Thus, it is essential to keep these networks energy-efficient in order to allow them to be expanded further and provide us better services with lesser environmental impact.

Energy-efficiency is also needed to let wireless devices operate for a longer duration. In many applications of wireless multi-hop networks nodes may run on batteries. High energy consumption reduces operational lifetime of battery-powered devices, and hence the autonomy of the system relying on them. Any communication mechanism for these networks should be energy-efficient to save the limited battery energy of nodes for data exchange over wireless links. Moreover, multi-hop communication of wireless devices has some hidden energy costs which must be minimized as well. In a networked environment, the energy consumption of a node for relaying packets which belong to other nodes could be even more than the energy that the node consumes for transmitting its own packets. Thus, each node needs to be aware of its scarce energy budget while it operates in a multi-hop wireless network. Relay traffic in the network should be balanced between nodes to prevent quick failure of those nodes which forward many packets on behalf of other nodes. Failure of nodes due to battery exhaustion not only isolates them from other nodes but also harms multi-hop connectivity of the network. *Therefore, energy-awareness should be considered in the design of a wireless multi-hop network to increase the operational lifetime of nodes individually and the operational lifetime of the network as a whole.*

1.3 Motivations and Research Questions

The motivation behind this research is to investigate energy-efficient and energy-aware communication in personal types of wireless multi-hop networks (e.g., PNs and home networks). We aim to reduce energy consumption in these networks and increase their operational lifetime keeping an eye on reliability aspects. Energy-efficiency and reliability are two important requirements for dependability of personal networks in

particular and wireless multi-hop networks in general [11]. This, in turn, is essential for their adoption by the end-user as a reliable communication architecture.

While there has been a large body of work addressing different aspects of wireless personal networks, there has been less attention to energy-awareness in these networks. Amongst studies related to personal networking, we can list architectures of personal networks [12], mobility and clustering of personal networks [13], impact of quality of wireless links in communication in personal networks [14], and service discovery is these networks [15]. Furthermore, we can highlight [16] as a study which investigates fundamental properties of wireless multi-hop networks, such as network connectivity, hop-count, network capacity, and interference. Our work, on the other hand, addresses an important open issue in wireless multi-hop network research, namely energy-awareness. We mention here personal networks as an important use-case. This enables us to get a clear picture of many issues and requirements. However, the mechanisms proposed and the analysis presented in this dissertation are generic and applicable to any type of wireless multi-hop network.

There has been an excessive attention within the research community on energy-aware and energy-efficient design of communication networks. Consortiums of academic and industry partners have been formed around the world (like *Green-Touch*[1]) aiming to reduce the energy consumption in communication networks. Having high performance may no longer be the dominant objective to design a communication network. Energy-efficiency is becoming more important. This dissertation investigates this important aspect of the design of wireless multi-hop networks; networks which are expected to become an integral part of human life in the future. We present novel ideas in energy-aware design and analysis of these networks on the basis of in-depth analytical models. More specifically, we address the following research issues:

R_1: Modeling the energy consumption for communication in wireless multi-hop networks.

R_2: Energy-efficient routing in wireless multi-hop networks.

R_3: Load balancing on the basis of battery energy of nodes.

R_4: Topology control for keeping fault-tolerant multi-hop connectivity using a lower transmission power.

R_5: Analyzing the lifetime of multi-hop connectivity between nodes.

R_6: Energy-efficiency of the physical layer.

---

[1]www.greentouch.org

There are other issues connected to this study such as power management using sleep and wake up mechanisms [17–20] and clustering [13,21,22] for energy efficiency. There are many solutions for these issues in the literature. However, the path taken here is indeed inclusive. That is, the solutions proposed in this thesis can co-exist with them. In the next section, we list all the contributions of this thesis and explain each of them.

1.4   Contributions of the Thesis

There are two concepts behind our contributions in this thesis. First, we believe that it is necessary to bring energy-efficiency to different layers of the communication stack, making it a *"Green Stack"*. We believe that designing energy-efficient and energy-aware schemes for only one layer is not effective. Energy-efficiency of other layers must also be taken into account. Second, while we design an energy-efficient mechanism for one layer, we need to consider the impact of other layers on that layer to provide a cross-layer optimization from an energy-efficiency viewpoint. Keeping these two aspects in mind, we develop a suite of communication schemes which together form a platform for energy-efficient and energy-aware communication in wireless multi-hop networks. In other words, our proposed platform considers different layers of the communication stack taking into account cross-layer dependency between them from energy-efficiency viewpoint (see Figure 1.6). We list our contributions as follows:

1. We propose routing schemes for finding the most energy-efficient routes between any two nodes of the network. To this aim, we consider the impact of the physical layer, data link layer, and transport layer on energy-efficient routes. The energy-efficient routing schemes are then enhanced with the capability to balance the traffic load between nodes according to their available battery energy. The proposed schemes could be deployed at the network layer (Layer 3). These contributions covers Research issues R_1 to R_3.

2. We propose a neighbor discovery mechanism for the data link layer (Layer 2) in the form of a network topology control algorithm. The proposed algorithm keeps the maximum transmission power of nodes as low as required for multi-hop connectivity of the network. This contribution covers Research issue R_4.

3. We analyze the expected duration that two nodes in a wireless multi-hop network with a random topology could communicate with each other from a transport layer (Layer 4) viewpoint. This contribution covers Research issues R_5.
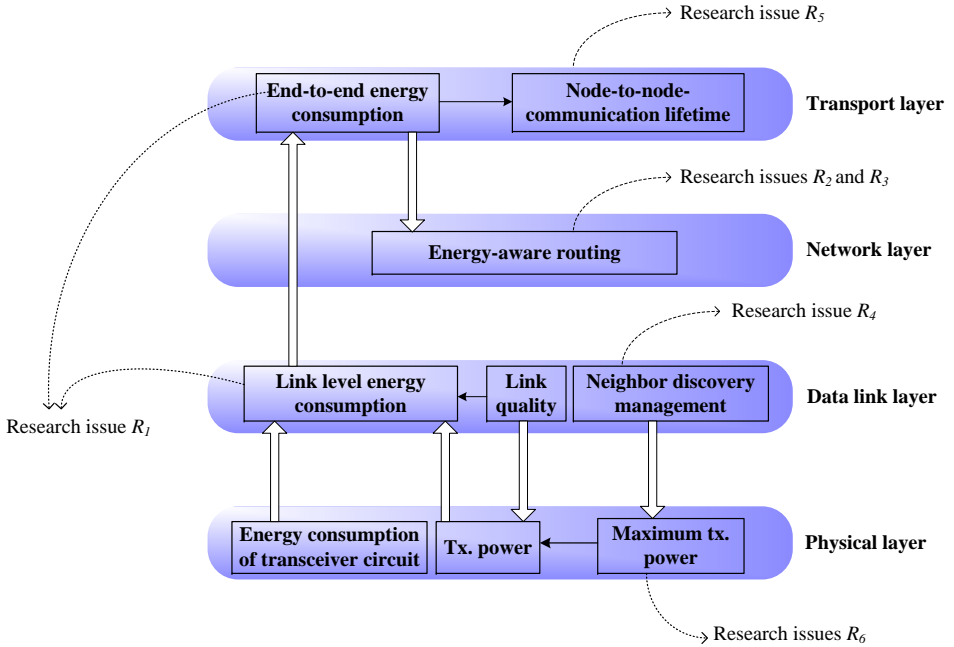
Figure 1.6 – Cross-layer dependencies for energy-aware communication in wireless multi-hop networks, and the corresponding research issues.

4. We propose cooperative signal transmission techniques to reduce the transmission power of nodes at the physical layer (Layer 1) without sacrificing link reliability. This covers Research issue R_6.

In each chapter, we will identify what is missing in the current literature and what are the questions that need our attention. We also show the drawbacks of existing schemes and the requirements for improving the current energy-aware communication schemes. We present the novelty of our proposed schemes thereafter. Background, the current literature, and related discussions will be provided while explicating each of the research issues in the forthcoming chapters of the thesis.

1.5   Outline of the Thesis

The rest of this thesis is organized as follows: In Chapter 2, we provide background information about wireless multi-hop networking. We explain how nodes communicate with each other in these networks, and which technologies could be used for multi-hop communication in wireless networks. Essentials of radio

signal propagation and modeling the topology of these networks are presented as well. Then in Chapter 3, we model the energy consumption for transmission and reception of packets over a wireless link. This creates the first step for designing the energy-aware communication mechanisms. Using the developed model, we analyze in Chapter 4 the energy consumption for multi-hop packet traversal between nodes. This analysis lays the foundation of designing energy-efficient routing algorithms for wireless multi-hop networks, which is tackled in Chapter 5. In Chapter 6, we enhance energy-efficient routing schemes presented in Chapter 5 with the capability to balance the traffic load amongst nodes. To this end, we consider the remaining battery-energy and the type of power supply of nodes. In Chapter 7, we study topology control in wireless multi-hop networks, and propose novel schemes for these networks. In Chapter 8, we analyze the duration that two arbitrary nodes in a wireless multi-hop network with a random topology could keep communicating with each other. This novel analysis is based on the energy consumption model that we developed in Chapter 3. Chapter 9 addresses cooperative signal transmission schemes for reducing energy consumption of nodes. We conclude the thesis and highlight future work in Chapter 10. The relation between chapters of the thesis and their sequence is shown Figure 1.7.
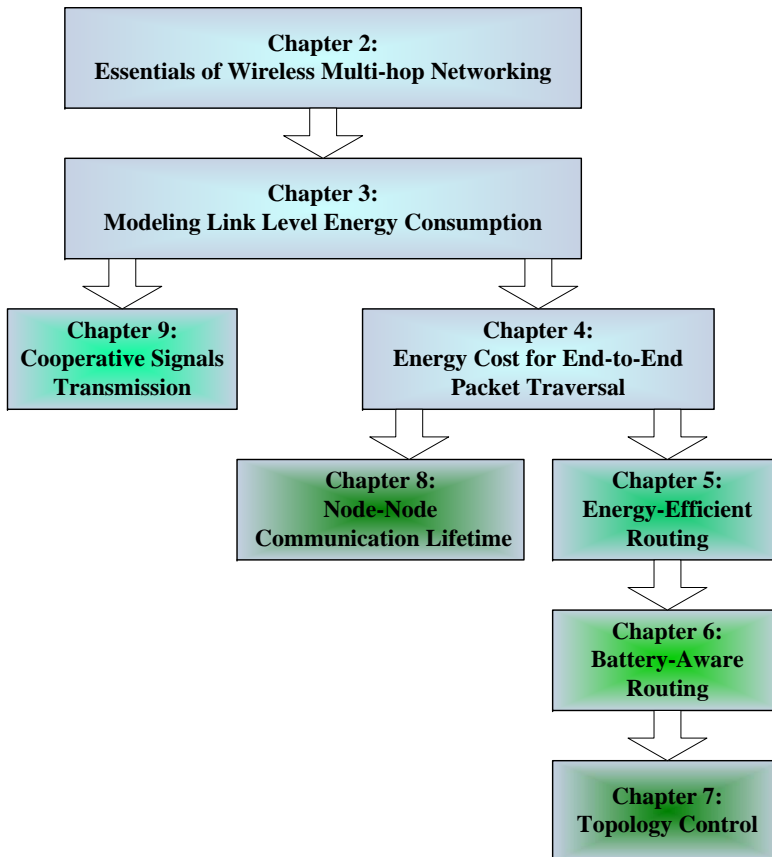
Figure 1.7 – Sequence of chapters of the thesis and the relation between them. Arrows show a logical relation between chapters. The proposed schemes in different chapters make the network more and more energy-efficient.

Chapter 2

Essentials of Wireless Multi-hop Networking

In this chapter, we provide general information about wireless multi-hop networks. This is essential for understanding the rest of the thesis. We introduce radio technologies suitable for multi-hop networks and explain routing and medium access control mechanisms in these networks. Essentials of radio signal propagation and topological representation of wireless multi-hop networks will be presented as well.

2.1   Radio Technologies

With the proliferation of wireless technologies, support for multi-hop communication has been considered in many of them. Various radio technologies developed for wireless personal area networks (WPANs), wireless local area networks (WLANs), and wireless metropolitan area networks (WMANs) support multi-hop communication. We briefly review these technologies.

2.1.1   WPAN Technologies

WPAN technologies support short-range wireless connectivity in the personal operating space (around 10-20m). IEEE 802.15.4 [23] and IEEE 802.15.3 [24] are two well-known standards for WPANs which can support multi-hop communication. IEEE 802.15.4 supports low data rate communication (up to 250 Kbps) for applications such as home automation, personal health-care, industrial automation, and wireless sensor networking. On the other hand, IEEE 802.15.3 supports high data rate (up to 55 Mbps) with QoS provisioning for video-streaming and large file transfer applications such as video or digital imaging.

IEEE 802.15.4 can support multi-hop communication in its *peer-to-peer* mode. In this mode, two nodes that are within transmission range of each other can communicate directly. Thus, a multi-hop network can easily be formed by creating direct links between nodes within each other's transmission range. In the IEEE 802.15.3 standard, multi-hop communication is supported only through the concept of child piconets associated with their parent piconets. A piconet is a one-hop wireless network whose communication is controlled by one of its nodes acting as the piconet controller (PNC). To support multi-hop communication, the PNC of a child piconet, which is a member of the parent piconet as well, has to forward packets from a device in the parent piconet to a device in the child piconet and vice versa. This results in a two-hop communication between devices in parent and child piconets. To have a three-hop communication, another piconet should be attached to the child piconet. The network could be expanded using successive child piconets attached to each other. Nevertheless, this scheme is not very efficient because the allocated bandwidth to a multi-hop connection reduces drastically as the number of hops increases [25]. A solution for this problem has been proposed in [25]. In this method, a parent-child relationship is not required for multi-hop communication anymore. Instead, a two-hop scheduling mechanism is used to reserve required time slots for two-hop communication between two neighboring piconets. The neighboring piconets are connected through one of their common nodes.

2.1.2   WLAN Technologies

WLAN technologies support high data rate wireless connectivity for fixed, portable, and mobile stations within a local area (of the order of 100m). IEEE 802.11b [26], IEEE 802.11g [27], and IEEE 802.11n [28] are well-known standards for WLANs which can easily support multi-hop communication in their *ad-hoc* modes. In this mode, no access point is required. IEEE 802.11n which supports data rates up to 300 Mbps is backward compatible with IEEE 802.11g and IEEE 802.11b. On the other hand, IEEE 802.11g which supports data rate up to 54 Mbps is backward compatible with IEEE 802.11b which supports data rates up to only 11 Mbps.

2.1.3   WMAN Technologies

WMAN technologies support wireless connectivity for fixed, portable, and moving stations within a metropolitan area (of the order of 1 km). IEEE 802.16 [29] is the well-know wireless standard for WMANs. It can support high data rate communication (up to 120 Mbps) with QoS provisioning. The primary goal of development of this standard is to support infrastructure-based communication. However, it can support multi-hop communication as well in *mesh* mode. To this end, the

IEEE 802.16 standard uses a complicated decentralized scheduling to coordinate transmission of nodes for multi-hop communication with QoS provisioning (see [29] for further details). This complex scheduling mechanism reduces the ability of the IEEE 802.16 standard to support multi-hop communication on a large scale compared to a standard such as IEEE 802.11b.

2.2   Medium Access Control

The goal of medium access control (MAC) protocol in wireless networks is to monitor and control how nodes access the shared wireless medium. Here, medium is referred to as the space through which the radio waves propagate. A MAC protocol is deployed in the MAC layer which corresponds to the data link layer in the OSI Reference Architecture[1].

Time division multiple access (TDMA) and carrier sense multiple access with collision avoidance (CSMA/CA) are well-accepted MAC mechanisms in wireless multi-hop networks. In TDMA, each node can only transmit data in time-slot(s) allocated to that node. Allocating time-slots to nodes is the responsibility of a central controller (e.g., a PNC in the IEEE 802.15.3 standard). This adds to the complexity of TDMA-based MAC protocols and reduces the scalability of these protocols to be deployed in a distributed environment such as wireless multi-hop networks. Moreover, the use of TDMA necessitates nodes to be synchronized and have a common sense of timing.

In CSMA/CA, each node senses the medium and sends its data if the medium is free. Medium access is of a probabilistic nature compared to that of TDMA which is of a deterministic nature. CSMA/CA is a scalable solution for wireless multi-hop networks. It does not require a centralized controller and time synchronization between nodes. However, the drawback of CSMA/CA is that no guaranteed QoS can be provisioned, while TDMA can guarantee QoS provisioning.

Among various wireless standards, the MAC protocol in IEEE 802.11b/g/n and IEEE 802.15.4 (in peer-to-peer non-beacon-enabled mode) uses CSMA/CA. MAC protocol in IEEE 802.15.3 uses a combination of CSMA/CA and TDMA. In the IEEE 802.15.3 standard, superframes are used to coordinate communication within a piconet. Each superframe starts with a beacon propagated by the PNC through which nodes can synchronize themselves with the PNC. Part of a superframe consists of time-slots, which are allocated to piconet nodes by the PNC, while channel access in the rest of the superframe is using CSMA/CA.

Apart from the type of channel access mechanism which can be used to categorize MAC protocols, they can be categorized based on their support for automatic repeat request (ARQ). If ARQ is supported, lost packets could be

---

[1]In this thesis, we will use MAC layer and data link layer interchangeably.

recovered through retransmissions triggered by the MAC layer. To this aim, the receiver must acknowledge correct reception of a packet through an acknowledgment packet (referred to as MAC acknowledgment). If the sender does not receive the acknowledgment, it will retransmit the packet after expiration of a timer. This may happen because either the packet or its acknowledgment is lost. The sender retransmits the packet until it receives an acknowledgment, or the maximum number of transmission attempts, M, is reached. Therefore, a packet or its acknowledgment might be transmitted $m \leq M$ times. Note that if the acknowledgement is lost and the receiver receives the retransmitted packet, there will be a duplicate packet at the receiver. The MAC layer or higher layers discard such packets.

MAC acknowledgments could be transmitted *per packet* or using *cumulative* acknowledgments. If per packet acknowledgments are supported, each packet is acknowledged separately. If commutative acknowledgments are used, several packets could be acknowledged using a single acknowledgement. Among wireless technologies, IEEE 802.11b/g/n support mandatory per packet acknowledgement, while IEEE 802.15.4 supports optional per-packet acknowledgment. In IEEE 802.15.4, the MAC header of each transmitted packet indicates whether the receiver needs to acknowledge the packet or an acknowledgement is not required. On the other hand, the IEEE 802.15.3 standard supports data transfer with per-packet acknowledgments, with cumulative acknowledgements, or without ARQ. If ARQ is not supported, the sender transmits each packet once and no acknowledgement is transmitted by the receiver. As we will discuss in the next chapter, support for ARQ at the MAC layer can affect the total amount of energy that a sender and a receiver consume to exchange a packet through the wireless link.

Considering the type of MAC mechanism in various WPAN, WLAN, and WMAN standards, we can conclude that *IEEE 802.11b/g/n* and *IEEE 802.15.4* are easier to be deployed in wireless multi-hop networks. Since these standards use CSMA/CA, a multi-hop network can be formed and expanded with less complexity. These standards are widely accepted by users and the research community. So far, no commercial device supporting the IEEE 802.15.3 standard is available, but 802.15.4 and 802.11 based devices exist commercially worldwide. Although 802.16 based devices are appearing recently, they are mainly for infrastructure-based communication. Support for multi-hop communication is optional in this standard. Most IEEE 802.16 based commercial devices do not support multi-hop communication.

2.3   Routing and Mobility

In wireless multi-hop networks, a routing protocol is required to keep nodes connected at the network layer level. The task of the routing protocol is to discover

and maintain a valid route between a pair of nodes. A route consists of a number of intermediate nodes between a source and a destination node which forward packets hop-by-hop to the destination. Design, analysis, and evaluation of routing protocols in wireless multi-hop networks have been the target of many research activities during the last decade [30–42]. Various protocols with different capabilities optimized for different applications have been proposed so far. A survey of these protocols can be found in [43, 44]. We can categorize routing protocols developed for wireless multi-hop networks based on different criteria. A main criterion for categorizing these protocols is the way they discover and maintain routes. In this way, routing protocols are categorized as proactive and reactive protocols.

2.3.1   Proactive Routing

Proactive protocols maintain routes proactively. Each node keeps an updated route to any other node in the network even if there is no session going on between that node and other nodes. When a node receives a packet from its application layer or its neighbors, it checks its routing table to find the next hop node towards the destination address. The packet is then forwarded to the determined next hop node. This continues until the destination node receives the packet. In order to keep valid routes, nodes maintain a complete map of the network topology. Thus, they can determine the optimal path (e.g., the path with the minimum number of hops) to any other node in the network using, for instance, Dijkstra's shortest-path routing algorithm.

In proactive protocols, the network topology at each node is constructed using *topology broadcast* messages that nodes propagate and through which they share with each other their view of the network topology. Topology broadcast messages are sent by nodes periodically, and flood the entire network. Another important message in proactive protocols is *Hello* message. Nodes use Hello messages to detect their neighbors and inspect physical links to their neighbors. Hello messages are transmitted periodically as well. Nevertheless, they do not flood the network.

As we may expect, the main drawback of proactive protocols is the high routing overhead generated by flooding by topology broadcast messages and broadcasting of Hello messages. Propagation of these messages occupies the bandwidth and consumes energy. Some protocols such as Optimized Link State Routing (OLSR) [40] try to reduce the routing overhead by smart propagation of topology broadcast messages. In OLSR, each node can select a set of nodes among its neighbors which are allowed to flood topology broadcast messages.

2.3.2   Reactive Routing

Reactive routing protocols discover routes on demand when a node has data to send
to another node and it does not know a valid route to its destination node. In such
a case, the source node broadcasts a route request (RREQ) message to discover a
valid route to the destination node. Each node, which has not received the RREQ
message already, may re-broadcast the message. When the destination receives the
RREQ message, it replies to it by a unicast route replay message (RREP). The
RREP message traverses the same route back to the source node that RREQ has
traversed from the source to the destination. Examples of reactive routing protocols
are Ad-hoc On-demand Distance Vector (AODV) [42] and Dynamic Source Routing
(DSR) [41, 45].

Many studies have shown that reactive protocols not only generate less
overhead compared to proactive protocols, but also have a better packet delivery
performance [46–49]. This is intuitively obvious in networks whose their topology
does not change frequently. In such networks, once a route is discovered, it could
be used for a long period. However, in networks with changing topology (e.g.,
mobile networks), reactive protocols may generate the same overhead as proactive
protocols [47], because route discovery may be triggered frequently. Nevertheless,
reactive protocols can react faster to topological changes. In proactive protocols,
once a change in the network topology happens, it may take relatively long before
all the nodes obtain the same view of the network topology again. Thus, while the
routing tables are being updated in all nodes, packets might be dropped due to lack
of knowledge of a valid route to the destination.

At the end, it is worthwhile to mention that the routing protocol in mobile
multi-hop networks is also a means for mobility support. The routing protocol
can maintain valid routes between nodes while they are moving. A data packet
originated by a source node can be routed to its destination node, even if they both
are mobile and intermediate nodes between them are mobile as well. Nevertheless,
topology changes due to mobility can induce a high routing overhead. For this
reason, the use of delay tolerant communication and opportunistic routing [36]
have been considered as efficient schemes for mobile multi-hop networks.

2.4   Network Topology Representation

The topology of a wireless multi-hop network determines how nodes are connected
to each other. Fading over wireless channels and mobility of nodes may cause
a break in existing links and the appearance of new links in the network. This,
in turn, changes the network topology. Nevertheless, at any instant of time, the

topology of a wireless multi-hop network could be represented by a graph $G(\mathbb{V}, \mathbb{E})$, where $\mathbb{V}$ and $\mathbb{E}$ are the set of nodes (vertices) and links (edges), respectively.

A node in the network could be identified by a unique identifier. The identifier of a node can be its MAC or IP address. Alternatively, we can simply use an integer value from the interval $[1, N]$ to identify a node, in which $N = |\mathbb{V}|$ is the number of nodes in the network. In this thesis, we will use this simple scheme to refer to a node in the network. Therefore, an integer $u \in [1, N]$ specifies the uth node in the network. Consequently, a link is represented by a pair of integer values (u, v), where u is the *sender/sending* end and v is the *receiver/receiving* end of the link. If there is a link between two nodes, then $(u, v) \in \mathbb{E}$. One implicit assumption for having a link between two nodes is that they are equipped with the same radio technology.

2.4.1   Related Terms

Directional and Bidirectional Links: A link $(u, v) \in \mathbb{E}$ is *bidirectional*, if $(v, u) \in \mathbb{E}$ as well. Otherwise, (u, v) is a *directional* link. In a wireless multi-hop network, there could be directional links between nodes if the transmission range of nodes is not the same. For instance, if two nodes use the same radio technology produced by different manufactures, their transmission range could be different. In such a case, it might be possible that one of them lies outside the transmission range of the other. Directional links in wireless networks could cause problems in communication when MAC acknowledgment is supported. If MAC acknowledgment is supported, the next packet will be transmitted by the sender only when the sender has already received the acknowledgment for the last transmitted packet. If there is a directional link between two nodes, the sender will not receive the acknowledgement. Thus, there will be no communication between the sender and the receiver.

Path (Route):   A path between a source node u and a destination node v is a set of nodes which connect the two nodes to each other in a multi-hop way. We represent a path in the network with $h \geq 1$ hops as $\mathcal{P} = \{n_1 = u, n_2, ..., n_h, n_{h+1} = v\}$ where $n_k \in \mathbb{V}$ is the kth node, $k = 1, ..., h + 1$, of the path, and $(n_k, n_{k+1}) \in \mathbb{E}$ is the kth link, $k = 1, ..., h$. Here, n_k, $k = 2, ..., h$, is an *intermediate (relay)* node. If $h = 1$, then the path consists of only one hop, which is the direct link between the source and the destination. Two paths between a pair of source-destination nodes could be *node-disjoint* or *non-disjoint*. They are node-disjoint, if they don't have any intermediate node in common. Otherwise, they are called non-disjoint routes.

Path and Link Weight: Path weight is a function of the weight of constituent links of the path. We denote the weight of a path $\mathcal{P}$ by $W(\mathcal{P})$, and the weight of a link (u, v) by $w_{u,v}$. There are three types of link weights: additive, concave, and multiplicative. If link weights are additive, the path weight is the summation of the weight of constituent links of the path. Consumed energy for packet transmission over a link and delay are examples of additive link weights. If link weights are concave, the path weight is the minimum weight of constituent links of the path. Bandwidth of a link is an example of concave link weights. If link weights are multiplicative, the path weight is obtained by multiplying weights of constituent links of the path. Reliability of links is an example of multiplicative link weights.

Neighbor: A node v is a neighbor of node u, if there is a direct link from u to v (i.e., $(u, v) \in \mathbb{E}$). That is, neighbors of a node are *one hop* away from the node. Neighbors of a node form a *neighborhood*.

Node Degree: The number of neighboring nodes of a node is referred to as degree of that node. The average node degree of all nodes in the network is called *mean degree of nodes*. Minimum degree among all nodes is referred to as *minimum degree* of the network.

Transmission Power: Transmission power is the output power of a node for signal transmission over the air. In general, we can assume that the transmission power of a node to its various neighboring nodes could be different. We denote $P_{u,v} \leq P_u$ as the transmission power of node u to node v, where P_u is the maximum transmission power of node u.

Transmission Range: Transmission range of a node in the network is the maximum radius from the node at which a target bit error rate is satisfied in the receiver when the node transmits with its maximum transmission power. We denote the transmission range of node u by D_u. The target bit error rate is usually a design parameter of the radio technology used.

Packet Delivery Ratio: Probability of error-free reception of a packet in a single transmission attempt is referred to as packet delivery ratio (PDR) of a link. PDR of a link depends on many factors such as modulation and channel coding schemes deployed at the physical layer, type of fading, and size of the packet. We denote $p_{u,v}(x)$ as the PDR of link (u, v) for a packet of size x bits.

Shortest Path: There might be several paths between a source and a destination node in a multi-hop network. The shortest path is the path which has the minimum cumulative weight.

Hop count: Hop count of a path is the number of hops in that path. The average value of hop count between all pairs of source-destination nodes in the network is referred to as *mean hop count*.

Connectivity: A multi-hop network is *connected*, if there is at least one path between any two nodes in the network. If there is a pair of nodes for which there is no path between them, the network is *disconnected*. Furthermore, a network in which there are at least k node-disjoint paths between any two nodes is called k-connected. k-connectedness ($k \geq 2$) is essential for having fault-tolerant communication in multi-hop networks, because communication between two nodes is not interrupted even after failure of the first path between them.

2.4.2 Homogenous and Heterogeneous Networks

In a homogenous network, all nodes are characteristically similar to each other. In a heterogeneous network, nodes have different characteristics. This may include, for instance, heterogeneity in radio technology, processing capabilities, energy consumption profile, and power supply. The heterogeneity may be attributed to only one or several of these characteristics.

A multi-hop network with heterogeneous radio technologies may consist of a number of interconnected *radio domains*. Each radio domain contains nodes which support the same radio technology. To connect two radio domains to each other, we need a node supporting both technologies. Such a node is referred to as a *bridge node*. The topology of such a multi-hop network can still be represented by a graph $G(\mathbb{V}, \mathbb{E})$. Nevertheless, we have $\mathbb{V} = \mathbb{V}_1 \cup \mathbb{V}_2 \cup ... \cup \mathbb{V}_n$ where n is the number of radio domains in the network and $\mathbb{V}_i$ is the set of nodes in the ith radio domain. Accordingly, we have $\mathbb{E} = \mathbb{E}_1 \cup \mathbb{E}_2 \cup ... \cup \mathbb{E}_n$, where $\mathbb{E}_i$ is the set of links in the ith radio domain.

A network consisting of several radio domains is a good example of a heterogeneous network. Nevertheless, all the nodes using the same radio technology may still be called heterogeneous if, for instance, they use different interfaces made by different manufactures. In such a case, the energy consumption profile of nodes and their transmission range could be different. Another example is having nodes with similar radio interfaces but different processing capabilities (e.g., a laptop and a smart phone with similar wireless interfaces).

Another type of heterogeneity in multi-hop networks is heterogeneity of the type of power supply of nodes. That is, even if wireless interfaces of nodes are

completely the same, nodes can be heterogeneous in terms of energy if they use different types of power supply. For instance, some devices in a wireless multi-hop network might be connected to the mains, but others may run on a battery. For such a network, we define $\mathbb{V}_b$ as the set of nodes which run on battery and $\mathbb{V}_m$ as the set of nodes which are connected to the mains (the grid). Accordingly, we define $\mathbb{E}_b = \{(u,v) \in \mathbb{E} : u \in \mathbb{V}_b\}$ as the set of links going out from battery-powered nodes (called *battery-powered links*), and $\mathbb{E}_m = \{(u,v) \in \mathbb{E} : u \in \mathbb{V}_m\}$ as the set of links going out from mains-powered nodes (called *mains-powered links*). In this thesis, we will consider mainly heterogeneity of power supply and energy consumption of nodes.

2.5   Radio Propagation Models

There are two common models for signal propagation in wireless multi-hop networks. They are the *path-loss* model and the *lognormal* model.

2.5.1   Path-loss Model

In the path-loss model, the average received power at a receiver is proportional to $d^{-\eta}$, in which η is the path-loss exponent of the environment, and d is the distance between the sender and the receiver. Parameter η varies from 2 in free space to 6 in heavily built urban areas. According to the path-loss model, if node u transmits signals with power P_u, the average received power by node v from node u is as follows:

$$P_{rx_{u,v}} = cP_u d_{u,v}^{-\eta} \tag{2.1}$$

in which c is a constant that depends on the wavelength and the receiving and the transmitting antenna gains. Note that the instantaneous received power is modeled as a random variable with mean value $P_{rx_{u,v}}$. If there is no line of sight (LOS) between the two nodes, the instantaneous received power is modeled as a random variable with Rayleigh distribution. If there is a LOS between the two nodes, the instantaneous received power is modeled as a random variable with Rician distribution [50].

According to the path-loss model, the transmission range of u is

$$D_u = \left(\frac{cP_u}{P_{rx_{min}}} \right)^{\frac{1}{\eta}}, \tag{2.2}$$

in which $P_{rx_{min}}$ is the minimum received power required for having a link between two nodes[1]. Since received power decays with distance, the received power at a

---

[1] The minimum received power depends on the target BER requirement which must be satisfied at the receiver.

distance greater than D_u from transmitter will be lower than $P_{rx_{min}}$. Thus, there is a link from u to v (i.e., $(u, v) \in \mathbb{E}$), only if $d_{u,v} \leq D_u$. In other words,

$$\Pr\{(u, v) \in \mathbb{E}\} = \begin{cases} 1 & d_{u,v} \leq D_u \\ 0 & d_{u,v} > D_u. \end{cases} \tag{2.3}$$

2.5.2   Lognormal Model

In the lognormal model, the average received power at distance d from a sender varies from location to location [51]. Remember that in the path-loss model, the average received power at distance d is the same at all locations. In the lognormal model, the average received signal at distance d is itself a random variable. The logarithmic value of this random variable is assumed to have a normal distribution with mean value as predicted by the path-loss model. More specifically, the average received power by a node v from a node u is expressed as follows:

$$10log(P_{rx_{u,v}}) = 10log\left(cP_u d_{u,v}^{-\eta}\right) + z, \tag{2.4}$$

where z is a zero-mean normal random variable.

Since the transmission power varies from location to location, the transmission range is not the same at different locations. The amount of variation in the transmission range of a node depends on the variance of z. The higher the variance of z, the more is the variation domain of the transmission range of the node. The average value, however, is as expressed in (2.2). Therefore, what is considered as the transmission range in the path-loss model is in fact the *average transmission range* according to the lognormal model. In this model, the probability of having a link between two nodes u and v is [52]

$$\begin{aligned} \Pr\left\{(u, v) \in \mathbb{E}\right\} &= \Pr\left\{z \geq 10log\left(\frac{cP_u d_{u,v}^{-\eta}}{P_{rx_{min}}}\right)\right\} \\ &= \Pr\left\{z \geq 10log\left(\left(\frac{d_{u,v}}{D_u}\right)^{\frac{1}{\eta}}\right)\right\} \\ &= \frac{1}{2}\left[1 - erf\left(\frac{10\eta}{\sqrt{2}\sigma log(10)}log\left(\frac{d_{u,v}}{D_u}\right)\right)\right], \end{aligned} \tag{2.5}$$

where $P_{rx_{min}}$ is the minimum received power for having a link between two nodes, and $erf(.)$ is the Gauss error function.

2.6   Geometric Random Graphs

Geographic random graphs have been widely accepted for modeling wireless multi-hop networks such as wireless sensor and ad hoc networks [53–55]. These

graphs are considered to be a more realistic model for wireless multi-hop networks than pure random graphs of Erdos and Renyi [52]. In Erdos and Renyi random graphs, there might be a link between any two nodes with a certain probability, regardless of their distance with each other. Furthermore, the existence of a link between two nodes is independent of the existence of a link between another pair of nodes. Nevertheless, in a wireless multi-hop network, there can not be a link between two nodes which are outside each other's transmission range. Moreover, links are locally correlated with each other. That is, there is a high probability that a link exists between two nodes which have a common neighbor.

A geometric random graph consisting of N nodes is constructed by distributing N points uniformly on a square area and adding edges to connect any two nodes for which their Euclidean distance to each other is less than a predefined value. Under some circumstances, a geometric random graph can model the topology of a wireless multi-hop network. First, nodes in the wireless multi-hop network are uniformly distributed. Second, the signal propagation model is the path-loss model. Third, all nodes have the same transmission range $D_u = D_{max} \ \forall u \in \mathbb{E}$. Such a graph is also known as *path-loss geometric random graph* [52], since it is based on the path-loss signal propagation model.

Another variant of geometric random graphs have been proposed in [52] as *lognormal geometric random graphs*. These graphs inherit some characteristics from path-loss geometric random graphs and some from pure random graphs of Erdos and Renyi. In lognormal geometric random graphs, the probability of having a link between two nodes is specified by (2.5). Note that, we can consider path-loss geometric random graph a good model for wireless multi-hop networks, if the variation of received signal strength at transmission range D_{max} is so small that it does not change the network topology. Unless stated otherwise, the term "geometric random graph" in this thesis will refer to the path-loss geometric random graph.

Penrose [55] proved that a geometric random graph G with $N \to \infty$ nodes located uniformly in a unit disk (or a unit cube) is almost surely k-connected if its minimum degree is k. In other words, for any random geometric graph G, the following expression holds:

$$Pr\{G \ is \ k - connected\} = Pr\{n_{min} \geq k\},$$

where n_{min} is the minimum degree of the graph. Thus, to have a k-connected graph, each node must at least have k neighbors.

Bettstetter [53] used this fact to determine the probability that a wireless multi-hop network is k-connected. To compute $Pr\{n_{min} \geq k\}$ in a wireless multi-hop networks, we need to know the probability density function of node degree in the network. If nodes are uniformly distributed in a square area, the probability density function of the degree of a node is approximated by a Poisson

density function with parameter $\tau = \frac{\pi N D_{max}^2}{A}$ [53]. Here, D_{max} is the common transmission range of nodes and A is the network deployment area. We can show that

$$Pr\{G \text{ is } k - connected\} = \left(1 - e^{-\tau} \sum_{i=0}^{k-1} \frac{(\tau)^i}{i}\right)^N.$$

$$(2.6)$$

This formula has been obtained assuming that $\frac{\pi D_{max}^2}{A} << 1$. That is, the coverage area of a node must be very small compared to the network deployment area.

An implication of the expression given in (2.6) is that we can determine the minimum node density (given the transmission range of nodes) or the minimum transmission range (given the node density) required to have a k-connected network with a certain probability. For instance, to have a 1-connected network with probability greater than b, we need to set the transmission range of nodes to

$$D_{max} \geq \sqrt{\frac{-A \ln\left(1 - b^{\frac{1}{N}}\right)}{N\pi}}.$$

$$(2.7)$$

Alternatively, if the transmission range D_{max} is known, we can determine the minimum number of nodes required to have a 1-connected network using the above inequality, which can be only solved numerically.

The probability of k-connectivity of the network has been plotted in Figure 2.1 as a function of the number of nodes in the network and the transmission range of nodes. In addition to theoretical values, simulation results have been plotted as well. To have a clear picture, we only have plotted simulation results for $k = 1$. The figure shows that the values obtained by simulations are smaller than those predicted theoretically. The reason for this mismatch is the border effect of the rectangular network area. Equation (2.6) has been obtained assuming an infinitely large area. In practice, the network area is bounded. Having a bounded area results in the border effect, because a node placed near the boundary of the rectangle area will cover less area than a node in the middle of the area. Thus, nodes located at the borders of the area on the average have a lower node degree compared to nodes in the middle of the area. The consequence of the border effect is reducing the probability of having a k-connected network from what is predicted by (2.6).

So far, we discussed connectivity of wireless multi-hop networks assuming all nodes have a common transmission range D_{max}. With this assumption, we presented an expression specifying the probability that the network is k-connected. In practice the transmission ranges of nodes might not be the same. This might happen either because of heterogeneity of radio interfaces of nodes or due to lognormal signal propagation. When transmission ranges of nodes are not the same, we can use (2.6) to determine *a lower bound* on the probability of k-connectivity
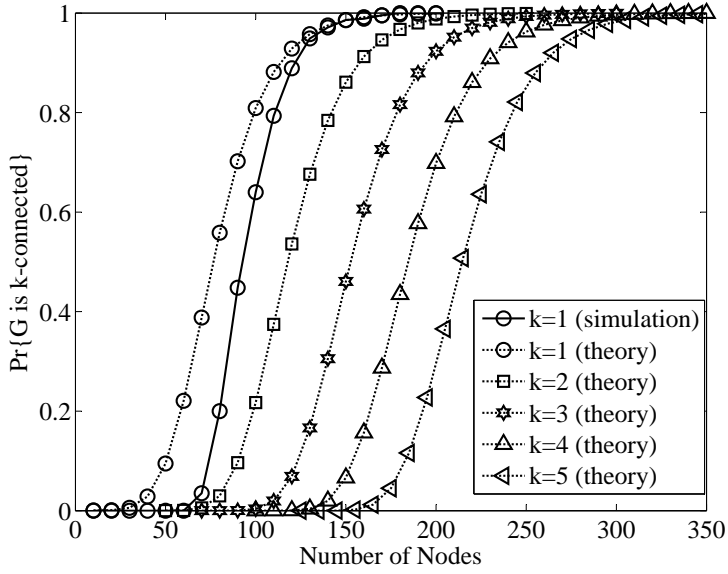
(a)
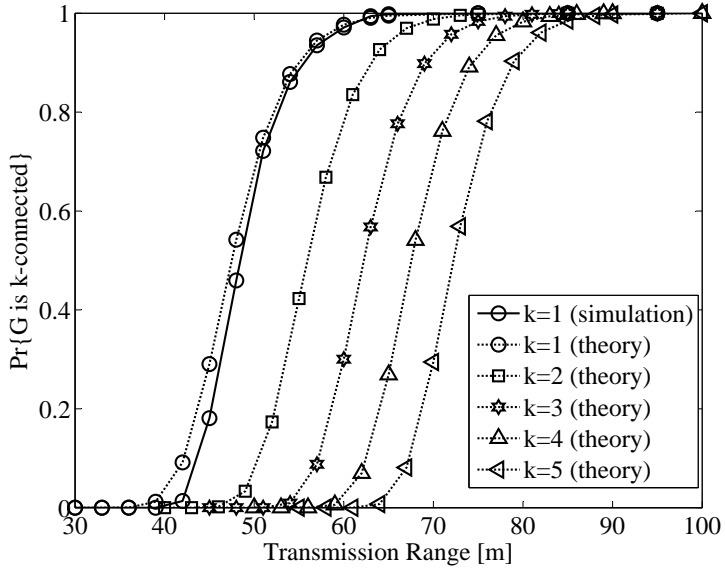
(b)

Figure 2.1 – (a) The probability that a wireless multi-hop network is connected as a function of (a) the number of nodes in the network and (b) the transmission range of nodes. The transmission range of nodes in Plot (a) is 70m, and the number of nodes in Plot (b) is 200. The network area is $500 \times 500 \text{m}^2$. The theoretical values have been obtained using (2.6).

of the network. To specify this lower bound, let b_{min} be the probability that the network is k-connected assuming the transmission range of each node is D_m, where D_m is the minimum transmission range amongst nodes of the network. We can determine b_{min} using (2.6) assuming $D_{max} = D_m$. Since, in practice the transmission range of some nodes might be greater that D_m, there will be more links in the network compared to the case that the transmission range of all nodes is D_m. This increases the probability of k-connectivity of the network. Therefore, if b denotes the probability that such a network is k-connected, we have $b \geq b_{min}$.

2.7 Summary

In this chapter, we introduced wireless standards which support multi-hop communication in wireless networks. These are IEEE 802.15.3 (using the parent-child relationship in piconets), IEEE 802.15.4 (in peer-to-peer mode), IEEE 802.11b/g/n (in ad hoc mode), and IEEE 802.16 (in mesh mode). Considering the scalability and complexity of MAC layer in these standards, IEEE 802.15.4 and IEEE 802.llb/g/n were recognized as suitable solutions for wireless multi-hop networks. We then discussed routing in multi-hop networks. Two main types of routing protocols were explained, namely reactive and proactive protocols. Studies show that reactive protocol are better choices for wireless multi-hop networks, since they generate less overhead and cope faster with topological changes. Next, we introduced some terms and notations related to the topological representation of wireless multi-hop networks, which will be used in the rest of the thesis. Two radio signal propagation models – path-loss and lognormal models – were presented, and geometric random graphs were introduced as suitable models for wireless multi-hop networks. Connectivity of these graphs was studied as well.

Chapter 3

Modeling Link Level Energy Consumption

In this chapter, we develop a mathematical model for energy consumption of nodes for packet exchange over wireless links. This model determines the amount of energy consumed by a sender and a receiver to exchange a packet over the wireless link between them. We will use this model in the design and evaluation of energy-aware communication schemes in the rest of the thesis. The developed model in this chapter is very detailed compared to other models [56–60]. It includes details such as reliability of wireless links, consumed energy by processing elements of transceivers, packet retransmission at the MAC layer, size of data and acknowledgment packets, and data rate of wireless links. Studies such as [56,57] only model consumed energy during a single transmission and reception of a packet. They do not take into account the effect of packet retransmission on energy consumed for packet exchange. By taking into account the effect of packet retransmission, the model we present in this chapter brings into picture the effect of reliability of wireless links on the energy consumption of nodes. Our model also enhances the proposed model in [60] by limiting the number of times that a lost packet is allowed to be retransmitted by the MAC layer. It is assumed in [60] that there is no limitation on the number of retransmissions. Furthermore, [60] assumes, without any verification, that the same amount of energy is consumed for receiving lost and error-free packets. We used 2.4 GHz IEEE 802.15.4 devices to verify this assumption. We show that *a high percentage* of lost packets over a wireless link are discarded after being completely detected by the receiver. This means, the consumed energy for receiving lost packets is comparable with the consumed energy for receiving packets successfully.

To develop the energy consumption model, we first study the structure of a transmitter and receiver (transceiver) in Section 3.1. Knowing the structure of a

transceiver, we then model energy consumption during a single transmission and reception of a packet over a link in Section 3.2. In Section 3.3, we introduce transmission power control technique in wireless multi-hop network and study its impact on the link level energy consumption model. Section 3.4 studies the effect of packet retransmission at the MAC layer on energy consumption of nodes. Since energy consumption of nodes is affected by quality of wireless links, we elaborate on this issue in Section 3.5. We compare our model with other models from the literature in Section 3.6. We summarize the chapter in Section 3.7.

3.1 Structure of a Transceiver

To model energy consumption of nodes, we consider three commercial transceivers: 1) Intersit PRISM I chipset which is based on the IEEE 802.11b standard, 2) Chipcon CC2420 which is based on the IEEE 802.15.4 standard, and 3) Chipcon CC1000 which is a very low power UHF wireless transceiver. Figure 3.1 shows a block diagram of these transceivers. If we look at these three different transceivers, we can recognize four common building blocks in all of them. The first block contains processing elements for baseband processing and possibly other types of digital data processing which could be performed by a microcontroller. The second block contains IF and RF parts for signal transmission excluding the power amplifier. The third block contains the power amplifier (PA). The PA generates the required power for signal transmission over the air. The fourth block contains IF and RF parts for signal reception which is followed by the low noise amplifier (LNA). The LNA amplifies the received signal in order to reduce the detection error. We can abstract different elements of a wireless transceiver as shown in Figure 3.2. Such a model has been used in other studies as well (e.g., [56–58,60]). In this model, we define the following parameters,

- P_{PT}: power consumption of processing elements during data transmission.

- P_{PR}: power consumption of processing elements during data reception.

- P_{CT}: power consumption of the transmission circuit (IF and RF parts without the PA).

- P_{CR}: power consumption of the receiving circuit (IF and RF parts).

- P_{LNA}: power consumption of the LNA.

- P_{PA}: power consumption of the PA.

- $P(d)$: Transmission power of the device (output power of the PA) which could be a function of the distance to the receiving node d.
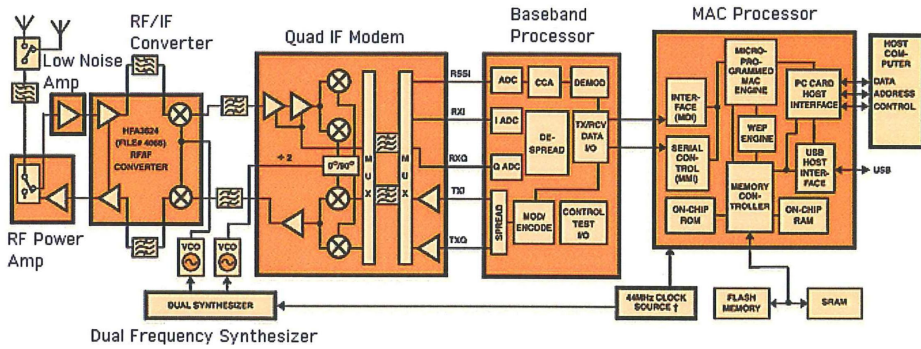
(a) PRISM I
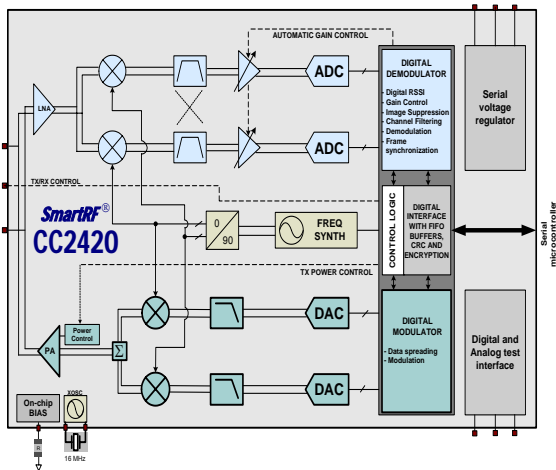
(b) CC2420 (T-mote)
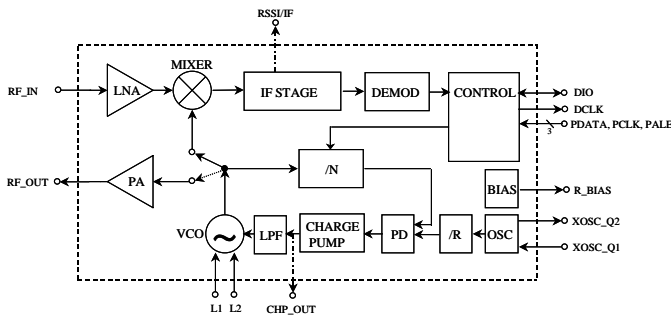
(c) CC1000

Figure 3.1 – Internal block diagram of three commercial chipsets [61–63].
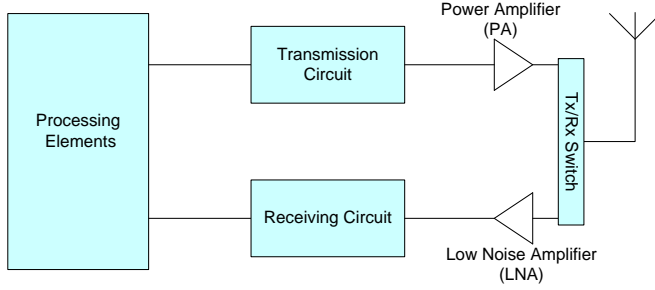
Figure 3.2 – General structure of a transceiver.

- $\kappa = \frac{P(d)}{P_{PA}}$: power efficiency of the PA.

Given these parameters, the power consumption of a device during packet transmission and reception can be computed as follows:

$$P_T = P_0 + \frac{P(d)}{\kappa}$$
$$P_R = P_{PR} + P_{CR} + P_{LNA}$$

$$(3.1)$$

where $P_0 = P_{PT} + P_{CT}$.

3.2 Energy Consumption for Single Transmission and Reception of a Packet

Suppose that node u wants to transmit a packet of length L bits to its neighbor v. Without loss of generality, we assume all nodes use the same transceiver chipset. Thus, their power consumption profiles are the same. The only thing which could differ from one node to another node is the transmission power. In wireless multi-hop networks, nodes might be able to adjust their transmission power according to the distance to their neighbors. This is known as *transmission power control* which will be discussed in the next section in detail. For the time being, we assume that $P_{u,v} = P(d_{u,v})$ is the transmission power from node u to node v. Therefore, the consumed energy by u during transmission of the packet to v is:

$$E_T(u, v, L) = P_T \times T$$
$$= \left(P_0 + \frac{P_{u,v}}{\kappa} \right) \frac{L}{r}$$

$$(3.2)$$

in which T is the time required to transmit L bits with the rate r bits/sec. Similarly, the consumed energy by v to receive a packet from u is:

$$
\begin{aligned}
E_R(u, v, L) &= P_R \times T \\
&= P_R \frac{L}{r} \\
&= \epsilon_r L
\end{aligned}
\tag{3.3}
$$

where we define $\epsilon_r = P_R/r$ (Joule/bit) as the energy consumed to receive one bit.

3.3   Impact of Transmission Power Control on Energy Consumption

Transmission power control (TPC) [64–68] is a well-accepted technique in wireless multi-hop networks to save energy. Nodes reduce their power to spend less energy for packet transmission to their neighboring nodes. Reducing the transmission power of nodes can also increase the network capacity due to reduced interference [69, 70]. In the design and evaluation of energy-aware communication schemes, we assume nodes can deploy TPC as defined bellow:

Definition 1. *TPC: Given the data transmission rate r, a sending node keeps its transmission power to the receiving node as low as required to satisfy a target BER requirement.*

To satisfy the target BER requirement, the average received signal to noise and interference ratio (SINR) must be above a threshold. This threshold depends on the modulation and channel coding schemes deployed by the wireless interface. According to path-loss fading model, if node u transmits signals with power $P_{u,v}$ to node v, the average received power by node v is:

$$
P_{rx_{u,v}} = cP_{u,v}d_{u,v}^{-\eta}
\tag{3.4}
$$

in which c is a constant which depends on the wavelength and the receiving and the transmitting antenna gains. Let γ_{min} be the average SINR required for having the target BER at the receiving node, and $\mathcal{N}$ be the noise and interference power. We need to have:

$$
\frac{c}{\mathcal{N}} P_{u,v} d_{u,v}^{-\eta} \geq \gamma_{min}.
\tag{3.5}
$$

The minimum transmission power required to satisfy the target BER requirement at the receiver is then:

$$
P_{u,v} = c_n d_{u,v}^{\eta},
\tag{3.6}
$$

where c_n is defined as $c_n = \frac{\mathcal{N}\gamma_{min}}{c}$.

We can normalize (3.6) with respect to c_n. To this end, we determine the adjusted transmission power when the receiver is at a reference distance d_0. Assume P_{ref} is the minimum transmission power such that the target BER requirement is satisfied at the reference distance d_0 from the sender. According to (3.6), we have

$$P_{ref} = c_n d_0^{\eta}.$$

The adjusted power for signal transmission from u to v is then obtained as follows:

$$P_{u,v} = P_{ref} \left(\frac{d_{u,v}}{d_0} \right)^{\eta}. \tag{3.7}$$

The reference distance d_0 is usually considered to be $1\,\mathrm{m}$ for indoor environments and $1\,\mathrm{km}$ for outdoor environments.

If we replace $P_{u,v}$ from (3.7) into (3.2), the energy consumption during packet transmission can be expressed as:

$$
\begin{aligned}
E_T(u,v,L) &= \left(P_0 + \frac{P_{ref}}{\kappa} \left(\frac{d_{u,v}}{d_0} \right)^{\eta} \right) \frac{L}{r} \\
&= \left(\alpha + \beta d_{u,v}^{\eta} \right) L,
\end{aligned}
\tag{3.8}
$$

where we define $\alpha = P_0/r$ and $\beta = P_{ref}/(\kappa d_0^{\eta})$. Parameter β is completely dependent on the environment that the network is deployed. This dependency is due to the dependency of P_{ref} and the path-loss exponent on the environment. The transmission power P_{ref} must be measured in the environment where the network is deployed. In other words, to compute β, we need to measure P_{ref} when the receiver is located at the reference distance d_0. Nevertheless, alternatively we can set P_{ref} to its maximum value P_{max} (maximum transmission power of nodes), and measure the distance d_0 from the sender at which the target BER requirement is satisfied. Let us define the transmission range of a node as follows:

> *the maximum distance from the node at which the target BER require-*
> *ment is satisfied in the network deployment environment, when the node*
> *transmits with the maximum transmission power P_{max}.*

With this definition, we obviously have $d_0 = D_{max}$ (the common transmission range of nodes). Therefore, β could alternatively be computed as:

$$\beta = \frac{P_{max}}{\kappa D_{max}^{\eta}}. \tag{3.9}$$

For the sake of completeness, we also consider the case when nodes are not able to adjust their transmission power according to the distance. In such a case, each node always transmits packets with its maximum transmission power.

Table 3.1 – Energy consumption parameters of commercial products. Data has been extracted from [61–63].

	CC2420 (IEEE 802.15.4)	CC1000 (868 MHz)	PRISM I (IEEE 802.11b)
P_0 [mW]	26.5	15.9	1400
P_R [mW]	59.1	22.2	1320
P_{max} [mW]	1	5	50
κ	3.7%	6.4%	10.2%
r	250 [Kbps]	76.8 [Kbps]	11 [Mbps]
D_{max} [m]	50	50	150
α [nJ/bit]	2.4	1.44	127
β [fJ/bit/m$^\eta$] ($\eta = 3$)	864	8138	13.2
ϵ_r [μJ/bit]	0.23	0.29	1.2
ϵ_t [μJ/bit]	2.14	1.22	0.57

That is, $P_{u,v} = P_{max}, \forall(u,v) \in \mathbb{E}$. Therefore, the energy consumption for packet transmission without TPC will be as follows:

$$E_T(u, v, L) = \left(P_0 + \frac{P_{max}}{\kappa} \right) \frac{L}{r}$$
$$= \epsilon_t L, \tag{3.10}$$

where we define $\epsilon_t = (P_0 + \frac{P_{max}}{\kappa})/r$ [J/bit] as the amount of energy required to transmit one bit of the packet with the maximum power. We have shown values of energy consumption parameters of our model for some commercial products in Table 3.1.

Note that if TPC is supported, the BER remains constant even if the distance to the receiver changes. Nevertheless, when TPC is not supported, the BER reduces if the distance between the transmitter and the receiver reduces. This is due to path loss experienced by electromagnetic waves, which results in increased received signal strength at shorter distances from the receiver. We should emphasize here that adjusting the transmission power to distance is subject to keeping the data transmission rate over wireless channels constant.

3.4 Impact of MAC Layer on Energy Consumption

ARQ mechanism of the MAC layer affects the total amount of energy that two nodes consume to exchange a packet. As mentioned in the previous chapter, some MAC

protocols support ARQ. That is, a lost packet is transmitted several times by the sender until the receiver receives a packet without errors. Thus, the actual energy consumed to exchange a packet between two nodes includes the energy consumed during retransmissions.

Let $\mathcal{X}_{u,v} \in \{1, 2, ..., M\}$ be the number of times that the packet is transmitted by u to v, including the first transmission, and $\mathcal{Y}_{v,u} \in \{0, 1, 2, ..., M\}$ be the number of acknowledgments transmitted by v for the packet. The value of $\mathcal{X}_{u,v}$ and $\mathcal{Y}_{v,u}$ depends on the quality of the forward link (u, v) and the quality of the reverse link (v, u). We will later determine $\Pr\{\mathcal{X}_{u,v} = m\}$, $\forall m \in \{1, 2, ..., M\}$, and $\Pr\{\mathcal{Y}_{v,u} = m\}$, $\forall m \in \{0, 1, 2, ..., M\}$.

Let L_d (bits) denote the size of the data packet transmitted from the transmitter to the receiver, and L_a (bits) denote the size of the acknowledgment. Without loss of generality, we assume that data packets and acknowledgments are transmitted with the same rate r[1]. For the time being, we also assume that the energy consumed by the receiver for receiving and decoding a corrupted packet is the same as the energy consumed for receiving an error-free packet. In Section 3.5, we will verify this assumption. With these assumptions, the total consumed energy by the transmitter to deliver the packet to the receiver is:

$$\mathcal{E}_T(u, v, L_d) = \mathcal{X}_{u,v} E_T(u, v, L_d) + \mathcal{Y}_{v,u} E_R(v, u, L_a). \tag{3.11}$$

If we replace $E_T(u, v, L_d)$ from its definition given in (3.8) and $E_R(v, u, L_a)$ from its definition given in (3.3), then we have:

$$\mathcal{E}_T(u, v, L_d) = \mathcal{X}_{u,v} \left(\alpha + \beta d_{u,v}^{\eta} \right) L_d + \mathcal{Y}_{v,u} \epsilon_r L_a. \tag{3.12}$$

The total energy consumed by the receiver to receive the packet is:

$$\mathcal{E}_R(u, v, L_d) = \mathcal{X}_{u,v} E_R(u, v, L_d) + \mathcal{Y}_{v,u} E_T(v, u, L_a). \tag{3.13}$$

If we replace $E_R(u, v, L_d)$ and $E_T(v, u, L_a)$ from their respective definitions, we can express (3.13) alternatively as follows:

$$\mathcal{E}_R(u, v, L_d) = \mathcal{X}_{u,v} \epsilon_r L_d + \mathcal{Y}_{v,u} \left(\alpha + \beta d_{u,v}^{\eta} \right) L_a. \tag{3.14}$$

Since values of $\mathcal{X}_{u,v}$ and $\mathcal{Y}_{v,u}$ depend on quality of links, the total consumed energy by nodes to exchange a packet over a wireless link depends on quality of links as well. Furthermore, due to the random nature of these two values, the energy consumption of the sender and the receiver are random variables too. Thus, we may even face a situation in which the receiver consumes more energy than the sender to exchange a packet over a wireless link.

---

[1] Wireless technologies may use different rates for data traffic and acknowledgments (e.g., IEEE 802.11b/g/n).

From (3.12) and (3.14), the expected amount of energy consumed by the sender and the receiver is obtained as follows:

$$
\begin{aligned}
\bar{\mathcal{E}}_T(u, v, L_d) &= \bar{\mathcal{X}}_{u,v} \left(\alpha + \beta d_{u,v}^{\eta} \right) L_d + \bar{\mathcal{Y}}_{v,u} \epsilon_r L_a \\
\bar{\mathcal{E}}_R(u, v, L_d) &= \bar{\mathcal{X}}_{u,v} \epsilon_r L_d + \bar{\mathcal{Y}}_{v,u} \left(\alpha + \beta d_{u,v}^{\eta} \right) L_a,
\end{aligned}
\tag{3.15}
$$

in which $\bar{x}$ is the expected value of x. To determine $\bar{\mathcal{E}}_T(u, v, L_d)$ and $\bar{\mathcal{E}}_r(u, v, L_d)$, we need to determine the expected values of $\mathcal{X}_{u,v}$ and $\mathcal{Y}_{v,u}$.

3.4.1 Expected Transmission Attempts of Data Packets

A packet will be transmitted m times if the packet itself or its acknowledgment is lost in the last $m - 1$ transmission attempts. Therefore,

$$
\Pr\{\mathcal{X}_{u,v} = m\} = \begin{cases} (1 - pq)^{m-1} pq, & m = 1, ..., M - 1, \\ (1 - pq)^{M-1}, & m = M, \end{cases}
\tag{3.16}
$$

where $p = p_{u,v}(L_d)$ is the packet delivery ratio (PDR) of (u, v) for a packet of size L_d bits, and $q = p_{v,u}(L_a)$ is the PDR of (v, u) for an acknowledgment of size L_a bits.

Figure 3.3 shows $\Pr\{\mathcal{X} = m\}$ for various values of p, q, and M. Plots depicted in Figure 3.3 have been obtained assuming q is greater than p, because acknowledgment packets are usually smaller than data packets. Thus, the error probability for acknowledgment packets is likely smaller than the error probability for data packets. The figure verifies that if the quality of the link is low ($p = 0.25$ and $q = 0.4$), the probability of transmitting a packet M times is much higher than the probability of transmitting a packet $m < M$ times. Nevertheless, when the quality of the link is good ($p = 0.85$ and $q = 1$), the probability of transmitting a packet once is the dominant value.

The expected value of $\mathcal{X}$ can be calculated as follows:

$$
\begin{aligned}
\bar{\mathcal{X}}_{u,v} &= M(1 - pq)^{M-1} + \sum_{m=1}^{M-1} mpq(1 - pq)^{m-1} \\
&= \frac{1 - (1 - pq)^M}{pq}.
\end{aligned}
\tag{3.17}
$$

To derive (3.17), we used $\sum_{m=1}^{n} z^m = z\frac{1-z^n}{(1-z)^2} - \frac{nz^{n+1}}{1-z}$ considering $z = 1 - pq$ and $n = M - 1$. Note that if there is no limitation on the number of transmission attempts (i.e., $M \to \infty$), then $\bar{\mathcal{X}} \to \frac{1}{pq}$. This implies that the following inequality is true for any limited value of M:

$$
\bar{\mathcal{X}}_{u,v} \leq \frac{1}{pq} \quad \forall M > 0.
\tag{3.18}
$$
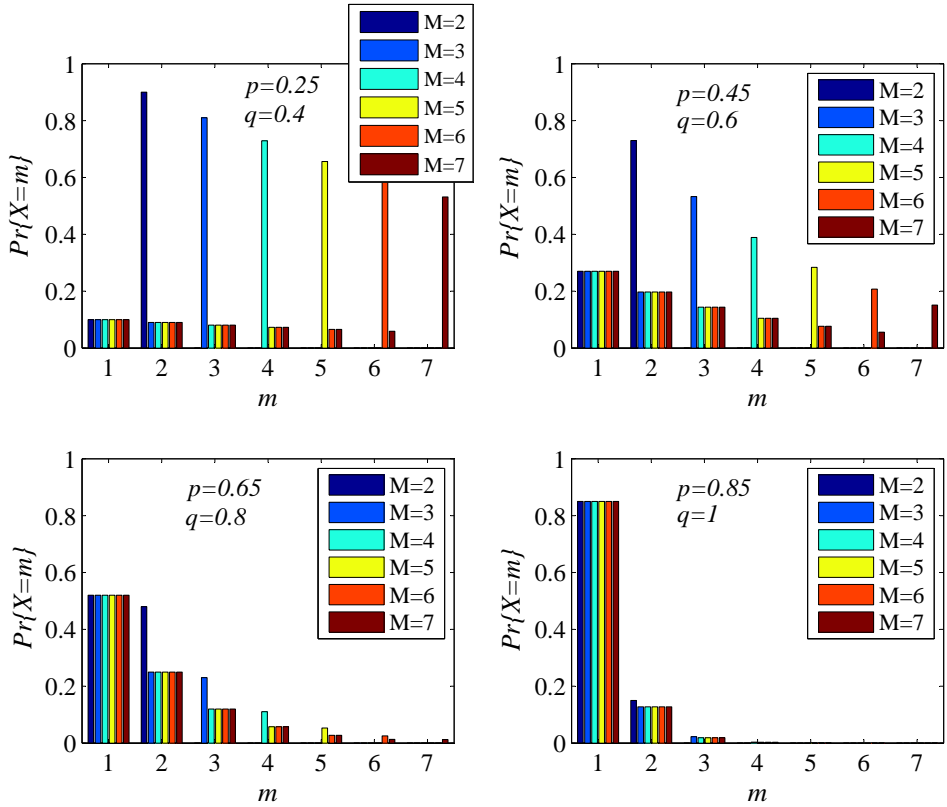
Figure 3.3 – Probability of transmitting a data packet m times.

Figure 3.4 shows $\bar{\mathcal{X}}$ for various values of M. We can see that for relatively high values of M ($M \geq 4$), the upper bound in (3.18) is a tight bound when the PDR of the link is greater than 0.5.

3.4.2 Expected Transmission Attempts of Acknowledgments

If a data packet is lost during all possible transmission attempts, no acknowledgment will be transmitted for it. Thus, $\Pr\{\mathcal{Y}_{v,u} = 0\} = (1-p)^M$. On the other hand, an acknowledgment will be transmitted M times for a data packet, if the data packet is received correctly in every transmission attempt, but all $M-1$ acknowledgments transmitted for it are lost. Therefore, $\Pr\{\mathcal{Y}_{v,u} = M\} = p^M(1-q)^{M-1}$.

To calculate the probability of transmitting $0 < m < M$ acknowledgments for a data packet, we should notice that an acknowledgment is transmitted only when the data packet is received correctly. Of course, a packet might be received correctly after a number of transmission attempts. If the acknowledgment transmitted for the packet is lost, the sender will retransmit the packet. This could be detected after expiration of a timer. If the data packet is again received correctly after a number of attempts, another acknowledgment will be transmitted.

Here, we consider two possible cases. In the first case, the Mth transmission of the data packet never happens, because the sender receives an acknowledgment for the packet before reaching the maximum transmission attempts M. In such a case, $m-1$ out of the first $n-1$, $\forall n \in \{m, m+1, m+1, ..., M-1\}$, transmission attempts of the data packet could be successful, but all $m-1$ acknowledgments transmitted for it should be lost. The mth transmission of the data packet must be successful as well, and its acknowledgment must also be received successfully. The probability of this event is:

$$A_1 = \sum_{n=m}^{M-1} \binom{n-1}{m-1} p^{m-1}(1-q)^{m-1}(1-p)^{n-1-(m-1)}pq.$$

In the second case, the sender transmits the data packet M times, because it has not received an acknowledgment after $M-1$ attempts. Here, we face with two subcases. In the first subcase, $m-1$ out of the first $M-1$ transmission attempts of the packet are successful, but all its $m-1$ acknowledgments are lost. The Mth transmission attempt of the packet is also successful, which triggers transmission of the mth acknowledgment. The probability of this event is:

$$A_2 = \binom{M-1}{m-1} p^{m-1}(1-p)^{M-1-(m-1)}(1-q)^{m-1}p.$$

In the second subcase, m out of the first $M-1$ transmission attempts of the packet are successful, but all m acknowledgments transmitted for it are lost. The Mth
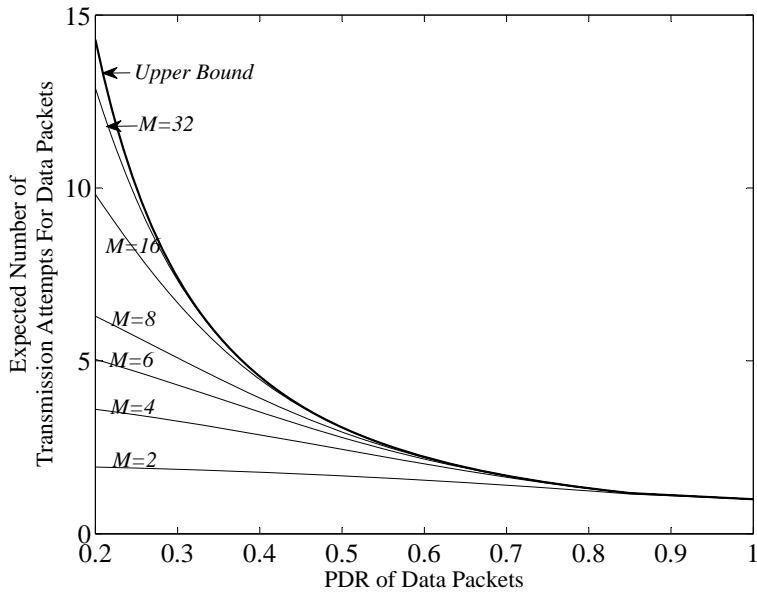
Figure 3.4 – Expected number of transmission attempts of a data packet
$\bar{\mathcal{X}}$ as a function of the PDR of the link. Since data packets are larger than
acknowledgments, we have assumed (for the sake of simplicity) that $p = q + t$.
Here, t is set to 0.15 except that $t = 0$ when $q = 1$. The upper bound is as
expressed in (3.18).

transmission attempt of the packet fails, which prevents transmission of another acknowledgment. The probability of this event is:

$$A_3 = \binom{M-1}{m} p^m (1-p)^{M-1-m} (1-q)^m (1-p).$$

The probability of transmitting $1 \leq m \leq M-1$ acknowledgments for the packet is then $= A_1 + A_2 + A_3$. In summary, we have:

$$\Pr\{\mathcal{Y}_{v,u} = m\} = \begin{cases} (1-p)^M, \ m = 0; \\\\ \sum_{n=m}^{M-1} \binom{n-1}{m-1} p^m (1-q)^m (1-p)^{n-m} \\ + \binom{M-1}{m-1} p^m (1-p)^{M-m} (1-q)^{m-1} \\ + \binom{M-1}{m} p^m (1-p)^{M-m} (1-q)^m, \ \ m = 1..M-1; \\\\ p^M (1-q)^{M-1}, \ m = M. \end{cases} \quad (3.19)$$

Figure 3.5 shows $\Pr\{\mathcal{Y}_{v,u} = m\}$ for various values of p, q, and M. We observe that as quality of the link improves, probability of transmitting one acknowledgment for a packet becomes much higher than the probability of transmitting no acknowledgment or more than one acknowledgment. When quality of link is low ($p = 0.25$ and $q = 0.4$) and M is not a very big value (here $M < 5$), there is a high probability that no acknowledgment is transmitted for the packet. This is due to the fact that the packet may not be received correctly within the limited transmission attempts.

Given p and q, we can compute the exact values of $\bar{\mathcal{Y}}_{v,u}$ for any value of M as follows:

$$\bar{\mathcal{Y}}_{v,u} = \sum_{m=0}^{M} m \Pr\{\mathcal{Y}_{v,u} = m\}. \quad (3.20)$$

Unfortunately, no closed-form expression could be found for $\bar{\mathcal{Y}}_{v,u}$ when M is finite. However, if there is no limitation on the number of transmission attempts of a packet ($M \to \infty$), we can find a closed-form expression. In such a case, a packet can be retransmitted as many times as required until the receiver receives the packet successfully. Hence, the expected number of times that an acknowledgment is transmitted for a packet is simply $\bar{\mathcal{Y}}_{u,v} = \frac{1}{q}$. As a result, the following inequality holds for any limited value of M:

$$\bar{\mathcal{Y}}_{v,u} \leq \frac{1}{q} \quad \forall M > 0. \quad (3.21)$$
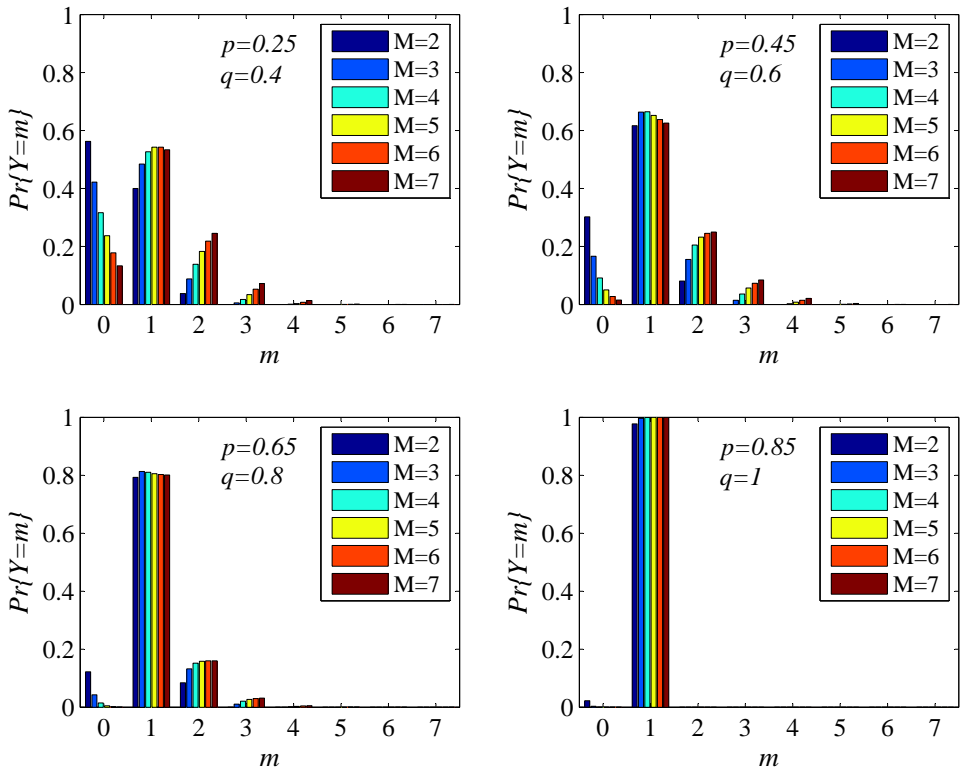
Figure 3.5 – Probability of transmitting m acknowledgments for a data packet.
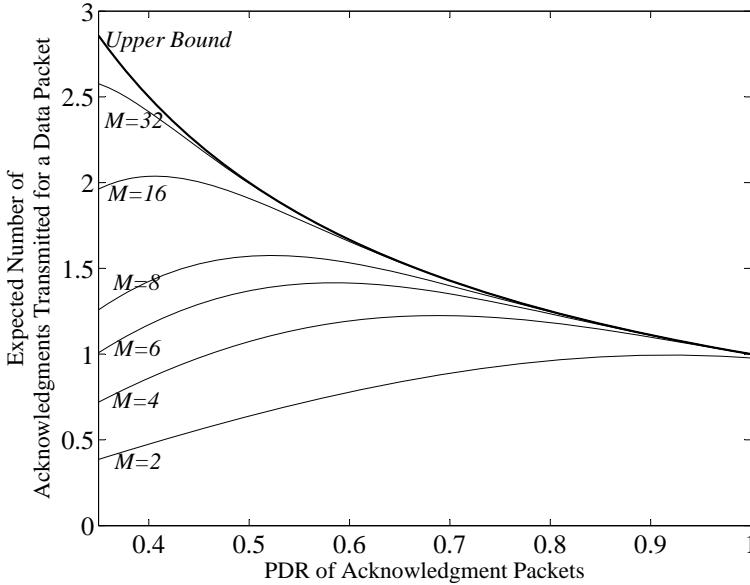
Figure 3.6 – Expected number of acknowledgments transmitted for a data packet $\bar{\mathcal{Y}}_{v,u}$ as a function of delivery probability of acknowledgments q. The upper bound is as expressed in (3.21)

The exact value of $\bar{\mathcal{Y}}_{v,u}$ and its upper bound have been plotted in Figure 3.6 for various values of M. We observe that the upper bound is a tight bound only if M is relatively a big value.

Using (3.15) and considering the two inequalities $\bar{\mathcal{X}}_{u,v} \leq \frac{1}{pq}$ and $\bar{\mathcal{Y}}_{v,u} \leq \frac{1}{q}$, the expected energy consumed by the sender and the receiver to exchange a packet over the wireless link is upper-bounded as:

$$
\begin{aligned}
\bar{\mathcal{E}}_T(u, v, L_d) &\leq \left(\alpha + \beta d_{u,v}^\eta\right) \frac{L_d}{pq} + \frac{\epsilon_r L_a}{q} \\
\bar{\mathcal{E}}_R(u, v, L_d) &\leq \frac{\epsilon_t L_d}{pq} + \left(\alpha + \beta d_{u,v}^\eta\right) \frac{L_a}{pq},
\end{aligned}
\tag{3.22}
$$

where the equality happens if M is unlimited.

It is clear that MAC level retransmission increases the total amount of energy consumed to exchange a packet over a wireless link. However, this provides a reliability gain, because a lost packet might be recovered during retransmissions. It is also possible that the packet is not recovered after several attempts. This of course depends on the quality of the link and the maximum number of transmissions allowed. When MAC level retransmission is supported, the reliability of a link is

the probability that the packet is ultimately delivered to the receiver before the number of allowed retransmissions is reached. That is:

$$R_{u,v}(L) = 1 - (1 - p_{u,v}(L))^M. \tag{3.23}$$

Here, we should notice that the reliability of a link is not affected by the probability of losing the acknowledgment. If the packet is received correctly but its acknowledgment is lost, the packet will be retransmitted. If the retransmitted packet is received correctly too, there will be a duplicate packet at the receiver. Duplicate packets are usually discarded silently, but acknowledgments are sent for them. Thus, to calculate the reliability of a link, we do not need to take into account the PDR of the reverse link for acknowledgment packets. This, however, affects the energy consumption of the transmitting and the receiving nodes, which was considered in computing their energy costs.

If MAC level retransmission is not supported, the reliability of the link is simply its PDR. That is:

$$R_{u,v}(L) = p_{u,v}(L). \tag{3.24}$$

3.5   Packet Delivery Ratio of Wireless Links

We observed that if MAC level retransmission is supported, the energy cost of nodes to exchange a packet over wireless links depends on the PDR of links between them. This relates the energy consumption of nodes to the quality of wireless links. In this section, we elaborate on the PDR of wireless links. To this end, we first study the format of a data and acknowledgment packets and the packet detection process at the receiver.

3.5.1   Packet Format and Experimental Results

In accordance with wireless standards such as IEEE 802.11b and IEEE 802.15.4, a packet transmitted on a physical link consists of a preamble for transmitter-receiver synchronization, physical layer (PHY) header, MAC header, data payload, and frame check sequence (FCS). The packet format has been shown in Figure 3.7. In this thesis, we refer to the packet length as the length of the entire packet including the header and the preamble. For a data packet, the data payload includes higher layer headers and the user data. For a MAC acknowledgment, the data payload length is zero. The FCS carries redundant bits for a cyclic redundancy check (CRC) which is used at the receiver to detect errors in the payload. Table 3.2 shows the size of different parts of a data and an acknowledgment packet in the IEEE 802.11b and 802.15.4 standards.

Table 3.2 – Length of preamble, physical layer header, and the payload for data packets and acknowledgments in IEEE 802.11b and IEEE 802.15.4 standards. All Values are per byte.

Standard	Packet Type	Preamble	PHY Header	MAC Header	FCS FCS	Data Payload	Packet Length
IEEE 802.11b (long preamble)	Data	24	24	30	4	0-2312	82-2394
IEEE 802.11 (long preamble)	MAC Ack.	24	24	14	4	0	66
IEEE 802.11b (short preamble)	Data	15	15	30	4	0-2312	64-2376
IEEE 802.11 (short preamble)	MAC Ack.	15	15	14	4	0	48
IEEE 802.15.4	Data	5	1	7-23	2	0-127	15-158
IEEE 802.15.4	MAC ACK	5	1	3	2	0	11

Preamble	PHY Header	MAC Header	Data Payload (including higher layers headers)	FCS

Packet Length
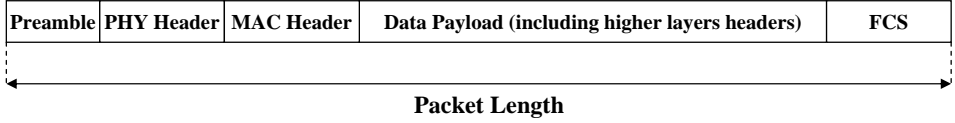
Figure 3.7 – Format of a packet transmitted over the physical link.

There could be four scenarios where a packet transmitted on a physical link is lost:

1. If the received power of the signal carrying the preamble is lower than the threshold required for detection, then the packet will not be detected at all.

2. If the receiver detects the preamble with an erroneous bit, then it will not continue detecting the rest of the packet.

3. When the preamble is detected error-free but the PHY header is detected with an erroneous bit, the receiver stops receiving the rest of the packet.

4. If both preamble and PHY header are detected error-free, the receiver detects the rest of the packet. However, if the packet failed to pass the CRC due to bit error, then the packet will be discarded (lost).

In the first scenario, a lost packet is not received at all. In the second and third scenarios, a lost packet is received partially. However, in the fourth scenario, a lost packet is received completely. Since the sizes of the preamble and the header are usually much smaller than the size of the rest of the packet, the probability that an error occurs in the preamble and in the header is much smaller. Thus, the receiver will continue to listen and receive (and decode) the rest of the packet. In other words, we can say that the probability that a lost packet is received completely is much higher than the probability that it is received partially. That is, we can assume that most lost packets are detected completely.

We have verified this fact using experimental results based on T-mote devices (the CC2420 chipset). To this aim, we programmed devices to report packets which do not pass the CRC. Only those which have not been detected at all due to lower received SNR or due to faulty synchronization are not reported. The receiver was placed at different distances from the sender to have different signal strengths. At each location, 100000 packets were transmitted by the sender, and the receiver counted both error-free received packets and CRC-failed packets. Figure 3.8 shows the measurement setup and Figure 3.9 shows the results.

As Fig. 3.9 shows, even if only 10% of the packets are received error-free, around 55% of them have been detected (correct reception or erroneous) for 25Byte packet sizes. This value is 65% for 115Byte packet sizes. That is, when practically there is

Figure 3.8 – Measurement setup.

no link between the two nodes due to high packet drop rate, many of the transmitted packets have been detected completely. When the quality of the link improves, the percentage of detected packets gets closer to 100%. For instance, in Fig. 3.9(b), when 65% of transmitted packets are received error free, 92% of them have been detected. Only 8% of them have not been detected at all (these packets are not even picked up by the PHY). Thus, if there is a link between two nodes with an acceptable quality, a high percentage of packets are detected completely. This means, the consumed energy for reception of lost packets is almost equal (on average) to the consumed energy for reception of error-free packets.

3.5.2 Mathematical Expressions

If we assume that bit errors occur independently from each other, we can calculate the PDR of a link for a packet of size L bits as follows:

$$p_{u,v}(L) = (1 - p_{c_{u,v}}(L))(1 - \delta_{u,v})^L \tag{3.25}$$

in which $\delta_{u,v}$ is the BER of the wireless link due to transmission errors caused by fading, and $p_{c_{u,v}}(L)$ is the collision probability of link (u, v). The assumption of having independent bit errors may not hold always in practice. When burst errors occur, bit errors are not independent anymore. Nevertheless, we can consider this model for calculating the PDR of a link as an acceptable model.
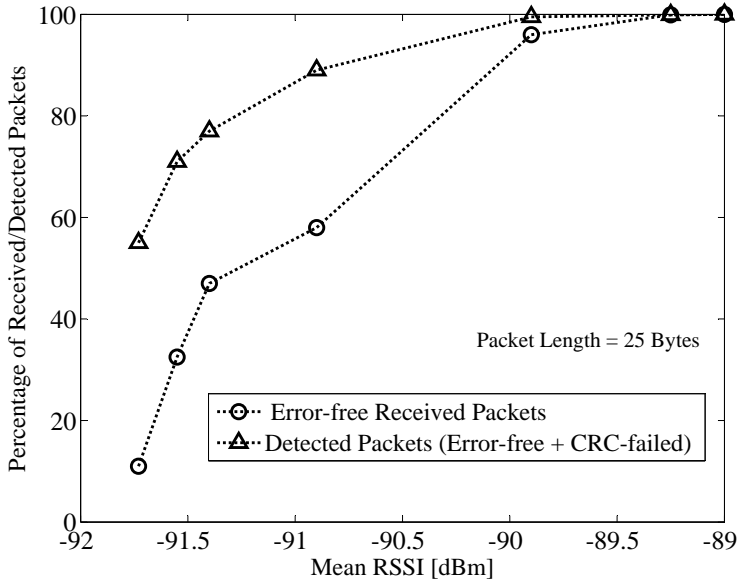
(a) 25 Byte packets
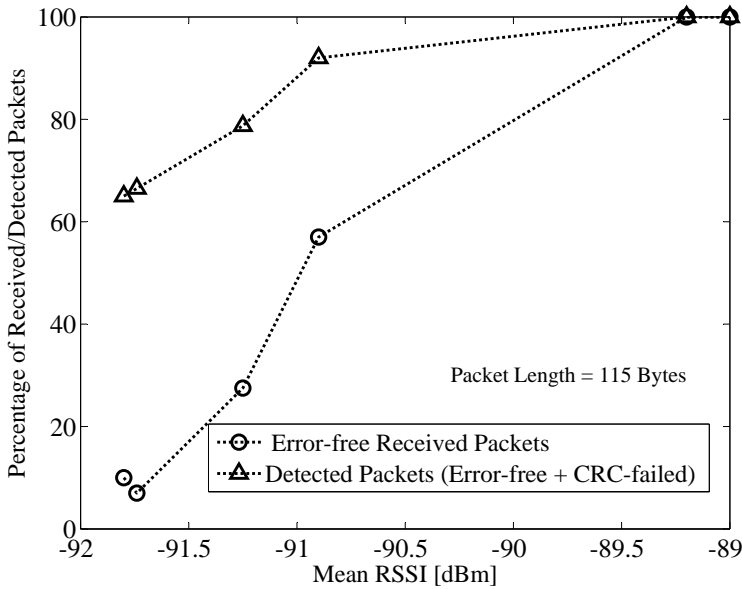
(b) 115 Byte packets

Figure 3.9 – Percentage of received and detected packets as a function of the mean received signal strength indicator (RSSI).

The BER of a link depends on modulation and channel coding schemes deployed at the physical layer and the type of the wireless channel. For instance, the BER for Q-ary CCK modulation over a slowly flat fading Rayleigh channel (no line-of-sight) is [71]:

$$\delta_{u,v} = \frac{2^{log_2(Q)-1}}{2^{log_2(Q)} - 1} \left(\sum_{i=1}^{Q-1} \frac{(-1)^{i+1} \binom{Q-1}{i}}{1 + i(1 + \bar{\gamma}_{u,v})} \right). \qquad (3.26)$$

The CCK modulation is used in the IEEE 802.11b standard to support 11 Mbps and 5.5 Mbps data rates. In (3.26), $Q = 8$ for 11 Mbps, and $Q = 4$ for 5.5 Mps. Furthermore, $\bar{\gamma}_{u,v}$ is the average received SNIR at node v when u transmits a packet. It is related to the transmission power $P_{u,v}$ as follows:

$$\bar{\gamma}_{u,v} = \frac{cP_{u,v}}{d_{u,v}^{\eta}\mathcal{N}}. \qquad (3.27)$$

For a slowly flat fading Rician channel (with line-of-sight), the probability of bit error for Q-ary CCK modulation is described as [71]:

$$\delta = \frac{2^{log_2(Q)-1}}{2^{log_2(Q)} - 1} \left(\sum_{i=1}^{Q-1} \frac{(-1)^{i+1} \binom{Q-1}{i}(1 + K)}{1 + K + i(1 + K + \bar{\gamma}_{u,v})} \right) \qquad (3.28)$$

where K represents the ratio between the direct-path (line-of-sight) power and the diffuse power.

As another example, we consider OQPSK modulation which is used in the IEEE 802.15.4 standard. The BER of OQPSK modulation over a slowly flat fading Rayleigh fading channel is [72]

$$\delta_{u,v} = \frac{1}{2(1 + \bar{\gamma}_{u,v})} \qquad (3.29)$$

and over a slowly flat Rician fading channel is

$$\delta_{u,v} = \frac{1}{2(1 + K + \bar{\gamma}_{u,v})}. \qquad (3.30)$$

3.6   Simulation Studies

In this section, we present simulation results to show quantitatively the impact of MAC level retransmission and transmission power control on energy consumption of nodes. We also use simulation results to show the significance of our model

compared to similar models from the literature. We developed a generic simulation platform for our experiments. See [73] for the ANSI C implementation. We emphasize here that since we attack various issues across many layers of the communication stack, it was indeed helpful to develop our own simulation model. In the following chapters as and when we introduce more mechanisms and algorithms, we incorporated them in the same model to take into effect all the proposed mechanisms together.

3.6.1   Effect of MAC Level Retransmissions

In the first experiment, we compare energy consumption per packet when MAC level retransmission is supported and when MAC level retransmission is not supported. In this experiment, the receiver is located at the border of the transmission range. Simulation parameters correspond to the data of the CC2420 and PRISM chipsets (see Table 3.1).

As Figure 3.10 shows, for both chipsets, if the packet size increases, retransmissions due to packet loss can significantly increase the total energy consumed by a sender and a receiver. For the CC2420 chipset, the total consumed energy for packets of length 155 Byte increases around 63%, if MAC level retransmission is supported. For the PRISM chipset, it increases around 272% for packets of length 2364 Byte. This shows that MAC level retransmissions (and eventually link quality) have a big impact on the energy consumption of nodes. Neglecting this effect in any energy consumption model (e.g., similar to [56–59]) can result in sub-optimum design of energy-efficient communication schemes for wireless networks. Figure 3.10 also shows that there is a good match between simulation values and theoretical values predicted by our model.

Results depicted in Figure 3.11 show that MAC retransmission provides a reliability gain, because a lost packet might be recovered during retransmissions. Here, we have assumed that the BER of the link, i.e., δ, is 3.2×10^{-4} for the CC2420 chipset and 6.4×10^{-5} for the PRISM chipset. The PDR of the link for a given packet length has been calculated using (3.25) assuming $p_c(L) = 0$. The default value of the number of transmission attempts is 7 for the PRISM chipset (IEEE 802.11b standard) and 4 for the CC2420 chipset (IEEE 802.15.4 standard).

3.6.2   Effect of Transmission Power Control

TPC can reduce the transmission power of nodes. On the other hand, without power adjustment, nodes transmit with the maximum power. If a node transmits with its maximum power to any of its neighbors, it consumes more energy for packet transmission. Nevertheless, this can increase the PDR of links, since the received signal power increases at the receiver. If MAC level retransmission is supported, a

(a) CC2420 chipset
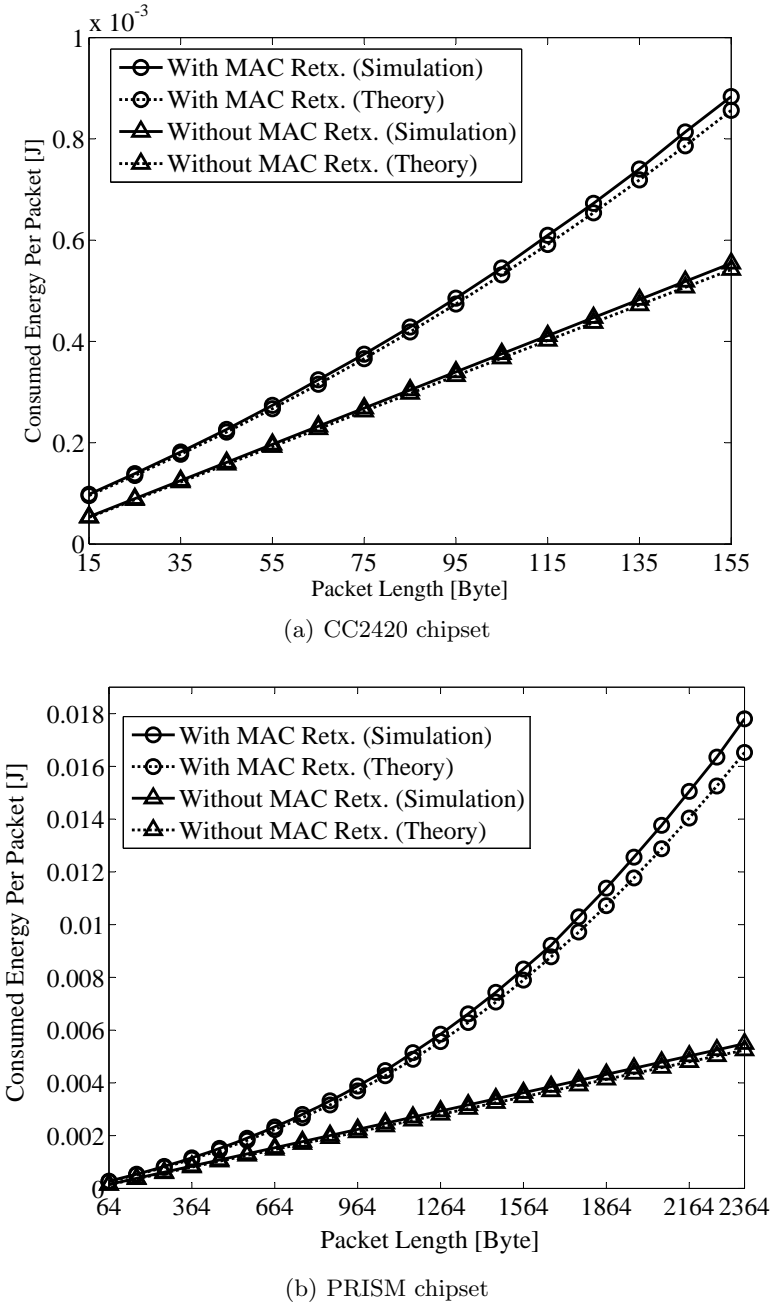
(b) PRISM chipset

Figure 3.10 – Total energy consumed by a sender and a receiver to exchange a packet over a wireless link as predicted by our mathematical model and simulations.
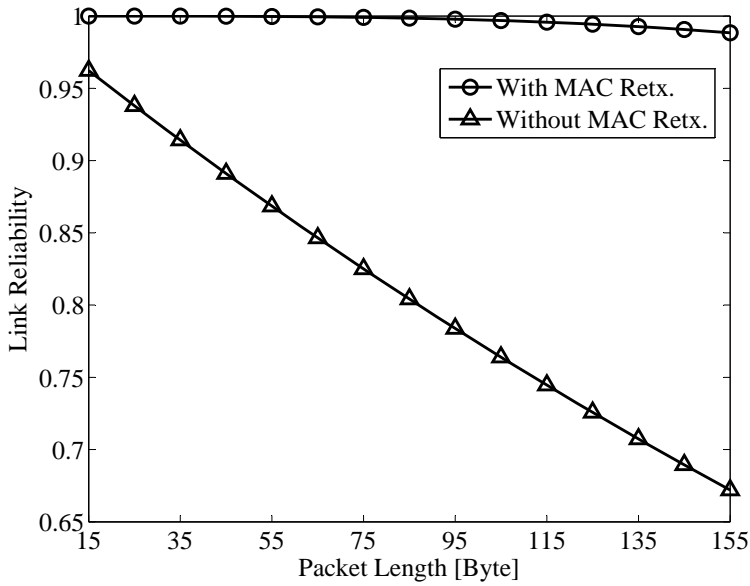
(a) CC2420 chipset
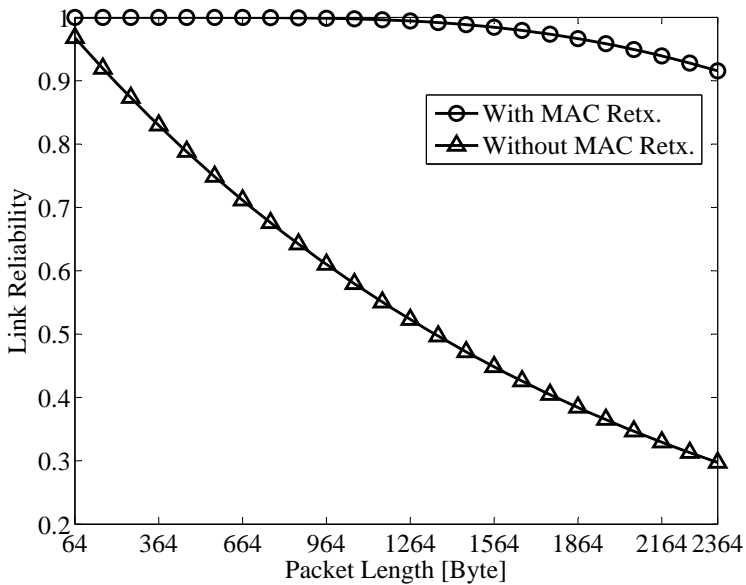
(b) PRISM chipset

Figure 3.11 – Link reliability in terms of the packet length for the CC2420 and the PRISM chipsets.

(a) CC2420 chipset

(b) PRISM chipset
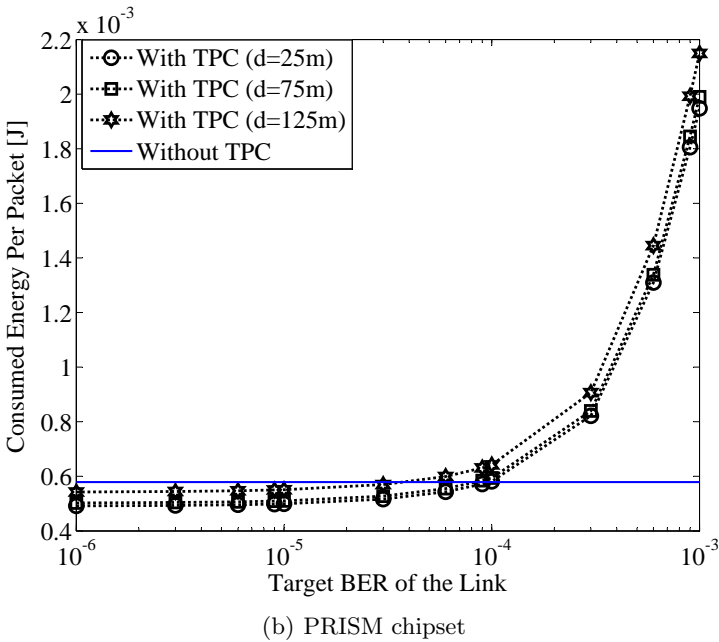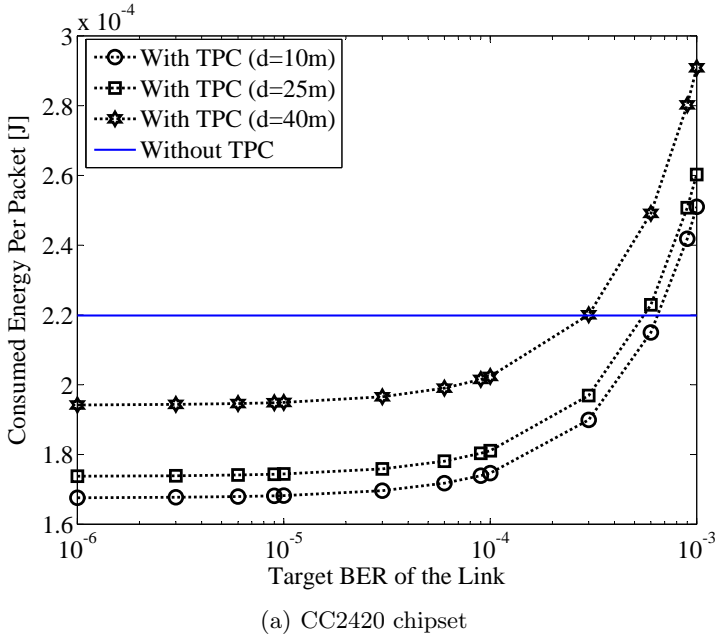
Figure 3.12 – Total energy consumed to exchange a packet over a wireless link as a function of the target BER of the link when MAC level retransmissions are supported.

consequence of having increased PDR is having less retransmissions. As a result, the overall energy consumption of nodes may even be reduced if TPC is not supported. The target BER requirement for which the transmission power is adjusted is critical here. We can observe in Figure 3.12 that if the target BER for TPC is higher than a specific value, then the overall energy consumption with TPC is even higher than the case without TPC. As could be seen in Figure 3.12, this specific value of the target BER requirement depends on the energy consumption profile of the nodes, the distance between the transmitter and the receiver, the size of data packets, and the maximum number of allowed retransmissions. *As a conclusion, we can state that if MAC level retransmission is supported, then TPC can save energy only if it does not harm the PDR of the link.* Nevertheless, if MAC level retransmission is not supported, TPC can always save energy. This might however be at the cost of reduced reliability.

3.6.3   Comparison with Other Energy Consumption Models

In this experiment, we compare our model with other models used in the design of energy-efficient communication schemes for wireless ad hoc networks in [74–82]. In [74–76], only the transmission power of nodes over the air is considered as the dominant source of energy consumption. Neither the energy consumption of transceiver circuits nor the effect of MAC level retransmission is considered. We refer to this model as PAMAS [74]. The energy consumption model used in [77–81] only considers the effect of MAC level retransmission. It neglects the consumed energy by processing elements of transceivers. We refer to this model as MRPC [79]. The model used in [82] considers energy consumed by the processing elements of the receiver. However, it does not consider the effect of MAC level retransmissions. We refer to this model as MTTPR [82]. Figure 3.13 shows values predicted by our model and other models. It is clear that existing models are not very accurate compared to the model developed in this chapter especially when the packet size increases.

3.7   Summary

In this chapter, we presented a detailed analytical model for energy consumption of nodes for exchanging a packet over a wireless link. To develop the model, we considered many details such as the effect of retransmission of lost packets, the size of data packets and acknowledgments, the PDR of links, and TPC. We also formulated the TPC for adjusting output power according to the distance. We observed that when ARQ is supported by the MAC protocol, TPC can reduce the energy consumption of nodes, only if it does not increase the number of
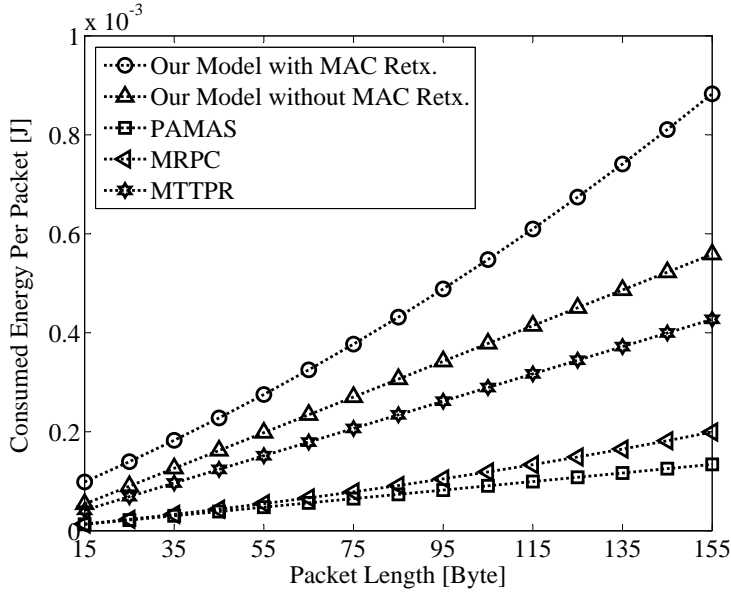
(a) CC2420 chipset
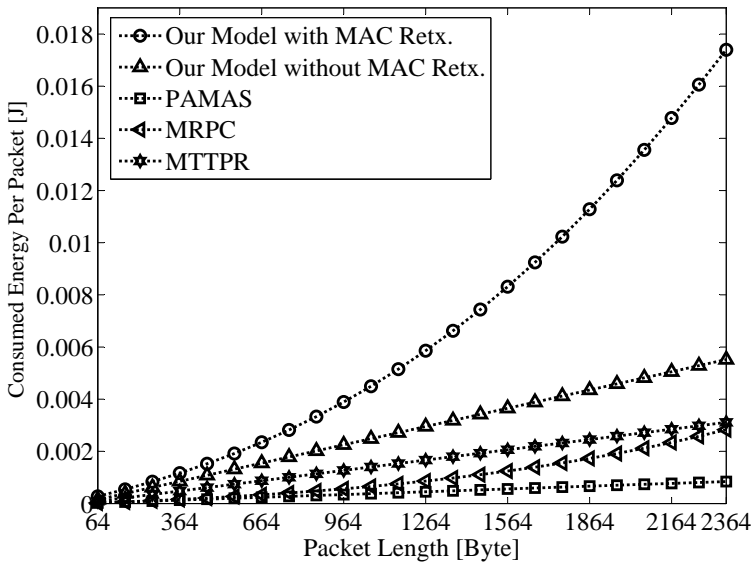
(b) PRISM chipset

Figure 3.13 – Total energy consumed by a sender and a receiver to exchange a packet over a wireless link as predicted by our model and models from the literature.

retransmissions. We used empirical results to show that most of the time, lost packets are detected completely, since most of the time packets are discarded due to CRC failure, which is performed on completely detected packets. Thus, the same amount of energy consumed to detect an error-free packet may be consumed to receive lost packets. Our simulation studies showed that the energy consumed by processing elements of a transceiver both during packet transmission and reception is quite considerable. Neglecting these sources of energy consumption can cause significantly sub-optimal designs for achieving energy-efficiency in wireless networks. The same is true regarding the impact of MAC level packet retransmission.

Chapter 4

Energy Cost for End-to-end Packet Traversal

Our goal in this chapter is to determine energy consumption in a wireless multi-hop network for end-to-end transmission of a packet from a source node to a destination node. We consider four types of packet transfer. These four types are various combinations of packet transmission with and without MAC retransmissions and with and without end-to-end retransmissions. We recall from the previous chapter that MAC retransmissions increase the reliability of packet transmission over wireless links. However, some MAC protocols may not support retransmissions of lost packet, or this option might have been disabled for particular applications. On the other hand, end-to-end retransmissions are supported by transport protocols (e.g., TCP) to ensure end-to-end reliability. Since the number of transmission attempts at the MAC layer could be limited, it is possible that the packet is lost during hop-by-hop transmission from the source to the destination. In such a case, the transport protocol triggers end-to-end retransmission of the lost packet. Nevertheless, there are some scenarios in which end-to-end retransmissions are not supported (e.g., UDP traffic).

Support for MAC and end-to-end retransmissions affect the total amount of energy consumed for transferring a packet from the source to the destination. By formulating this energy cost, we can design routing protocols which find energy-efficient routes between nodes. This is an issue which will be tackled in the next chapter. In this chapter, we mainly analyze and compare the energy consumption of nodes in the four possible types of packet transfer in wireless multi-hop networks. Our analysis in this chapter is on the basis of the detailed energy consumption model that we developed in the previous chapter. On the

basis of this model, we specify the minimum required energy for end-to-end packet traversal in wireless multi-hop networks.

This chapter is organized as follows: In Section 4.1, we explain the required preliminaries. In Section 4.2 and 4.3, we formulate energy consumption for packet traversal with and without end-to-end retransmissions, respectively. Then, in Section 4.4, we compare energy consumption in various types of packet transfer by analyzing the minimum required energy in each type. Section 4.5 presents simulation studies, and Section 4.6 summarizes the chapter.

4.1 Preliminaries

In this section, we introduce some notations and terms which are required in the rest of the chapter.

4.1.1 Link Level Energy Consumption

As introduced in the previous chapter, $\bar{\mathcal{E}}_T(u, v, L_d)$ denotes the expected amount of energy consumed by u to transmit a packet to v, and $\bar{\mathcal{E}}_R(u, v, L_d)$ denotes the expected amount of energy consumed by v to receive the packet from u. If MAC retransmission is supported $\bar{\mathcal{E}}_T(u, v, L_d)$ and $\bar{\mathcal{E}}_R(u, v, L_d)$ are calculated using (3.15):

$$
\begin{aligned}
\bar{\mathcal{E}}_T(u, v, L_d) &= \bar{\mathcal{X}}_{u,v} \left(\alpha + \beta d_{u,v}^{\eta} \right) L_d + \bar{\mathcal{Y}}_{u,v} \epsilon_r L_a \\
\bar{\mathcal{E}}_R(u, v, L_d) &= \bar{\mathcal{X}}_{u,v} \epsilon_r L_d + \bar{\mathcal{Y}}_{u,v} \left(\alpha + \beta d_{u,v}^{\eta} \right) L_a,
\end{aligned}
\tag{4.1}
$$

where $\bar{\mathcal{X}}_{u,v}(L_d)$ is the expected number of times that a data packet is transmitted by u to v, and $\bar{\mathcal{Y}}_{v,u}(L_a)$ is the expected number of acknowledgments transmitted for a data packet by v to u. If MAC retransmission is not supported, $\bar{\mathcal{E}}_T(u, v, L_d)$ and $\bar{\mathcal{E}}_R(u, v, L_d)$ are calculated as follows:

$$
\begin{aligned}
\bar{\mathcal{E}}_T(u, v, L_d) &= \left(\alpha + \beta d_{u,v}^{\eta} \right) L_d \\
\bar{\mathcal{E}}_R(u, v, L_d) &= \epsilon_r L_d.
\end{aligned}
\tag{4.2}
$$

Let us define $\bar{\mathcal{E}}(u, v, L_d)$ as the total energy consumed by u and v to exchange a packet of length L_d bits over the physical link (u, v). We simply have:

$$
\bar{\mathcal{E}}(u, v, L_d) = \bar{\mathcal{E}}_T(u, v, L_d) + \bar{\mathcal{E}}_R(u, v, L_d).
\tag{4.3}
$$

4.1.2 End-to-end Retransmission

We explained in the previous chapter that MAC retransmission is triggered when the sender does not receive the acknowledgment from the receiver within a predefined period. End-to-end retransmission is triggered using the same mechanism, but in

an end-to-end way. The destination node sends an end-to-end acknowledgment to the source node when it receives the packet correctly. If the source node does not receive an acknowledgment from the destination, it retransmits the packet. This may happen either because the packet is lost during its transmission from the source to the destination, or because the acknowledgment is lost during transmission from the destination to the source. There are several ways for issuing end-to-end acknowledgments. We introduce them briefly.

4.1.2.1   Per Packet Acknowledgment

In this scheme, an end-to-end acknowledgement is transmitted for each packet. The next packet is transmitted by the source node, only when it has already received an acknowledgment from the destination node for the previously transmitted packet. This is a well-accepted scheme by the community working on wireless ad hoc networks [60, 77–81]. It could be implemented in tiny devices with low data rates, since it is a low complexity scheme. However, it is not a very efficient technique for high data rate applications.

4.1.2.2   Cumulative Acknowledgments

This scheme is used in TCP. In this scheme, one acknowledgement can confirm the reception of several packets by indicating the sequence number of the last correctly received packet. An acknowledgment packet can acknowledge up to W packets, where W is the transmission window size at the source node. The transmission window size specifies the maximum number of packets which could be transmitted by the source node waiting to be acknowledged by the destination. If the timer at the source node expires before reception of an acknowledgment, it will retransmit all packets whose sequence numbers are higher than the sequence number of the last acknowledged packet. Thus, unnecessary transmissions could happen, which is the main drawback of this scheme. Furthermore, correctly received packets with a sequence number higher than the sequence number of a lost packet can not be acknowledged until the lost packet is acknowledged. To mitigate this problem, selective acknowledgement has been proposed to be used in TCP [83]. With selective acknowledgments, the destination informs the source node about all packets that have been received successfully. Therefore, the sender retransmits only the packets that have actually been lost. The selective acknowledgment is sent in a cumulative way again. However, the sequence number of the lost packets is also mentioned in addition to the sequence number of the last packet that has been received successfully.

To analyze the energy cost for end-to-end packet traversal, we assume, similar to [60, 77, 78], that end-to-end acknowledgments are sent per packet. Since

wireless links are usually unreliable and introduce errors, transmission of cumulative acknowledgments may introduce excessive delays. Furthermore, the energy cost when per packet acknowledgments are used upper-bounds the energy cost when selective acknowledgments are transmitted in a cumulative way.

4.2 Energy Cost without End-to-end Retransmissions

We denote $\mathcal{C}(\mathcal{P}(n_1, n_{h+1}))$ as the expected amount of energy consumed for end-to-end packet traversal through a path $\mathcal{P} = \{n_1, n_2, ..., n_h, n_{h+1}\}$ from the source node n_1 to the destination node n_{h+1}. Since each packet is transmitted by the source node once, $\mathcal{C}(\mathcal{P}(n_1, n_{h+1}))$ is the summation of the expected amount of energy consumed by each node along the path. Here, we should notice that a packet could be lost while it is being transferred to the destination. This means, the remaining nodes of the path may not consume energy to forward a particular packet. This fact brings the reliability of the path into the picture for computing the energy cost.

Let $R_{n_i}(L_d)$ denote the end-to-end reliability of the path up to node n_i, $i = 1, ..., h + 1$, for data packets of length L_d bits. $R_{n_i}(L_d)$ is defined as:

$$R_{n_i}(L_d) = \begin{cases} 1, & i = 1 \\ \prod_{k=1}^{i-1} R_{n_k, n_{k+1}}(L_d), & i = 2, ..., h+1, \end{cases} \tag{4.4}$$

where $R_{n_k, n_{k+1}}(L_d)$ is the reliability of link $(n_k, n_{k+1}) \in \mathcal{P}$ for packets of length L_d bits, which is computed as:

$$R_{n_k, n_{k+1}}(L_d) = \begin{cases} p_{n_k, n_{k+1}}(L_d), & \text{no MAC Retx.} \\ 1 - \left[1 - p_{n_k, n_{k+1}}(L_d)\right]^M, & \text{with MAC Retx.} \end{cases} \tag{4.5}$$

The expected energy cost when end-to-end retransmission is not supported is as follows:

$$\mathcal{C}(\mathcal{P}(n_1, n_{h+1})) = \sum_{i=1}^{h} R_{n_i}(L_d) \bar{\mathcal{E}}(n_i, n_{i+1}, L_d), \tag{4.6}$$

where $\bar{\mathcal{E}}(n_i, n_{i+1}, L_d)$ is the energy consumed to exchange the packet between n_i and n_{i+1} in the path. It is computed using (4.3).

4.3 Energy Cost with End-to-end Retransmissions

When end-to-end retransmission is supported, a data packet may be sent again by the source node, if the source node does not receive an acknowledgment from the

destination. We assume that the destination node uses the same route but in the reverse direction to send the acknowledgment to the source node. This we call the *reverse route*. The reverse route of $\mathcal{P}$ is denoted by $\mathcal{P}^{'}$, which consists of the same links as that of $\mathcal{P}$ but in the reverse direction. That is, if (n_k, n_{k+1}) is the kth link in $\mathcal{P}$, (n_{k+1}, n_k) is the $(h - k + 1)^{th}$ link in $\mathcal{P}^{'}$. Though it is possible that the forward and reverse paths could be different, we assume them being the same. This stem from the fact that most of the routing protocols select the reverse path to be consisting of nodes (links) in the reverse order. For instance, in reactive routing protocols such as DSR and AODV, RREP messages are transmitted to the source node using such a reverse path.

To determine the energy cost, we first consider a case in which MAC retransmission is not supported. In this case, the expected energy consumed for end-to-end traversal of a data packet is the expected amount of energy consumed during a single transmission from the source to the destination multiplied by the expected number of times that the source transmits the packet (including the first transmission). If L_e denotes size of the end-to-end acknowledgment, we have:

$$\mathcal{C}(\mathcal{P}(n_1, n_{h+1})) = F_{\mathcal{P}}(L_d) \sum_{i=1}^{h} \left[R_{n_i}(L_d) \bar{\mathcal{E}}(n_i, n_{i+1}, L_d) \right] +$$
$$B_{\mathcal{P}}(L_e) \sum_{i=1}^{h} \left[R^{'}_{n_{i+1}}(L_e) \bar{\mathcal{E}}(n_{i+1}, n_i, L_e) \right]. \tag{4.7}$$

in which $F_{\mathcal{P}}(L_d)$ is the expected number of times that a data packet of length L_d bits is transmitted from the source to the destination (including the first transmission), and $B_{\mathcal{P}}(L_e)$ is the expected number of times that an end-to-end acknowledgement of length L_e bits is transmitted by the destination for the data packet. Furthermore, $R^{'}_{n_{i+1}}(L_e)$ is the end-to-end reliability of the reverse path $\mathcal{P}^{'}$ from the destination node up to node n_{i+1}. $R^{'}_{n_i}(L_e)$, $i = 1, 2, ..., h + 1$, is computed as:

$$R^{'}_{n_i}(L_e) = \begin{cases} \prod_{k=i}^{h} R_{n_{k+1}, n_k}(L_e), & \forall i = 1, ..., h \\ 1, & i = h + 1, \end{cases} \tag{4.8}$$

where, $R_{n_{k+1}, n_k}(L_e)$ is the reliability of link $(n_{k+1}, n_k) \in \mathcal{P}^{'}$ for packets of length L_e bits. Since MAC retransmission is not supported, we have $R_{n_{k+1}, n_k}(L_e) = p_{n_{k+1}, n_k}(L_e)$.

Values of $F_{\mathcal{P}}(L_d)$ and $B_{\mathcal{P}}(L_d)$ depend on the reliability of forward path $\mathcal{P}$ for data packets and the reliability of reverse path $\mathcal{P}^{'}$ for end-to-end acknowledgments. Assuming there is no limitation on the number of retransmissions by the source node, $F_{\mathcal{P}}(L_d)$ and $B_{\mathcal{P}}(L_e)$ are computed as:

$$\begin{cases} F_{\mathcal{P}}(L_d) = \frac{1}{R_{n_{h+1}}(L_d) R^{'}_{n_1}(L_e)} \\ B_{\mathcal{P}}(L_e) = \frac{1}{R^{'}_{n_1}(L_e)}. \end{cases}$$

Now, we consider a case in which MAC retransmission is supported. In this case, we need to consider the dependency between the number of times that a packet is retransmitted by the source node and the number of times that a packet is retransmitted in each hop. Due to this dependency, $\mathcal{C}(\mathcal{P}(n_1, n_{h+1}))$ is not necessarily the multiplication of the expected energy consumed during a single transmission of the packet from source to destination and the expected number of times that a packet is transmitted by the source. However, if we assume that the maximum allowed transmission attempts in each physical link, M, is large enough and the quality of the link is good enough to ultimately have reliable links after possibly M transmissions, we can find an approximate expression for $\mathcal{C}(\mathcal{P}(n_1, n_{h+1}))$. If all links are ultimately reliable, all routes will be reliable as well. That is, $R_{n_h}(L_d) \approx 1$ and $R'_{n_1}(L_e) \approx 1$ (neglecting packet loss due to buffer overflow at intermediate nodes). In such a case, we have:

$$\begin{cases} F_{\mathcal{P}}(L_d) \approx 1 \\ B_{\mathcal{P}}(L_e) \approx 1. \end{cases}$$

In other words, each packet and its end-to-end acknowledgment will be transmitted almost once. Therefore, the expected energy consumed during end-to-end packet traversal could be approximated as:

$$\mathcal{C}(\mathcal{P}(n_1, n_{h+1})) \approx \sum_{i=1}^{h} \bar{\mathcal{E}}(n_i, n_{i+1}, L_d) + \sum_{i=1}^{h} \bar{\mathcal{E}}(n_{i+1}, n_i, L_e). \tag{4.9}$$

Note that if M is unlimited (i.e., $M \to \infty$), (4.9) gives us the exact value of the consumed energy. Nevertheless, in such a case, no end-to-end acknowledgement is required.

4.4 Minimum Energy Cost for End-to-end Packet Traversal

In this section, we analyze the minimum amount of energy required to transmit a packet from a source node to a destination node. Since we want to find the minimum value, we assume nodes deploy TPC provided that the PDR of links is not harmed due to reduced transmission power. We recall from the previous chapter, that when nodes support TPC, the PDR of all links remains be the same, regardless of the distance between the sender and the receiver. That is, $p_{u,v}(x) = p(x)$, $\forall (u,v) \in \mathbb{E}$, $\forall x > 0$[1]. With this assumption, we determine *the minimum* value of $\mathcal{C}(\mathcal{P}(n_1, n_{h+1}))$ for various cases. To simplify the presentation, we use the following notation in this section: $p_{u,v}(L_d) = p_d$, $p_{u,v}(L_e) = p_e$, $p_{u,v}(L_a) = p_a$, $\bar{\mathcal{X}}_{u,v}(L_d) = \bar{\mathcal{X}}_d$, $\bar{\mathcal{Y}}_{u,v}(L_a) = \bar{\mathcal{Y}}_a$, $\bar{\mathcal{X}}_{u,v}(L_e) = \bar{\mathcal{X}}_e$, $\forall (u,v) \in \mathbb{E}$.

---

[1]This is subjected to having negligible or the same collision probability for all links.

When neither MAC retransmission nor end-to-end retransmission is supported, $\mathcal{C}(\mathcal{P}(n_1, n_{h+1}))$ in (4.6) is simplified to:

$$\mathcal{C}(\mathcal{P}(n_1, n_{h+1})) = L_d \sum_{i=1}^{h} \left[(\alpha + \epsilon_r + \beta d_{n_i,n_{i+1}}^{\eta}) p_d^{i-1} \right]. \tag{4.10}$$

We can easily show that the minimum value of $\sum_{i=1}^{h} d_{n_i,n_{i+1}}^{\eta}$ is achieved if $d_{n_i,n_{i+1}} = \frac{d_{sd}}{h}$, where d_{sd} is the distance between the source and the destination. That is, all intermediate nodes between the source and the destination are equally spaced. Thus, (4.10) changes to:

$$\mathcal{C}(\mathcal{P}(n_1, n_{h+1})) = L_d \left(\epsilon_r + \alpha + \beta \frac{d_{sd}^{\eta}}{h^{\eta}} \right) \frac{1 - p_d^h}{1 - p_d}. \tag{4.11}$$

Given L_d, to minimize $\mathcal{C}(\mathcal{P}(n_1, n_{h+1}))$ in (4.11), we need to find the optimal value of h (i.e., the number of equally spaced hops between the source and the destination). Our observations show that depending on the values of various parameters in (4.11), $\mathcal{C}(\mathcal{P}(n_1, n_{h+1}))$ might be an increasing function, a decreasing function, or a convex function of h. Figure 4.1 shows different plots of $\mathcal{C}(\mathcal{P}(n_1, n_{h+1}))$ as a function of h for different values of source-destination distance. As we can observe, for $d_{sd} = 500$ m, the energy cost is a convex function of h, where there is an optimum value for h minimizing the energy cost. For $d_{sd} = 100$ m, the energy cost is an increasing function of h, which means a smaller value of h results in a smaller energy cost. For $d_{sd} = 2000$ m, the energy cost is a decreasing function of h, which means a higher value of h ensures higher energy-efficiency. The significance of this result is that it *violates what is predicted by simplified models of energy consumption used in* [74–76, 79]. These models predict that for any given source-destination distance d_{sd}, a higher value of h always ensures higher energy-efficiency. However, we observe that this is not always true. The realistic energy consumption model which we used in this thesis can predict a different result. Depending on energy consumption parameters of wireless interfaces and distance between the source and the destination, a higher, a lower, or an optimum value of h could result in a higher energy-efficiency. The main problem of the simplified models in [74–76, 79] is that they only consider the transmission power of nodes, and neglect other sources of energy consumption of transceivers.

Now, we continue with the other three cases. When end-to-end retransmission is not supported, but MAC retransmission is supported, we have:

$$\mathcal{C}(\mathcal{P}(n_1, n_{h+1})) = \left[L_d \bar{\mathcal{X}}_d + L_a \bar{\mathcal{Y}}_a \right] \left(\epsilon_r + \alpha + \beta \frac{d_{sd}^{\eta}}{h^{\eta}} \right) \frac{1 - f_d^h}{1 - f_d}, \tag{4.12}$$

in which $f_d = 1 - (1 - p_d)^M$.

(a) $d_{sd} = 500$ m

(b) $d_{sd} = 100$ m

(c) $d_{sd} = 2000$ m
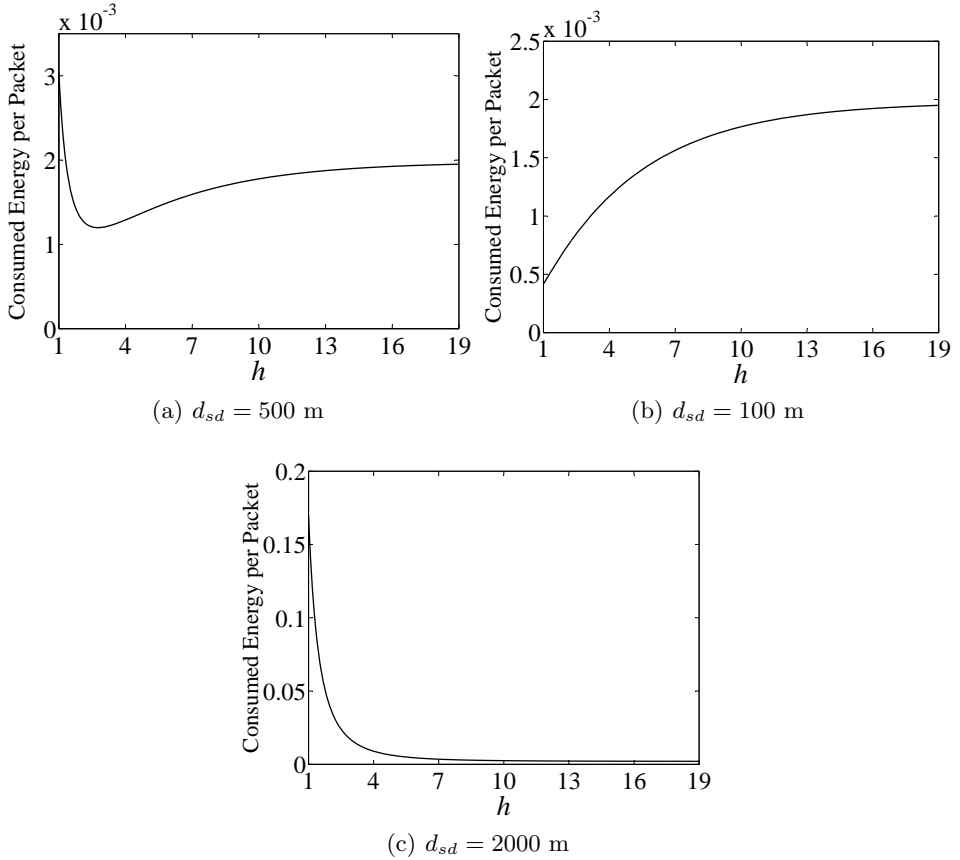
Figure 4.1 – Energy cost for end-to-end packet transfer as a function of h, when neither end-to-end nor MAC retransmissions are supported, and the PDR of links is identical. Results are for the PRISM chipset. Values of various parameters are as follows: $p_a = 0.9$, $p_d = 0.8$, $\eta = 4$, and $L_d = 1600$ [bit]. The plot of the minimum energy may have different shapes depending on the distance between the source and the destination node d_{sd}.

When end-to-end retransmission is supported, but MAC retransmission is not supported, we have:

$$\mathcal{C}(\mathcal{P}(n_1, n_{h+1})) = \frac{1}{p_e^h} \left(\frac{L_d}{p_d^h} + L_e \right) \left(\epsilon_r + \alpha + \beta_t \frac{d_{sd}^\eta}{h^\eta} \right) \frac{1 - p_d^h}{1 - p_d}.$$

Finally, when both end-to-end and MAC retransmissions are supported, we have:

$$\mathcal{C}(\mathcal{P}(n_1, n_{h+1})) \approx \left[L_d \bar{\mathfrak{X}}_d + 2\bar{\mathfrak{y}}_a L_a + L_e \bar{\mathfrak{X}}_e \right] \left(h(\epsilon_r + \alpha) + \beta \frac{d_{sd}^\eta}{h^{\eta-1}} \right). \qquad (4.13)$$

In general, the value of h which minimizes the energy cost for each of the four cases might be different from the other case. Let h_{opt} denotes the value of h minimizing the energy cost $\mathcal{C}(\mathcal{P}(n_1, n_{h+1}))$, and E_{min} denotes the corresponding value of the energy cost when $h = h_{opt}$. Given a fixed data rate for all nodes and a fixed PDR for all links, E_{min} is in fact *the minimum expected energy that is consumed to transfer a data packet to a destination node located at distance d_{sd} from the source node.* Since h_{opt} might be a real value and not necessarily an integer value, E_{min} is in fact the benchmark. In practice, the optimal number of hops is the closest integer to h_{opt}. Thus, the required energy will be higher than E_{min}. Here, we use E_{min} as a means to compare energy cost of four types of packet transfer.

4.4.1 Effect of Distance between Source and Destination

We have plotted E_{min} and h_{opt} in Figure 4.2 for various cases as a function of the distance between the source and the destination. There are some points that we can extract from the plots in Figure 4.2(a):

1. For all the cases, routes with a higher number of hops are more energy efficient as the distance between the source and the destination increases.

2. Support for MAC retransmission or end-to-end retransmission reduces the value of h_{opt} compared to the case that no type of retransmission is supported.

3. Support for MAC retransmission causes h_{opt} to remain almost the same, regardless of support or lack of support for end-to-end retransmission. Observations show that this, however, depends on the number of allowed maximum transmission attempts at the MAC layer. If the number of allowed transmissions decreases, the difference between h_{opt} of the two cases increases.

Regarding the value of E_{min}, we list the inferences from Figure 4.2(b):

1. The lowest value of E_{min} belongs to the case in which neither end-to-end nor MAC retransmission is supported, because no energy will be consumed for retransmissions of the packet.

(a)

(b)
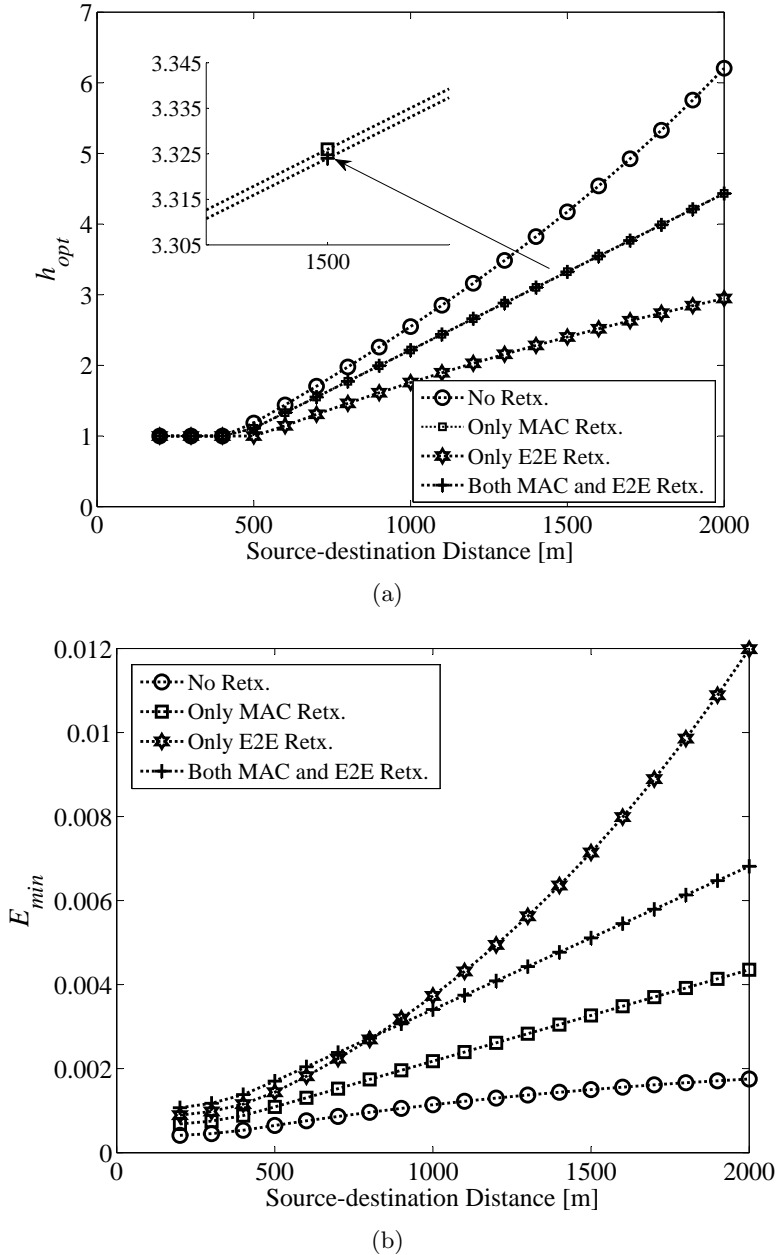
Figure 4.2 – E_{min} and h_{opt} as a function of the distance between the source and the destination. Results are for PRISM chipset. Values of other parameters are as follows: $p_a = 0.9$, $p_d = p_e = 0.8$, $L_d = 1600$ [bit], $L_a = 384$ [bit], $L_e = 768$ [bit], $M = 7$, $\eta = 4$, and $r = 11$ [Mbps].

2. When end-to-end retransmission is supported, E_{min} increases exponentially as the distance between the source and the destination increases. On the other hand, if only MAC retransmission is supported, E_{min} increases almost linearly with the distance. This means, *end-to-end retransmissions in wireless multi-hop networks can dramatically increase the overall energy consumption as the network size increases. If instead of end-to-end retransmissions, only MAC retransmissions are supported, the minimum energy cost scales better with the network size.*

4.4.2   Closed-Form Expression of Optimal Hop Count

For the cases in which MAC retransmission is supported, we can find a closed-form expression for h_{opt}, when there is no limitation on the number of transmissions attempts (i.e., $M \to \infty$). In such a case, $f_d = 1$ (see 4.12). Thus, for the case of packet transfer without end-to-end retransmission, (4.12) simplifies to

$$\mathcal{C}(\mathcal{P}(n_1, n_{h+1})) = (L_d \bar{\mathcal{X}}_d + L_a \bar{\mathcal{Y}}_a) \left(h(\epsilon_r + \alpha) + \beta \frac{d_{sd}^\eta}{h^{\eta-1}} \right). \qquad (4.14)$$

If end-to-end retransmission is supported, we have:

$$\mathcal{C}(\mathcal{P}(n_1, n_{h+1})) \approx \left[L_d \bar{\mathcal{X}}_d + 2\bar{\mathcal{Y}}_a L_a + L_e \bar{\mathcal{X}}_e \right] \left(h(\epsilon_r + \alpha) + \beta \frac{d_{sd}^\eta}{h^{\eta-1}} \right). \qquad (4.15)$$

By taking the first derivative of $\mathcal{C}(\mathcal{P}(n_1, n_{h+1}))$ in (4.14) and (4.15), h_{opt} is obtained as follows:

$$h_{opt} = \left(\frac{\beta d_{sd}^\eta (\eta - 1)}{\epsilon_r + \alpha} \right)^{\frac{1}{\eta}}. \qquad (4.16)$$

As predicted in (4.16), h_{opt} decreases, if α and/or ϵ_r increases. In other words, *as the energy consumed by the processing elements of the transceiver increases, routes with a shorter number of hops will be more energy-efficient.*

4.4.3   Effect of Path-loss Exponent

E_{min} and h_{opt} are directly dependent on the path-loss exponent η of the environment. It may seem that parameter β, which was introduced in Chapter 3 for modeling link level energy cost, indirectly relates E_{min} to the path-loss exponent as well. Recall from Chapter 3 that β is defined as:

$$\beta = \frac{P_{ref}}{\kappa r d_0^\eta},$$

in which P_{ref} is the minimum transmission power required to satisfy the target BER requirement at reference distance d_0. We can find an alternative expression

for β considering the fact that P_{ref} itself is also affected by the path-loss exponent. According to the path-loss fading model expressed in (3.6), we have:

$$P_{ref} = c_n d_0^\eta,$$

where c_n is a constant depending on noise power, antenna gain, and wavelength. Therefore, β can be expressed alternatively as:

$$\beta = \frac{c_n}{\kappa r}.$$

To study the impact of the path-loss exponent on energy-efficiency of routes, we use this alternative expression for β.

We have plotted h_{opt} and E_{min} in Figure 4.3 as a function of the path-loss exponent. What we observe in Figure 4.3(a) is that the number of hops in an energy-efficient path increases as the path-loss exponent of the environment increases. The physical phenomenon behind this behavior is the high signal attenuation in environments with large path-loss exponent. Thus, a higher transmission power is required to receive signals with the required power to satisfy the target BER requirement. To keep the energy cost minimal as the path-loss exponent increases, we may need to increase the number of hops. This, however, depends on the energy consumption of processing elements of the transceiver. If this energy is much greater than the transmission power, the hop count of the minimal energy path may remain unchanged even if the path-loss exponent increases. This is due to the fact that the energy consumption of the processing elements of the transceiver will be the dominant factor, not the transmission power which is affected by the path-loss exponent of the environment.

Figure 4.3(a) also shows that except for the case of packet transfer without any kind of retransmission, h_{opt} always has a limited value. That is, if packet retransmission is not supported, h_{opt} does not take a limited value when the path-loss exponent is high. We observe that h_{opt} has been limited by the maximum value in the plot (50 in this figure). This means, for such a case, a higher value of h_{opt} theoretically provides better energy-efficiency. A practical implication of this phenomenon is that when neither MAC retransmission nor end-to-end retransmission is supported, routes with a higher number of hops could be more energy-efficient in environments with high path-loss exponent such as heavily built urban areas. This, however, is not true for environments with small path-loss exponent such as indoor environments, or for the cases in which either MAC retransmission or end-to-end retransmission is supported (regardless of the value of the path-loss exponent).

Regarding the value of E_{min}, Figure 4.3(b) shows that if only end-to-end retransmission is supported, E_{min} increases exponentially as the path-loss exponent

(a)

(b)
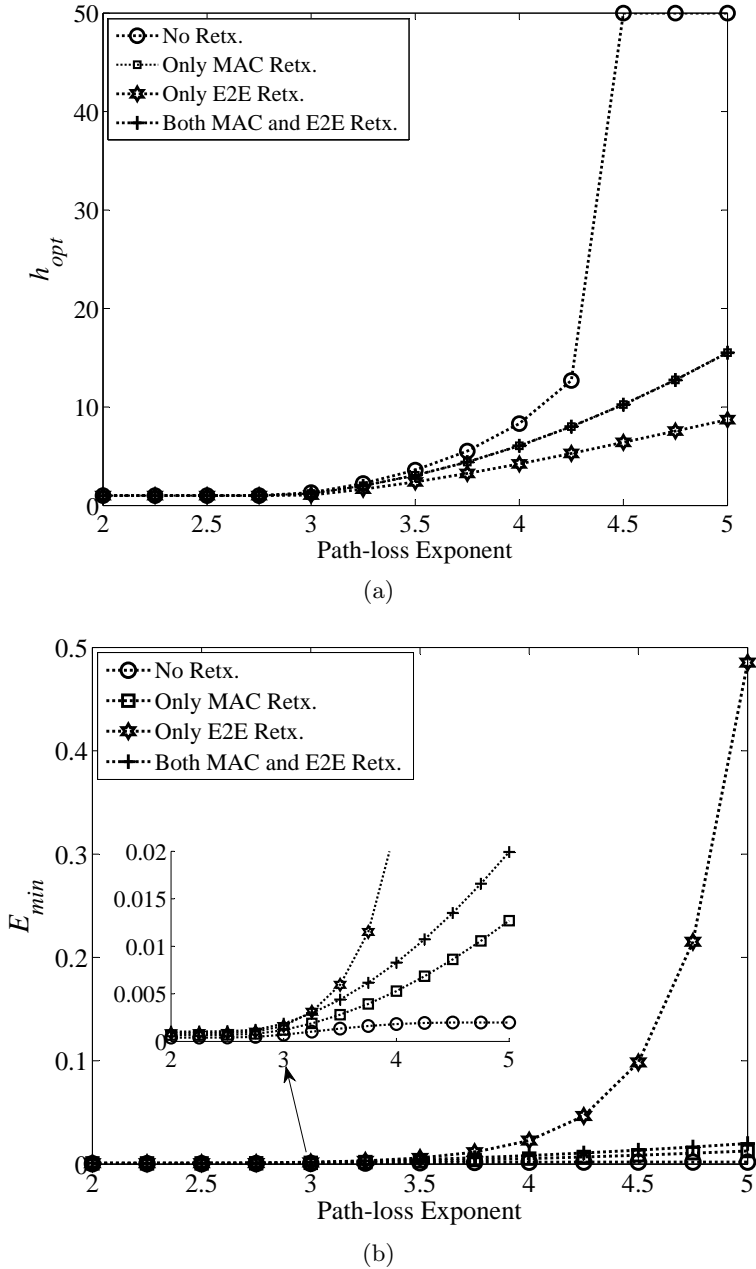
Figure 4.3 – E_{min} and h_{opt} as a function of the path-loss exponent of the environment. Results are for the PRISM chipset. Values of other parameters are as follows: $p_a = 0.9$, $p_d = p_e = 0.8$, $L_d = 1600$ [bit], $L_a = 384$ [bit], $L_e = 768$ [bit], $M = 7$, $r = 11$ [Mbps], and $d_{sd} = 500$ [m].

increases. The rate of increase is less when MAC retransmission is supported as
well. This again shows that support for MAC retransmission can reduce energy
consumption for end-to-end packet transfer with end-to-end acknowledgment (at
the cost of increased hop-count or latency). It is also interesting to note that if
no retransmission is supported, E_{min} increases slightly as the path-loss exponent
increases. Nevertheless, this is also at the cost of increased hop-count (latency) as
shown in Figure 4.3(a).

4.5   Simulation Studies

In this section, we present simulation results to 1) verify the accuracy of the
analytical models presented in this chapter and 2) to study the impact of
transmission power control on energy consumption for end-to-end packet traversal.
We consider a network in which nodes are uniformly distributed in a square area of
size 750×750 [m^2]. Nodes are equipped with a PRISM chipset. In each simulation
run, we pick up a pair of source-destination nodes randomly. The min-hop route
between them is determined using the Dijkstra's routing algorithm. Then, 10000
data packets of size $L_d = 1600$ bit are transmitted between the source and the
destination. In each simulation run, the consumed energy per packet is calculated
by dividing the total amount of energy consumed by all nodes along the route to
the number of transmitted packets by the source node. The expected consumed
energy per packet in the network is calculated by averaging over 2000 distinct pairs
of source-destination nodes. Theoretical values are calculated using the expressions
given in Section 4.1 and Section 4.2. The target BER requirement in this experiment
is set to 5×10^{-5}.

4.5.1   Accuracy of the Analytical Model

Results depicted in Figure 4.4 show that there is a good match between the
analytical and simulation results in all cases. Furthermore, we observe that the
average energy cost reduces as the mean degree of nodes increases, regardless of
the type of packet transfer. Since the network area is fixed, increasing the mean
degree of nodes corresponds to increasing the density of nodes in the network. If the
node density increases, it is more probable to find routes consisting of shorter links.
Such routes are more energy-efficient. This means, *increasing the mean degree of*
nodes (node density) in wireless multi-hop networks can reduce the energy cost for
end-to-end packet traversal.
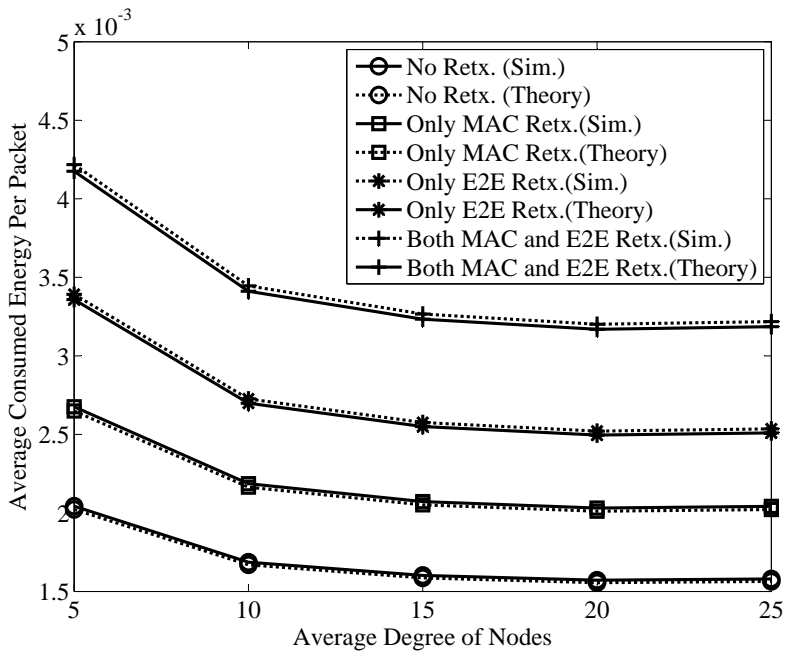
Figure 4.4 – The average energy cost for end-to-end packet traversal as a function of the mean degree of nodes for various types of packet transfer.

4.5.2   Effect of Transmission Power Control

The concept of TPC in wireless multi-hop networks was introduced in the previous chapter. We observed that TPC can save energy for packet exchange over wireless links provided that the PDR of the link is not harmed due to reduced transmission power. Here, we compare energy cost for end-to-end packet traversal in multi-hop networks with and without TPC.

TPC can save energy consumption of nodes in a wireless multi-hop network in two ways. First, it saves energy consumption of nodes for packet exchange over wireless links. Second, it reduces energy consumption of nodes by reducing the collision probability due to reduced transmission power. As a result, the PDR of links increases. This, in turn, reduces the number of retransmissions of a packet when any kind of packet retransmission is supported. Consequently, more amount of energy is saved. To demonstrate this, we conduct a simulation study. We set the maximum collision probability (MCP) in the network when TPC is not supported to 0.5. Then, we increase the collision probability when TPC is supported, from 0 to the MCP without TPC (i.e., 0.5). The collision probability in each link is chosen randomly between zero and the MCP. Plots in Figure 4.5 show that if MAC retransmission is supported, reducing the collision probability due to TPC increases energy efficiency of end-to-end packet transmission. However, if MAC retransmission is not supported, reducing the collision probability due to TPC increases the energy cost. The reason behind this phenomenon lies in the fact that if the PDR of links increases, intermediate nodes between the source and the destination forward more packets. As a result, they consume more energy. This, of course, provides a reliability gain.

4.6   Summary

In this chapter, the energy cost of a route for end-to-end packet transfer was formulated. We considered four types of packet transfer: without retransmission, with MAC retransmission, with end-to-end transmission, with both MAC and end-to-end retransmissions. For each case, the minimum energy cost for packet exchange between two nodes in a multi-hop network was determined. We observed that if only end-to-end retransmission is supported, the minimum energy cost increases exponentially as the network size increases. It increases linearly, if MAC retransmission is supported instead.
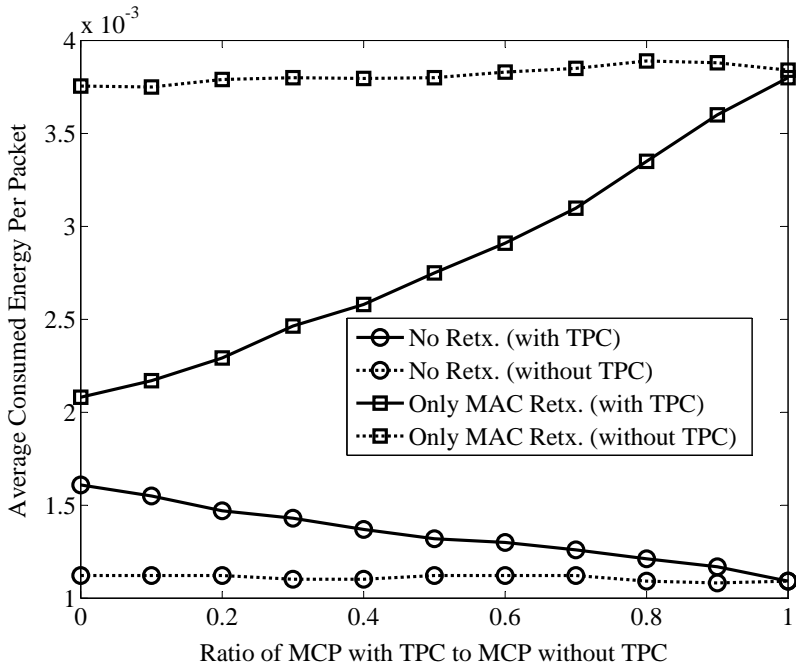
Figure 4.5 – Impact of reduced collision probability in the network due to transmission power control on the average energy cost of routes for end-to-end packet traversal.

Chapter 5

Energy-efficient Routing

In the previous chapter, we determined the required amount of energy to transfer a packet from a source node to a destination node in wireless multi-hop networks. In this chapter, we study energy-efficient routing in these networks. Energy-efficient routing deals with finding routes which minimize the energy required for end-to-end transmission of a packet from a source node to a destination node. This is an effective way to reduce the energy cost of data communication in wireless multi-hop networks. Nevertheless, finding energy-efficient routes should not result in finding routes with low quality. If packet retransmission techniques are supported, the use of low-quality links can increase energy consumption of nodes, because lost packet over such links have to be retransmitted. Reliability of wireless links has to be taken into account to take the full advantage of energy-efficient routing in wireless multi-hop networks. By considering reliability of wireless links in route selection, we can also find reliable routes which increase quality of service [84].

Energy-efficient routing has been studied in the literature [74–76, 76–78, 80–82, 82, 85–88]. However, the existing schemes have not been designed on the basis of realistic energy consumption models. Most schemes (e.g., [74–81]), only consider the energy consumed for packet transmission over the air. As we observed in Chapter 3, a realistic energy consumption model should consider the energy consumed by processing elements of the transceiver as well. Furthermore, we observed in Chapter 4 that the actual amount of energy consumed to deliver a packet to its destination includes the energy consumed for retransmission and reception of data and acknowledgment packets. Proposed schemes in [74–76, 82] do not consider the effect of packet retransmission. On the other hand, although the effect of packet retransmission is considered in [77,78,80,81], these studies do not consider consumed energy by processing elements of transceivers. The use of such unrealistic energy consumption models results in suboptimal solutions for energy-efficient routing in

wireless multi-hop networks. It is essential to use energy consumption models which take into account all the details.

In this chapter, we design a suite of algorithms for energy-efficient routing in wireless multi-hop networks on the basis of the energy consumption model that we developed so far in this thesis. In the previous chapter, we observed that support for MAC retransmission, end-to-end retransmission, or both affect the energy efficiency of routes. As we will see in this chapter, this also affects the design of energy-efficient routing algorithms. A key characteristic of the routing algorithms that we present in this chapter is that they consider both energy cost and reliability of links in route selection. For this reason, we call this suite of algorithms Reliable Minimum Energy Routing (RMER). This chapter presents design and evaluation of RMER for wireless multi-hop networks.

The rest of this chapter is organized as follows: we provide some background knowledge about routing algorithms in wireless multi-hop networks in Section 5.1. Then, we introduce RMER algorithms in Section 5.2. Section 5.3 provides a comparison between RMER and energy-efficient routing algorithms proposed in prior studies. Section 5.4 describes practical considerations for deploying RMER in wireless multi-hop networks. In Section 5.5, we present simulation studies, and we summarize the chapter in Section 5.6.

5.1 Preliminaries

A routing algorithm finds the optimal route between a pair of nodes in a multi-hop network. Dijkstra's algorithm and Bellman-Ford algorithm are two well-known routing algorithms which can find shortest paths between nodes. The main difference between them is that Bellman-Ford algorithm can find shortest paths in networks with negative link weights, while Dijkstra's algorithm can only be used in networks with positive link weights. Without loss of generality, we focus on Dijkstra's algorithm, because for energy-efficient routing link weights should be proportional to the energy consumption of nodes (which are positive values). Dijkstra's algorithm is also faster than Bellman-Ford algorithm.

Dijkstra's algorithm, shown in Algorithm 1, is an iterative algorithm. At each iteration the shortest path from the source node s to one of the nodes in the network is determined. The algorithm stops when the shortest path from the source node to any other node in the network has been discovered (if there is a path).

The principle behind convergence of Dijkstra's algorithm is that the weight of a path $\mathcal{P}(s, v)$ can be calculated in a recursive way as follows:

$$\mathcal{C}(\mathcal{P}(s, v)) = \mathcal{C}(\mathcal{P}(s, u)) + w_{u,v}, \tag{5.1}$$

Algorithm 1 Dijkstra's algorithm for finding the shortest-path between a source node s and other nodes of the network. In this algorithm, $C(v)$ maintains the path-weight from s to v, and $\mathcal{T}(v)$ maintains the constituent links of the shortest-path from s to v.

Dijkstra$(G(\mathbb{V}, \mathbb{E}), s)$
$C(s) = 0$
for each node $v \in \mathbb{V} - \{s\}$ **do**
$\quad C(v) \leftarrow \infty$
$\quad \mathcal{T}(v) \leftarrow \emptyset$
end for
$\mathcal{Q} \leftarrow \mathbb{V}$
while $\mathcal{Q} \neq \emptyset$ **do**
$\quad u \leftarrow v \in \mathcal{Q} \mid C(v)$ is minimum
$\quad \mathcal{Q} \leftarrow \mathcal{Q} - u$
$\quad$**for** each neighbor $v \in \mathcal{Q}$ of u **do**
$\quad\quad temp \leftarrow C(u) + w_{u,v}$
$\quad\quad$**if** $temp < C(v)$ **then**
$\quad\quad\quad C(v) \leftarrow temp$
$\quad\quad\quad \mathcal{T}(v) \leftarrow \mathcal{T}(u) \cup (u, v)$
$\quad\quad$**end if**
$\quad$**end for**
end while

---

in which $\mathcal{C}(\mathcal{P}(s, v))$ is the weight of the path $\mathcal{P}(s, v)$, $\mathcal{C}(\mathcal{P}(s, u))$ is the weight of the path $\mathcal{P}(s, u)$, and $w_{u,v}$ is the weight of the link (u, v). Here, it is assumed that u precedes v in $\mathcal{P}(s, v)$. To refer to (5.1), we name it *Dijkstra's recursive equation*. This equation has a critical role in the proof of the following theorem, which proves convergence of Dijkstra's algorithm [89]:

Theorem 1. *In Dijkstra's algorithm, each time a node v is extracted from $\mathcal{Q}$ (see Algorithm 1), links in $\mathcal{T}(v)$ form a shortest path from s to v.*

The time complexity of the Dijkstra's algorithm depends on the network topology and how the minimum cost node is extracted from $\mathcal{Q}$ in each iteration of the algorithm. In the worst-case scenario, each node can have a link to any other node of the network. Thus, $|\mathbb{V} - 1|$ comparisons are made on $|\mathbb{V} - 1|$ nodes to extract the minimum cost node from $\mathcal{Q}$. This means, the time complexity of Dijkstra's algorithm is $O(|\mathbb{V}|^2)$. Nevertheless, Fredman and Tarjan [90] showed that in sparse networks the time complexity of the Disjktra's algorithm can be reduced to $O(|\mathbb{E}| + |\mathbb{V}| \log(|\mathbb{V}|))$. For sparse graphs with far fewer links than dense graphs, the Dijkstra's algorithm can be implemented more efficiently by storing the graph in the form of adjacency lists using Fibonacci heaps. In such a case, extracting the

minimum cost node from $\mathcal{Q}$ could be done more efficiently. We refer the interested readers to [90] for details about implementation of the Dijsktra's algorithm using Fibonacci heaps.

5.2 Reliable Minimum Energy Routing

RMER is an energy-efficient routing algorithm based of the Dijkstra's algorithm. RMER can find minimum energy paths between nodes.

Definition 2. *Minimum Energy Path (MEP): The MEP between a source and a destination node is a path which minimizes the expected amount of energy required to transfer a packet from the source to the destination.*

To find MEPs between nodes, we face with some questions. Can we use Dijkstra's algorithm to find MEPs? If Dijkstra's algorithm could be used, then how should we calculate the link weights? If Dijkstra's algorithm can not be used, then what changes are required for finding MEPs? Should we design a new algorithm or modify the Dijkstra's algorithm? Or should we alter definition of MEP to be able to use the Dijkstra's algorithm to find energy-efficient routes? To answer these questions, we examine the consumed energy for end-to-end packet traversal, which was analyzed in the previous chapter. We again consider four types of packet transfer: 1) without retransmission 2) with MAC retransmission 3) with end-to-end retransmission, and 4) with both MAC and end-to-end retransmissions. Our approach is to find a recursive equation similar to (5.1) to calculate the required energy for packet transfer from a source node s to a destination node v. This allows us to determine whether Dijkstra's algorithm could be used for finding MEPs or should we need some modifications to it.

5.2.1 Packet Transfer without Retransmission

When packet retransmission is not supported neither by the MAC layer nor in an end-to-end manner, the expected consumed energy for end-to-end packet traversal along a path $\mathcal{P}(n_1, n_{h+1})$ was expressed in (4.6):

$$\mathcal{C}(\mathcal{P}(n_1, n_{h+1})) = \sum_{i=1}^{h} R_{n_i}(L_d)\bar{\mathcal{E}}(n_i, n_{i+1}, L_d). \tag{5.2}$$

We can express the consumed energy $\mathcal{C}(\mathcal{P}(n_1, n_{h+1}))$ alternatively as follows:

$$
\begin{aligned}
\mathcal{C}(\mathcal{P}(n_1, n_{h+1})) &= \\
&\left(\sum_{i=1}^{h-1} \left[R_{n_i}(L_d) \bar{\mathcal{E}}(n_i, n_{i+1}, L_d) \right] \right) + R_{n_h}(L_d) \bar{\mathcal{E}}(n_h, n_{h+1}, L_d) \\
&= \mathcal{C}(\mathcal{P}(n_1, n_h)) + \frac{R_{n_{h+1}}(L_d)}{R_{n_h, n_{h+1}}} \bar{\mathcal{E}}(n_h, n_{h+1}, L_d).
\end{aligned}
\tag{5.3}
$$

Equation (5.3) shows how we can calculate the consumed energy for packet transfer from node n_1 to node n_{h+1} in terms of the consumed energy from n_1 to n_h, where n_h precedes n_{h+1} in the path $\mathcal{P}(n_1, n_{h+1})$. In order to express (5.3) similar to Dijkstra's recursive equation, we assume $n_1 = s$ is the source node, $n_{h+1} = v$ is the destination node, and $n_h = u$ precedes v in the path $\mathcal{P}(s, v)$ from s to v. Thus, according to (5.3), the expected consumed energy for transferring a packet of length L_d bits from a source node s to a destination node v could be calculated in a recursive way as follows:

$$
\begin{cases}
\mathcal{C}(\mathcal{P}(s, v)) = \mathcal{C}(\mathcal{P}(s, u)) + R(\mathcal{P}(s, v), L_d) \times \frac{\bar{\mathcal{E}}(u, v, L_d)}{R_{u, v}(L_d)} \\
R(\mathcal{P}(s, v), L_d) = R(\mathcal{P}(s, u)) \times R_{u, v}(L_d)
\end{cases}
\tag{5.4}
$$

where $R_{u, v}(L_d)$ is the reliability of the link (u, v) for data packets of size L_d bits as given by (4.5), and $R(\mathcal{P}(s, v), L_d)$ is the end-to-end reliability of $\mathcal{P}(s, v)$ for data packet of length L_d bits. If we compare the recursive equation in (5.4) with Dijkstra's recursive equation in (5.1), it is clear that in order to be able to use Dijkstra's algorithm to find MEPs, we need to define the link weight $w_{u,v}$ as

$$
w_{u, v} = R(\mathcal{P}(s, v), L_d) \times \frac{\bar{\mathcal{E}}(u, v, L_d)}{R_{u, v}(L_d)}.
\tag{5.5}
$$

This, however, means that the weight of each link depends on the reliability of upstream links from the source node to that link. Thus, the same link may have different weights in different paths between the same source and destination. Note that Dijkstra's algorithm works on the basis of the fact that the weight of a link is not dependent on which path the link belongs to. We can prove that if we define link weights as in (5.5), then Dijkstra's algorithm cannot find MEPs. To this end, we prove that Theorem 1 is not true anymore, if link weights are defines as (5.5).

Let the path formed by links in $\mathcal{T}(i)$, $\forall i \in \mathbb{V}$, be denoted by $\mathcal{P}^*(s, i)$. Let u be the last node extracted so far from $\mathcal{Q}$, and $\mathcal{P}^*(s, u)$ be the shortest path from s to u. Now, suppose that we are about to extract v from $\mathcal{Q}$ in the next iteration of Dijkstra's algorithm. If link weights are defined as (5.5), we can show that $\mathcal{P}^*(s, v)$ may not be the shortest-path from s to v. We show that there might be another path $\mathcal{P}_1(s, v)$ which its weight is smaller that the weight of $\mathcal{P}^*(s, v)$.

Assume that $\mathcal{P}_1(s, v) = \mathcal{P}_1(s, u) \cup \{v\}$, where $\mathcal{P}_1(s, u)$ is a path between s and u. Since $\mathcal{P}^*(s, u)$ is the shortest path from s to u, we have

$$\mathcal{C}(\mathcal{P}^*(s, u)) \leq \mathcal{C}(\mathcal{P}_1(s, u)). \tag{5.6}$$

If we want $\mathcal{P}^*(s, v)$ be the shortest path from s to v, then we must have

$$\mathcal{C}(\mathcal{P}^*(s, v)) \leq \mathcal{C}(\mathcal{P}_1(s, v)).$$

Since u has been extracted just before v, then $\mathcal{P}^*(s, v) = \mathcal{P}^*(s, u) \cup \{v\}$. Thus, according to (5.4), we must have

$$\begin{aligned}
\mathcal{C}(\mathcal{P}^*(s, u)) + R(\mathcal{P}^*(s, v), L_d) \times \frac{\bar{\mathcal{E}}(u, v, L_d)}{R_{u,v}(L_d)} \leq \\
\mathcal{C}(\mathcal{P}_1(s, u)) + R(\mathcal{P}_1(s, v), L_d) \times \frac{\bar{\mathcal{E}}(u, v, L_d)}{R_{u,v}(L_d)}
\end{aligned} \tag{5.7}$$

From (5.7) and (5.6), we can conclude that in order to have $\mathcal{C}(\mathcal{P}^*(s, v)) \leq \mathcal{C}(\mathcal{P}_1(s, v))$, we need to have

$$R(\mathcal{P}^*(s, v), L_d) \leq R(\mathcal{P}_1(s, v), L_d). \tag{5.8}$$

Nevertheless, since we have not made any assumption regarding the reliability of routes with respect to each other, there is no guarantee that the reliability of $\mathcal{P}^*(s, v)$ is smaller than that of $\mathcal{P}_1(s, v)$. It may happen that $R(\mathcal{P}^*(s, v), L_d) > R(\mathcal{P}_1(s, v), L_d)$. Thus, $\mathcal{P}^*(s, v)$ may not necessarily be the shortest path from s to v. This shows that Theorem 1 is not true anymore.

What causes this? If we review the above-mentioned proof again, we observe that the dependency of link weight on the reliability of paths in (5.5) is the source of the problem. Now, let us remove this dependency by simplifying the energy cost of a path as follows:

$$\mathcal{C}(\mathcal{P}(n_1, n_{h+1})) = \sum_{i=1}^{h} \bar{\mathcal{E}}(n_i, n_{i+1}, L_d). \tag{5.9}$$

With this simplification, the energy cost of a path is the energy consumed by all nodes along the path to *successfully* transfer a packet from the source to the destination. Considering this definition of path cost, the recursive expression in (5.4) changes to

$$\mathcal{C}(\mathcal{P}(s, v)) = \mathcal{C}(\mathcal{P}(s, u)) + \bar{\mathcal{E}}(u, v, L_d). \tag{5.10}$$

It is obvious that (5.10) is characteristically similar to Dijkstra's recursive equation in (5.1). Therefore, if we define $w_{u,v}$ in Dijkstra's algorithm as the energy cost for

packet exchange over a wireless link, i.e., $w_{u,v} = \bar{\mathcal{E}}(u, v, L_d)$, then we can use this algorithm as a heuristic solution to find MEPs when packet retransmission is not supported. For this case, we can expand $\bar{\mathcal{E}}(u, v, L_d)$ using (4.3) and (4.2) as follows:

$$w_{u,v} = \bar{\mathcal{E}}(u, v, L_d) = L_d(\epsilon + \alpha + \beta d_{u,v}^{\eta}). \tag{5.11}$$

We can also use the normalized value of $w_{u,v}$ with respect to the packet size L_d without changing the ranking of routes with respect to their energy efficiency. Thus, the link weight $w_{u,v}$ could simply be calculated as

$$w_{u,v} = \epsilon + \alpha + \beta d_{u,v}^{\eta}, \tag{5.12}$$

where the energy consumption parameters ϵ, α, and β are defined and explained in Chapter 3.

5.2.2   Packet Transfer with MAC Retransmission

If only MAC retransmission is supported, the energy consumption for end-to-end transfer of a packet is expressed similar to that of packet transfer without retransmission. The only difference is the way that the energy consumed on a link is calculated. The design of the energy-efficient routing algorithm for this case is completely similar to that of packet transfer without retransmission. Thus, we can again use Dijkstra's algorithm as a heuristic solution to find MEPs, if we define the link weight $w_{u,v}$ as

$$w_{u,v} = \bar{\mathcal{E}}(u, v, L_d).$$

Nevertheless, the impact of retransmissions must be taken into account while we calculate $\bar{\mathcal{E}}(u, v, L_d)$. For this case, we can expand $\bar{\mathcal{E}}(u, v, L_d)$ using (4.3) and (4.1). Hence, the link weight $w_{u,v}$ is calculated as follows:

$$w_{u,v} = \left(L_d \bar{\mathcal{X}}_{u,v}(L_d) + L_a \bar{\mathcal{Y}}_{v,u}(L_a) \right) (\epsilon_r + \alpha + \beta d_{u,v}^{\eta}). \tag{5.13}$$

We recall that $\bar{\mathcal{X}}_{u,v}(L_d)$ is the expected number of times that a data packet of length L_d bits is transmitted over (u, v) before it is delivered to v, and $\bar{\mathcal{Y}}_{v,u}(L_a)$ is the expected number of acknowledgments transmitted for the packet by v. Due to dependency of $\bar{\mathcal{X}}_{u,v}(L_d)$ and $\bar{\mathcal{Y}}_{v,u}(L_a)$ to the quality of links, the link weight in (5.13) is a function of both energy consumption characteristics of nodes and quality of links.

5.2.3 Packet Transfer with End-to-end Retransmission

If only end-to-end retransmission is supported, the expected amount of energy consumed to transfer a packet from a source node to a destination node was expressed in (4.7):

$$
\mathcal{C}(\mathcal{P}(n_1, n_{h+1})) = \frac{1}{R_{n_{h+1}}(L_d) R'_{n_1}(L_e)} \sum_{i=1}^{h} \left[R_{n_i}(L_d) \bar{\mathcal{E}}(n_i, n_{i+1}, L_d) \right] +
$$
$$
\frac{1}{R'_{n_1}(L_e)} \sum_{i=1}^{h} \left[R'_{n_{i+1}}(L_e) \bar{\mathcal{E}}(n_{i+1}, n_i, L_e) \right]. \tag{5.14}
$$

If we replace $R_{n_i}(L_d)$ from (4.4) and $R'_{n_{i+1}}$ from (4.8) into (4.7), we can express $\mathcal{C}(\mathcal{P}(n_1, n_{h+1}))$ in (5.14) as

$$
\mathcal{C}(\mathcal{P}(n_1, n_{h+1})) = \sum_{i=1}^{h} \frac{\bar{\mathcal{E}}(n_i, n_{i+1}, L_d)}{\prod_{j=i}^{h} R_{n_j, n_{j+1}}(L_d) \prod_{j=1}^{h} R_{n_{j+1}, n_j}(L_e)}
$$
$$
+ \sum_{i=1}^{h} \frac{\bar{\mathcal{E}}(n_{i+1}, n_i, L_e)}{\prod_{j=1}^{i} R_{n_{j+1}, n_j}}, \tag{5.15}
$$

which is equivalent to

$$
\mathcal{C}(\mathcal{P}(n_1, n_{h+1})) = \frac{\sum_{i=1}^{h-1} \left(\frac{\bar{\mathcal{E}}(n_i, n_{i+1}, L_d)}{\prod_{j=i}^{h-1} R_{n_j, n_{j+1}}(L_d) \prod_{j=1}^{h-1} R_{n_{j+1}, n_j}(L_e)} \right)}{R_{n_h, n_{h+1}}(L_d) R_{n_{h+1}, n_h}(L_e)}
$$
$$
+ \frac{\frac{\bar{\mathcal{E}}(n_h, n_{h+1}, L_d)}{\prod_{j=1}^{h-1} R_{n_{j+1}, n_j}(L_e)}}{R_{n_h, n_{h+1}}(L_d) R_{n_{h+1}, n_h}(L_e)}
$$
$$
+ \sum_{i=1}^{h-1} \left(\frac{\bar{\mathcal{E}}(n_{i+1}, n_i, L_e)}{\prod_{j=1}^{i} R_{n_{j+1}, n_j}} \right) + \frac{\bar{\mathcal{E}}(n_{h+1}, n_h, L_e)}{\prod_{i=1}^{h} R_{n_{j+1}, n_j}(L_e)}. \tag{5.16}
$$

If we define

$$
\mathcal{C}_1(\mathcal{P}(n_1, n_h)) = \sum_{i=1}^{h-1} \frac{\bar{\mathcal{E}}(n_i, n_{i+1}, L_d)}{\prod_{j=i}^{h-1} R_{n_j, n_{j+1}}(L_d) \prod_{j=1}^{h-1} R_{n_{j+1}, n_j}(L_e)},
$$

and

$$
\mathcal{C}_2(\mathcal{P}(n_1, n_h)) = \sum_{i=1}^{h-1} \frac{\bar{\mathcal{E}}(n_{i+1}, n_i, L_e)}{\prod_{j=1}^{i} R_{n_{j+1}, n_j}},
$$

we can express (5.16) alternatively as follows:

$$\mathcal{C}(\mathcal{P}(n_1, n_{h+1})) = \frac{1}{R_{n_h, n_{h+1}}(L_d) R_{n_{h+1}, n_h}(L_e)} \times$$
$$\left[\mathcal{C}_1(\mathcal{P}(n_1, n_h)) + \frac{\bar{\mathcal{E}}(n_h, n_{h+1}, L_d)}{\prod_{j=1}^{h-1} R_{n_{j+1}, n_j}(L_e)} \right] \qquad (5.17)$$
$$+ \left[\mathcal{C}_2(\mathcal{P}(n_1, n_h)) + \frac{\bar{\mathcal{E}}(n_{h+1}, n_h, L_e)}{\prod_{j=1}^{h} R_{n_{j+1}, n_j}(L_e)} \right].$$

In (5.17), $\prod_{j=1}^{h} R_{n_{j+1}, n_j}(L_e)$ is the end-to-end reliability of the reverse path from node n_{h+1} to node n_1 as given in (4.8). Similarly, $\prod_{j=1}^{h-1} R_{n_{j+1}, n_j}(L_e)$ is the end-to-end reliability of the reverse path from node n_h to node n_1. Equation (5.17) expresses the energy cost of the path from n_1 to n_{h+1} in terms of the energy cost from n_1 to n_h and the cost of the link between n_h and n_{h+1}. If we again denote $n_1 = s$, $n_{h+1} = v$ and $n_h = u$, we can calculate the energy consumed to transfer a packet of length L_d bits from source node s to destination node v in a recursive way as

$$\begin{cases} \mathcal{C}_1(\mathcal{P}(s, v)) = \frac{1}{R_{u,v}(L_d) R_{v,u}(L_e)} \left(\mathcal{C}_1(\mathcal{P}(s, u)) + \frac{\bar{\mathcal{E}}(u, v, L_d)}{R(\mathcal{P}'(u, s), L_e)} \right) \\ \mathcal{C}_2(\mathcal{P}(s, v)) = \mathcal{C}_2(\mathcal{P}(s, u)) + \frac{\bar{\mathcal{E}}(v, u, L_e)}{R(\mathcal{P}'(v, s), L_e)} \\ \mathcal{C}((\mathcal{P}(s, v)) = \mathcal{C}_1(\mathcal{P}(s, v)) + \mathcal{C}_2(\mathcal{P}(s, v)) \\ R(\mathcal{P}'(v, s), L_e) = R_{v,u}(L_e) \times R(\mathcal{P}'(u, s), L_e). \end{cases} \qquad (5.18)$$

Here, $R_{u,v}(L_d)$ is the reliability of link (u, v) for data packets of length L_d bits, and $R_{v,u}(L_e)$ is the reliability of link (v, u) for end-to-end acknowledgments of length L_e bits. Furthermore, $R(\mathcal{P}'(u, s), L_e)$ and $R(\mathcal{P}'(v, s), L_e)$ are the reliability of reverse paths $\mathcal{P}'(u, s)$ and $\mathcal{P}'(v, s)$ for end-to-end acknowledgments.

It is clear that (5.18) is not characteristically similar to Dijkstra's recursive equation in (5.1). even if instead of (5.1), we use the recursive equation of (5.18) in Dijkstra's algorithm, we can again show that Theorem 1 is not true anymore. The problem originates from the fact that the energy cost of a path depends on the energy cost of its reverse path for transferring the acknowledgment from the destination to the source. Thus, to calculate the energy cost from the source to any intermediate node, we need to know the energy cost of the reverse path from the destination to that intermediate node as well. This *reverse path dependency* adds to the complexity of finding MEPs. The dependency is resulted by $R'_{n_{i+1}}$ in (5.14), which itself depends on the reliability of links in the reverse path from the destination to the intermediate node n_i in that path (see (4.8)). To be able to find MEPs when only end-to-end retransmission is supported, we propose two heuristic solutions $\mathcal{H}_1$ and $\mathcal{H}_2$.

5.2.3.1 Heuristic Solution $\mathcal{H}_1$

Assume that we can neglect the effect of acknowledgement packets on the expected amount of energy consumed for end-to-end transmission of data packets. With this assumption, (5.14) reduces to

$$
\begin{aligned}
\mathcal{C}(\mathcal{P}(n_1, n_{h+1})) &= \frac{1}{R_{n_{h+1}}} \sum_{i=1}^{h} R_{n_i} \bar{\mathcal{E}}(n_i, n_{i+1}, L_d) \\
&= \sum_{i=1}^{h} \frac{\bar{\mathcal{E}}(n_i, n_{i+1}, L_d)}{\prod_{j=i}^{h} R_{n_j, n_{j+1}}} \\
&= \frac{1}{R_{n_h, n_{h+1}}} \left[C(\mathcal{P}(n_1, n_h)) + \bar{\mathcal{E}}(n_h, n_{h+1}, L_d) \right].
\end{aligned}
\tag{5.19}
$$

On the basis of the expression given for $\mathcal{C}(\mathcal{P}(n_1, n_{h+1}))$ in (5.19), we can extract the following recursive expression for computing the energy cost of a path from a source node s to a destination node v:

$$
\begin{cases}
\mathcal{C}(\mathcal{P}(s, v)) = \frac{1}{R_{u,v}(L_d)} \left[\mathcal{C}(\mathcal{P}(s, u)) + w_{u,v} \right] \\
w_{u,v} = \bar{\mathcal{E}}(u, v, L_d)
\end{cases}
\tag{5.20}
$$

The recursive equation in (5.20) is a generalized version of Dijkstra's recursive equation in (5.1), because (5.20) simplifies to (5.1) if we assume $R_{u,v}(L_d) = 1$. Hence, on the basis of (5.20), we can design a generalized version of Dijkstra's shortest-path routing algorithm for finding MEPs when only end-to-end retransmission is supported. This is achieved by replacing the command $temp \leftarrow C(u) + w_{u,v}$ in Dijkstra's algorithm (Algorithm 1) with $temp \leftarrow \frac{1}{R_{u,v}(L_d)} [C(u) + w_{u,v}]$. With this change, we can easily show that Theorem 1 is still valid.

If only end-to-end retransmission is supported, $\bar{\mathcal{E}}(u, v, L_d)$ is similar to the one defined for the case of packet transfer without MAC retransmission in (5.11). Therefore, the link weight $w_{u,v}$ could again be calculated using (5.12) after normalizing with respect to the packet size L_d:

$$
w_{u,v} = \epsilon + \alpha + \beta d_{u,v}^{\eta}.
\tag{5.21}
$$

Note that although reliability of links are not considered in computing $w_{u,v}$ in (5.21), it is considered in computing the total energy cost in (5.20).

5.2.3.2 Heuristic Solution $\mathcal{H}_2$

$\mathcal{H}_1$ neglects the effect of acknowledgement packet on the energy cost. Nevertheless, if size of the acknowledgement packet is not small compared to size of the data packet, this assumption may not be a valid assumption. In heuristic solution $\mathcal{H}_2$,

we consider the impact of the acknowledgement packet on the energy cost. In this solution, the energy cost of packet transfer from source node s to destination node v is calculated using a recursive expression which is given as follows:

$$\begin{cases} \mathcal{C}(\mathcal{P}(s,v)) = \frac{1}{R_{u,v}(L_d)R_{v,u}(L_e)} \left[\mathcal{C}(\mathcal{P}(s,u)) + w_{u,v} \right] \\ w_{u,v} = \bar{\mathcal{E}}(u,v,L_d) + \bar{\mathcal{E}}(v,u,L_e). \end{cases} \tag{5.22}$$

As (5.22) suggests, $\mathcal{H}_2$ considers the effect of reliability of reverse links as well as the energy consumed to forward the acknowledgement across reverse links. $\mathcal{H}_2$ also resolves the reverse path dependency that (5.18) suffers from, since the energy cost from source node s to destination node v only depends on the reliability of links between the source node and the destination node.

It is clear that (5.22) is also a generalized version of Dijkstra's recursive equation (5.1), because it simplifies to (5.1) if we assume $R_{u,v}(L_d) = 1$ and $R_{v,u}(L_e) = 1$. Hence, on the basis of (5.22), we can design another generalized version of Dijkstra's shortest-path routing algorithm for finding MEPs when only end-to-end retransmission is supported. This is achieved by replacing the command $temp \leftarrow C(u) + w_{u,v}$ in Dijkstra's algorithm (Algorithm 1) with $temp \leftarrow \frac{1}{R_{u,v}(L_d)R_{u,v}(L_d)} [C(u) + w_{u,v}]$.

To calculate the link weight $w_{u,v}$ in $\mathcal{H}_2$, we expand $\bar{\mathcal{E}}(u,v,L_d)$ and $\bar{\mathcal{E}}(v,u,L_e)$ using (4.3) and (4.2). Thus, we have

$$w_{u,v} = (L_d + L_e)(\epsilon + \alpha + \beta d_{u,v}^{\eta}).$$

Since the constant term $L_d + L_e$ appears in the energy cost of all links, we can use a normalized version of $w_{u,v}$ to resolve the dependency of energy costs of routes to the size of data and acknowledgment packets. Thus, $w_{u,v}$ in $\mathcal{H}_2$ could be simply computed as

$$w_{u,v} = \epsilon + \alpha + \beta d_{u,v}^{\eta}. \tag{5.23}$$

This is similar to the link weight in $\mathcal{H}_1$, but the way the the energy cost of a path is computed is different from that of $\mathcal{H}_1$.

5.2.4 Packet Transfer with MAC and End-to-end Retransmissions

For this case, (4.9) defines the expected amount of energy which is approximately consumed for end-to-end packet transfer:

$$\mathcal{C}(\mathcal{P}(n_1, n_{h+1})) \approx \sum_{i=1}^{h} \bar{\mathcal{E}}(n_i, n_{i+1}, L_d) + \sum_{i=1}^{h} \bar{\mathcal{E}}(n_{i+1}, n_i, L_e). \tag{5.24}$$

We use this approximate expression to devise a heuristic solution for finding MEPs when both MAC and end-to-end retransmissions are supported. To this end, we express (5.24) alternatively as

$$\mathcal{C}(\mathcal{P}(n_1, n_{h+1})) = \mathcal{C}(\mathcal{P}(n_1, n_h)) + \left[\bar{\mathcal{E}}(n_h, n_{h+1}, L_d) + \bar{\mathcal{E}}(n_{h+1}, n_h, L_e)\right]. \qquad (5.25)$$

On the basis of (5.25), we can calculate the energy cost for packet transfer from a source node s to a destination node v in a recursive way as follows:

$$\begin{cases} \mathcal{C}(\mathcal{P}(s, v)) = \mathcal{C}(\mathcal{P}(s, u)) + w_{u,v} \\ w_{u,v} = \bar{\mathcal{E}}(u, v, L_d) + \bar{\mathcal{E}}(v, u, L_e) \end{cases} \qquad (5.26)$$

where $\bar{\mathcal{E}}(u, v, L_d)$ is the energy cost for transferring the data packet through (u, v) and $\bar{\mathcal{E}}(v, u, L_e)$ is the energy cost for transferring the end-to-end acknowledgment through (v, u). The recursive equation in (5.26) is characteristically similar to Dijkstra's recursive equation. Therefore, we can use Dijkstra's algorithm to find the MEP from a source node s to destination node v, if we define the link weight as

$$w_{u,v} = \bar{\mathcal{E}}(u, v, L_d) + \bar{\mathcal{E}}(v, u, L_e).$$

Since MAC retransmission is supported, $\bar{\mathcal{E}}(u, v, L_d)$ and $\bar{\mathcal{E}}(v, u, L_e)$ are computed using (4.3) and (4.1). Thus, we have

$$w_{u,v} = \left[L_d\bar{\mathcal{X}}_{u,v}(L_d) + L_a\left(\bar{\mathcal{Y}}_{u,v}(L_a) + \bar{\mathcal{Y}}_{v,u}(L_a)\right) + L_e\bar{\mathcal{X}}_{v,u}(L_e)\right](\epsilon + \alpha + \beta d_{u,v}^\eta). \tag{5.27}$$

It is obvious that the link weight in (5.27) is a function of the energy consumption parameters of nodes (ϵ, α, and β) as well as the expected transmission counts of data and acknowledgment packets ($\bar{\mathcal{X}}_{u,v}(L_d)$, $\bar{\mathcal{Y}}_{u,v}(L_a)$, $\bar{\mathcal{Y}}_{v,u}(L_a)$, and $\bar{\mathcal{X}}_{v,u}(L_e)$).

We have summarized in Algorithm 2, the suite of RMER algorithms which we designed in this section for various types of packet transfer. Since the RMER algorithm is based on the Dijkstra's algorithm, its complexity is the same as the complexity of the Dijkstra's algorithm. In other words, the time complexity of the RMER algorithms is $O(|\mathbb{V}|^2)$ in dense networks and $O(|\mathbb{E}| + |\mathbb{V}|\log(|\mathbb{V}|))$ in sparse networks.

5.3   Comparison of RMER with Earlier Schemes

In this section, we review other energy-efficient routing schemes from the literature to show the significance of RMER with regard to these schemes.

Algorithm 2 RMER algorithm for finding MEP from a source node s to any other node in the network. If no retransmission is supported, $w_{u,v}$ is as given in (5.12). If only MAC retransmission is supported, $w_{u,v}$ is as given in (5.13). For the heuristic solution $\mathcal{H}_1$, $w_{u,v}$ is given in (5.21). For the heuristic solution $\mathcal{H}_2$, $w_{u,v}$ is given in (5.23). If both MAC and end-to-end retransmissions are supported, $w_{u,v}$ is given in (5.27).

  RMER($G(\mathbb{V}, \mathbb{E})$, s)
  $C(s) = 0$
  for each node $v \in \mathbb{V} - \{s\}$ **do**
    $C(v) \leftarrow \infty$
    $\mathcal{T}(v) \leftarrow \emptyset$
  end for
  $\mathcal{Q} \leftarrow \mathbb{V}$
  while $\mathcal{Q} \neq \emptyset$ **do**
    $u \leftarrow v \in \mathcal{Q} \mid C(v)$ is minimum
    $\mathcal{Q} \leftarrow \mathcal{Q} - u$
    for each neighbor $v \in \mathcal{Q}$ of u **do**
      if Only E2E Retransmission **then**
        if $\mathcal{H}_1$ **then**
          $temp \leftarrow \frac{1}{R_{u,v}(L_d)} \left[C(u) + w_{u,v} \right]$
        end if
        if $\mathcal{H}_2$ **then**
          $temp \leftarrow \frac{1}{R_{u,v}(L_d)R_{u,v}(L_e)} \left[C(u) + w_{u,v} \right]$
        end if
      else
        $temp \leftarrow C(u) + w_{u,v}$
      end if
      if $temp < C(v)$ **then**
        $C(v) \leftarrow temp$
        $\mathcal{T}(v) \leftarrow \mathcal{T}(u) \cup (u, v)$
      end if
    end for
  end while

5.3.1   PAMAS, PARO, and MTTPR Algorithms

PAMAS [74], PARO [75], and MTTPR [82] are amongst the first energy-efficient routing schemes proposed for wireless multi-hop networks. They find routes in which the total *transmission power* required to transmit a packet to the destination is minimized. Since the required transmission power in each hop is proportional to the distance between the sender and receiver in that hop, these schemes calculate the cost of a path from s to v as

$$\begin{cases} \mathcal{C}(\mathcal{P}(s,v)) = \mathcal{C}(\mathcal{P}(s,u)) + w_{u,v} \\ w_{u,v} = d_{u,v}^{\eta}. \end{cases} \tag{5.28}$$

They use Dijkstra's algorithm to find the energy-efficient paths. Nevertheless, this traditional definition of energy-efficient path neither considers the energy consumed by processing elements of transceivers nor the effect of packet retransmission. RMER considers both of them.

5.3.2   MPR Algorithm

The drawback of PAMAS, PARO, and MTTPR, has partially been addresses in [77] by taking into account the effect of MAC retransmissions on energy consumption of nodes. The proposed scheme in [77] calculates the cost of a path from s to v in a recursive way as

$$\mathcal{C}(\mathcal{P}(s,v)) = \mathcal{C}(\mathcal{P}(s,u)) + \frac{d_{u,v}^{\eta}}{p_{u,v}(L_d)}, \tag{5.29}$$

in which $p_{u,v}(L_d)$ is the PDR of (u,v) for packets of length L_d bits. We refer to this scheme as Minimum Power Routing (MPR). The main drawback of MPR is neglecting the energy consumed by processing elements of transceivers.

5.3.3   BAMER Algorithm

BAMER has been proposed in [78] for packet transfer with only end-to-end retransmissions. BAMER calculates the energy cost of a path from s to v in a recursive way as follows:

$$\begin{cases} \mathcal{C}(\mathcal{P}(s,v)) = \frac{1}{R_{u,v}(L_d)} \left(\mathcal{C}(\mathcal{P}(s,u)) + w_{u,v} \right) \\ w_{u,v} = d_{u,v}^{\eta}. \end{cases} \tag{5.30}$$

BAMER is similar to our proposed heuristic solutions $\mathcal{H}_1$ and $\mathcal{H}_2$. Nevertheless, $\mathcal{H}_1$ includes the energy consumed by processing elements of transceivers while BAMER neglects it. Apart from this, BAMER does not consider the fact that a data packet might be retransmitted by the source node if the acknowledgment is lost while being

routed from the destination to the source. Our proposed heuristic solution $\mathcal{H}_2$ takes this fact into account.

Compared to the existing schemes, we covered all possible cases of packet transfer (with and without MAC and end-to-end retransmissions), while we also used a more realistic energy consumption model in the design of the RMER algorithm.

5.4   Practical Considerations

In this section, we clarify some issues regarding implementation of RMER in wireless multi-hop networks. We explain how we can compute link weights as defined by the RMER algorithm, and how we can implement RMER on top of a routing protocol.

5.4.1   Computing Link Weights in RMER

To compute link weights in RMER, the following information is required:

1. *Energy Consumption Parameters of Nodes:* Each node needs to know its energy consumption parameters ϵ_r, α, and β as defined and explained in Chapter 3. These parameters could be calculated offline and saved in a configuration file in each node.

2. *Distance Between Nodes:* Each node needs to know its distance to its neighbors. Lightweight localization techniques proposed for wireless networks could be used to estimate distance between nodes (e.g., [91–94]). These localization techniques usually use the received signal strength to estimate the distance between a sending and a receiving node. Since the transmission power attenuates according to the power law with the distance, the received signal strength have some information about the traversed distance by the wave. Enhanced signal processing techniques are used to extract this information and obtain an accurate estimate of distance between the sender and the receiver.

3. *PDR of Links:* Depending on whether MAC and end-to-end retransmissions are supported, $p_{u,v}(L_d)$, $p_{u,v}(L_a)$ and $p_{u,v}(L_e)$ must be known for computing the link weight $w_{u,v}$. Knowing these values, nodes can calculate the expected number of transmission attempts for data packets $\bar{\mathcal{X}}_{u,v}(L_d)$, end-to-end acknowledgments $\bar{\mathcal{X}}_{v,u}(L_e)$, and MAC acknowledgments $\bar{\mathcal{Y}}_{v,u}(L_a)$. We can use any link quality estimation methods proposed for wireless networks to estimate the PDR of links. It could be a packet based technique in which periodic Hello messages [84], periodic unicast packets [95] or data traffic [96] are used to estimate the PDR of links. We can also use an SNR-based technique [97, 98],

which uses the received signal strength to determine the PDR of links using an SNR to PDR mapping profile.

Here, we briefly explain how the PDR of a link (u, v) could be estimated using periodic Hello messages. To this end, u broadcasts Hello messages with sequence numbers. Its neighbor v counts the number of received Hello messages from u to estimate the PDR of the link (u, v). Similarly, u can estimate the PDR of (v, u) counting the Hello messages that it receives from v[1]. Each node broadcasts the measured values in Hello messages that it propagates. In this way, nodes learn about the PDR of links between themselves and their neighbors as well as links between their neighbors and themselves. These values can approximate the PDR of links for data packets $p_{u,v}(L_d)$, end-to-end acknowledgments $p_{u,v}(L_e)$, and MAC acknowledgments $p_{u,v}(L_a)$.

5.4.2   Dependency of Energy-efficient Routes to Packet Size

Energy-efficient routes found by RMER could be dependent on the size of data and acknowledgment packets. In two types of packet transfer, with only MAC retransmission and with both MAC and end-to-end retransmissions, this dependency could be observed through direct dependency of link weights on size of data and acknowledgement packets. Such a direct dependency is not observed in the two other types, i.e., when retransmission is not supported or only end-to-end retransmission is supported. Nevertheless, since the PDR of links is considered in finding optimal routes by the heuristic solutions $\mathcal{H}_1$ and $\mathcal{H}_2$, and the PDR is generally dependent on the packet size, energy-efficient routes in $\mathcal{H}_1$ and $\mathcal{H}_2$ are indirectly dependent to the packet size. This type of dependency is also observed in packet transfer with only MAC retransmission and with both MAC and end-to-end retransmissions. We, however, should notice that energy-efficient routes should be independent of the size of data packets, because packets with different sizes might be routed through the same routes. Finding energy-efficient routes for any size of data packets adds to the complexity of routing protocol.

Regarding the direct dependency of energy-efficient routes to the packet size, we discuss the two cases of packet transfer, i.e., with only MAC retransmission and with both MAC and end-to-end retransmissions, separately. First, we assume that only MAC retransmission is supported. In this case, we can neglect $L_a \bar{\mathcal{Y}}_{v,u}(L_a)$ compared to $L_d \bar{\mathcal{X}}_{u,v}(L_d)$, because usually $L_d \bar{\mathcal{X}}_{u,v}(L_d) >> L_a \bar{\mathcal{Y}}_{v,u}(L_a)$. To clarify the point, let us take an example. Suppose that $L_d = 1600$, $L_a = 384$ (in the IEEE 802.11b standard), and BER of the forward link (u, v) and reverse link (v, u) is

---

[1]At the same time, nodes can also estimate their distance to each other using the signal strength indicator of the received Hello messages

5×10^{-4}. Thus, $p_{u,v}(L_d) = 0.44$ and $p_{v,v}(L_a) = 0.96$. If there is no limitation on the number of MAC retransmissions, then $\bar{\mathcal{X}}_{u,v}(L_d) = 1/(p_{u,v}(L_d)p_{v,u}(L_a)) = 2.36$, and $\bar{\mathcal{Y}}_{u,v}(L_a) = 1/p_{v,u}(L_a) = 1.04$. It is obvious that $L_d\bar{\mathcal{X}}_{u,v}(L_d) = 3824 >> L_a\bar{\mathcal{Y}}_{v,u}(L_a) = 399.3$. Therefore, when only MAC retransmission is supported, we can simplify the link weights in RMER by neglecting $L_a\bar{\mathcal{Y}}_{v,u}(L_a)$ compared to $L_d\bar{\mathcal{X}}_{u,v}(L_d)$. This results in

$$w_{u,v} = L_d\bar{\mathcal{X}}_{u,v}(L_d)(\epsilon_r + \alpha + \beta d_{u,v}^\eta).$$

We can further normalize $w_{u,v}$ with respect to the packet size L_d without changing the ranking of routes. Hence, when only MAC retransmission is supported, $w_{u,v}$ can be simply calculated as follows:

$$w_{u,v} = \bar{\mathcal{X}}_{u,v}(L_d)(\epsilon_r + \alpha + \beta d_{u,v}^\eta). \tag{5.31}$$

This resolves the direct dependency of link weights on the packet size L_d. Nevertheless, we still can observe the indirect dependency through dependency of $\bar{\mathcal{X}}_{u,v}(L_d)$ to the packet size L_d. This will be discussed later.

Now, assume both MAC and end-to-end retransmissions are supported. For this case, the link weight was defined in (5.27):

$$w_{u,v} = \left[L_d\bar{\mathcal{X}}_{u,v}(L_d) + L_a\left(\bar{\mathcal{Y}}_{u,v}(L_a) + \bar{\mathcal{Y}}_{v,u}(L_a)\right) + L_e\bar{\mathcal{X}}_{v,u}(L_e)\right](\epsilon + \alpha + \beta d_{u,v}^\eta).$$

In this case, we neglect $L_a\bar{\mathcal{Y}}_{v,u}(L_a)$ compared to $L_d\bar{\mathcal{X}}_{u,v}(L_d)$, and $L_a\bar{\mathcal{Y}}_{u,v}(L_a)$ compared to $L_e\bar{\mathcal{X}}_{v,u}(L_e)$. This results in

$$w_{u,v} = \left[L_d\bar{\mathcal{X}}_{u,v}(L_d) + L_e\bar{\mathcal{X}}_{v,u}(L_e)\right](\epsilon + \alpha + \beta d_{u,v}^\eta),$$

Note that $\bar{\mathcal{X}}_{u,v}(L_d)$ is estimated using broadcast Hello messages or unicast packets with fixed sizes. To resolve the direct dependency of the link weight to the packet size, we can replace L_d with the size of Hello message L_{hello} (or the unicast packets) and let the size of a Hello message be the size of the end-to-end acknowledgement (i.e., $L_{hello} = L_e$). With these choices, we have

$$w_{u,v} = L_{hello}\left[\bar{\mathcal{X}}_{u,v}(L_d) + \bar{\mathcal{X}}_{v,u}(L_e)\right](\epsilon + \alpha + \beta d_{u,v}^\eta).$$

which could be simplified to

$$w_{u,v} = \left[\bar{\mathcal{X}}_{u,v}(L_d) + \bar{\mathcal{X}}_{v,u}(L_e)\right](\epsilon + \alpha + \beta d_{u,v}^\eta). \tag{5.32}$$

We again note that the link weight in (5.32) is not directly proportional to the packet size. However, there is still the indirect dependency on packet size through the expected transmission counts of data and acknowledgement packets.

There is an important point regarding the indirect dependency of energy-efficient routes on packet size. We notice that the PDR of a link needs to be estimated using a link quality estimation method. The estimated PDR, however, is for a specific packet size (e.g., the size of Hello messages). Estimating the PDR of links for various packet sizes using a single packet size may not be very accurate as shown in Figure 5.1. The figure, however, shows that if BER of links is very small, such estimation could still be accurate. Estimation of the PDR of links using a reference packet size has the benefit that we do not need to estimate the PDR of a link for different packet sizes.

5.4.3   Cross Layer Dependency of Energy-efficient Routes

Finding energy-efficient routes using RMER necessitates a cross-layer dependency between routing (which is handled at the network layer) to the physical, MAC, and transport layers. This dependency comes from the energy consumption parameters of nodes and the PDR of links, which are dependent on the physical layer, and the impact of retransmissions triggered by the MAC and transport layers. Although this dependency can result in a cross-layer optimization across various layers of the communication stack, it may add to the complexity of routing at the network layer.

The main complexity originates from the dependency of energy-efficient routes to the support of MAC and end-to-end retransmissions. In some multi-hop networks, we may only face one of the four types of packet transfer. Thus, nodes need to deploy only the variant of RMER algorithm designed and optimized for such type of packet transfer. For instance, in a network which deploys IEEE 802.11g as the link technology and only supports UDP traffic, packet transfer is supported with only MAC retransmissions. Hence, all nodes need to find MEPs for the case of packet transfer with only MAC retransmission. In some other networks, however, we may face more than one type of packet transfer. For instance, assume in addition to UDP traffic, TCP traffic is also supported in an IEEE 802.11g network. This means, two types of packet transfer will be supported in the network: with only MAC retransmission and with both MAC and end-to-end retransmissions. Hence, each node needs to find MEPs to any other node suitable for these two types of packet transfer. Now, assume instead of IEEE 802.11g, we deploy IEEE 802.15.4 as the link technology and both UDP and TCP traffic is supported. Since in the IEEE 802.15.4 standard support for MAC retransmission is optional, for some traffic MAC retransmission might not be supported. This means, we can have all four types of packet transfer in the network. In such a case, each node has to maintain four different routes to any other node in the network. Depending on whether MAC and end-to-end retransmissions are supported for a session between a source and a destination, appropriate routes must be used. This, indeed, adds to the complexity of the routing protocol. The question is, whether for such cases we can reduce this
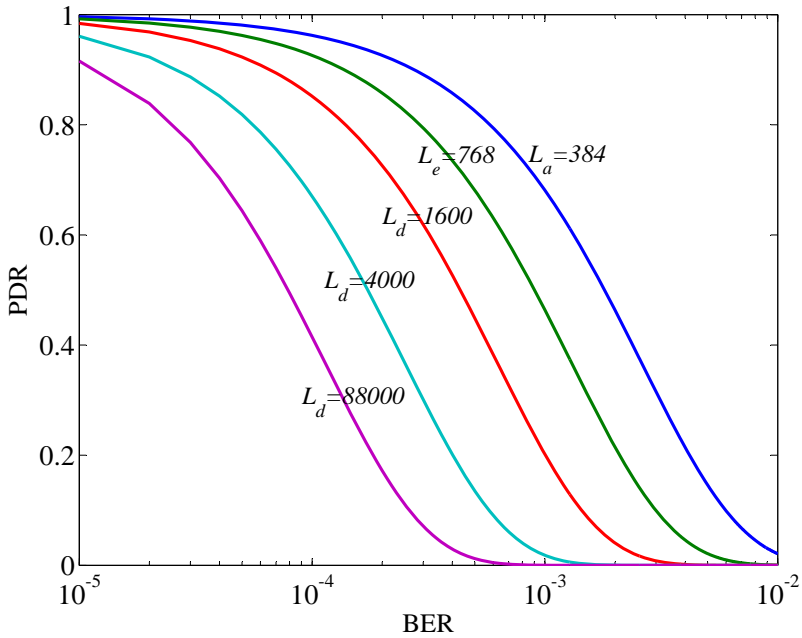
Figure 5.1 – PDR of a link in terms of its BER for various packet sizes. Here, $L_a = 384$ [bit] is the size of the MAC acknowledgment in the IEEE 802.11b standard with short preamble. $L_e = 768$ [bit] is the size of end-to-end acknowledgment if we use the IEEE 802.11 standard with short preamble plus the TCP/IPv4 suite and assuming the end-to-end acknowledgement has the same format as that of a TCP acknowledgment.

Table 5.1 – The definition of link weight in various energy-efficient routing algorithms.

Algorithm	Link Weight $w_{u,v} =$
RMER (no retx.)	$\epsilon_r + \alpha + \beta d_{u,v}^\eta$
RMER (MAC retx.)	$\left(L_d \bar{\mathcal{X}}_{u,v}(L_d) + L_a \bar{\mathcal{Y}}_{v,u}(L_a) \right)(\epsilon_r + \alpha + \beta d_{u,v}^\eta)$
RMER (E2E retx. $\mathcal{H}_1$)	$\epsilon_r + \alpha + \beta d_{u,v}^\eta$
RMER (E2E retx. $\mathcal{H}_2$)	$\epsilon_r + \alpha + \beta d_{u,v}^\eta$
RMER (MAC and E2E retx.)	$\left[L_d \bar{\mathcal{X}}_{u,v}(L_d) + L_a \left(\bar{\mathcal{Y}}_{u,v}(L_a) + \bar{\mathcal{Y}}_{v,u}(L_a) \right) + L_e \bar{\mathcal{X}}_{v,u}(L_e) \right](\epsilon_r + \alpha + \beta d_{u,v}^\eta)$
Unified RMER	$\bar{\mathcal{X}}_{u,v}(\epsilon_r + \alpha + \beta d_{u,v}^\eta)$
PAMAS	$d_{u,v}^\eta$
PARO	$d_{u,v}^\eta$
MTTPR	$d_{u,v}^\eta$
MPR	$d_{u,v}^\eta / p_{u,v}(L_d)$
BAMER	$d_{u,v}^\eta$

complexity without sacrificing energy-efficiency of routes. More specifically, can we use a unified algorithm for finding energy-efficient routes in various types of packet transfer?

Although the optimal route in different modes[1] of the RMER algorithm might be different, three out of four modes consider both energy consumption characteristics of nodes and reliability of links in route selection. We use this fact to come up with a unified energy-efficient routing algorithm which considers information about energy consumption characteristics of nodes and reliability of links. In the unified algorithm that we propose, link weights are calculated using the simplified expression in (5.31), which was obtained for the case of packet transfer with only MAC retransmissions. Although, this definition of link weight is different from that of packet transfer in the other three modes, we will show through simulation results that the same energy efficiency could be achieved if link weights are defined as in (5.31). Algorithm 3 shows our proposed unified algorithm for finding MEPs, which we name *Unified RMER*. In the Unified RMER algorithm, $\bar{\mathcal{X}}_{u,v}$ is the Expected Transmission Count (ETX) of (u, v) which is estimated using Hello messages or any other link quality estimation technique. We have summarized in Table 5.1 the definition of link weight in various energy-efficient routing algorithms introduced in this chapter including the Unified RMER.

---

[1]Here, mode refers to the type of packet transfer.

Algorithm 3 Unified RMER algorithm for finding MEP from a source node s to any other node v in the network.

$\text{RMER}(G(\mathbb{V}, \mathbb{E}), s)$
$C(s) = 0$
for each node $v \in \mathbb{V} - \{s\}$ **do**
    $C(v) \leftarrow \infty$
    $\mathcal{T}(v) \leftarrow \emptyset$
end for
$\mathcal{Q} \leftarrow \mathbb{V}$
while $\mathcal{Q} \neq \emptyset$ **do**
    $u \leftarrow v \in \mathcal{Q} \mid C(v)$ is minimum
    $\mathcal{Q} \leftarrow \mathcal{Q} - u$
    for each neighbor $v \in \mathcal{Q}$ of u **do**
        $w_{u,v} \leftarrow \bar{\mathcal{X}}_{u,v}(\epsilon_r + \alpha + \beta d_{u,v}^\eta)$
        $temp \leftarrow C(u) + w_{u,v}$
        if $temp < C(v)$ **then**
            $C(v) \leftarrow temp$
            $\mathcal{T}(v) \leftarrow \mathcal{T}(u) \cup (u, v)$
        end if
    end for
end while

5.4.4 Impact of Transmission Power Control

In the design of RMER and Unified RMER algorithms, we assumed that nodes deploy TPC. The definition of TPC says that nodes adjust their transmission power to their neighbors to a minimum value satisfying a target BER requirement (see Chapter 3). If such a scheme is deployed in the network, then theoretically all links will have the same PDR assuming collision is the same or negligible for all links. As a result, the ETX of all links will be the same. That is, $\bar{\mathcal{X}}_{u,v} = \bar{\mathcal{X}}$, $\forall (u,v) \in \mathbb{E}$. Therefore, the definition of link weight, for instance in Unified RMER, could be simplified to

$$w_{u,v} = \epsilon_r + \alpha + \beta d_{u,v}^\eta$$

without changing the ranking of routes between two nodes with respect to their energy-efficiency. In such a case, Unified RMER can only find an energy-efficient route, which may not necessarily be the most reliable path. Since all links have the same PDR, the most reliable path between two nodes is the path with the minimum number of hops.

Now, let us consider a case in which nodes are not able to adjust their transmission power. They transmit signals with their maximum power to any of their neighbors. Thus, the reliability of different links may not be the same anymore.

Assuming all nodes are equipped with the same chipsets, the link weight in Unified RMER must be calculated in this way

$$w_{u,v} = \bar{\mathcal{X}}_{u,v}(\epsilon_r + \alpha + \beta D_{max}^{\eta}), \tag{5.33}$$

in wich D_{max} is the transmission range of nodes. Since the term in parentheses is the same for all links, the link weight can simply be calculated as

$$w_{u,v} = \bar{\mathcal{X}}_{u,v}$$

without changing the ranking of routes between two nodes with respect to their energy-efficiency. This means, Unified RMER selects the path with the minimum accumulated ETX similar to the proposed routing scheme in [84]. However, if various nodes have different energy consumption profiles, the link weight must still be calculated using (5.33). Considering all these various cases, we can see that Unified RMER (as well as RMER) is a generalized algorithm which considers both reliability and energy-efficiency aspects to select optimal routes in wireless multi-hop networks.

5.5   Simulation Studies

In this section, we present simulation results to study the performance of RMER and Unified RMER algorithms. The simulation set up is the same as the set up in Section 4.5. That is, 200 nodes are uniformly distributed in a square area of size 750×750 [m^2], and they are equipped with the PRISM chipset. The sizes of data, acknowledgments, and Hello packets are: $L_d = 1600$ [bit], $L_a = 384$ [bit], $L_e = 768$ [bit], and $L_{hello} = 800$ [bit]. To study the performance of the RMER algorithm, we compare the energy-efficiency and the reliability of routes discovered by RMER, Unified RMER and similar algorithms from the literature. These similar algorithms will be introduced accordingly.

5.5.1   Energy Efficiency and Reliability of Routes

To measure energy-efficiency of routes discovered by various algorithms, we compare the average amount of energy consumed to transfer a packet from a source node to a destination node. We refer to this value as *Expected Energy per Packet (EPP)*. The end-to-end reliability of a route is computed by multiplying the reliability of the constituent links of the route. When MAC level retransmission is supported, link reliability is computed considering the impact of packet retransmissions. If MAC level retransmission is not supported, link reliability is in fact the PDR of the link.

5.5.1.1 Packet Transfer without Retransmission

For this case, we compare the energy efficiency and the reliability of routes discovered by the RMER, Unified RMER, and the MTTPR algorithm [82]. When retransmission is not supported by MAC and transport layers, RMER only considers energy consumption characteristics of nodes. MTTPR considers energy consumption characteristics of nodes as well. However, it neglects the energy consumption of the transmission circuit. On the other hand, Unified RMER considers both energy consumption characteristics of nodes and reliability of links.

As depicted in Figure 5.2(b), Unified RMER finds more reliable routes compared to the other algorithms. Nevertheless, we observe in Figure 5.2(a) that this gain in reliability is at the cost of increased energy consumption when Unified RMER is used instead of RMER. The reduced energy consumption of RMER compared to Unified RMER is due to transmission of less packets by intermediate nodes as a sign of finding less reliable routes by RMER.

Energy-efficiency of routes discovered by Unified RMER might be better or worse than that of routes found by MTTPR. This depends on the link quality. When links are of low quality on the average, MTTPR is more energy efficient. When links are of high quality on the average, Unified RMER is more energy efficient. The reason again lies in the fact that when links are of low quality, nodes consume less energy to forward packets, because they receive less packets to forward. On the other hand, Unified RMER finds more reliable routes in which nodes consume more energy for packet forwarding. Nevertheless, when links are of good quality, finding longer routes by MTTPR consisting of many short hops (we have skipped the result here) is the reason for increased energy consumption by this algorithm. In each hop, the sender and the receiver have to consume energy for processing the packet. The discovered route by MTTPR may seem to be energy-efficient. However, since MTTPR neglects the energy consumed by senders for packet processing, the route is not energy-efficient in practice.

5.5.1.2 Packet Transfer with MAC Retransmission

For this case, we compare energy-efficiency and reliability of routes discovered by RMER, Unified RMER, and MPR [77]. MPR is an example from the literature which considers quality of links in route selection, but neglects the energy consumed by processing elements of transceivers. When only MAC retransmission is supported, both RMER and Unified RMER consider quality of links in route selection. The difference between them is that Unified RMER neglects the impact of MAC acknowledgments. Results depicted in Figure 5.3 show that if only MAC retransmission is supported, performance of Unified RMER is very close to that of RMER with regard to both energy-efficiency and reliability of
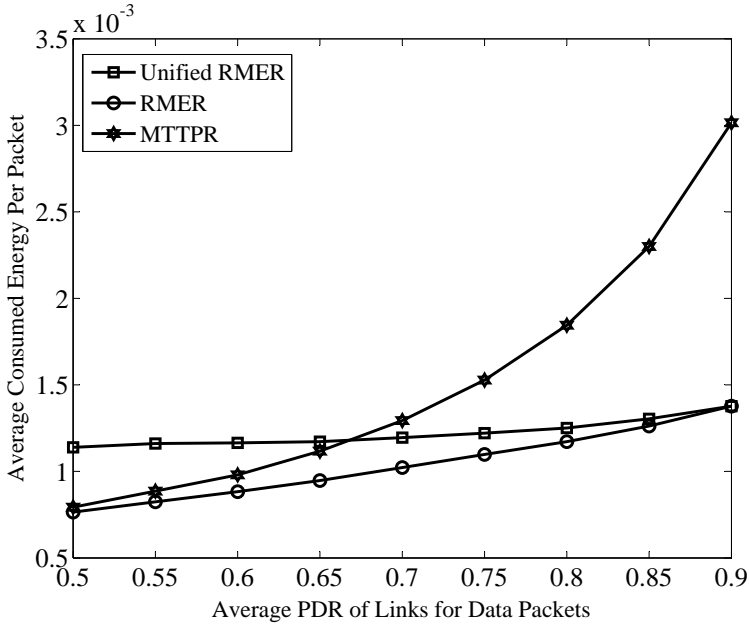
(a)
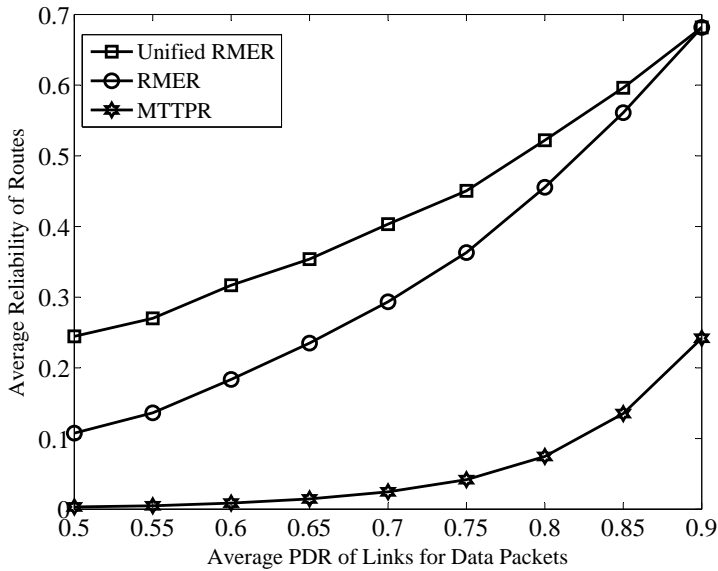
(b)

Figure 5.2 – (a) Energy-efficiency and (b) reliability of routes discovered by various routing algorithms when no retransmission is supported.

(a)
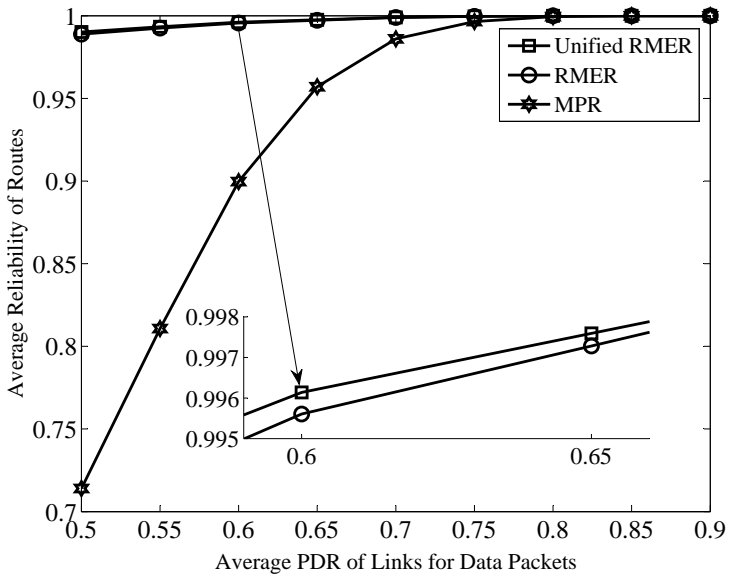
(b)

Figure 5.3 – (a) Energy-efficiency and (b) reliability of routes discovered by various routing algorithms when only MAC retransmission is supported.

routes. Furthermore, RMER and Unified RMER both are able to find more reliable and more energy-efficient routes compared to MPR. MPR only considers the transmission power of nodes. Since transmission power decays with distance, short hops are more energy-efficient than long hops. Thus, MPR will favor routes consisting of many short hops to routes consisting of few long hops. However, if the processing power is not neglected, routes consisting of many short hops can not be energy-efficient anymore. This is why RMER and Unified RMER can find more energy-efficient routes as well as more reliable routes compared to MPR.

Regarding the reliability, we notice that although transmission error in short hops is lower compared to long hops, but collision probability in wireless networks may even result in a lower PDR for short hops. As a result, when the packet has to be forwarded through many short hops probability of packet loss might even be greater compared to the case where a few long hops are used. This is why we can expect to have more reliable routes in RMER and Unified RMER rather than MPR. Considering only quality of links in route selection by MPR may not necessarily result in finding more reliable routes. A realistic energy consumption model which considers energy consumption of processing elements of transceivers is also important. The important conclusion is that *undermining the energy consumption of nodes in wireless multi-hop networks can severely affect the reliability of energy-efficient routes.*

5.5.1.3   Packet Transfer with End-to-end Retransmission

For this case, we consider RMER with heuristic solutions $\mathcal{H}_1$ and $\mathcal{H}_2$, Unified RMER and the BAMER algorithm [78]. Similar to previous cases, we plot the average reliability of routes and the expected energy consumed per packet. Furthermore, we plot the average reliability of reverse routes which transfer the end-to-end acknowledgment from the destination to the source.

Plots in Figure 5.4 show that routes discovered by Unified RMER are the most energy-efficient and reliable routes. Although $\mathcal{H}_1$ and $\mathcal{H}_2$ are designed to find MEPs when only end-to-end retransmissions are supported, we should not forget that they are only heuristic solutions. For the configuration that we have considered in our simulations, Unified RMER has been able to find more energy efficient and more reliable routes. We also observe that $\mathcal{H}_2$, which considers the effect of energy consumed for routing the end-to-end acknowledgments, can find more energy-efficient routes compared to $\mathcal{H}_1$ and BAMER, which neglects this effect. Nevertheless, routes discovered by $\mathcal{H}_1$ are more reliable than routes discovered by $\mathcal{H}_2$. However, reverse routes are more reliable when $\mathcal{H}_2$ is used. This is due the fact that $\mathcal{H}_2$ considers reliability of both forward and reverse links, while $\mathcal{H}_1$ only considers reliability of forward links. In summary, we can say that compared to $\mathcal{H}_1$, $\mathcal{H}_2$ provides a better compromise between reliability of forward and reverse routes.
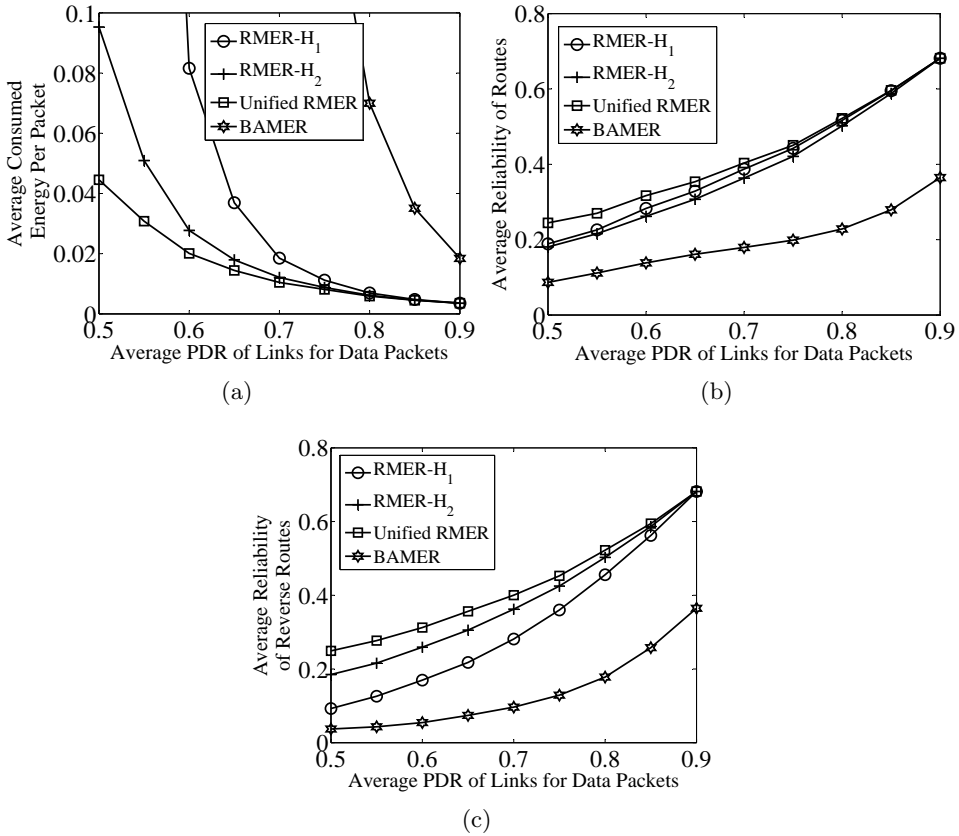
Figure 5.4 – (a) Energy-efficiency, (b) reliability of forward routes, and (c) reliability of reverse routes discovered by various routing algorithms when only end-to-end retransmission is supported.

5.5.1.4   Packet Transfer with MAC and End-to-end Retransmissions

For this case, we consider RMER designed for this type of packet transfer as well as Unified RMER and MPR [77] algorithms. Results depicted in Figure 5.5 show that energy-efficiency and reliability of routes discovered by RMER and Unified RMER are very close to each other and much better than those of MPR.

5.5.2   Packet Transfer without Power Control

So far, we observed that Unified RMER is able to find more energy-efficient and reliable routes compared to other energy-efficient routing algorithms from the literature. In this section, we compare energy-efficiency of routes discovered by Unified RMER with that of min-hop routes and routes discovered by Unified RMER when transmission power control is not supported.

The first set of results show the EPP of discovered routes by various schemes as a function of average node degree in the network (Figure 5.6). Unified RMER with transmission power control finds more energy-efficient routes compared to other schemes. The second set of results show the energy cost of routes when maximum collision probability with power control is a fraction of the maximum collision probability without power control (Figure 5.7). We observe that reducing the collision probability due to TPC improves energy efficiency of routes discovered by Unified RMER compared to other schemes.

5.6   Summary

In this chapter, a suite of novel energy-efficient routing algorithms, named Reliable Minimum Energy Routing (RMER), were proposed. In the design of RMER, different types of packet transfer were considered. They are various combinations of packet transfer with and without MAC and end-to-end retransmissions. This resulted in various types of RMER algorithms optimized for different types of packet transfer in wireless multi-hop networks. To reduce the complexity of finding energy-efficient routes when all types of packet transfer are supported in a network, Unified RMER was proposed. Similar to RMER, Unified RMER considers both reliability of links and the energy consumption of nodes for selecting optimal routes. Simulation studies showed that the performance of Unified RMER is close to the performance of RMER both in terms of reliability and energy-efficiency of routes. Compared to the existing energy-efficient routing algorithms, RMER and Unified RMER save energy in wireless multi-hop networks and increase the reliability of these networks. RMER and Unified RMER do not neglect the energy cost of transmitting and receiving circuits of transceivers. Neglecting these sources of energy consumption in the design of energy-efficient routing algorithms not only
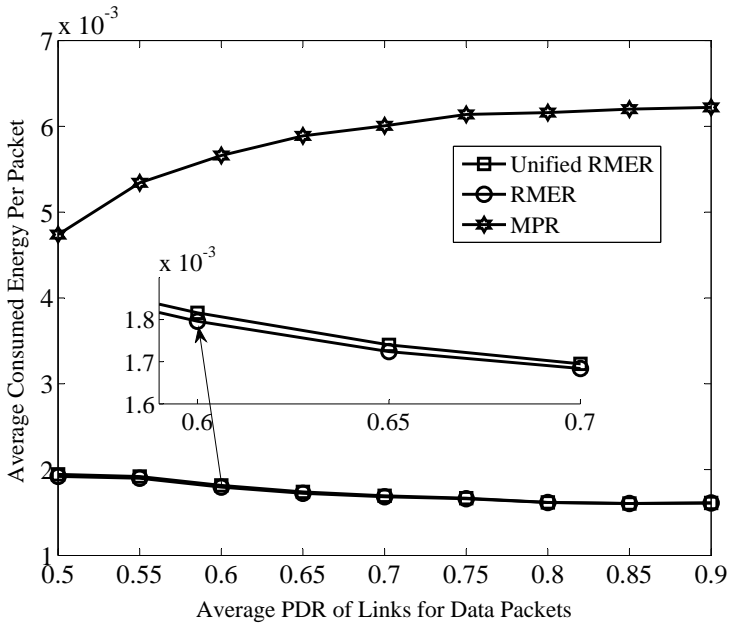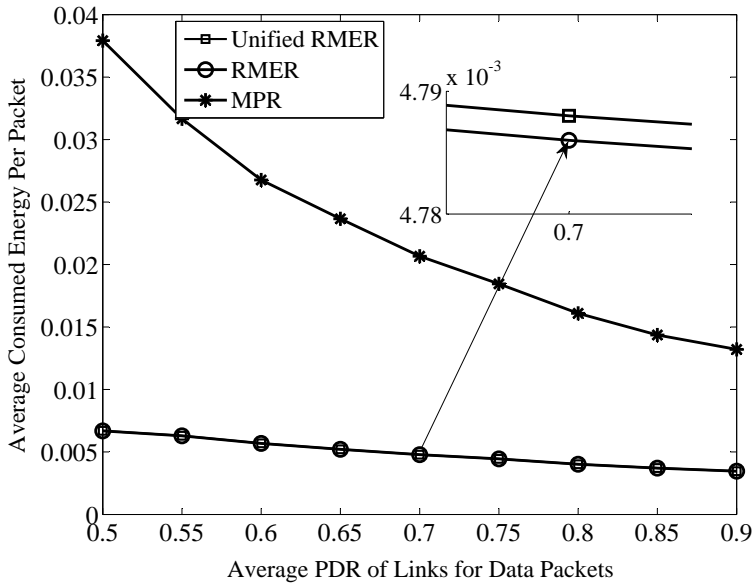
(a)
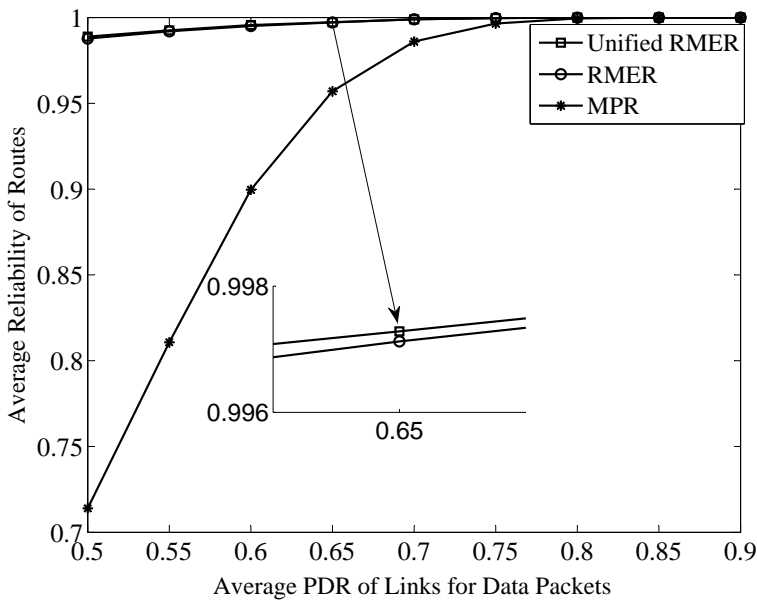
(b)

Figure 5.5 – (a) Energy-efficiency and (b) reliability of routes discovered by various routing algorithms when both MAC and end-to-end retransmissions are supported.

results in choosing high-energy cost routes in multi-hop networks, but also reduces the reliability of packet transfer in these networks.
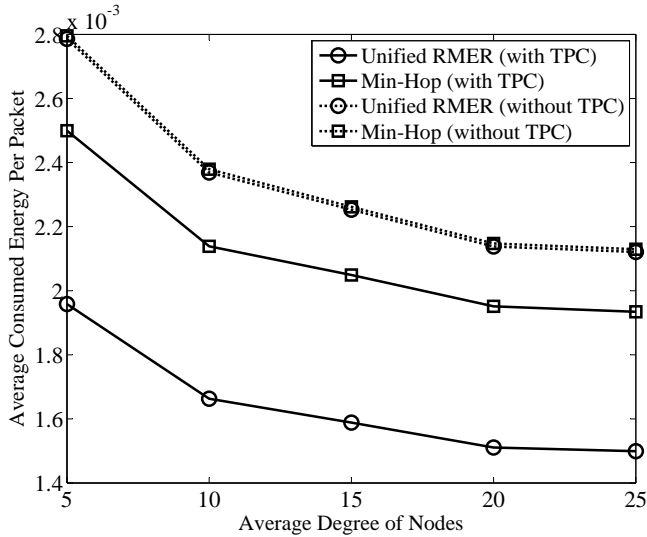
Figure 5.6 – Energy cost of discovered routes by various routing algorithms as a function of the average node degree in the network. In this experiment, the collision probability is assumed to be zero.
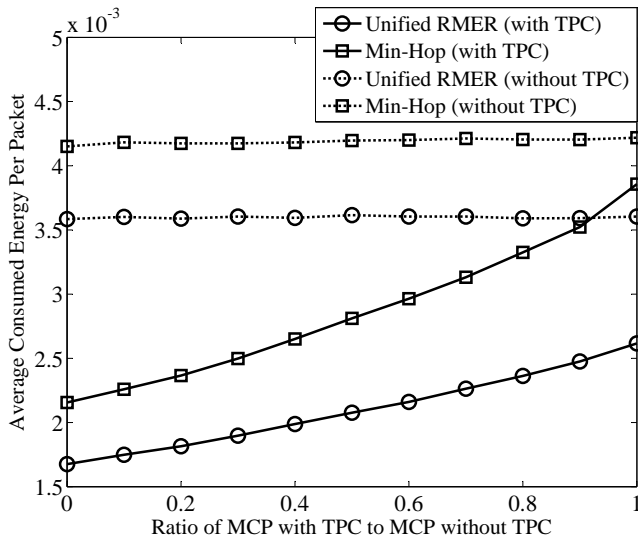
Figure 5.7 – Energy cost of discovered routes by various routing algorithms as a function of the ratio of maximum collision probability (MCP) with power control to MCP without power control. The MCP without power control has been set to 0.5, and the average node degree in the network is 10.

Chapter 6

Battery-aware Routing

In the previous chapter, we studied energy-efficient routing in wireless multi-hop networks. Although energy-efficient routing can reduce the overall energy consumption in the network, it has a drawback. Some nodes, especially those located in the center of the network, might be selected frequently as intermediate nodes of energy-efficient routes between different pairs of source-destination nodes. Such nodes need to forward many packets belonging to other nodes, which in turn, can result in their quick failure. Consequently, the network will be partitioned quickly if failed nodes are critical nodes that are keeping the network connected. We address this problem in depth in this chapter, and provide some novel solutions for it.

The key idea is to consider the remaining battery energy of nodes in route selection to avoid relaying over nodes which have low battery energy. This we call battery-aware routing. Furthermore, if there are some mains-powered nodes in the network, we can also exploit this to direct the relay traffic towards such nodes. There are several scenarios where we can have both mains-powered and battery-powered nodes in a wireless multi-hop network. For instance, in a meeting scenario, laptops of participants can form a wireless ad hoc network to exchange information during the meeting. Some laptops may be connected to the mains, while others use their batteries. Another example is home networking where devices at home exchange context [7]. In a home network, most devices are connected to the mains (e.g., appliances), while some handheld devices may run on battery (e.g., a smart phone). In these scenarios and other similar scenarios of wireless multi-hop networking, battery-aware routing schemes could be devised considering the heterogeneity of power supply of nodes to avoid –as much as possible– relaying over battery-powered devices.

As we will show in this chapter, considering the power supply and remaining battery energy of nodes in routing can prolong the operational lifetime of the network significantly. However, we should notice that routes selected in this way

may not be energy-efficient anymore. Here, there are two main research questions to be answered:

1. How to use information about remaining battery energy of nodes as well as the type of their power supply in routing.

2. How to design battery-aware routing schemes which not only prolong the operational lifetime of nodes by balancing the traffic load between them, but also provide an acceptable level of energy-efficiency and reliability.

In this chapter, we answer these questions. To this end, we first provide a succinct background of battery-aware routing in wireless multi-hop networks (Section 6.1). This helps us to partially answer the first question and also highlight weaknesses of the existing schemes. Then, we introduce our proposed battery-aware routing algorithm, called Reliable Minimum Energy Cost Routing (RMECR), in Section 6.2. RMECR resolves the drawbacks of the existing schemes by taking into account not only battery-energy of nodes in route selection but also their energy consumption characteristics as well as the reliability of links. In Section 6.3, we study battery-aware routing in networks consisting of both battery-powered and mains-powered nodes. We propose several algorithms which can differentiate between mains-powered and battery-powered nodes in routing. Section 6.4 elaborates on implementation issues of the proposed algorithms. In Section 6.5, we evaluate the performance of the battery-aware routing algorithms using simulations. We show that to take the full advantage of battery-aware routing for load balancing in wireless multi-hop networks, it must be accompanied by energy-efficiency. If energy-efficiency is not achieved, then load balancing can not be achieved either. The chapter is summarized in Section 6.6.

6.1   Background

Authors in [76,79,82,85–88,99,100] have proposed various schemes for battery-aware routing in wireless multi-hop networks. Minimum Battery Cost Routing (MBCR), Min-Max Battery Cost Routing (MMBCR), and Conditional Max-Min Battery Capacity Routing (CMMBCR) [76, 82] are among earliest proposed schemes. Schemes such as Maximum Residual Packet Capacity (MRPC) and Conditional MRPC (CMRPC) [79] and more complex schemes proposed in [86–88, 99, 100] use the principle behind the design of MBCR, MMBCR, or CMMBCR. For this reason, we briefly describe how MBCR, MMBCR, CMMBCR as well as MRPC and CMRPC, which were proposed later, use the residual battery energy of nodes in route selection.

6.1.1 MBCR Algorithm

MBCR selects a path which minimizes the accumulated battery cost of nodes to
send a packet from a source node to a destination node. The battery cost of a node
is defined as the inverse of its remaining battery energy. If a node has lower battery
energy compared to other nodes, its battery cost for packet forwarding is higher.
MBCR defines the optimal path between a source and a destination node as follows:

$$\mathcal{P}_{mbcr} = \text{argmin } \{\mathcal{C}_{mbcr}(\mathcal{P}_k)\} \qquad \forall \mathcal{P}_k \in \mathbb{Q},$$

in which, $\mathbb{Q}$ is the set of paths between the source and the destination node, and
$\mathcal{P}_k$ is the kth path between them. The path weight $\mathcal{C}_{mbcr}(\mathcal{P}_k)$ is defined as

$$\mathcal{C}_{mbcr}(\mathcal{P}_k) = \sum_{i=1}^{h_k} \frac{1}{B_{n_i} - B_{th}}, \qquad (6.1)$$

where, B_{n_i} is the residual battery energy of the ith node of the path, and h_k is
the hop count of the path. Here, B_{th} is the threshold of the remaining battery
energy of nodes for deciding whether a nodes is dead. According to (6.1), the
path cost in MBCR is the summation of the weight of individual links of the path,
where the weight of a link is the inverse value of the remaining battery energy of
the transmitting node of the link. Therefore, MBCR could be implemented using
Dijkstra's shortest-path routing algorithm, if we define the weight of each link as
follows:

$$w_{u,v}^{mbcr} = \frac{1}{B_u - B_{th}} \qquad \forall (u,v) \in \mathbb{E}. \qquad (6.2)$$

By finding a path with the minimum accumulated battery cost, MBCR tries to
find routes in which nodes are *likely* to have more remaining battery power. This
can avoid nodes from being overused, and balance the traffic load between them.
However, since the total battery cost of a route is the summation of the battery cost
of individual nodes, MBCR may not completely prevent selection of nodes with low
battery energy as relaying nodes. This problem can be mitigated by MMBCR.

6.1.2 MMBCR Algorithm

MMBCR finds a path in which the remaining battery energy of the *critical node* is
higher than that of the other paths. The critical node of a path is a node which
has the lowest battery energy in that path. In other words, the optimal path in
MMBCR is defined as follows:

$$\mathcal{P}_{mmbcr} = \text{argmax } \{\mathcal{C}_{mmbcr}(\mathcal{P}_k)\} \qquad \forall \mathcal{P}_k \in \mathbb{Q}, \qquad (6.3)$$

in which, the path weight $\mathcal{C}_{mmbcr}(\mathcal{P}_k)$ is defined as

$$\mathcal{C}_{mmbcr}(\mathcal{P}_k) = \min\{B_{n_i}\}_{i=1}^{h_k} \qquad n_i \in P_k. \qquad (6.4)$$

According to (6.4), the weight of a path in the MMBCR algorithm is the minimum residual battery energy in that path. As suggested by (6.3), MMBCR selects a path with the maximum weight between a source and a destination node. This means MMBCR uses a max-min route selection scheme, which can not be implemented using Dijkstra's shortest-path routing algorithm. Nevertheless, if we consider the remaining battery energy of the critical node of a path as the *width* of that path, which must be maximized, then the optimal path in the MMBCR algorithm will be *the widest path* between the source and the destination. Algorithm 4 shows how to find the widest path between a source node and any other node in the network according to MMBCR. In this algorithm, the weight of a link is defined as the remaining battery energy of the transmitting node of the link. That is,

$$w_{u,v}^{mmbcr} = B_u \qquad \forall (u,v) \in \mathbb{E}. \qquad (6.5)$$

The max-min route selection scheme of MMBCR can prevent selection of nodes with low battery energy as relaying nodes. Nevertheless, it could also result in selection of long routes, because there is no control on hop count of selected routes. This we will verify later in Section 6.5. Using long routes for packet transfer can increase the total energy consumption in the network. Consequently, the average energy consumption rate of individual nodes will increase. This, in turn, can reduce the lifetime of nodes. CMMBCR has been suggested in [82] to partially mitigate this problem.

6.1.3 CMMBCR Algorithm

CMMBCR is a hybrid routing algorithm that works in two different modes: MTTPR[1] mode and MMBCR mode. CMMBCR acts in MTTPR mode, if there are some paths between a source and a destination node where the remaining battery energy of their critical node lies above a certain threshold $0 \leq \gamma \leq B$ (B is the maximum battery energy of a node). Amongst such paths, CMMBCR finds the path minimizing the total transmission power required to transmit a packet from the source to the destination (similar to the MTTPR algorithm). Nevertheless, if there are no paths between the source and the destination for which the remaining battery energy of their critical nodes lies above the threshold γ, CMMBCR acts in MMBCR mode. That is, when the remaining battery energy of *at least* one node in each available path between the source and the destination falls below γ, CMMBCR selects a path according to the MMBCR algorithm.

---

[1]MTTPR is an energy-efficient routing algorithm which was introduced in Section 5.3.1

Algorithm 4 Implementation of the MMBCR algorithm using a widest-path routing algorithm for finding the optimal path from a source node s to any other node in the network.

MMBCR$(G(\mathbb{V}, \mathbb{E}), s)$
for each node $v \in \mathbb{V}$ **do**
  if v is a neighbor of s **then**
    $C(v) \leftarrow B_s$
    $\mathcal{T}(v) \leftarrow \{(s,v)\}$
  else
    $C(s) \leftarrow 0$
    $\mathcal{T}(v) \leftarrow \emptyset$
  end if
end for
$\mathcal{Q} \leftarrow \mathbb{V}$
while $\mathcal{Q} \neq \emptyset$ **do**
  $u \leftarrow v \in \mathcal{Q} \mid C(v)$ is maximum
  $\mathcal{Q} \leftarrow \mathcal{Q} - u$
  for each neighbor $v \in \mathcal{Q}$ of u **do**
    $temp \leftarrow \min(C(u), B_u)$
    if $temp > C(v)$ **then**
      $C(v) \leftarrow temp$
      $\mathcal{T}(v) \leftarrow \mathcal{T}(u) \cup (u,v)$
    end if
  end for
end while

To explain the operation of CMMBCR better, we define $\mathbb{Q}_1 \subset \mathbb{Q}$ as a set containing all paths in $\mathbb{Q}$ which satisfy the following condition:

$$\mathcal{C}_{mmbcr}(\mathcal{P}_k) > \gamma \qquad \forall \mathcal{P}_k \in \mathbb{Q},$$

where, $\mathcal{C}_{mmbcr}(\mathcal{P}_k)$ is as defined in (6.4). If $\mathbb{Q}_1 \neq \emptyset$, ($\emptyset$ is the empty set), CMMBCR selects a path from $\mathbb{Q}_1$ which minimizes the total transmission power required to transmit a packet from the source to the destination. If $\mathbb{Q}_1 = \emptyset$, then a path is selected from $\mathbb{Q}$ according to the MMBCR algorithm.

Algorithm 5 shows how CMMBCR can find the optimal path between a source node s and any other node in the network. In this algorithm, we first remove those links in $G_1(\mathbb{V}, \mathbb{E}_1)$ with a link weight smaller than γ. Let the resulting graph be $G_1'(\mathbb{V}, \mathbb{E}_1)$. Then, we find the optimal path according to MTTPR between the source node s and each node in $G_1'(\mathbb{V}, \mathbb{E}_1)$. If no path could be found to a node, it means that there is at least one node in each path between the source node and that node, whose remaining battery energy is less than γ. In such a case, the optimal path to such a node must be found by running Algorithm 4 on $G_2(\mathbb{V}, \mathbb{E}_2)$.

Algorithm 5 Finding the optimal path between a source node s and any other node in the network according to CMMBCR. Here, $G_1(\mathbb{V}, \mathbb{E}_1)$ is the network topology in which link weights are calculated according to MTTPR (see (5.28)). $G_2(\mathbb{V}, \mathbb{E}_2)$ is the network topology in which link weights are calculated according to MMBCR (see (6.5)). In other words, the two graphs are the same, but their link weights are different.

$\text{CMMBCR}(G_1(\mathbb{V}, \mathbb{E}_1),\ G_2(\mathbb{V}, \mathbb{E}_2),\ \gamma,\ s)$
  for each $(u, v) \in \mathbb{E}_2$ **do**
    if $w_{mmbcr}(u, v) < \gamma$ **then**
      $\mathbb{E}_1 \leftarrow \mathbb{E}_1 - (u, v)$
    end if
  end for
  $\mathcal{T}_1(v) = \text{MTTPR}(G_1(\mathbb{V}, \mathbb{E}_1),\ s)$
  $\mathcal{T}_2(v) = \text{MMBCR}(G_2(\mathbb{V}, \mathbb{E}_2),\ s)$
  for each $v \in \mathbb{V}$ **do**
    if $\mathcal{T}_1(v) = \emptyset$ **then**
      $\mathcal{T}(v) \leftarrow \mathcal{T}_2(v)$
    else
      $\mathcal{T}(v) \leftarrow \mathcal{T}_1(v)$
    end if
  end for

6.1.4   MRPC and CMRPC Algorithms

MRPC and CMRPC were proposed in [79]. In addition to the remaining battery energy of nodes, they consider the impact of MAC retransmission on optimal routes. The weight of a link in these two battery-aware routing schemes is a combination of the remaining battery energy of the transmitting node of the link and the reliability of the link. MRPC uses a max-min formulation similar to MMBCR (see (6.3)). Nevertheless, the path weight in MRPC is the number of packets which can ideally be transmitted through the path when there is no other traffic going through that path. That is,

$$\mathcal{C}_{mrpc}(\mathcal{P}_k) = \min\{\frac{B_{n_i}}{T_{n_i, n_{i+1}}}\}_{i=1}^{h_k}$$

where $T_{n_i, n_{i+1}} = \frac{d_{n_i, n_{i+1}}^{\eta}}{p_{n_i, n_{i+1}}}$ is the required transmission power for reliable transmission of a packet over (n_i, n_{i+1}). Similar to MMBCR, the path with the maximum weight is selected.

CMRPC is a conditional version of MRPC. It is similar to CCMBCR with the difference that CMRPC acts in MRPC and MPR modes. CMRPC finds the minimum energy path based on the MPR scheme (introduced in Section 5.3.2) among paths that have a MRPC weight above a threshold. If there are no such

paths, CMRPC acts in MRPC mode and finds the optimal path according to this scheme.

6.1.5 Other Schemes

Other battery-aware routing schemes proposed in the literature are based on principles similar to the explained schemes. We briefly review them. In [85], Minimum Drain Rate (MDR) and the Conditional Minimum Drain Rate (CMDR) algorithms were proposed. MDR monitors the drain rate of battery of nodes to predict their lifetime according to their remaining battery energy and their packet forwarding rate. MDR tries to avoid using nodes with short lifetime as relaying nodes. CMDR is the conditional version of MDR which guarantees that the total transmission power of the chosen route is minimized among those that have a lifetime above a threshold. The basic idea behind CMDR is similar to CMMBCR, but CMDR works in MDR and MTTPR modes. Wang et al. [99] introduced an on-demand battery-aware routing protocol in which the path weight is a weighted combination of its hop-count and the remaining battery energy of its critical node (similar to MMBCR). Chang et al. [86] proposed a battery-aware routing scheme in which the weight of a link is a weighted combination of the energy consumption rate and the residual battery energy of the two end-nodes of the link. Battery-aware routing schemes in [87, 100] define the link weight as a combination of the delay of the link and the residual battery energy of the transmitting node of the link. The proposed algorothm in [88] uses a bi-criteria route selection scheme considering the minimum residual battery energy along a path (similar to MMBCR) as the first criterion, which must be maximized, and the total transmission power along the path (similar to MTTPR), which must be minimized.

6.1.6 Drawbacks of the Existing Schemes

The battery-aware routing schemes proposed so far have two main drawbacks:

1. Some schemes such as MBCR and MMBCR only consider the remaining battery energy of nodes without paying attention to the energy-efficiency of routes. Although this problem has been addressed by schemes such as CMMBCR, CMDR, MRPC, and CMRPC, they do not use a realistic energy consumption model for finding energy-efficient routes. Another problem holds specifically for schemes which use a min-max route selection formulation (e.g., MMBCR and MRPC). Such schemes suffer from the increased hop count of routes. This, in turn, increases the overall energy consumption in the network.

2. The existing energy-aware routing schemes are not optimized for networks with heterogeneous power supplies, where there are both mains-powered and battery-powered nodes in the network. Although we can deploy the existing schemes in such networks by considering no battery cost for packet forwarding by mains-powered nodes, such solutions may not be optimal. One problem is again the increased hop count. Considering no battery cost for mains-powered nodes may increase the number of hops of the selected routes, because longer routes consisting of many mains-powered nodes will be preferred to shorter routes consisting of few battery-powered nodes.

Our proposed battery-aware routing schemes in this chapter circumvent these drawbacks. We first present the state-of-the-art battery-aware routing algorithm RMECR. RMECR has been designed for networks with only battery-powered nodes. Then, we propose single-objective and multi-objective battery-aware routing algorithms based on RMECR for networks with heterogeneous power supplies. Furthermore, we investigate in depth the effect of various parameters such as routing overhead, mobility, transmission power control, and node density on the performance of the proposed algorithms.

6.2 Reliable Minimum Energy Cost Routing Algorithm

RMECR is an enhanced version of the Unified RMER algorithm which in addition to energy consumption characteristics of nodes and reliability of links takes into account the remaining battery energy of nodes in route selection. The only difference between RMECR and Unified RMER is the way they calculate link weights. Unified RMER defines the energy cost of a link as the amount of energy consumed to exchange a packet over the link. RMECR, on the other hand, defines the energy cost of a link as *the fraction of the remaining battery energy of the sending and the receiving node of the link which is consumed to exchange a packet between them.* We recall from the previous chapter that the link weight in Unified RMER is defined as

$$w_{u,v}^{urmer} = \bar{\mathcal{X}}_{u,v} \left[\epsilon_r + \alpha + \beta d_{u,v}^{\eta} \right], \tag{6.6}$$

where $\bar{\mathcal{X}}_{u,v}(L_d)$ is the ETX (expected transmission count) of the link and ϵ_r, α, and β are energy consumption parameters. Furthermore, $d_{u,v}$ is the distance between u and v, and η is the path-loss exponent of the environment. According to (6.6), the energy consumed by the sending node is $\bar{\mathcal{X}}_{u,v}(L_d)(\alpha + \beta d_{u,v}^{\eta})$ and that of the

receiving node is $\bar{\mathfrak{X}}_{u,v}(L_d)\epsilon_r$. Thus, in RMECR, the weight of a link is defined as follows:

$$w_{u,v}^{rmecr} = \bar{\mathfrak{X}}_{u,v} \left[\frac{\alpha + \beta d_{u,v}^{\eta}}{B_u} + \frac{\epsilon_r}{B_v} \right], \qquad (6.7)$$

where, B_u is the remaining battery energy of u and B_v is the remaining battery energy of v. The path with the minimum accumulated weight is selected by RMECR as the optimal path. This means, we can use Dijkstra's routing algorithm to find optimal routes between nodes according to RMECR provided that the link weight is defined as (6.7). We observe that the link weight in RMECR considers not only the remaining battery energy of nodes, but also the energy consumption characteristics of the wireless interface as well as the reliability of links.

RMECR is a minimum cost routing algorithm similar to MBCR. As mentioned before, the use of max-min route selection scheme in battery-aware routing algorithms such as MMBCR and MRPC increases the hop count of routes. This increases the latency of end-to-end packet transfer. The total energy consumption in the network increases either. On the other hand, battery-aware routing algorithms such as MBCR which find the minimum cost routes can achieve a lower hop count and a higher network lifetime [101].

6.3 Networks with Heterogeneous Power Supplies

In this section, we explain how information about the type of power supply of nodes could be considered for battery-aware routing. The key point that we should consider in designing a battery-aware routing algorithm for networks with heterogeneous power supplies is that a mains-powered (MP) node does not lose battery energy for packet forwarding. A battery-powered (BP) node, however, consumes part of its limited battery energy to relay a packet. We can direct the relay traffic to MP nodes of the network in order to avoid using BP nodes of the network as relaying nodes. However, the challenge is to design routing algorithms which are able to consider not only the heterogeneity of power supply of nodes but also the energy cost of packet exchange over wireless links, the reliability of wireless links, and the remaining battery energy of BP nodes of the network. Here, we introduce several routing algorithms which take into account these factors altogether in routing. First, single-objective algorithms are introduced, and then their bi-objective variants are presented.

6.3.1 Single-Objective Routing Algorithms

In the sequel, two single-objective battery-aware routing algorithms are presented for networks with heterogeneous power supplies.

6.3.1.1   RMLNR Algorithm

Let us define a parameter f_u for node u as follows:

$$f_u = \begin{cases} 1, & \forall u \in \mathbb{V}_b \\ 0, & \forall u \in \mathbb{V}_m, \end{cases} \tag{6.8}$$

where $\mathbb{V}_m$ is the set of MP nodes of the network, and $\mathbb{V}_b$ is the set of BP nodes of the network. To capture the effect of power supply in routing, we modify the link weight of RMECR as follows:

$$w_{u,v}^{rmlnr} = \bar{\mathfrak{X}}_{u,v} \left[\frac{f_u(\alpha + \beta d_{u,v}^{\eta})}{B_u} + \frac{f_v \epsilon_r}{B_v} \right]. \tag{6.9}$$

The link weight in (6.9) implies that the *battery cost* for packet transmission and reception is considered to be zero for an MP node. Considering no battery cost for MP nodes means that the cost of a path is in fact the accumulated battery cost of its BP nodes. If there is a path between two nodes which consist of only MP nodes, it will be the optimal path between them. Otherwise, the path with a lower batter cost for BP nodes is optimal. We name this routing algorithm *Reliable Minimum battery cost with Least BP Nodes Routing (RMLNR)*. RMLNR is a generalized version of RMECR, because if all nodes are battery powered, the definition of link weight in RMLNR will be the same as that of RMECR.

6.3.1.2   RLBNR Algorithm

Using the same way that we modified the link weight in RMECR to arrive at RMLNR, we can modify the link weight in Unified RMER to consider the type of power supply of nodes in routing. That is, we modify the link weight in Unified RMER as follows:

$$w_{u,v}^{rlbnr} = \bar{\mathfrak{X}}_{u,v} \left[f_u(\alpha + \beta d_{u,v}^{\eta}) + f_v \epsilon_r \right]. \tag{6.10}$$

This means we again do not consider any battery cost for packet transmission or reception by an MP node. The optimal route between two nodes can be determined using Dijkstra's algorithm. We name the resulting routing algorithm as *Reliable Least BP Nodes Routing (RLBNR)*. Obviously, RLBNR is a generalized version of Unified RMER, because if all nodes are battery powered, the definition of link weight in RLBNR will be the same as that of Unified RMER.

RLBNR and RMLNR differ from each other in the similar manner as RMECR and Unified RMER differ from each other. We remember that RMECR is an enhanced version of Unified RMER which in addition to the energy consumption characteristics of nodes and quality of links takes into account the remaining battery energy of nodes in routing. Similarly, RMLNR is an enhanced version of RLBNR which in addition to the energy consumption characteristics of nodes, quality of

links, and type of power supply of nodes, takes into account the remaining battery energy of BP nodes in routing.

The main drawback of RMLNR and RLBNR is that they may find longer routes, because they do not consider any battery cost for MP nodes. If the hop count of the selected routes increase, the latency of packet transfer will increase as well. Furthermore, end-to-end reliability of routes will also decrease, which in turn can increase the overall energy consumption for packet transfer if end-to-end retransmissions are supported. Because of these drawbacks, we need to consider other objectives such as latency and hop-count in battery-aware routing in networks with heterogeneous power supplies.

6.3.2 Bi-objective Routing Algorithms

Single-objective algorithms RMLNR and RLBNR define the optimal path between two nodes as the path which minimizes the energy cost. Here, the energy cost of a path is the summation of the energy cost of the constituent links of that path. The bi-objective algorithms that we introduce in this section consider a second criterion in routing. The goal of considering the second criterion is to limit the hop count of minimum energy cost routes. The natural choice will be to minimize the hop count of routes in addition to minimizing their energy cost. Nevertheless, a better choice is to minimize the total ETX of routes, where ETX of a route is the summation of the ETX of constituent links of that route. The ETX of a route is not only related to the hop count of the route, but also captures the latency of end-to-end packet transfer due to retransmissions.

6.3.2.1 General Formulation of the Routing Problem

Let $\mathcal{C}(\mathcal{P})$ denote the energy cost of $\mathcal{P}$, and $\bar{\mathcal{X}}(\mathcal{P})$ denote the ETX of $\mathcal{P}$ defined as

$$\begin{cases} \mathcal{C}(\mathcal{P}) = \sum_{i=1}^{h} w_{n_i,n_{i+1}} \\ \bar{\mathcal{X}}(\mathcal{P}) = \sum_{i=1}^{h} \bar{\mathcal{X}}_{n_i,n_{i+1}} \end{cases}, \tag{6.11}$$

where $w_{n_i,n_{i+1}}$ is the energy cost of link (n_i, n_{i+1}) and $\bar{\mathcal{X}}_{n_i,n_{i+1}}$ is the ETX of this link. We define the optimal path between a pair of source-destination nodes as a path whose energy cost and its ETX are smaller than the energy cost and ETX of any other path between the source and the destination. In other words, the optimal path is $\mathcal{P}_m \in \mathbb{Q}$ such that

$$\begin{cases} \mathcal{C}(\mathcal{P}_m) \leq \mathcal{C}(\mathcal{P}_q), \\ \bar{\mathcal{X}}(\mathcal{P}_m) \leq \bar{\mathcal{X}}(\mathcal{P}_q), \\ \forall \ \mathcal{P}_q \in \mathbb{Q}. \end{cases} \tag{6.12}$$

Thus, to find the optimal path, we need to solve a bi-criteria decision making problem. Note that a bi-criteria (generally a multi-criteria) decision making problem

may not have a solution optimizing both (all) criteria. Although, there might be a solution that optimizes one of the criteria, there may not be a solution optimizing both (all) criteria simultaneously. The *lexicographic method* and the *weighted sum approach* are two methods that we can use to solve multi-criteria decision making problems [102]. Based on these two methods, we design different bi-objective battery-aware routing algorithms for wireless multi-hop networks with heterogeneous power supplies.

6.3.2.2 Lexicographic-based Algorithms

This suite of algorithms uses the lexicographic method (LM) to find the optimal routes. The LM considers the priority of different criteria in the decision making process. Since minimizing the energy cost has a higher priority than minimizing the ETX in the design of battery-aware routing schemes, we give a higher priority to minimizing the energy cost. Thus, according to the LM, the optimal path between two nodes is a path with the minimum energy cost. However, if there are several paths between a source and a destination which have the minimum energy cost, the path with the minimum ETX is selected amongst them. In other words, let $\mathbb{Q}_1 \subset \mathbb{Q}$ be as follows:

$$\mathbb{Q}_1 = \left\{ \mathcal{P}_n \in \mathbb{Q} : \mathcal{C}(\mathcal{P}_n) \leq \mathcal{C}(\mathcal{P}_q) \; \forall \mathcal{P}_q \in \mathbb{Q} \right\}.$$

If $|\mathbb{Q}_1| = 1$, the only element of $\mathbb{Q}_1$ is the optimal path. If $|\mathbb{Q}_1| > 1$, the optimal path is $\mathcal{P}_m \in \mathbb{Q}_1$, where

$$\bar{\mathcal{X}}(\mathcal{P}_m) \leq \bar{\mathcal{X}}(\mathcal{P}_n) \qquad \forall \mathcal{P}_n \in \mathbb{Q}_1.$$

The optimal path between two nodes in LM-based routing algorithms is called *lexicographically shortest path*.

Based on the two different definitions of energy cost of links that we introduced for RMLNR and RLBNR, we can design two LM-based algorithms. To refer to these algorithms, we name them RMLNR-LM and RLBNR-LM, respectively. In RMLNR-LM the energy cost of a link is calculated using (6.9), while in RLBNR-LM, it is calculated using (6.10). Nevertheless, the main question is how to design a routing algorithm similar to Dijkstra's algorithm to find lexicographically shortest paths between nodes in a multi-hop network.

There are two types of routing algorithms that we can use to find lexicographically shortest paths: *label correcting* algorithms [103–105] and *label setting* algorithms [106, 107]. Both label setting and label correcting algorithms consider a label for each path originating from a source node s terminating on a destination node v in the network. We represent a label as $\mathcal{L}(v) = (l_1, l_2, u, v)$. Here, l_1 and l_2 are the weight of the path from source node s to destination node v with respect to the two objectives, and u is the node preceding v in the path from s to v. Two

labels are different from each other if any of their elements are different. In our case, l_1 specifies the energy cost of the path and l_2 specifies the ETX of the path.

The difference between the label setting and label correcting algorithms is in the way they find the lexicographically shortest path from the source node to any other node iteratively. Raitha and Ehrgotta [108] have shown that label-setting algorithms are faster than label-correcting algorithms. Thus, in the sequel, we explain how we can find the lexicographically shortest path using a label setting algorithm.

In the label setting approach, a list of tentative labels is maintained for all nodes. The source node is initially labeled as $\mathcal{L}(s) = (0, 0, s)$. There is no label for other nodes. At each iteration, a label that is lexicographically smaller than other labels is removed from the list of all tentative labels. Here, we say a label $\mathcal{L}(i) = (a_1, a_2, u, i)$ is lexicographically smaller that a label $\mathcal{L}(j) = (b_1, b_2, h, j)$ if $a_1 < b_1$ or $a_1 = b_1$ and $a_2 < b_2$. The removed label at each iteration, which for instance belongs to node u, is extended via all outgoing links (u, v) from u, where v is a neighbor of u. Extension of a label $\mathcal{L}(u)$ means that a new label is created as

$$ExtendLabel(v) = \mathcal{L}(u) + \left(w_{u,v}, \bar{\mathbb{X}}_{u,v}\right)$$
$$= (l_1 + w_{u,v}, l_2 + \bar{\mathbb{X}}_{u,v}).$$

New labels generated by extending the removed label are inserted into the list of tentative labels. If there are several labels for the same node, the one which is lexicographically the smallest is kept and other labels for that node are eliminated from the list of tentative labels. The algorithm iterates until no label remains in the list of tentative labels. The optimal path to any node can be backtracked using labels. Algorithm 6 shows the label setting algorithm [107] for finding lexicographically shortest paths between a source node s and all other nodes of the network.

The time complexity of the label setting algorithm is similar to the complexity of the Dijkstra's algorithm, i.e., $O(|\mathbb{V}|^2)$. In fact, the Dijktra's algorithm is a label setting algorithm in which each label composed of only one element. Similar to the Dijkstra's algorithm, the complexity of Algorithm 6 could be reduced to $O(|\mathbb{E}| + |\mathbb{V}| \log(|\mathbb{V}|))$ using Fibonacci heaps.

6.3.2.3 WSA-based Algorithms

This suite of algorithms uses the weighted sum approach (WSA) to find the optimal routes. WSA considers the relative weight of different criteria with respect to each other. A single objective is defined for decision making, which is the weighted sum of all the objectives. The optimal solution of the multi-criteria decision making

---

Algorithm 6 Label setting bi-objective routing algorithm for finding the lexico-graphically shortest path from a source node s to any other node in the network.

Label-Setting($G(\mathbb{V}, \mathbb{E})$, s)
$\mathcal{L}(s) = (0, 0, s)$
$\mathbb{L} = \{(0, 0, s)\}$
while $\mathbb{L} \neq \emptyset$ **do**
    $u \leftarrow i \in \mathbb{V} \mid \mathcal{L}(i)$ is lexicographically the smallest in $\mathbb{L}$
    $\mathbb{L} \leftarrow \mathbb{L} - \{\mathcal{L}(u)\}$
    for each neighbor v of u **do**
        $TempLabel \leftarrow \mathcal{L}(u) + (w_{u,v}, \bar{\mathfrak{X}}_{u,v})$
        Remove any label of v from $\mathbb{L}$ which is greater than $TempLabel$
        if the label set of v has changes **then**
            $\mathbb{L} = \mathbb{L} \cup TempLabel$
        end if
    end for
end while

---

problem is a solution which optimizes the resulting single objective. Thus, according to WSA, we define a single cost function for each path $\mathcal{P}$ as

$$\mathcal{Z}(\mathcal{P}) = a\frac{\mathcal{C}(\mathcal{P})}{b} + (1-a)\bar{\mathfrak{X}}(\mathcal{P}). \tag{6.13}$$

The path which minimizes $\mathcal{Z}(\mathcal{P})$ is then selected as the optimal path. This could again be done using Dijkstra's shortest path routing algorithm. Here, $0 \leq a \leq 1$ is the relative weight of minimizing the energy cost of routes to minimizing their ETX in the decision making process. Parameter b is a normalizing coefficient to match unit and variation range of the energy cost of a route to that of the ETX of the route, such that these two values could be added to each other. Since energy cost and ETX have different units, they can not be summed without being normalized.

By replacing $\mathcal{C}(\mathcal{P})$ in (6.13) with its definition given in (6.11), $\mathcal{Z}(\mathcal{P})$ expands to

$$\mathcal{Z}(\mathcal{P}) = \sum_{i=1}^{h} \left(\frac{a}{b}w_{n_i,n_{i+1}} + (1-a)\bar{\mathfrak{X}}_{n_i,n_{i+1}}\right). \tag{6.14}$$

Equation (6.14) suggests that in WSA a new energy weight function is defined for each link as

$$\mathcal{W}_{u,v} = \frac{a}{b}w_{u,v} + (1-a)\bar{\mathfrak{X}}_{u,v}, \tag{6.15}$$

and the path with the minimum accumulated weight is selected as the optimal path. We refer to $\mathcal{W}_{u,v}$ as the *WSA weight* of link (u, v) to distinguish it from the *actual weight* of the link (i.e., $w_{u,v}$).

6.3.2.4   Choice of Normalizing and Weighing Coefficients

The main issue in the WSA approach is choosing the normalizing coefficient b and weighing coefficient a. Coefficient b must be chosen in such a way that the unit and variation range of the energy cost of a route is adjusted in such a way it could be added to the ETX of the route. For example, if the unit of the energy cost of a path is Joule, b must be in Joule as well, because ETX has no unit. Furthermore, to bring the energy cost of a path to the same order as that of ETX, we can define b as *the maximum energy cost of the path when the ETX of each link is one*. For instance, if the energy cost of a path with 3 hops is 0.08 [J] and the maximum energy cost for forwarding a packet once in each hop is 0.02 [J], then we choose $b = 3 \times 0.02 = 0.06$ [J]. With this choice, the normalized energy cost of the path will be $0.08/0.06 = 8/6$. Note that although the normalized energy cost of a path might be smaller than its ETX, it does not necessarily mean that in WSA the ETX is favored to the energy cost. The tunable parameter a has a critical role to play here. It controls the relative priority of energy cost to ETX in route selection. We discuss some extreme cases.

If $a = 0$, we have $\mathcal{W}_{u,v}|_{a=0} = \bar{\mathcal{X}}_{u,v}$. This means the optimal path in WSA will be the path with the minimum ETX. In other words, if $a = 0$, any battery-aware routing algorithm devised on the basis of WSA turns out to be Min-ETX routing. Nevertheless, for $a = 1$, we have

$$\mathcal{W}_{u,v}|_{a=1} = \frac{1}{b} w_{u,v}. \tag{6.16}$$

Since b is a constant term, it has no influence in selecting the optimal path if the link weight is defined as (6.16). Therefore, we can simplify the WSA link weight as

$$\mathcal{W}_{u,v}|_{a=1} = w_{u,v}, \tag{6.17}$$

without changing the optimal path. Equation (6.17) implies that when $a = 1$, the WSA link weight is the actual weight of the link. In other words, if $a = 1$, any battery-aware routing algorithm devised on the basis of WSA only considers the energy cost of links as the routing metric and finds a route with the minimum energy cost as the optimal route. For any value of a between its two limits 0 and 1, the energy cost might be favored to the ETX in route selection or vice versa. We will further discuss the effect of coefficient a on the performance of WSA-based routing algorithms in Section 6.5.

6.3.2.5   Similarity between Lexicographic and WSA Methods

In general, the optimal routes between two nodes found according to the LM and WSA methods may have some nodes in common. To clarify this, we discuss the

special case of $a = 1$ to give an impression about the similarity between routes in these two methods. We observed that when $a = 1$, the WSA link weight is the energy cost of the link. Recall that LM considers minimizing the actual energy cost of routes as the primary criterion for route selection. Thus, the optimal route found by WSA when $a = 1$ could be similar to the optimal path found by LM. However, they may not be completely the same either. LM considers minimizing the total ETX of the path as the second criterion. If there are several paths which have minimum energy cost, LM chooses the path with the minimum accumulated ETX amongst them. On the other hand, in WSA with $a = 1$, minimizing the energy cost is the only criterion for route selection. Therefore, if there are several paths with the minimum energy cost, one of them will be chosen randomly (tie breaking). Only if by chance the path with the minimum ETX among those with the minimum energy cost is selected, or there is only one path which has the minimum energy cost, the optimal path found by WSA when $a = 1$ will be the same as the optimal path found by LM.

6.3.2.6   RLMNR-WSA and RLBNR-WSA Algorithms

We can introduce two WSA-based routing algorithms based on the two different definitions of energy cost of links that we introduced for RMLNR and RLBNR. We refer to these algorithms as RMLNR-WSA and RLBNR-WSA. RMLNR-WSA defines the energy cost of a link similar to RMLNR, i.e., using (6.9). RLBNR-WSA defines it similar to RLBNR, i.e., using (6.10).

Another difference between these two algorithms is in the way they define the normalizing coefficient b. For RLBNR-WSA, we define the normalizing coefficient b as the maximum energy consumed for transmission and reception of a single bit over a wireless link during a single transmission. That is,

$$b_{wrlbnr} = \epsilon_r + \alpha + \beta D_{max}^{\eta},$$

where D_{max} is the transmission range of nodes. For RMLNR-WSA, we define b as the fraction of the maximum battery energy of a BP node which is consumed to transmit and receive a single bit over a wireless link when nodes transmit with their maximum transmission power. That is,

$$b_{wrmlnr} = \frac{\epsilon_r + \alpha + \beta D_{max}^{\eta}}{B} = \frac{b_{wrlbnr}}{B}.$$

To summarize, the WSA link weight in RLBNR-WSA and RMLNR-WSA are calculated as follows:

$$\begin{aligned}
\mathcal{W}_{u,v}^{wrlbnr} &= \frac{a}{b_{wrlbnr}} \bar{\mathcal{X}}_{u,v}(\epsilon_r + \alpha + \beta d_{u,v}^{\eta}) + (1-a)\bar{\mathcal{X}}_{u,v} \\
&= \bar{\mathcal{X}}_{u,v} \left[\frac{a}{b_{wrlbnr}}(\epsilon_r + \alpha + \beta d_{u,v}^{\eta}) + 1 - a \right],
\end{aligned} \tag{6.18}$$

Table 6.1 – The definition of battery cost in various battery-aware routing algorithms.

Algorithm	Battery Cost $w_{u,v} =$
RMECR	$\bar{\mathcal{X}}_{u,v} \left(\frac{\alpha + \beta d_{u,v}^{\eta}}{B_u} + \frac{\epsilon_r}{B_v} \right)$
RMLNR	$\bar{\mathcal{X}}_{u,v} \left(\frac{f_u(\alpha + \beta d_{u,v}^{\eta})}{B_u} + \frac{f_v \epsilon_r}{B_v} \right)$
RMLNR-LM	$\bar{\mathcal{X}}_{u,v} \left(\frac{f_u(\alpha + \beta d_{u,v}^{\eta})}{B_u} + \frac{f_v \epsilon_r}{B_v} \right)$
RMLNR-WSA	$\bar{\mathcal{X}}_{u,v} \left(\frac{aB}{b_{wrlbnr}} \left(\frac{\epsilon_r}{B_v} + \frac{\alpha + \beta d_{u,v}^{\eta}}{B_u} \right) + 1 - a \right)$
RLBNR	$\bar{\mathcal{X}}_{u,v} \left(f_u(\alpha + \beta d_{u,v}^{\eta}) + f_v \epsilon_r \right)$
RLBNR-LM	$\bar{\mathcal{X}}_{u,v} \left(f_u(\alpha + \beta d_{u,v}^{\eta}) + f_v \epsilon_r \right)$
RLBNR-WSA	$\bar{\mathcal{X}}_{u,v} \left(\frac{a}{b_{wrlbnr}} (\epsilon_r + \alpha + \beta d_{u,v}^{\eta}) + 1 - a \right)$
MBCR	$\frac{1}{B_u}$
MMBCR	B_u
CMMBCR	B_u
MRPC	$\frac{B_u p_{u,v}}{d_{u,v}^{\eta}}$
CMRPC	$\frac{B_u p_{u,v}}{d_{u,v}^{\eta}}$

$$
\begin{aligned}
\mathcal{W}_{u,v}^{wrlmnr} &= \frac{aB}{b_{wrlbnr}} \bar{\mathcal{X}}_{u,v} (\frac{\epsilon_r}{B_v} + \frac{\alpha + \beta d_{u,v}^{\eta}}{B_u}) + (1 - a) \bar{\mathcal{X}}_{u,v} \\
&= \bar{\mathcal{X}}_{u,v} \left[\frac{aB}{b_{wrlbnr}} \left(\frac{\epsilon_r}{B_v} + \frac{\alpha + \beta d_{u,v}^{\eta}}{B_u} \right) + 1 - a \right].
\end{aligned}
\tag{6.19}
$$

We can find the optimal path between two nodes in WSA-based algorithms using Dijkstra's algorithm provided that link weights are calculated using (6.18) and (6.19). Table 6.1 summarizes the definition of the link weight in various battery-aware routing algorithms introduced in this chapter.

6.4   Implementation Issues

To compute link weights as defined by any of the battery-aware routing algorithms that we proposed in this chapter, nodes need to know all parameters that are required to compute link weights as discussed for Unified RMER in Section 5.4. In networks with only BP nodes, they also need to know their remaining battery energy. In networks that consist of both MP and BP nodes, nodes need to know the type of their power supply as well. Discovering whether the node is connected

to the mains or runs on battery and specifying the remaining battery energy of a BP node are implementation issues. The important issue is to discuss how the proposed routing algorithms could be deployed in a routing protocol. We mentioned in Chapter 2 that routing protocols in wireless multi-hop networks fall into two categories: reactive and proactive. We discuss these two cases separately.

6.4.1 Implementation issues with Proactive Protocols

The proposed battery-aware routing algorithms could be deployed directly in a proactive routing protocol provided that each node can have a complete view of the network topology. This includes updated values of the link weights. Knowing the network topology, each node can find the optimal route to any other node in the network using the battery-aware routing algorithm in force. As discussed in Chapter 2, in proactive protocols each node has to periodically propagate its view of the network topology to help other nodes to update their view of the network topology. This, indeed, generates a large amount of routing overhead in large networks. The problem could be solved by deploying reactive routing protocols, where routes are discovered on-demand only when a route is needed.

6.4.2 Implementation issues with Reactive Protocols

In reactive protocols, the source node should broadcast a single local route request (RREQ) message, which is received by (approximately) all nodes currently within wireless transmission range of the source node. The RREQ contains the source node and the destination node identifiers and a unique sequence number determined by the source node. Each replica of the RREQ should collect the energy cost of the links it traverses. The address of each intermediate node that forwards a particular copy of the RREQ is also recorded by that replica of the RREQ message. The format of a RREQ is shown in Figure 6.1, which is the modified version of the Route Request Option in the DSR protocol [45]. The only difference between the RREQ in Figure 6.1 and the original Route Request Option in DSR is the Path Cost field, which records the accumulated energy cost of the traversed routes.

When a node other than the destination node receives the RREQ for the first time, it should check whether it has a valid route to the destination. If the node knows a valid route, it sends the valid route to the source node using a unicast route reply (RREP) message. Otherwise, the node records the route that the RREQ has traversed so far, as well as the accumulated energy cost of the traversed route (summing the link weights). If the energy cost of the received RREQ is smaller than the last recorded value from other replicas of the RREQ, then the node forwards the RREQ. Otherwise, it drops the received RREQ. In case of a bi-objective routing algorithm, if the energy costs of two routes are the same, the node compares the total

Octet 1	Octet 2	Octet 3 and 4
Option Type	Option Data Len.	Sequence Number
Target address		
Path Cost		
Address [1]		
Address [2]		
…		
Address [n]		

Figure 6.1 – The modified format of a RREQ message in the DSR protocol [45]. According to [45], Option Type must be Route Request, and Option Data Length must specify the length of the option in octets excluding the length of Option Type and Option Data Length fields. Target Address must specify the address of the destination node. Path Cost is the cumulative cost of the path. For bi-objective routing algorithms another Path Cost field must be considered for gathering the path weight with regard to the second objective. Address[i] is the address of the ith intermediate node recorded in the RREQ message.

ETX of the two routes to determine which route is better. This filtering procedure at each node helps in reducing the routing overhead. The destination node follows the same procedure as other nodes, but it does not forward the RREQ. Instead, it waits to receive all replicas of the same RREQ. Then, it chooses the optimal route according to the algorithm used, and sends a unicast RREP message to the source node. The waiting time at the destination node will depend on the network size and traffic conditions, and usually is a design choice. A simple example of the reactive route discovery mechanism which could be used by RLBNR and RMLNR algorithms is depicted in Figure 6.2.

6.4.3 Route Refreshment Frequency

Route refreshment is an important issue in deployment of battery-aware routing in wireless multi-hop networks. Route refreshing is needed to avoid overusing the same set of BP nodes. With time, the remaining battery energy of nodes changes, and optimal routes might be different from the used routes. If a proactive routing protocol is deployed, route refreshment can happen when a node obtains an updated version of link weights. In this case, the key parameter is the period that nodes should propagate their view of network topology. On the other hand, if a reactive routing protocol is used, route refreshment can happen by propagating a new RREQ

@ t_0: cost=∞
@ t_1: 1--> 2 (cost=0.8): forwarded
@ t_2: 1--> 3-->2 (cost=0.6): forwarded

@ t_0: cost=∞
@ t_2: 1-->2 -->4 (cost=1.3)
@ t_2: 1-->3-->4 (cost=1.1): Optimal path
@ t_3: 1-->3-->2-->4 (cost=1.1)

@ t_0: cost=∞
@ t_1: 1--> 3 (cost=0.6): forwarded
@ t_2: 1--> 2-->3 (cost=0.8): dropped

(a) LM-based algorithms

@ t_0: cost=∞
@ t_1: 1--> 2 (cost=0.8): forwarded
@ t_2: 1--> 3-->2 (cost=0.6): forwarded

@ t_0: cost=∞
@ t_2: 1-->2 -->4 (cost=1.3)
@ t_2: 1-->3-->4 (cost=1.1): Optimal path
@ t_3: 1-->3-->2-->4 (cost=1.1)

@ t_0: cost=∞
@ t_1: 1--> 3 (cost=0.6): forwarded
@ t_2: 1--> 2-->3 (cost=0.8): dropped

(b) WSA-based algorithms

Figure 6.2 – Reactive route discovery using RREQ and RREP messages in LM-based and WSA-based routing algorithms. In Figure (a), values on each link show the actual energy cost of the link. In Figure (b), they are WSA energy cost of links which are related to the actual energy cost of links according to (6.15) assuming $a = 0.5$. Here, we have assumed ETX of each link is 1. t_0, t_1, t_2, and t_3 are time samples.

message. In this case, the key parameter is the frequency of transmitting RREQ messages for route re-discovery.

Whether a reactive or a proactive protocol is deployed, frequency of route refreshment affects the routing overhead of battery-aware routing. If routes are not refreshed, nodes will be overused. If routes are refreshed too frequently, the energy consumption of nodes will increase. This, in turn, reduces the lifetime of nodes. Choosing the appropriate value of route refreshment frequency is another design parameter which we examine in the next section.

6.5   Performance Comparison

We use simulations to compare the performance of various battery-aware routing algorithms. We compare them in various scenarios: static networks, mobile networks, networks with and without TPC, and network with homogeneous and heterogeneous power supplies. This helps us to have a complete picture of the performance of these routing schemes in wireless multi-hop networks.

6.5.1   Simulation Setup

We consider a network in which nodes are uniformly distributed in a square area of size $5D_{max} \times 5D_{max}$, where D_{max} is the transmission range of nodes. We assume nodes are all equipped with the PRISM chipset. We assume that a reactive routing protocol is deployed in the network. We also assume only MAC layer retransmission is supported.

6.5.1.1   Traffic Generation Model

We use a dynamic traffic generation model to provide a situation where battery energy of nodes changes with time. Sessions are generated between randomly chosen source and destination nodes. Each node may establish concurrent sessions to different nodes, or be the destination node of several sessions at the same time. The inter-arrival time between two successive sessions generated in the network is assumed to be exponentially distributed with mean ρ. The duration of each session is also assumed to be exponentially distributed with mean μ. The source node of each session generates packets with rate λ packets per unit of time. Note that such a traffic model may not always be the case in every type of wireless multi-hop networks. However, by changing values of parameters μ, ρ, and λ we can have a flexible model which can fit the requirements of many applications. If we increase ρ, sessions will be generated more frequently. If we increase μ, sessions last for a longer time and more concurrent sessions may exist in the network.

6.5.1.2   Performance Measures

To compare various routing schemes, we consider several performance measures. They are:

1. Mean ETX which reflects quality and latency of selected routes by various algorithms.

2. Mean Hop Count which also reflects latency of selected routes by various algorithms.

3. Mean EPP which reflects the energy-efficiency of selected routes by various algorithms.

4. Network Lifetime which shows the capability of a routing algorithm in balancing the traffic load in the network.

We can use several definitions for the lifetime of a wireless multi-hop networks:

1. The time at which the first (BP) node fails due to battery exhaustion.

2. The time at which the network is partitioned due to failure of nodes.

3. The time at which no new session could be established, because the source and the destination are no longer connected to each other.

4. The time at which a fraction of the nodes survive in the network.

Depending on the network application, some of these definitions could not be suitable to measure the lifetime of a wireless multi-hop network. For instance, when there are both MP and BP nodes in the network, the network may not be partitioned due to failure of BP nodes, and there might always be a route between the source and the destination of a newly established session. Another example is mobile networks in which a disconnected network might be connected a few seconds later due to movements of nodes (or a connected network might be partitioned). In such scenarios, the time at which the first node fails or the time at which a fraction of the nodes survive could be a more appropriate measure. If a routing scheme can delay the first node failure, failure of other nodes will be delayed as well. The time to first node failure could also be an appropriate definition in networks where each node may provide a service for a user. The first failed node might be the node that provides the required service for a user in the network. Failure of such a node interrupts the service delivery to the user.

6.5.1.3 Routing Overhead

To take into account the effect of the routing overhead, we introduce δ as the route refreshment interval. After δ units of time of the establishment of a session, the source node will propagate another RREQ to refresh its route to the destination (if the session is still alive). The newly discovered route might be different from the previously discovered route. In our simulations, we investigate the effect of route refreshment frequency on the performance of battery-aware routing algorithms.

Propagation of Hello messages to measure the reliability of links is another source of overhead. As we explained in Section 5.4, each node needs to broadcast Hello messages through which the quality of wireless links is estimated. The use of Hello messages is required in routing schemes that utilize information about the reliability of links in route selection. This includes Unified RMER and various algorithms we proposed in this section. To capture this source of overhead, we assume nodes transmit every T_{hello} seconds a Hello message.

6.5.1.4 Collecting Results

To collect simulation results, different algorithms are compared in a completely similar setting. In each simulation run, we deploy a network randomly. A replica of the deployed network is created for each routing algorithm to measure the network lifetime when that routing algorithm is deployed in the network. We then generate similar sessions in each replica of the network. In other words, we have several samples of the same randomly deployed network which are completely the same (including the active sessions in these networks), but the deployed routing algorithms are different. To increase the confidence in our results, we repeated this procedure 300 times and plotted the average values for each algorithm. We skipped confidence intervals to have clear plots. Nonetheless we have a minimum 98% confidence level. Table 6.2 shows the default values of various parameters that we use in our simulations.

6.5.2 Networks with Homogeneous Power Supplies

We first compare the performance of battery-aware routing algorithms in networks with all BP nodes. We consider the battery-aware routing algorithms RMECR, MBCR, MMBCR, CMMBCR, and MRPC as well as the energy-efficient routing algorithm Unified RMER.

Table 6.2 – Values of Simulation Parameters

Parameter	Simulation value
Maximum battery energy of BP nodes (B)	5 [J]
Transmission range (D_{max})	150 [m]
Network area	$5D_{max} \times 5D_{max}$ [m^2]
Mean session inter-arrival time (ρ)	20 [s]
Mean session duration (μ)	200 [s])
Size of data packets	200 [Byte]
Target BER of the system	1×10^{-5}
RREQ packet size	54+4(hop-count) [Byte]
RREP packet size	50+4(hop-count) [Byte]
Number of retransmissions allowed	7
Path-loss exponent (η)	3
Decision threshold for CMMBCR (γ)	$\frac{B}{2}$ [J]
Packet rate (λ)	1 [packets/s]
Period of Hello message broadcast (T_{hello})	7 [s]
Number of nodes in the network	100
Fraction of MP nodes (in networks with heterogeneous power supplies)	0.5
Route refreshment interval (δ)	100 [s]

6.5.2.1   Definition of Network Lifetime

We mentioned several definitions for the network lifetime. The question is how they relate to each other? To answer this question, we have compared three definitions of the network lifetime with each other in Figure 6.3(a). The figure shows that the time to network partition and the time to first node failure are very close to each other regardless of the average node degree in the network. However, depending on the average node degree in the network, the time till a session fails due to lack of routes could be much higher than the time at which the first node fails or the network is partitioned. In other words, shortly after the failure of the first node, the network might be partitioned, but nodes could still communicate for a relatively long time. To explain this fact, we should notice that a network is partitioned even if a few nodes are isolated from the rest of the network. If the average node degree (node density) is high, then the rest of the network could still be a big component. As we can see in Figure 6.3(a), if the average node degree is low, then

the time to session failure could be very close to the time to partition the network. In Figure 6.3(b), we have shown the number of packets sent by source nodes during the network lifetime. Comparing plots in Figure 6.3(a) and Figure 6.3(b) shows that the number of packets sent could also be considered as an indicator of the network lifetime, because the higher the network lifetime the higher is the number of packets sent. This is because of the dynamic traffic generation pattern that we use in our simulations. In this model, sessions are generated with time. Therefore, the longer the network is operational, the more will be the number of generated sessions. As a result, more packets will be transmitted during the network lifetime. As Figure 6.3(b) shows, this is true regardless of the definition of the network lifetime.

6.5.2.2   Performance of Various Algorithms in Static Networks

Which algorithm can achieve a higher network lifetime? The answer to this question can be found in Figure 6.4 and Figure 6.5. These figures show different definitions of the network lifetime for various routing algorithms. What we observe in these figures is that RMECR outperforms other algorithms with regard to different definitions of the network lifetime. We also observe that the performance of MBCR is close to the performance of RMECR. The fact is, both RMECR and MBCR define the weight of a link as a function of the inverse of the remaining battery energy of nodes and find the path with the minimum accumulated weight. That is why their performances are closer to each other compared to other algorithms which use different weight functions. However, the question is why RMECR outperforms MBCR. Note that MBCR only considers the pure value of the remaining battery energy of nodes, while RMECR includes other factors such as link quality and energy consumption parameters of nodes as well. Thus, we may expect that MBCR balances the traffic more effectively than RMECR. The point is, since RMECR considers the required energy for packet forwarding by nodes, it is able to find more energy-efficient routes compared to MBCR (see Figure 6.6(b)). As a result, it can reduce the total energy consumption in the network, which increases the lifetime of the network as a whole.

There are some more points that we can extract from the results in Figure 6.4. Surprisingly, we observe that Unified RMER provides a higher network lifetime compared to MMBCR, MRPC, and CMMBCR. We notice that Unified RMER is not a battery-aware routing algorithm, while MMBCR, MRPC, and CMMBCR are battery-aware algorithms. We may expect them to have a better load balancing capability compared to Unified RMER. These three algorithms, however, increase the overall energy consumption in the network due to the increased hop-count of the selected routes. This fact can be seen in Figure 6.6(b), which shows that a high amount of energy is consumed for end-to-end traversal of a packet if these three algorithms are deployed in the network. The reason is the increased hop count of the selected routes by these three algorithms (see Figure 6.7). This, in
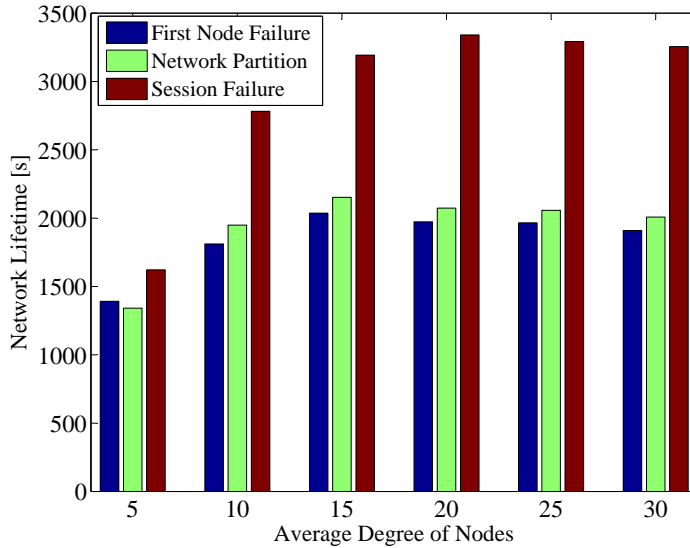
(a)
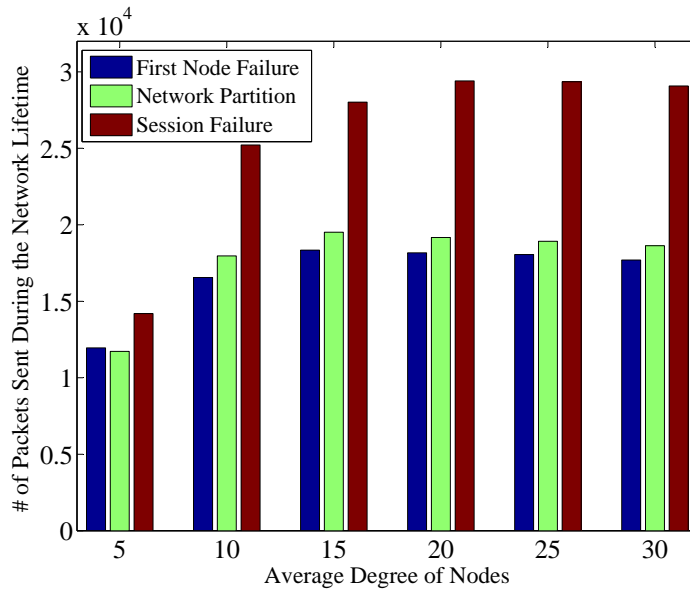
(b)

Figure 6.3 – Various definitions of network lifetime for RMECR algorithm in static networks consisting of only BP nodes capable of controlling their transmission power: (a) the network lifetime per second, (b) the number of data packets transmitted by source nodes during the network lifetime. The average PDR of links for data packets was set to 0.9.
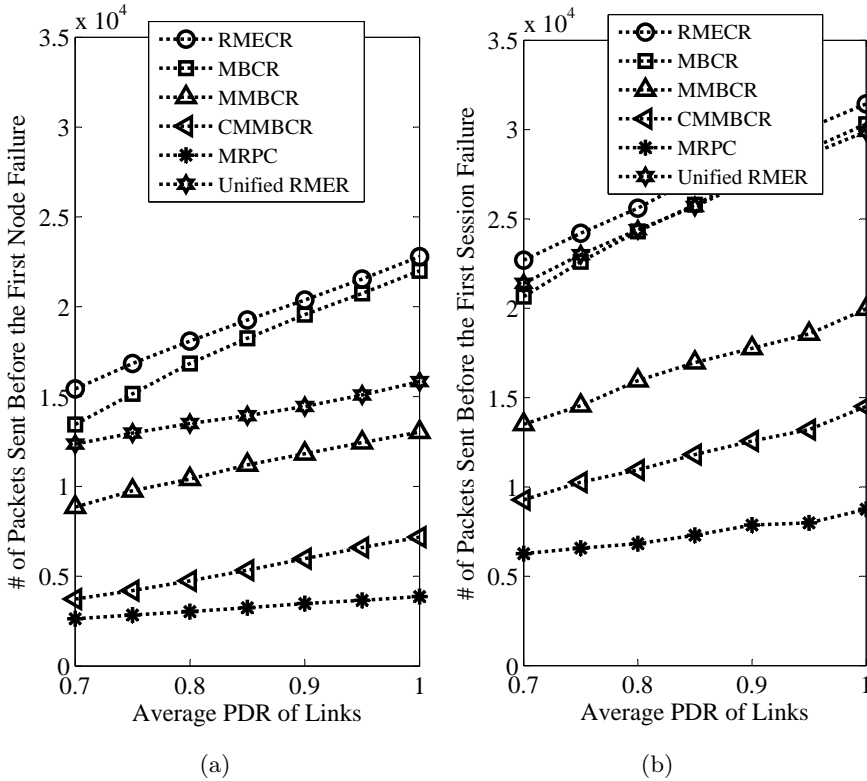
Figure 6.4 – Two different measures of the network lifetime for various routing algorithms. Nodes are static and they all are battery powered and capable of controlling the transmission power.
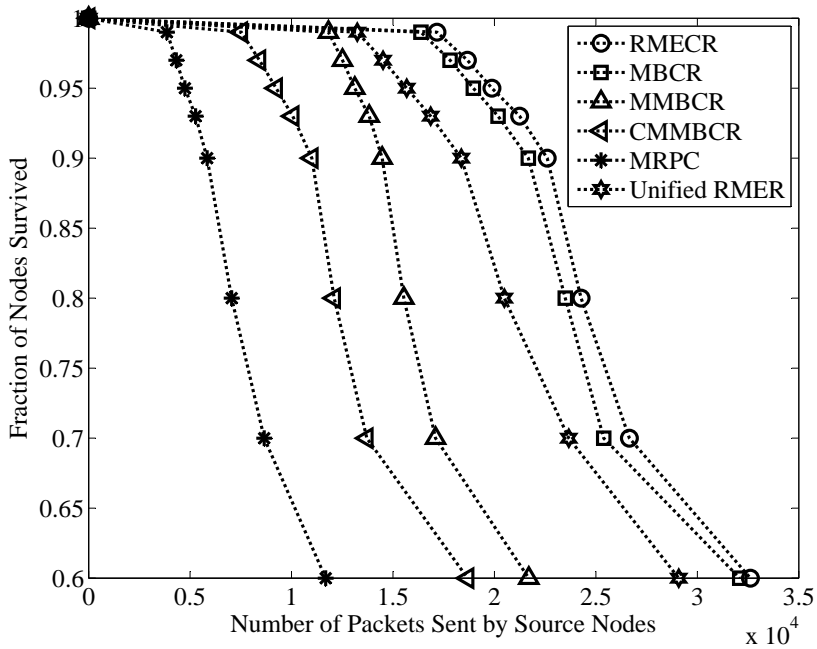
Figure 6.5 – Network lifertime in terms of the fraction of the nodes which are survived after transmission of a certain number of packets by the source nodes. Nodes are static and they all are battery powered and capable of controlling the transmission power. The average PDR of links is 0.9.
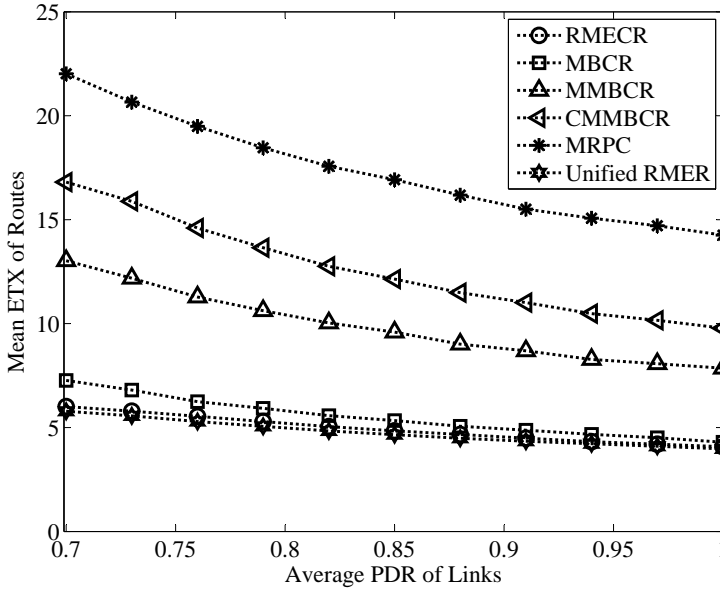
(a)
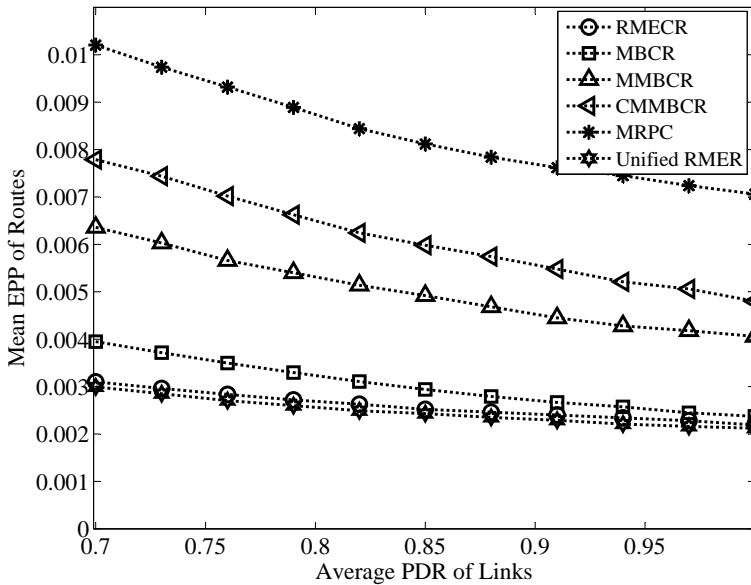
(b)

Figure 6.6 – Mean ETX and mean EPP of routes selected by various routing algorithms. Nodes are static and they all are battery powered and capable of controlling the transmission power. The number of nodes is 150.
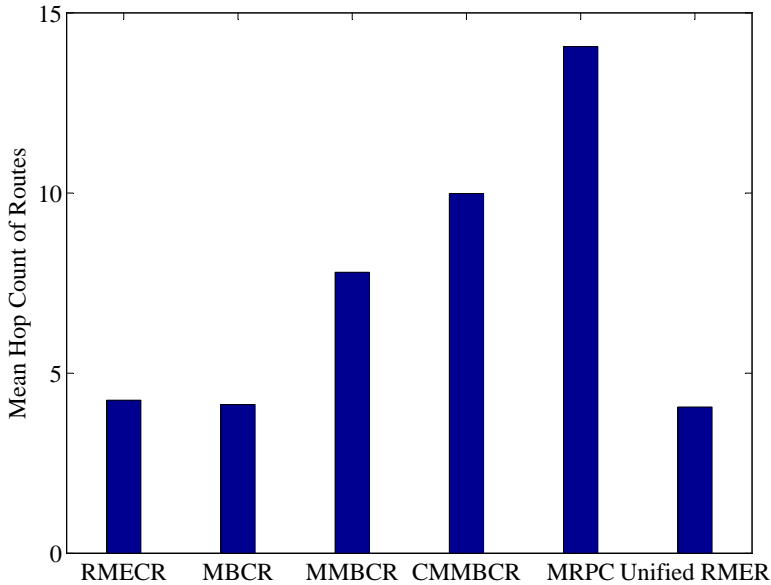
Figure 6.7 – Mean hop count of routes selected by various routing algorithms. Nodes are static and they all are battery powered and capable of controlling the transmission power. The number of nodes is 150.

turn, is due to the max-min route selection scheme by these algorithms, which increases the hop-count unboundedly. Therefore, we can say that *load balancing must be accompanied by energy-efficiency, otherwise it can not provide any gain in extending the operational lifetime of wireless multi-hop networks.* This has been our motivation in the design of RMECR algorithm as an algorithm which not only provides load balancing but also finds energy-efficient routes. Furthermore, as we can observe in Figure 6.4(a), RMECR can find reliable routes that require less retransmissions either.

Let us go one step further and discuss the performance of MMBCR, CMMBCR and MRPC. MRPC results in the lowest lifetime for the network compared to the other two algorithms, because it results in the highest EPP and the highest mean hop count. This bad performance results by a combination of the max-min route selection and the unrealistic energy consumption model unsed by MRPC. MRPC ignores the energy consumed by processing elements of transceivers. After MRPC, it is CMMBCR which results in the lowest network lifetime. Although CMMBCR does not use the max-min route selection in its MTTPR mode, but it uses an unrealistic energy consumption model to find energy-efficient routes in this mode.

This also explains why MMBCR achieves a higher network lifetime compared to MRPC and CMMBCR.

6.5.2.3   Impact of Node Density

Does node density change the performance of various routing algorithms with respect to each other? The answer is no as verified by the results depicted in Figure 6.8. However, there are some issues that should be highlighted. As the number of nodes in the network increases, we face with two phenomena affecting the network lifetime in different directions:

1. The probability that a node is selected frequently as part of a route decreases. This can reduce the possibility that a node is overused. Hence, the lifetime of nodes and consequently the network lifetime increases.

2. When the node degree increases, each node will receive more unicast and broadcast packets transmitted by its neighboring nodes. This increases the energy consumption rate of nodes. Therefore, the lifetime of nodes and consequently the network lifetime decrease.

Figure 6.8 shows that these phenomena have different combined effects on the performance of various algorithms. For RMECR, MBCR, MMBCR, and Unified RMER, for a specific node degree lower than 25, the first phenomenon is the dominant factor in determining the network lifetime. After this threshold, the second phenomenon becomes the dominant factor, where the network lifetime tends to decreases as the average node degree increases. For CMMBCR and MRPC, the second phenomenon is always the dominant factor.

To verify the second phenomenon, we showed in Figure 6.9 the average amount of energy consumed for end-to-end traversal of a data packet. The energy consumed to transmit and receive route discovery messages (RREQs which are broadcast and RREPs which are unicast) and data packets (which are unicast too) are shown separately. The figure clearly shows that the energy consumed by nodes to *receive* packets is the major source of energy consumption in the network. Furthermore, as the average node degree in the network increases, the energy consumed to *receive broadcast RREQ messages* becomes the dominant source of energy consumption. Thus, we can imagine how ignoring the energy consumed by nodes during packet reception in an energy consumption model can affect performance of battery-aware routing algorithms.
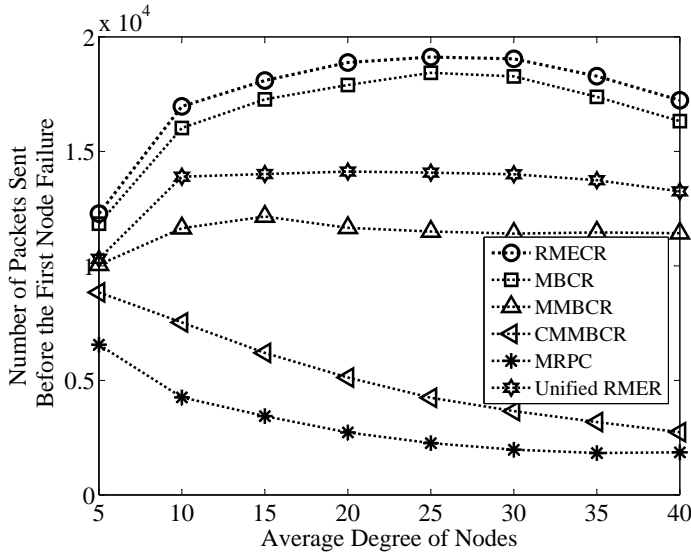
Figure 6.8 – Impact of the average degree of nodes on the network lifetime for various routing algorithms in networks with static BP nodes capable of controlling their transmission power. The average PDR of links for data packets is 0.9.
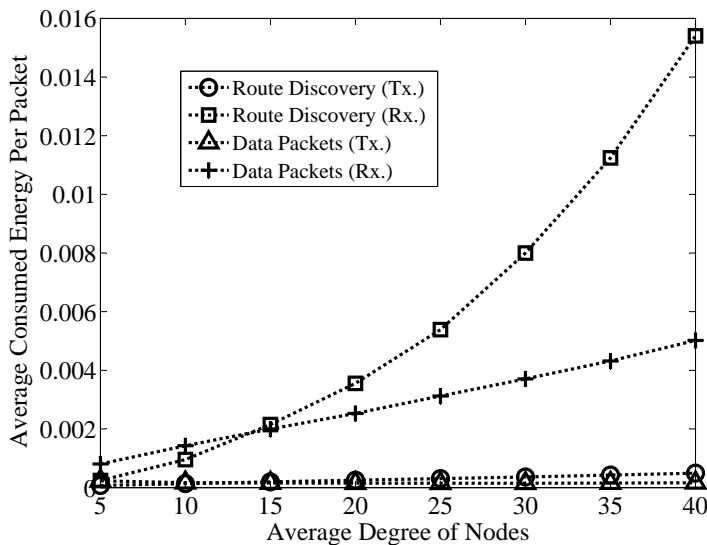
Figure 6.9 – The average amount of energy consumed per packet for transmission and reception of the packet and the route discovery messages. The illustrated results are for the RMECR algorithm.

6.5.2.4 Impact of Route Refreshing Frequency

Here, we show how route refreshment frequency in battery-aware algorithms affects the network lifetime. To this end, we fix the mean session duration μ, and we change the value of the route refreshing period δ. This means, the route refreshment frequency decreases when the ratio of $\frac{\delta}{\mu}$ increases. We have provided results for our proposed algorithm RMECR, which outperforms other battery-aware routing algorithms.

When the route refreshment frequency decreases, we encounter two phenomena that have opposite effects on the network lifetime.

1. Since nodes along a discovered route will be used for a longer time, they might be overused. This reduces the network lifetime.

2. Since route refreshing will happen less frequently, the overhead of route discovery decreases. Consequently, the energy consumption rate of nodes reduces. This increases the network lifetime:

We observe in Figure 6.10 that before a specific value of $\frac{\delta}{\mu}$, the second phenomenon is the dominant factor. After this threshold, the first phenomenon is the dominant factor. This is true for both values of the mean session duration, i.e., 200 and 1000 [s]. Nevertheless, for large values of $\frac{\delta}{\mu}$, the network lifetime remains unchanged for all the algorithms. This is a case in which the refreshment interval is much higher than the average lifetime of a session. Thus, route refreshment may not happen during the lifetime of the session. As a result, the discovered route at the session start-up may remain unchanged.

6.5.2.5 Impact of Transmission Power Control

How does TPC impact the performance of our proposed battery-aware routing algorithm RMECR? To answer this question, we conducted simulation studies in which the number of nodes is fixed to 150. As mentioned in Chapter 5, TPC can increase the PDR of links by reducing the collision probability. Hence, we fix the maximum collision probability (MCP) when TPC is not utilized to 0.5, and we change the ratio between MCP with TPC to MCP without TPC. We observe in Figure 6.11 that TPC increases the network lifetime, since it reduces the overall energy consumption of nodes. As explained in Chapter 5, this is due to decreasing the transmission power of nodes and decreasing the number of retransmissions due to collision.
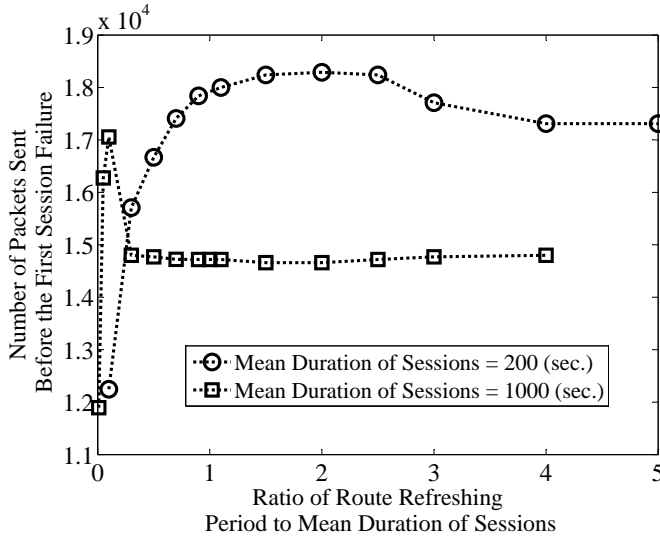
Figure 6.10 – Impact of the route refreshment frequency on the network lifetime for the RMECR algorithm in a network with 150 static BP nodes capable of controlling their transmission power. The average PDR of links for data packets is 0.9.
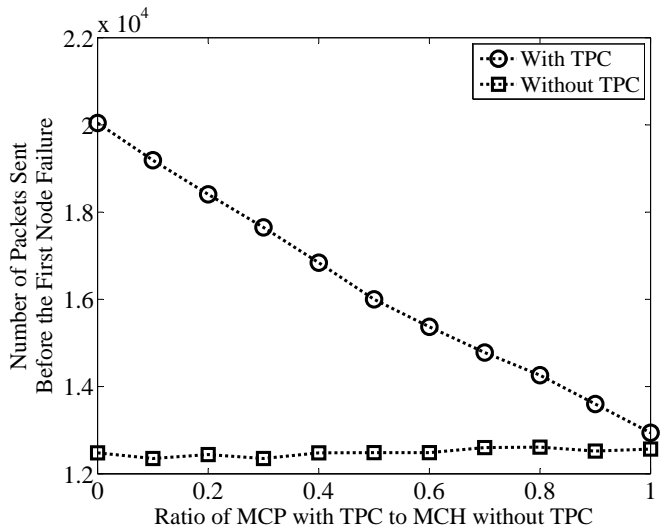
Figure 6.11 – Impact of TPC on the network lifetime for the RMERCR algorithm in a network with 150 static BP nodes. The horizontal axis is the ratio between maximum collision probability (MCP) of links when TPC is utilized to that of the network when TPC is not utilized.

6.5.2.6   Impact of Mobility

How does mobility affect the performance of battery-aware algorithms? In this section, we compare the performance of these algorithms in mobile networks. To this end, we consider a Random Waypoint [109] mobility model for nodes. Each node chooses a random destination point (within the network area) and moves towards that destination point with a velocity which is chosen randomly from the interval $(0, \mathcal{V}_m)$. When the node arrives at the destination point, it waits for a random duration which is known as pause time. The pause time is chosen randomly from the interval $(0, \mathcal{T}_p)$.

In mobile networks, the rate of topology change increases, because the source and the destination node of a session as well as the intermediate nodes between them change their positions. This will cause frequent route failures. As a result, the energy consumption rate of nodes increases due to the increased rate of route discovery in the network. This fact could be observed in Figure 6.12(a). In this figure, a mobility speed of zero means that all nodes are static. We observe that compared to static nodes, mobile nodes consume more energy for route discovery. This explains why the network lifetime tends to decrease in Figure 6.12(b) and Figure 6.12(c) when the maximum speed of nodes increases.

By comparing plots in Figure 6.12(b) with those in Figure 6.12(c), we can conclude that the network lifetime decreases with a bigger slope when there are 150 nodes in the network. While the static network with 150 nodes has a lifetime higher than that of a network with 75 nodes (regardless of the routing algorithm), a mobile network with 75 nodes has a higher lifetime. In fact, frequent route re-discoveries due to mobility reduce the network lifetime dramatically in dense networks, because nodes will receive more broadcast packets from their neighbors.

6.5.3   Networks with Heterogeneous Power Supplies

When it comes to networks with heterogeneous power supplies, we can consider the type of power supply of nodes in routing. Here, we highlight some facts regarding the performance of battery-aware algorithms RMLNR, RLBNR, RMLNR-LM, RMLNR-WSA, RLBNR-LM and RLBNR-WSA in such networks.

We may think that if we connect some nodes of the network to the mains, the network lifetime will increase, because the probability that BP nodes act as a relay reduces. Thus, directing the traffic load towards MP nodes could be seen as an effective scheme to further increase the network lifetime. Our investigation, however, show that this may not always be true. Directing the traffic load towards MP nodes, as being done by single objective algorithms RMLNR and RLBNR, or bi-objective algorithms RMLNR-LM and RLBNR-LM, can even reduce the network lifetime (see Figure 6.13(a)). The figure shows that any of these four algorithms
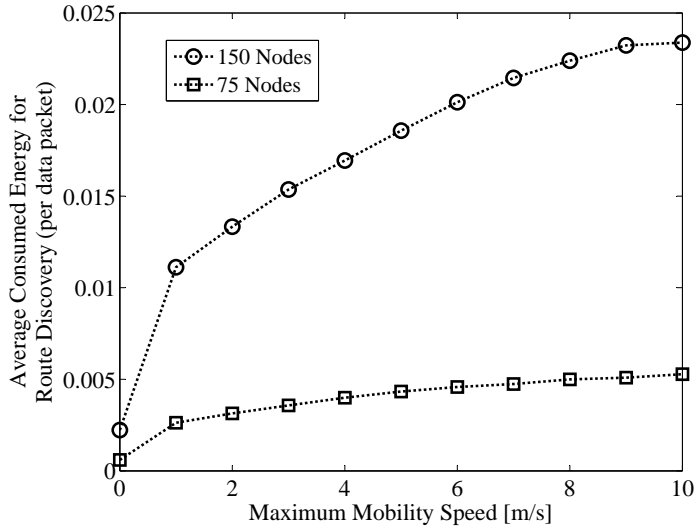
(a)
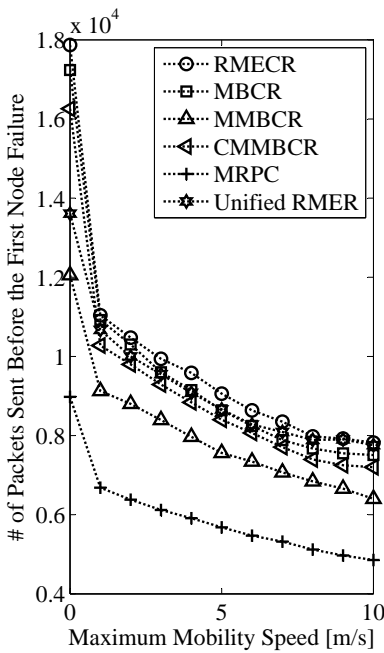
(b) 75 Nodes
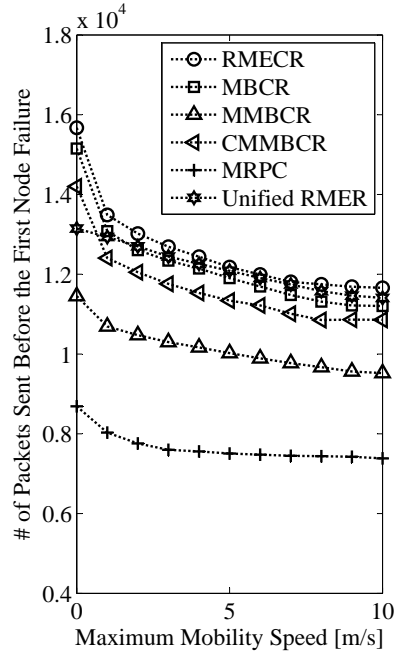
(c) 150 Nodes

Figure 6.12 – Plot (a) shows the average amount of energy consumed per data packet for route discovery. The illustrated results are for the RMECR algorithm. Plots (b) and (c) show the number of packets sent before the first node failure in networks with 75 and 150 nodes, respectively. The value of the maximum pause time is 15 [s].

achieve a higher network lifetime if there is no MP node in the network. This is even true for RMECR which does not explicitly distinguish (like RMLNR and RLBNR) between MP and BP nodes. However, RMECR implicitly does this by considering a constant value for the remaining battery energy of MP nodes, while that of BP nodes reduces with time. The only algorithm which benefits from having MP nodes in the network is Unified RMER, which does not consider the battery energy of nodes in route selection at all.

The reason for this phenomenon lies in the fact that directing the traffic load towards MP nodes imposes a lot of overhearing on BP nodes around MP nodes. Even if such BP nodes do not forward packets, they have to overhear a large number of packets from their neighboring MP nodes. Since directing the traffic load to MP nodes increases the hop-count of routes as suggested by Figure 6.13(b)[1], it requires more BP nodes to overhear forwarded packets by MP nodes. This causes faster failure of these BP nodes. The problem is more severe if MP nodes are a minority in the network, because all the traffic will be directed towards this minority set of MP nodes. If MP nodes are a majority, the adverse effect of directing the traffic load towards them is less. This explains the concave shape of the plots in Figure 6.13(a).

The severity of the above mentioned problem is less by considering the second objective in route selection, i.e., minimizing the total ETX of routes. This reduces the hop count of the selected routes as implied by Figure 6.13(b). The figure shows that when the majority of nodes are MP, the bi-objective algorithms RMLNR-LM and RLBNR-LM find shorter routes compared to their corresponding single-objective algorithms RMLNR and RLBNR. As a result, less BP nodes will overhear, and the network lifetime will increase for bi-objective algorithms. This, however, can not resolve the problem completely.

Is there any other solution? How can we benefit from having MP nodes in the network? One solution is to reduce overhearing of nodes[2]. This could be done using *sleep and wake up* MAC protocols which puts node in sleep mode most of the time. Alternatively, we can reduce the energy cost of nodes for packet reception by designing ultra low power receiving circuits. To give an impression on how reducing the overhearing can affect the network lifetime, we have repeated the results of Figure 6.13(a) in Figure 6.14 assuming overhearing is avoided. The figure clearly shows that RMLNR, RLBNR, RMLNR-LM and RLBNR-LM can increase the network lifetime compared to RMECR and Unified RMER through directing the traffic load towards MP nodes.

---

[1]The higher total ETX for routes selected by RMLNR, RLBNR, RMLNR-LM and RLBNR-LM compared to RMECR and Unified RMER is the result of a higher hop-count not the lower reliability of their constituent links.

[2]Another solution is the use of topology control algorithms, which will be studied in the next chapter.

(a)   (b)
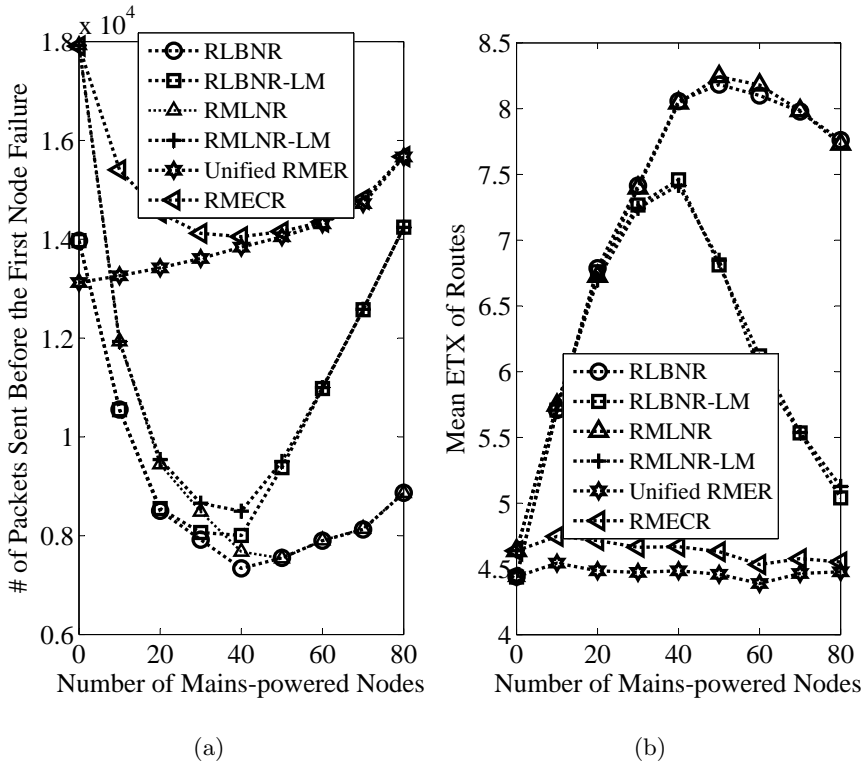
Figure 6.13 – Performance of various routing algorithms in networks with heterogeneous power supplies. Nodes are static and deploy TPC. The horizontal axis in both plots is the number of MP nodes. There are 100 nodes in the network.
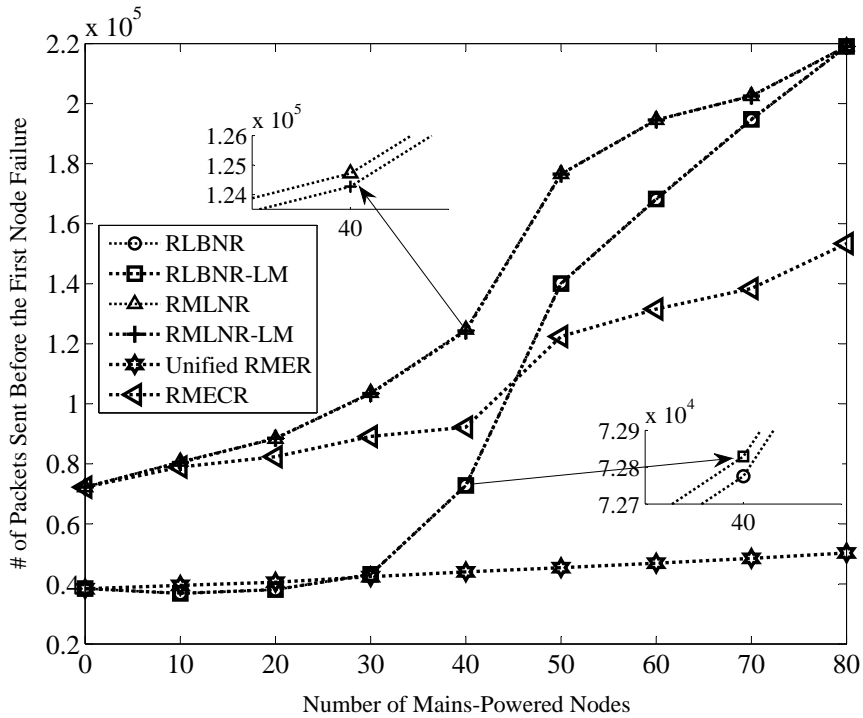
Figure 6.14 – Performance of battery-aware routing algorithms in networks with heterogeneous power supplies when energy consumption for packet reception is negligible. Nodes are static and deploy TPC. The total number of nodes in the network is 100.

Let us compare the performance of WSA-based algorithms with that of LM-based algorithms. To this end, we first study the choice of the weighing coefficient a in WSA-based algorithms. This coefficient controls the weight of minimizing the energy cost to minimizing the total ETX of routes in route selection. Results depicted in Figure 6.15 show that at the cost of increased ETX of routes, we may increase the achievable network lifetime by RMLNR-WSA through increasing the value of the weighing coefficient a from 0 to 1. When MP nodes are a minority (here 25 out of 100 nodes), the increase in rate of the network lifetime is smaller compared to the case that MP nodes are a majority (here 75 out of 100 nodes). According to the plots in Figure 6.15, we can choose $a = 0.5$ as a reasonable choice for RMLNR-WSA algorithms. Similar results are valid for RLBNR-WSA (we skipped the plots). With this choice, we have compared the performance of WSA-based and LM-based algorithms in Figure 6.16. The figure suggests that the performance of each WSA-based algorithm is similar to that of its corresponding LM-based algorithm. In other words, RMLNR-WSA (RLBNR-WSA) and RMLNR-LM (RLBNR-LM) have a similar performance.

6.6   Summary

In this chapter, we studied battery-aware routing in wireless multi-hop networks. Battery-aware routing specifies how information about remaining battery energy of nodes and type of their power supplies can be used in route selection. Several novel battery-aware routing schemes were proposed. RMECR was proposed as an algorithm for networks with all battery powered nodes. RMECR considers the remaining battery-energy of nodes to balance the traffic load among nodes. This can increase the lifetime of nodes as well as the lifetime of the network as a whole. Furthermore, the energy-efficiency and reliability of routes selected by RMECR is close to the one for routes discovered by Unified RMER. Simulation studies show that RMECR outperforms the battery-aware routing algorithms proposed so far for wireless multi-hop networks in several aspects (network lifetime, reliability of routes, and energy-efficiency of routes) and scenarios (static and mobile networks). We then proposed RLBNR and RMLNR algorithms. They are single-objective battery-aware routing algorithms which can differentiate between mains-powered and battery-powered nodes in route selection. They direct the traffic load to mains-powered nodes through considering no battery cost for packet forwarding by these nodes. RLBNR is based on Unified RMER and RMLNR is based on RMECR. In other words, RLBNR only considers the type of power supply of nodes, while RMLNR also considers the remaining battery-energy of battery-powered nodes. Nevertheless, simulation studies showed that directing the traffic load towards mains-powered nodes, as being done by RLBNR and

(a)   (b)
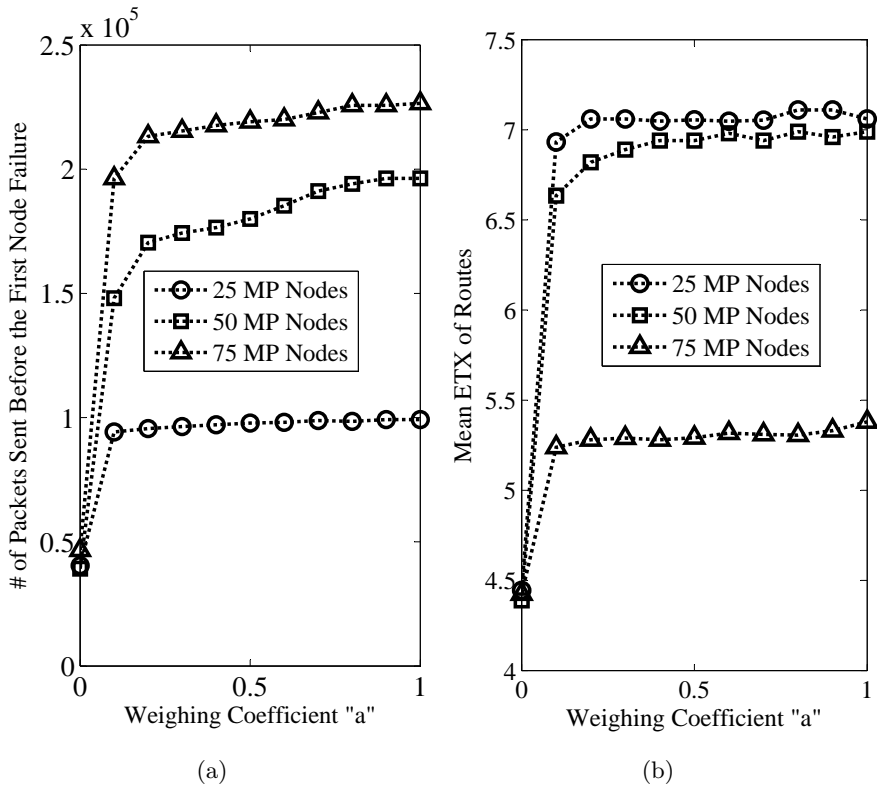
Figure 6.15 – The impact of weighing coefficient a on the performance of RMLNR-WSA. Nodes are static and deploy TPC. The total number of nodes in the network is 100, and overhearing could be avoided.

(a)

(b)
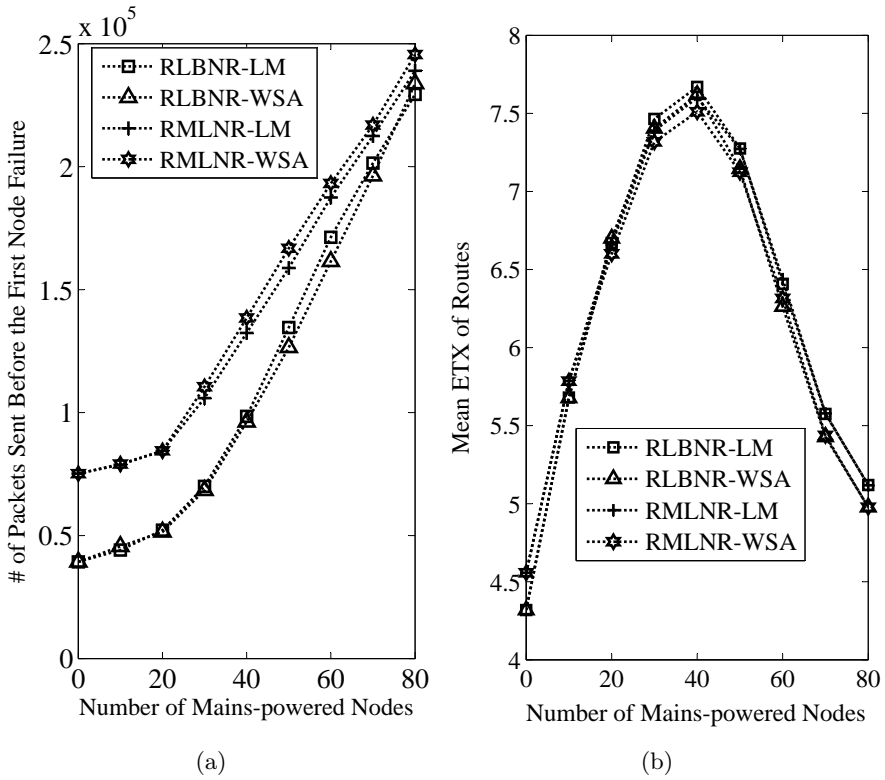
Figure 6.16 – Performance of WSA-based and LM-based algorithms in networks with static nodes capable of controlling their transmission power. The total number of nodes in the network is 100, and overhearing could be avoided.

RMLNR, can reduce the lifetime of battery-powered nodes which are neighbors of mains-powered nodes, because they overhear many packets. Directing the traffic load to mains-powered nodes can increase the network lifetime, only if energy consumption for overhearing is reduced. We also proposed bi-objective routing algorithms for wireless multi-hop networks with mains-powered nodes. The bi-objective algorithms consider minimizing the energy cost of routes (same as single-objective algorithms) and minimizing the accumulated ETX of routes as two objectives in route selection. The lexicographic method (LM) and the weighted sum approach (WSA) were used to design various bi-objective battery-aware routing algorithms. RLBNR-LM and RMLNR-LM use LM and RLBNR-WSA and RMLNR-WSA use WSA. Simulation studies showed that bi-objective algorithms can reduce the hop-count of routes compared to single-objective algorithms, when the majority of nodes is mains-powered. Nevertheless, LM-based and WSA-based algorithms achieve the same network lifetime. We also discussed issues regarding the implementation of the proposed algorithms using reactive and proactive protocols. The impact of node density, route refreshment frequency, mobility, and transmission power control on the lifetime of wireless multi-hop networks was also studied.

Chapter 7

Topology Control

In the previous chapter, we observed that overhearing consumes a considerable amount of energy of nodes in wireless multi-hop networks. It can dramatically reduce the lifetime of individual nodes as well as the lifetime of the whole network. Reducing the energy consumption of transceivers for packet reception and deploying sleep and wake up MAC protocols are two effective ways for reducing overhearing of nodes, which we concluded in the previous chapter. Another effective mechanism which could be deployed in conjunction with these two solutions is reducing the transmission power (range) of nodes. If nodes reduce their transmission range, they will have fewer neighbors. As a result, they will be exposed to overhearing by fewer nodes in the network. The important question, however, is to what extent nodes are allowed to reduce their transmission range such that the network remains connected. Topology control is a technique which deals with this issue.

In this chapter, we study topology control in wireless multi-hop networks. To this end, we first provide the background knowledge on topology control in these networks in Section 7.1. Then, in Sections 7.3 and 7.4, we present two topology control algorithms that we propose for wireless multi-hop networks. Section 7.5 presents practical considerations for deploying the proposed algorithms, and Section 7.6 presents simulation studies. We summarize the chapter in Section 7.7.

7.1 Background

In a dense wireless multi-hop network, each node could have links to many other nodes within its transmission range. Nevertheless, since nodes communicate with each other in a cooperative way, we can remove many of these links without harming the network connectivity. This concept has been illustrated in Figure 7.1, which

shows that the network is still connected even if we remove some links between nodes.

The result of topology control in wireless multi-hop network is a network with less links. This is achieved by reducing the transmission range, or equivalently the transmission power of nodes. In other words, if G and G' present the network topology before and after topology control, respectively, $G' \subset G$ will be an *energy-efficient spanning subgraph* of G which results from reducing the transmission power. A *topology control algorithm* specifies how G' is created using G.

A topology control algorithm determines which links have to remain between nodes, and which links are not necessary to keep the network connected. This means that a topology control algorithm could even be considered as a neighbor discovery algorithm which considers the impact of selecting a node as a neighbor on the connectivity of the whole network. Note that we can also consider topology control as a type of power control in wireless multi-hop network. Nevertheless, we differentiate between these two concepts in this thesis. TPC, as it was defined in Chapter 3, deals with adjusting the transmission power of nodes according to the distance to their neighbors. On the other hand, a topology control algorithm controls the *maximum* power that a node is allowed to consume for signal transmission in the network.

We can list at least three benefits for topology control in wireless multi-hop networks. First, reducing the transmission range (power) of nodes reduces their energy consumption for packet exchange with their neighbors. Second, since nodes have fewer neighbors, they will overhear fewer packets from their neighbors. Third, collision probability will be reduced, because nodes will interfere less with each other. The major drawback of topology control is, however, the reduction of the number of alternative routes between nodes. This makes the network more vulnerable to node failure. Furthermore, since traffic load should be carried through less links, each node may relay more packets. Thus, the energy consumption rate of nodes increases. Consequently, their failure rates increase.

The solution for this problem is what we call *fault-tolerant topology control*. In this technique, the network is kept fault-tolerant while the transmission range of nodes is reduced. To achieve a specific level of fault tolerance in a network, from the connectivity point of view, each node should have a certain number of disjoint paths to every other node. That is, instead of keeping the network 1-connected, it is kept k-connected ($k > 1$). Fault-tolerant topology control ensures that there are at least k node-disjoint routes between every two nodes even after removing some links in the network. In summary, we can categorize topology control algorithms into *ordinary and fault-tolerant* algorithms. Ordinary algorithms reduce the transmission range of nodes such that the network remains only 1-connected. On the other hand, fault-tolerant algorithms maintain k-connectivity ($k > 1$).
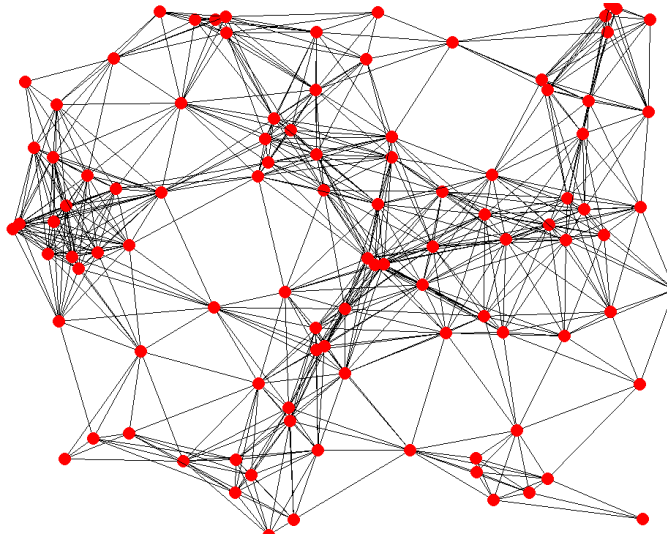
(a) Without Topology Control
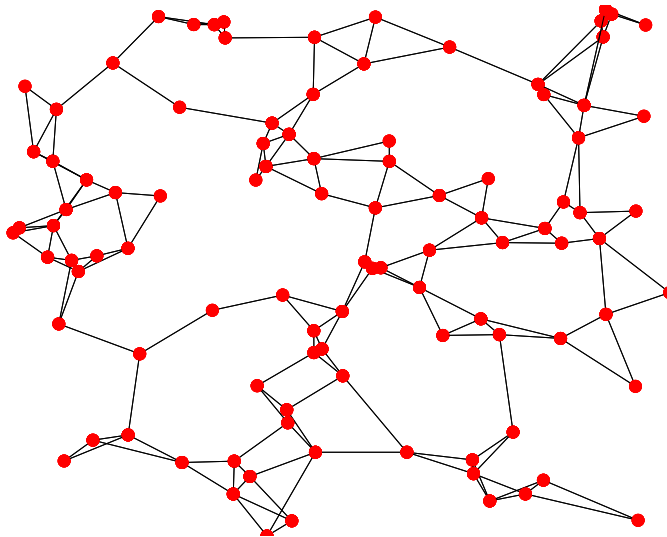
(b) With Topology Control

Figure 7.1 – Topology of a wireless multi-hop networks before and after topology control. The graph in Plot (a) is the result of nodes using their maximum transmission power (range), while in Plot (b) nodes use reduce their transmission power (range).

In another categorization, topology control algorithms can either be *centralized* or *localized (distributed)*. A localized algorithm only uses information gathered locally by each node to adjust the transmission range of nodes without having the global image of the network topology. On the other hand, a centralized algorithm requires the global image of the network topology to construct an energy-efficient spanning subgraph of the network. It is obvious that the deployment of a centralized topology algorithm is more difficult, because all nodes need to have a complete view of the network topology. Although this could be obtained using a link state proactive routing protocol like OLSR, it generates high overhead. On the other hand, in a localized algorithm, global view of the network topology is not required. Each node only needs to know its neighbors.

The state-of-the-art algorithm for fault-tolerant localized topology control is FLSS (Fault-tolerant Local Spanning Subgraph) [70]. FLSS is able to reduce the transmission power of nodes in such a way that the highest transmission power among all the nodes[1] of the network is minimized (min-max optimality) keeping the network k-connected. It has been proven that the maximum transmission power amongst all nodes of the network is smaller if FLSS is used instead of other fault-tolerant topology control algorithms such as CBTC (Cone-Based distributed Topology Control) [110] and Yao [111]. Compared to the recently proposed algorithm LTRT (Local Tree-based Reliable Topology) [112], which only preserves k-edge connectivity, preserving k-vertex connectivity by FLSS is more valuable, because the failure of a node (vertex) removes all the associated links (edges) with the failed node.

The existing schemes, however, have one characteristic in common. All of them have been designed and optimized for networks which consist of only battery-powered devices. This, of course, is a valid assumption for many applications of wireless multi-hop networks such as wireless sensor networks, in which all nodes are running on batteries. However, as mentioned before, in many applications such as ad hoc networking in conference centers, wireless mesh networking, and in-home multi-hop networking, nodes could have heterogeneous power supplies. While some nodes may run on battery, there might be nodes connected to the mains. Since mains-powered nodes can be considered to have infinite energy for communication, the heterogeneity of power supply of nodes could be exploited to provide a performance gain through topology control.

The novelty in this chapter is the proposal of a localized fault-tolerant topology control algorithm, named HFLTC (Heterogeneous Fault-Tolerant Localized Topology Control), designed and optimized for multi-hop networks with heterogeneous power supplies. HFLTC uses the advantage of having mains-powered nodes in the

---

[1]Note that topology control may result in different values for the transmission power of different nodes.

network to reduce the transmission power of battery-powered nodes while keeping the network k-connected. This is done by creating a backbone of mains-powered nodes formed using the most energy-efficient links between them, and then attaching battery-powered nodes to this backbone also using the most energy-efficient links. We prove that HFLTC distinctively achieves min-max optimality for the battery-powered nodes of the network. That is, the maximum transmission power of battery-powered nodes of the network required to keep the network k-connected is minimized. FLSS cannot guarantee such optimality in networks with heterogeneous power supplies. Furthermore, simulation results show that the average degree and average transmission range of battery-powered nodes in the topology generated by HFLTC is smaller than these values in the topology generated by FLSS. Furthermore, HFLTC can also provide a higher lifetime for wireless multi-hop networks. In this chapter, we also present a centralized version of HFLTC called Heterogeneous Fault-Tolerant Centralized Topology Control (HFCTC). HFCTC will be used as a benchmark to evaluate the effectiveness of its distributed version HFLTC.

7.2   Notations and Definitions

We consider a multi-hop network which its original topology (without topology control) represented by a directed graph $G(\mathbb{V}(G), \mathbb{E}(G))$, where $\mathbb{V}(G)$ is the set of nodes and $\mathbb{E}(G)$ is the set of links of G. In other words, $G(\mathbb{V}(G), \mathbb{E}(G))$ is the network topology when all nodes use their maximum transmission power. The set of battery-powered (BP) nodes of G is denoted by $\mathbb{V}_b(G)$, and the set of its mains-powered (MP) nodes are denoted by $\mathbb{V}_m(G)$. We define $\mathbb{E}_b(G) = \{(u,v) \in \mathbb{E}(G) | u \in \mathbb{V}_b(G)\}$ as the set of links going out from BP nodes of G (i.e., set of BP links). Similarly, $\mathbb{E}_m(G) = \{(u,v) \in \mathbb{E}(G) | u \in \mathbb{V}_m(G)\}$ is defined as the set of links going out from MP nodes of G (i.e, set of MP links).

For creating an energy-efficient spanning subgraph, the weight of each link should be the energy required for packet exchange between the two-end nodes of the link. We know that such an energy is a linear function of the power η of the Euclidean distance d between the two-end nodes, i.e., $c_0 d^\eta + c_1$, where c_0 and c_1 are constants. Under the assumption of using the same wireless interface in different nodes, for the algorithms presented in this chapter, it suffices to use the Euclidean distance as the weight function, because $c_0 d^\eta + c_1$ is a strictly increasing function of the Euclidean distance d. We use the identifiers of nodes as a tie-breaker, when different edges with different vertices have the same Euclidean distance[1].

---

[1]In this chapter, we will use edge and link as well as node and vertex interchangeably.

Definition 3. *Weight Function:* *For an edge (u, v), the weight function $w : \mathbb{E} \mapsto R^3$ maps to a 3-tuple. That is,*

$$w(u, v) = (d(u, v), \max\{id(u), id(v)\}, \min\{id(u), id(v)\}).$$

Given $(u_1, v_1), (u_2, v_2) \in \mathbb{E}$, we have

$$
\begin{aligned}
&w(u_1, v_1) > w(u_2, v_2) \\
&\Leftrightarrow d(u_1, v_1) > d(u_2, v_2) \\
&or \; \big(d(u_1, v_1) = d(u_2, v_2) \\
&\quad \&\& \max\{id(u_1), id(v_1)\} > \max\{id(u_2), id(v_2)\}\big) \\
&or \; \big(d(u_1, v_1) = d(u_2, v_2) \\
&\quad \&\& \max\{id(u_1), id(v_1)\} = \max\{id(u_2), id(v_2)\} \\
&\quad \&\& \min\{id(u_1), id(v_1)\} > \max\{id(u_2), id(v_2)\}\big).
\end{aligned}
$$

In the definition given for the link weight, $id(u)$ is the unique identifier of node u. This definition of link weight implies that two edges with different end-vertices will have different weights. Nevertheless, if two edges have the same end-vertices, their weights will be the same. In other words, $w(u, v) = w(v, u)$. Other definitions that we will use in this chapter are as follows:

Definition 4. *Visible Neighborhood:* *The visible neighborhood of node u, denoted as $\mathbb{N}(u)$, is the set of nodes that node u can reach in the network when it uses its maximum transmission power. That is, $\mathbb{N}(u) = \{v \in \mathbb{V}(G) | (u, v) \in \mathbb{E}(G)\}$. For each node $u \in \mathbb{V}(G)$, $G_u^{\mathbb{V}} = (\mathbb{V}(G_u^{\mathbb{V}}), \mathbb{E}(G_u^{\mathbb{V}}))$ is defined as the induced subgraph of G such that $\mathbb{V}(G_u^{\mathbb{V}}) = \{u\} \cup \mathbb{N}(u)$ and $\mathbb{E}(G_u^{\mathbb{V}}) = \{(u_0, v_0) \in \mathbb{E}(G) | u_0, v_0 \in \mathbb{V}(G_u^{\mathbb{V}})\}$.*

Definition 5. *Neighbor Relation:* *Node v is a neighbor of node u under an algorithm ALG –denotes as $u \xrightarrow{ALG} v$– if and only if there is a directed edge (u, v) in the topology generated by ALG.*

Definition 6. *Topology:* *The topology generated by an algorithm ALG is a directed graph $G_{ALG} = (\mathbb{V}(G_{ALG}), \mathbb{E}(G_{ALG}))$, in which $\mathbb{V}(G_{ALG}) = \mathbb{V}(G)$, and $\mathbb{E}(G_{ALG}) = \{(u, v) \in \mathbb{E}(G) | u \xrightarrow{ALG} v\}$.*

Definition 7. *Radius:* *The radius of node u under an algorithm ALG is denoted by $R_{ALG}(u)$, and is defined as the Euclidean distance between node u and its farthest neighbor in the topology generated by ALG. That is, $R_{ALG}(u) = \max_{v \in \mathbb{N}_{ALG}(u)}\{d(u, v)\}$.*

Definition 8. *Degree:* *The degree of a node u under an algorithm ALG, denoted as $Deg_{ALG}(u)$, is defined as the number of neighboring nodes of u in the topology generated by ALG. That is, $Deg_{ALG}(u) = |\mathbb{N}_{ALG}(u)|$.*

Definition 9. *Connectivity: Node u is connected to node v in a topology generated by algorithm ALG, if there exists a path $\mathcal{P} = \{n_1 = u, n_2, n_3, ..., n_h, n_{h+1} = v\}$ such that $n_i \xrightarrow{ALG} n_{i+1}$, $i = 1...h$, and $n_i \in \mathbb{V}(G_{ALG})$, $i = 1...n + 1$. If there are k node-disjoint paths (paths without intermediate nodes in common), u and v are k-connected.*

Definition 10. *Addition and Removal: The Addition operation adds an extra edge (v, u) into G_{ALG}, if $(u, v) \in \mathbb{E}(G_{ALG})$ and $(v, u) \notin \mathbb{E}(G_{ALG})$. The Removal operation removes any edge $(u, v) \in \mathbb{E}(G_{ALG})$, if $(v, u) \notin \mathbb{E}(G_{ALG})$.*

7.3 Heterogeneous Fault-Tolerant Centralized Topology Control

The key idea behind topology construction by our proposed algorithms HFCTC and HFLTC is the same. As mentioned before, they create a backbone of mains-powered nodes formed using the most energy-efficient links, and then attach battery-powered nodes to this backbone also using the most energy-efficient links. The difference between these two algorithms is that, HFCTC requires the complete knowledge of the network topology, i.e., $G(\mathbb{V}, \mathbb{E})$, while HFLTC only requires local information gathered by each node, i.e., $G_u^{\mathbb{V}} = (\mathbb{V}(G_u^{\mathbb{V}}), \mathbb{E}(G_u^{\mathbb{V}}))$. In this section, we present HFCTC. HFLTC will be presented in the next section.

The way that HFCTC constructs the network topology is explained in Algorithm 7. In order to create a backbone of MP nodes using the most energy-efficient links between them, at the beginning it is assumed that there is no link between nodes in the network. We sort all links going out from MP nodes of the network (i.e., MP links) in the ascending order of weight. Each link from the ordered set is added to the network topology only if the two end nodes of the link are not k-connected. If they are already k-connected, that link is not necessary to be added. Next, BP nodes are attached to this backbone again using the most energy-efficient links. To this aim, we inspect links going out from BP nodes of the network (i.e., BP links) in the same way that we inspected MP links. That is, a BP link is added to the topology only if the two end-nodes of that link are not k-connected. By the use of the Dinic's algorithm [113, 114], proposed for solving the max-flow problem, we can determine whether two nodes are k-connected in at most $O(|\mathbb{V}|^{1/2}|\mathbb{E}|)$ stepts. Thus, the time complexity of the HFCTC algorithm is $O(|\mathbb{V}|^{1/2}|\mathbb{E}|^2)$. It is worth-noticed that the generated topology by HFCTC may contain some directional links. In the sequel, we prove that if a topology is created in this way, it will be k-connected assuming the original topology is k-connected too. Moreover, we prove that the maximum transmission power among BP nodes of the network required to keep the network k-connected is minimized.

Algorithm 7 HFCTC: a centralized topology control algorithm for preserving k-connectivity in networks with heterogeneous power supplies. $\mathbb{V}_m$ is the set of mains-powered nodes and $\mathbb{V}_b$ is the set of battery-powered nodes of the network.

Procedure FCTC
Input $G(\mathbb{V}, \mathbb{E})$
Output $G_k(\mathbb{V}_k, \mathbb{E}_k)$
$\mathbb{V}_k \leftarrow \mathbb{V}, \mathbb{E}_k \leftarrow \emptyset$
$\mathbb{E}_m \leftarrow \{(u, v) \in \mathbb{E} \mid u \in \mathbb{V}_m\}$
$\mathbb{E}_b \leftarrow \mathbb{E} - \mathbb{E}_m$
sort all edges in $\mathbb{E}_m$ is ascending order of weight
for each edge (u_1, v_1) in the order **do**
  if u_1 is not k-connected to v_1 in G_k **then**
    $\mathbb{E}_k \leftarrow \mathbb{E}_k \cup (u_1, v_1)$
  end if
end for
sort all edges in $\mathbb{E}_b$ is ascending order of weight
for each edge (u_2, v_2) in the order **do**
  if u_2 is not k-connected to v_2 in G_k **then**
    $\mathbb{E}_k \leftarrow \mathbb{E}_k \cup (u_2, v_2)$
  end if
end for

7.3.1 Correctness

To prove the correctness of the HFCTC algorithm, we first assume that the maximum transmission range of all nodes is the same. This means, the original network topology is an undirected graph. Later we relax this assumption by considering a case in which the maximum transmission range of nodes is not the same.

The following two lemmas are required to prove the correctness of HFCTC:

Lemma 1. *Let u_1 and u_2 be two vertices in a k-connected undirected graph F. If u_1 and u_2 are k-connected after removal of edge (u_1, u_2), then $F - (u_1, u_2)$ is still k-connected.*

Proof. See [70].   □

Lemma 2. *Let $G' \subset G$ be a subgraph of undirected graph G such that $\mathbb{V}(G') = \mathbb{V}(G)$. If G is k-connected, and every edge $(u, v) \in \mathbb{E}(G) - \mathbb{E}(G')$ satisfies that u is k-connected to v either in $G - \mathbb{E}_b(G) - \{(u_0, v_0) \in \mathbb{E}_m(G) \mid w(u_0, v_0) \geq w(u, v)\}$, or in $G - \{(u_0, v_0) \in \mathbb{E}_b(G) \mid w(u_0, v_0) \geq w(u, v)\}$, then G' is also k-connected.*

Proof. Let $\mathbb{E}_{diff} = \mathbb{E}(G) - \mathbb{E}(G') = \{(u_1, v_1), (u_2, v_2), ..., (u_l, v_l)\}$ be the set of edges belonging to $\mathbb{E}(G)$ which are not in $\mathbb{E}(G')$. Without loss of generality, we

assume $w(u_1, v_1) \geq w(u_2, v_2) \geq ... \geq w(u_l, v_l)$. We define a series of graphs that
are subgraphs of G: $A_0 = G$ and $A_i = A_{i-1} - (u_i, v_i)$, $i = 1, 2, ..., l$. We need to
show that $A_l = G'$ is k-connected. The proof is by induction. Obviously, $A_0 = G$
is k-connected. Therefore, we need to show that if A_{i-1} is k-connected, then A_i,
$i = 1, 2, ..., l$, will be k-connected as well. To this end, we define a subgraph of G as
$G_i = G - \mathbb{E}_b(G) - \{(u_0, v_0) \in \mathbb{E}_m(G) \mid w(u_0, v_0) \geq w(u_i, v_i)\}$ and another subgraph
as $H_i = G - \{(u_0, v_0) \in \mathbb{E}_b(G) \mid w(u_0, v_0) \geq w(u_i, v_i)\}$. G_i contains only MP links
that their weight is greater than $w(u_i, v_i)$. H_i contains all MP links and those BP
links that their weight is greater than $w(u_i, v_i)$. We obviously have

$$\begin{aligned} G_i &\subseteq A_{i-1} - (u_i, v_i), \\ H_i &\subseteq A_{i-1} - (u_i, v_i). \end{aligned} \tag{7.1}$$

Considering (7.1) and the fact that u_i is k-connected to v_i either in G_i or in H_i
(according to our assumptions), we can conclude that u_i is k-connected to v_i in
$A_{i-1} - (u_i, v_i)$ as well. Thus, based on Lemma 1, $A_i = A_{i-1} - (u_i, v_i)$ is still
k-connected.   □

Theorem 2. *HFCTC can preserve k-connectivity of G. That is, if G is
k-connected, the generated subgraph by HFCTC (denoted by G_k) is k-connected
as well.*

Proof. In HFCTC, at first, edges in $\mathbb{E}_m(G)$ are added to G_k in an ascending order.
Thus, the fact that u is k-connected to v at the moment before $(u, v) \in \mathbb{E}_m(G)$
is added to G_k depends only on the edges in $\mathbb{E}_m(G)$ which have smaller weights.
Furthermore, since edges of $\mathbb{E}_b(G)$ are added to G_k in an ascending order after
adding edges of $\mathbb{E}_m(G)$, whether u is k-connected to v at the moment before $(u, v) \in$
$\mathbb{E}_b(G)$ is added, depends only on all edges in $\mathbb{E}_m(G)$ and those in $\mathbb{E}_b(G)$ which have
smaller weights. Therefore, every edge $(u, v) \in \mathbb{E}(G) - \mathbb{E}(G_k)$ satisfies that u is
k-connected to v either in $G - \mathbb{E}_b(G) - \{(u_0, v_0) \in \mathbb{E}_m(G) \mid w(u_0, v_0) \geq w(u, v)\}$,
or in $G - \{(u_0, v_0) \in \mathbb{E}_b(G) \mid w(u_0, v_0) \geq w(u, v)\}$. We can prove that G_k preserves
k-connectivity of G by applying Lemma 2 to G_k (assuming $G' = G_k$).   □

7.3.2 Optimality

Let $\mathbb{S}_k(G)$ be the set of all k-connected spanning subgraphs of G, and $\rho_b(F)$ be
the largest radius of all BP nodes in the spanning subgraph $F \in \mathbb{S}_k(G)$. That is,
$\rho_b(F) = \max_{u \in \mathbb{V}_b(F)}\{R(u)\}$. Assuming G_k is the subgraph generated by HFCTC,
we prove that $\rho_b(G_k) = \min\{\rho_b(F) | F \in \mathbb{S}_k(G)\}$. That is, HFCTC achieves a
min-max optimality for BP nodes of the network by minimizing the maximum
radius among them.

Theorem 3. *The maximum radius (or equivalently power) among all battery
-powered nodes in the network is minimized by HFCTC.*

Proof. Suppose G is k-connected. Based on Theorem 2, G_k is also k-connected. Assume (u, v) is the last edge that is inserted into G_k. Since BP links are inserted after MP links, we have $w(u, v) = \max_{(u_0, v_0) \in \mathbb{E}_b(G)} \{w(u_0, v_0)\}$, and $R(u) = \rho_b(G_k)$. We define $G'_k = G_k - (u, v)$. Since (u, v) is in G_k, u and v must not be k-connected to each other in G'_k. This means, G'_k is not k-connected.

Now, consider a graph $H = (\mathbb{V}(H), \mathbb{E}(H))$, in which $\mathbb{V}(H) = \mathbb{V}(G)$ and $\mathbb{E}(H) = \mathbb{E}_m(G_k) \cup \{(u_0, v_0) \in \mathbb{E}_b(G) | w(u_0, v_0) < w(u, v)\}$. To prove the theorem, we need to show that H is not k-connected. If so, we will be able to conclude that any $F \in \mathbb{S}_k(G)$ must have at least one edge whose length is equal to or longer than that of (u, v). That is, $\rho_b(G_k) = \min\{\rho_b(F) | F \in \mathbb{S}_k(G)\}$.

We prove that H is not k-connected by contradiction. Assume H is k-connected. Thus, two nodes u and v are k-connected to each other in H. This means, $\mathbb{E}(G'_k) \subseteq \mathbb{E}(H)$, because nodes u and v are not k-connected to each other in G'_k. Therefore, $\mathbb{E}_0 = \mathbb{E}(H) - \mathbb{E}(G'_k) \neq \emptyset$. Since BP links are inserted into G'_k in an ascending order after all MP links are inspected, every link $(u_1, v_1) \in \mathbb{E}_0$ satisfies that u_1 is k-connected to v_1 in $H - \{(u_0, v_0) \in \mathbb{E}_b(G) | w(u_0, v_0) \geq w(u_1, v_1)\}$. Since H is k-connected, G'_k must be k-connected according to Lemma 2. However, this is in contradiction with the earlier statements that G'_k is not k-connected. Therefore, H can not be k-connected. $\square$

HFCTC may not preserve this max-min optimality for all nodes (both BP and MP) of the network (like the centralized algorithm FGSS [70]), because HFCTC inspects all MP links before BP links. It might be possible that an MP link with a high transmission power is added to G_k before BP links with lower weights are added. We show this using an example. Consider the 1-connected graph G in Figure 7.2. This figure shows a connected spanning subgraph G_{FGSS} produced by FGSS [70] and another connected spanning subgraph G_{HFCTC} produced by HFCTC. Assuming $d(1,3) > d(2,3) > d(1,2) > d(3,4)$, we observe that the maximum radius among all nodes in G_{FGSS} is $d(2,3)$, but this value in G_{HFCTC} is $d(1,3)$ which is greater than $d(2,3)$. Nevertheless, we clearly observe that the maximum radius of BP nodes in G_{HFCTC} is $d(2,1)$. This is smaller than the maximum radius of BP nodes in G_{FGSS} (i.e., $d(2,3)$)

In HFCTC, each node needs to have the complete view of the network topology to be able to determine its radius required to keep the network k-connected. This adds to the complexity and overhead of the algorithm. In the next section, we present HFLTC. HFLTC is the localized version of HFCTC algorithm which eliminates this requirement.
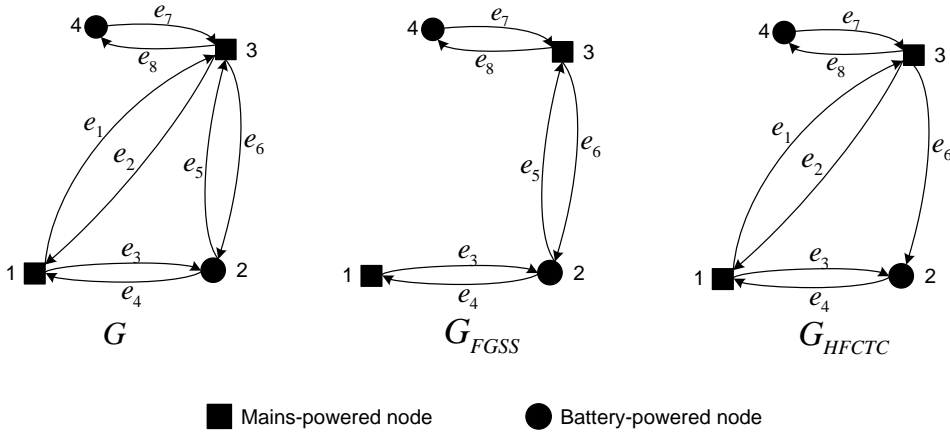
Figure 7.2 – A 1-connected graph G and its spanning subgraphs G_{FGSS} and G_{HFCTC}.

7.4 Heterogeneous Fault-Tolerant Localized Topology Control

In HFLTC, each node adjusts its transmission power based on locally collected information in its neighbor set. Similar to the localized algorithm FLSS proposed in [70], HFLTC consists of three phases:

1. Information Collection: Each node u collects local information of neighbors such as their positions and identifiers, and discovers its Visible Neighborhood $\mathbb{N}(u)$ by broadcasting Hello messages to its neighbors.

2. Topology Construction: Each node u defines, based on the information in $\mathbb{N}(u)$, the proper list of neighbors using Algorithm 8. This is done based on u's local spanning subgraph $S_u(\mathbb{V}(S_u), \mathbb{E}(S_u))$ generated by Algorithm 8 considering $G_u^{\mathbb{V}}$ as the input.

3. Construction of Topology with Only Bidirectional Links (Optional): Each node u adjusts its list of neighbors to make sure that all edges are bidirectional.

7.4.1 Correctness

We prove that if the network is k-connected without topology control, it will remain k-connected after reducing the transmission power of nodes according to the HFLTC algorithm. Before we proceed with the proof, we provide some definitions required for contracting the network topology using local spanning subgraphs of nodes.

Definition 11. *Neighbor Relation in HFLTC:* *In the topology generated by HFLTC, node v is a neighbor of node u –denoted by $u \xrightarrow{HFLTC} v$– if and only if $(u, v) \in \mathbb{E}(S_u)$. That is, v is a neighbor of u, if and only if v is an immediate neighbor on u's local spanning subgraph S_u.*

Definition 12. *Topology* G_{HFLTC}**:** *The topology $G_{HFLTC} = (\mathbb{V}(G_{HFLTC}), \mathbb{E}(G_{HFLTC}))$ –derived under HFLTC– is a directed graph, where $\mathbb{V}(G_{HFLTC}) = \mathbb{V}(G)$ and $\mathbb{E}(G_{HFLTC}) = \{(u, v) \in \mathbb{E}(G) | u \xrightarrow{HFLTC} v\}$*

Definition 13. *Topology* G_{HFLTC}^+**:** *The topology $G_{HFLTC}^+(\mathbb{V}(G_{HFLTC}^+), \mathbb{E}(G_{HFLTC}^+))$ is an undirected graph, where $\mathbb{V}(G_{HFLTC}^+) = \mathbb{V}(G_{HFLTC})$ and $\mathbb{E}(G_{HFLTC}^+) = \{(u, v) \in \mathbb{E}(G) | (u, v) \in \mathbb{E}(G_{HFLTC})$ or $(v, u) \in \mathbb{E}(G_{HFLTC})\}$.*

Definition 14. *Topology* G_{HFLTC}^-**:** *The topology $G_{HFLTC}^-(\mathbb{V}(G_{HFLTC}^-), \mathbb{E}(G_{HFLTC}^-))$ is an undirected graph, where $\mathbb{V}(G_{HFLTC}^-) = \mathbb{V}(G_{HFLTC})$ and $\mathbb{E}(G_{HFLTC}^-) = \{(u, v) \in \mathbb{E}(G) | (u, v) \in \mathbb{E}(G_{HFLTC})$ and $(v, u) \in \mathbb{E}(G_{HFLTC})\}$.*

Theorem 4. *If G is a k-connected undirected graph, then G_{HFLTC}, G_{HFLTC}^-, and G_{HFLTC}^+ all are k-connected.*

Proof. We only need to prove that G_{HFLTC}^- is k-connected, because $G_{HFLTC}^- \subseteq G_{HFLTC} \subseteq G_{HFLTC}^+$. Since undirected links have been removed from G_{HFLTC}^-, it is an undirected graph. Let $\mathbb{E}_{diff} = \mathbb{E}(G) - \mathbb{E}(G_{HFLTC}^-)$. For any link $(u, v) \in \mathbb{E}_{diff}$, at least one of the links (u, v) or (v, u) has not been in G_{HFLTC}, when G_{HFLTC}^- is formed. Without loss of generality, we assume that (u, v) has not been in G_{HFLTC}. This has two implications. First, in the process of local topology construction by node v, (v, u) has been required for k-connectivity of v to u. Second, in the process of local topology construction by node u, u has been already connected to v in S_u before (u, v) is inspected. Notice that G_{HFLTC}^- is a directed graph. This means, (u, v) could be treated as a bidirectional link. Thus, by removing (v, u), k-connectivity of v to u is maintained through k-connectivity of u to v.

Now, assume u is an MP node. Since MP edges in $G_u^{\mathbb{V}}$ are inserted into S_u in an ascending order of weight before BP edges, u must be k-connected to v in $A_m = G_u^{\mathbb{V}} - \mathbb{E}_b(G_u^{\mathbb{V}}) - \{(u_0, v_0) \in \mathbb{E}_m(G_u^{\mathbb{V}}) \mid w(u_0, v_0) \geq w(u, v)\}$. Let us define $B_m = G - \mathbb{E}_b(G) - \{(u_0, v_0) \in \mathbb{E}_m(G) \mid w(u_0, v_0) \geq w(u, v)\}$. We have $A_m \subseteq B_m$. Therefore, if u is k-connected to v in A_m, it is k-connected to v in B_m either.

Next, we assume u is a BP node. This means, (u, v) will be inspected after all MP edges in $G_u^{\mathbb{V}}$ and all BP edges with smaller weights are inspected. Thus, u must be k-connected to v in $A_b = G_u^{\mathbb{V}} - \{(u_0, v_0) \in \mathbb{E}_b(G_u^{\mathbb{V}}) \mid w(u_0, v_0) \geq w(u, v)\}$. Let us define $B_b = G - \{(u_0, v_0) \in \mathbb{E}_b(G) \mid w(u_0, v_0) \geq w(u, v)\}$. We have $A_b \subseteq B_b$. Thus, if u is k-connected to v in A_b, u is k-connected to v in B_b either. In summary, any link $(u, v) \in \mathbb{E}_{diff}$ is k-connected to v either in $G - \mathbb{E}_b(G) - \{(u_0, v_0) \in \mathbb{E}_m(G) \mid w(u_0, v_0) \geq w(u, v)\}$ or in $G - \{(u_0, v_0) \in \mathbb{E}_b(G) \mid w(u_0, v_0) \geq w(u, v)\}$. We can conclude that G_{HFLTC}^- is k-connected using Lemma 2.   □

Algorithm 8 HFLTC: a localized topology control algorithm for preserving k-connectivity in networks with heterogeneous power supplies.

Procedure HFLTC
Input $G_u^{\mathbb{V}}$, u's visible neighborhoods;
Output S_u, a spanning subgraph of $G_u^{\mathbb{V}}$;
$\mathbb{V}(S_u) \leftarrow \mathbb{V}(G_u^{\mathbb{V}})$
$\mathbb{E}(S_u) \leftarrow \emptyset$
$\mathbb{E}_m(G_u^{\mathbb{V}}) \leftarrow \{(u,v) \in \mathbb{E}(G_u^{\mathbb{V}}) \mid u \in \mathbb{V}_m(G_u^{\mathbb{V}})\}$
$\mathbb{E}_b(G_u^{\mathbb{V}}) \leftarrow \mathbb{E}(G_u^{\mathbb{V}}) - \mathbb{E}_m(G_u^{\mathbb{V}})$
sort all edges in $\mathbb{E}_m(G_u^{\mathbb{V}})$ is ascending order of weight
for each edge (u_1, v_1) in the order **do**
  if u_1 is not k-connected to v_1 in S_u **then**
    $\mathbb{E}(S_u) \leftarrow \mathbb{E}(S_u) \cup (u_1, v_1)$
  end if
end for
sort all edges in $E_b(G_u^{\mathbb{V}})$ is ascending order of weight
for each edge (u_2, v_2) in the order **do**
  if u_2 is not k-connected to v_2 in G_k **then**
    $\mathbb{E}(S_u) \leftarrow \mathbb{E}(S_u) \cup (u_2, v_2)$
  end if
end for

In a complete graph where there is a link between every two nodes, the complexity of the HFLTC algorithm is the same as its centralized version HFCTC. That is, the complexity is $O(|\mathbb{V}|^{1/2}|\mathbb{E}|^2)$. Nevertheless, in a graph with much less links than a complete graph, the complexity reduces. In fact, since HFLTC works on $G_u^{\mathbb{V}}$, its complexity is $O(n_u^{1/2} m_u^2)$, where n_u is the number of nodes in $G_u^{\mathbb{V}}$ and m_u is the number of links in $G_u^{\mathbb{V}}$.

7.4.2 Optimality

HFLTC achieves min-max optimality for BP nodes of the network. To elaborate on this, we use the following definition:

Definition 15. *__Strictly Localized Algorithm:__ An algorithm is strictly localized if its operation at any node u is only based on $G_u^{\mathbb{V}}$.*

Theorem 5. *Let $\mathbb{L}_k(G)$ be the set of all k-connected spanning subgraphs of G that are constructed by various strictly localized algorithms. HFLTC achieves the min-max optimality among all strictly localized algorithms. That is, $\rho_b(G_{HFLTC}) = \min\{\rho_b(F) | \forall F \in \mathbb{L}_k(G)\}$.*

Proof. Suppose G is k-connected. Based on Theorem 4, G_{HFLTC} is k-connected too. Let (u, v) be an edge in G_{HFLTC} such that

$$w(u, v) = \max_{(u_0, v_0) \in \mathbb{E}_b(G_{HFLTC})} \{w(u_0, v_0)\}.$$

Then, $\rho(G_{HFLTC}) = R(u)$. Let $G_0(\mathbb{V}(G_0), \mathbb{E}(G_0))$ be the induced subgraph of G_{HFLTC} when $\mathbb{V}(G_0) = \mathbb{V}(G_u^{\mathbb{V}})$. Obviously, $(u, v) \in \mathbb{E}(G_0)$. Furthermore, (u, v) is required to keep u k-connected to v. This means, $G_0' = G_0 - (u, v)$ is not k-connected. Now, consider a graph $H_0 = (\mathbb{V}(H_0), \mathbb{E}(H_0))$, in which $\mathbb{V}(H_0) = \mathbb{V}(G_u^{\mathbb{V}})$ and $\mathbb{E}(H_0) = \mathbb{E}_m(G_u^{\mathbb{V}}) \cup \{(u_0, v_0) \in \mathbb{E}_b(G_u^{\mathbb{V}}) | w(u_0, v_0) < w(u, v)\}$. If we replace G, G_k, G_k', and H with $G_u^{\mathbb{V}}$, G_0, G_0', and H_0, respectively, and we follow the corresponding proof in Theorem 3, we can prove that H_0 is not k-connected.

Since $G_u^{\mathbb{V}}$ is an induced subgraph of G, we may face two cases:

1. u is k-connected to v in $G_u^{\mathbb{V}}$. Since H_0, which does not contain (u, v), is not k-connected, any $F \in \mathbb{L}_k(G)$ should have at least one edge equal to or longer than (u, v).

2. u is not k-connected to v in $G_u^{\mathbb{V}}$. In this case, to preserve the connectedness of the network as much as possible, any $F \in \mathbb{L}_k(G)$ must include (u, v).

In both cases, $\rho_b(F) \geq \rho_b(G_u^{\mathbb{V}}) = \rho_b(G_{HFLTC})$. This proves the theorem. $\square$

7.5 Practical Considerations

To prove the optimality and correctness of the HFCTC and HFLTC algorithms, we assumed nodes to have the same maximum transmission range. Nevertheless, due to the lognormal fading in wireless channels, this assumption may not be practical even if we assume all nodes to have the same wireless interface. Thus, it is possible that the maximum transmission range for different nodes is different. In such a case, the original network topology can not be an undirected graph. It will be a directed graph. However, we can still show that HFCTC and HFLTC preserve k-connectivity of the network and maintain their optimality even if the network topology is a directed graph. We can easily prove the following lemmas and theorems for directed graphs using the same method that as for undirected graphs.

Lemma 3. *Let u_1 and u_2 be two vertices in a k-connected directed graph F. If u_1 and u_2 are k-connected after the removal of edge (u_1, u_2), then $F - (u_1, u_2)$ is still k-connected [70].*

Lemma 4. *Let G and G' be two directed graphs such that $\mathbb{V}(G) = \mathbb{V}(G')$. If G is k-connected, and every edge $(u, v) \in \mathbb{E}(G) - \mathbb{E}(G')$ satisfies that u is k-connected to v eigher in $G - \mathbb{E}_b(G) - \{(u_0, v_0) \in \mathbb{E}_m(G) \mid w(u_0, v_0) \geq w(u_1, v_1)\}$, or in $G - \{(u_0, v_0) \in \mathbb{E}_b(G) \mid w(u_0, v_0) \geq w(u_2, v_2)\}$, then G' is also k-connected.*

Theorem 6. *Let G be a k-connected directed graph. HFCTC can preserve k-connectivity of G.*

Theorem 7. *The maximum transmission radius (or equivalently power) among all battery-powered nodes in the network is minimized by HFCTC. That is, $\rho_b(G_k) = \min\{\rho_b(F)|F \in \mathbb{S}_k(G)\}$, where G is a directed graph.*

Theorem 8. *Among all strictly localized algorithms, HFLTC minimizes the maximum transmission radius (or power) of battery-powered nodes in the network. That is, $\rho_b(G_{HFLTC}) = \min\{\rho_b F|F \in \mathbb{L}_k(G)\}$, where G is a directed graph.*

The only exception is with regard to Theorem 4. If G is a directed graph, then we cannot prove that G^-_{HFLTC} is k-connected. We used the assumption that G is an undirected graph to prove Theorem 4. However, we can still show that G_{HFLTC} and G^+_{HFLTC} are both k-connected. The proof is slightly different from the proof of Theorem 4.

Theorem 9. *If G is a k-connected directed graph, then G_{HFLTC} and G^+_{HFLTC} are both k-connected.*

Proof. We only need to prove that G_{HFLTC} is k-connected, because $G_{HFLTC} \subseteq G^+_{HFLTC}$. Let $\mathbb{E}_{diff} = \mathbb{E}(G) - \mathbb{E}(G_{HFLTC})$. For any edge $(u, v) \in \mathbb{E}_{diff}$, u must already be k-connected to v when it has been inspected during the construction of the local spanning subgraph S_u. u is either BP or it is MP. Since MP edges in $G^\mathbb{V}_u$ are inserted into S_u in an ascending order of weight before BP edges are inspected, u must be k-connected to v in $A_m = G^\mathbb{V}_u - \mathbb{E}_b(G^\mathbb{V}_u) - \{(u_0, v_0) \in \mathbb{E}_m(G^\mathbb{V}_u) \mid w(u_0, v_0) \geq w(u, v)\}$. Let us define $B_m = G - \mathbb{E}_b(G) - \{(u_0, v_0) \in \mathbb{E}_m(G) \mid w(u_0, v_0) \geq w(u, v)\}$. We have $A_m \subseteq B_m$. Therefore, if u is k-connected to v in A_m, it is k-connected to v in B_m as well.

Next, we assume u is BP. This means, (u, v) will be inspected after all MP edges as well as all BP edges in $G^\mathbb{V}_u$ with smaller weights than $w_{u,v}$ are inspected. This means that u must be k-connected to v in $A_b = G^\mathbb{V}_u - \{(u_0, v_0) \in \mathbb{E}_b(G^\mathbb{V}_u) \mid w(u_0, v_0) \geq w(u, v)\}$. Let us define $B_b = G - \{(u_0, v_0) \in \mathbb{E}_b(G) \mid w(u_0, v_0) \geq w(u, v)\}$. We have $A_b \subseteq B_b$. Therefore, if u is k-connected to v in A_b, then u is k-connected to v in B_b as well. In summary, any link $(u, v) \in \mathbb{E}_{diff}$ is k-connected to v either in $G - \mathbb{E}_b(G) - \{(u_0, v_0) \in \mathbb{E}_m(G) \mid w(u_0, v_0) \geq w(u, v)\}$ or in $G - \{(u_0, v_0) \in \mathbb{E}_b(G) \mid w(u_0, v_0) \geq w(u, v)\}$. We can conclude that G_{HFLTC} is k-connected using Lemma 4. $\square$

7.6 Simulation Studies

In this section, we present simulation studies to show the effectiveness of our proposed topology control algorithms in networks with heterogeneous power supplies. We specifically show that our proposed algorithms take advantage of MP

nodes in the network to substantially reduce the transmission range of BP nodes. In addition to HFLTC, we consider FLSS [70] as an algorithm which does not exploit the heterogeneity of power supplies of nodes in topology control. As mentioned before, FLSS is also a localized and fault-tolerant algorithm which outperforms other similar topology control algorithms proposed so far for networks with homogeneous power supplies. We also consider the centralized algorithm HFCTC as a benchmark to see how its distributed version, HFLTC, performs comparatively.

7.6.1   Radius and Degree of Nodes

We first study the performance of topology control algorithms with respect to radius and degree of nodes. We assume nodes are uniformly distributed over an area of size 1000×1000 [m^2]. The maximal transmission range of all nodes is $D_{max} = 250$ [m]. We vary the number of nodes from 70 to 300 assuming half of them are mains powered. Each data point in our plots is the average over 100 simulation runs. Results are obtained for $k = 2$.

7.6.1.1   Maximum Radius

In a topology generated by a topology control algorithm, radius of different nodes might be different. The maximum radius in a topology is the highest radius among nodes in that topology. It is a measure which shows how that topology control algorithm succeeds to reduce the transmission power of nodes. Here, we compare the *maximum radius* among all nodes of the network, among only BP nodes of the network, and among only MP nodes of the network, when different topology control algorithms are deployed. To this aim, in each simulation run, the maximum radius among all nodes, for BP nodes only, and for MP nodes only is determined in the generated topology by the used algorithm. The average value over 100 simulation runs is recorded as the average maximum radius for that algorithm. Figure 7.3 shows this measure for the HFLTC, FLSS, and HFCTC algorithms. The figure shows that all three algorithms reduce the average maximum radius of nodes as the total number of nodes increases in the network. The maximum radius among all nodes of the network and among MP nodes only is greater, if HFLTC is deployed instead of FLSS. However, the maximum radius among BP nodes is smaller for HFLTC. We also observe that the average maximum radius among BP nodes of the network for HFLTC and HFCTC gets closer to each other, as the total number of nodes increases.
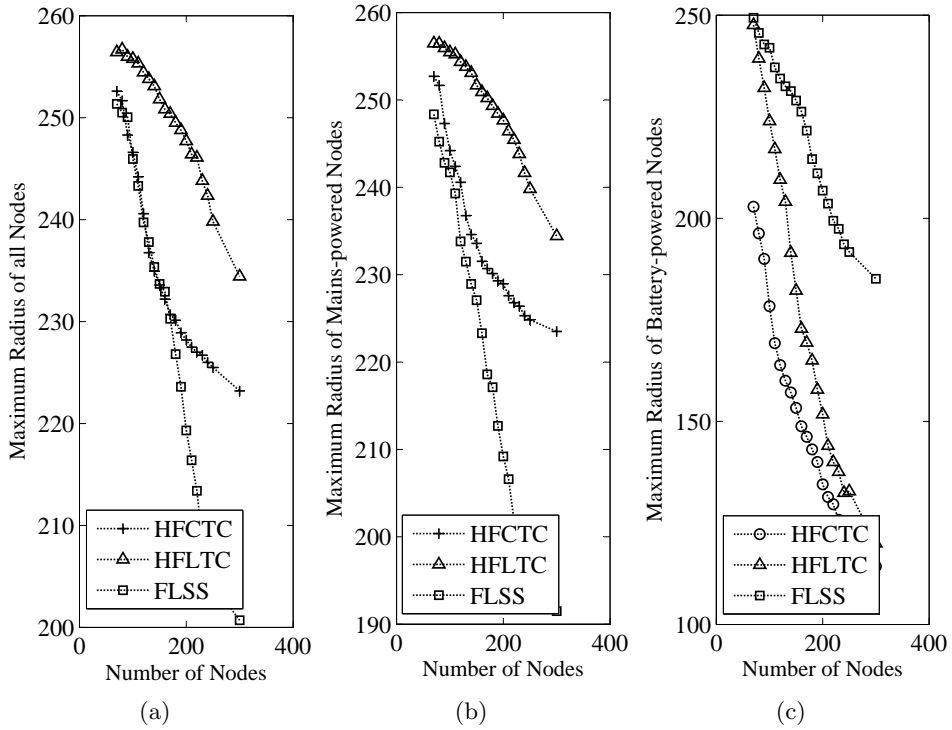
Figure 7.3 – (a) Average maximum radius of all nodes, (b) average maximum radius of mains-powered nodes, and (c) average maximum radius of battery-powered nodes as a function of the total number of nodes in the network.

7.6.1.2 Average Radius

The average radius of nodes in a topology is another measure which can show the effectiveness of a topology control algorithm in reducing the transmission range of nodes. To compute the average radius of nodes (or a specific set of nodes) in a topology, we only need to sum the radius of nodes and divide it by their number. Here, we compare this measure for various topology control algorithms. We again measure this value for all nodes, BP nodes only, and MP nodes only separately. To this end, the average radius of nodes in the generated graph by the used algorithm is determined in each simulation run. Then, the mean value over 100 simulation runs is recorded as the average radius of nodes for that algorithm. Figure 7.4 shows this measure for the HFLTC, FLSS, and HFCTC algorithms. We observe that these topology control algorithms can profoundly reduce the radius of nodes on average. Although the HFLTC algorithm increases the radius of MP nodes compared to the FLSS algorithm as seen in Figure 7.4(b), it considerably reduces the radius of BP nodes as seen in Figure 7.4(c). Furthermore, the average radius of all nodes in the subgraph generated by HFLTC is almost the same as the average radius of all nodes in the subgraph generated by FLSS. We also observe that the localized algorithm HFLTC performs almost similar to the centralized algorithm HFCTC.

7.6.1.3 Average Node Degree

The average node degree specifies the average number of neighbors of a node in the network. Reducing the average node degree in the network while the network is kept fault-tolerant is another sign of effectiveness of a topology control algorithm. Here, we compare this measure for the HFCTC, FLSS, and HFLTC algorithms. We again compute the average degree of all nodes, BP nodes only, and MP nodes only separately. To this aim, the average degree of these nodes in the generated graph by the algorithm is determined in one simulation run. Then, the mean value over 100 simulation runs is recorded as the average node degree for that algorithm. Figure 7.5 shows this measure for the HFCTC, FLSS, and HFLTC algorithms. As shown in Figure 7.5(b), the average degree of MP nodes is lower for FLSS compared to HFLCT, but the one of BP nodes is lower for HFLTC, as shown in Figure 7.5(c). The average degree of BP nodes with HFLTC is also very close to that of the centralized algorithm HFCTC. Furthermore, we observe in Figure 7.5(a) that our proposed algorithms HFLTC and HFCTC can even achieve a lower degree for all nodes of the network (both BP and NP) compared to FLSS. We have shown the average degree of nodes in the original graph (i.e., when none of these topology control algorithms are utilized) in Fig. 7.6. The average degree of nodes when no topology control algorithm is utilized increases almost linearly, if the number of nodes in the network increases. Nevertheless, all three topology control algorithms
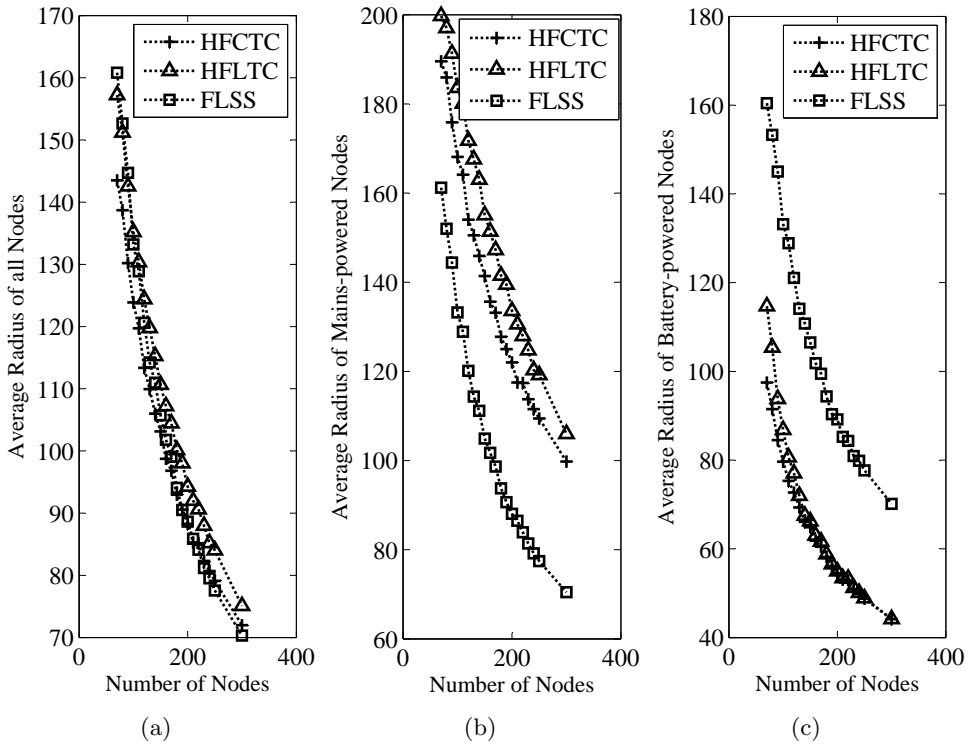
Figure 7.4 – (a) Average radius of all nodes, (b) average radius of mains-powered nodes, (c) average radius of battery-powered nodes as a function of the total number of nodes in the network.
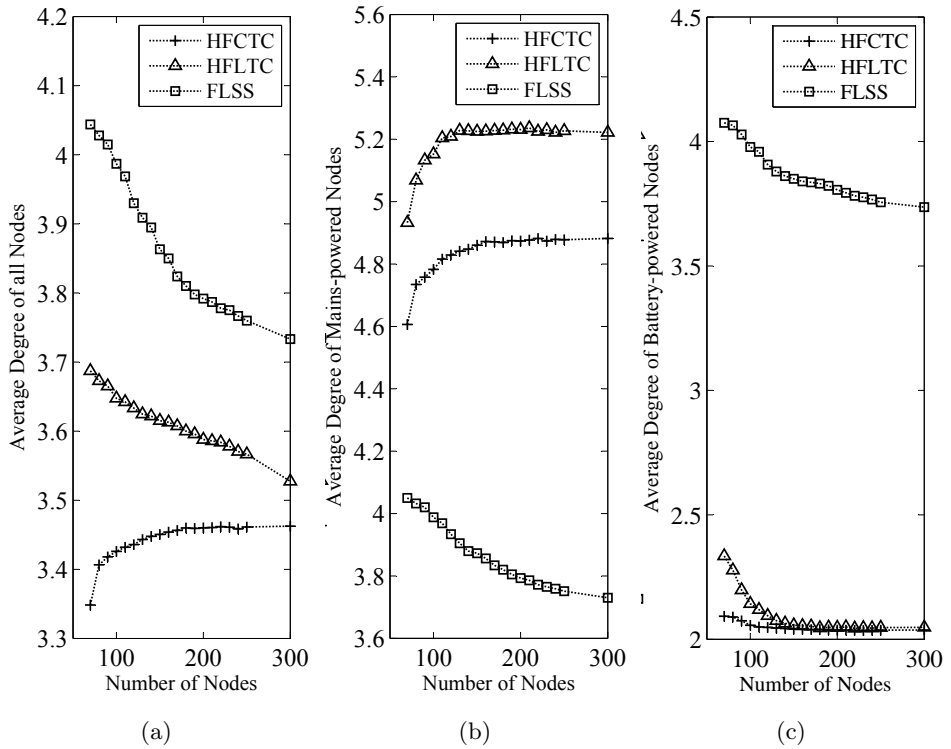
Figure 7.5 – (a) Average degree of all nodes, (b) average degree of mains-powered nodes, and (c) average degree of battery-powered nodes as a function of the total number of nodes in the network.
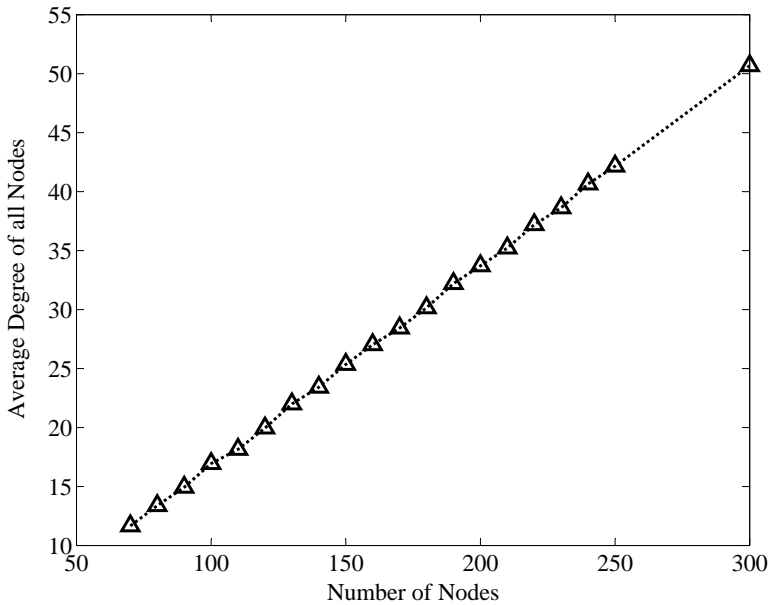
Figure 7.6 – Average degree of nodes (both mains-powered and battery-powered) in the original graph as a function of the total number of nodes.

tremendously reduce the degree of nodes as the number of nodes increases. They keep the node degree almost constant even if the node density increases.

7.6.1.4   Impact of Density of Mains-Powered Nodes

In this section, we study the impact of the density of MP nodes on the average radius of nodes when various topology control algorithms are deployed. The total number of nodes is set to 150. The fraction of MP nodes is changed from $\sigma = 0$ (all nodes are BP) to $\sigma = 1$ (all nodes are MP). Since the network area is fixed, increasing the fraction of MP nodes means that their density increases in the network. As we can observe in Figure 7.7(a), when the fraction of MP nodes increases from 0 to 0.1, the average radius of nodes (both BP and MP) decreases in the graph generated by HFLTC compared to the average radius in the graph generated by FLSS. From $\sigma = 0.2$ to $\sigma = 0.6$, we observe an increasing trend for HFLTC, while after $\sigma = 0.6$, there is again a decreasing trend. In the sequel, we explain the reasons for this behavior.

When all nodes are battery powered, HFLTC acts similar to FLSS. If the fraction of MP nodes increases, the average radius of BP nodes decreases in HFLTC, and
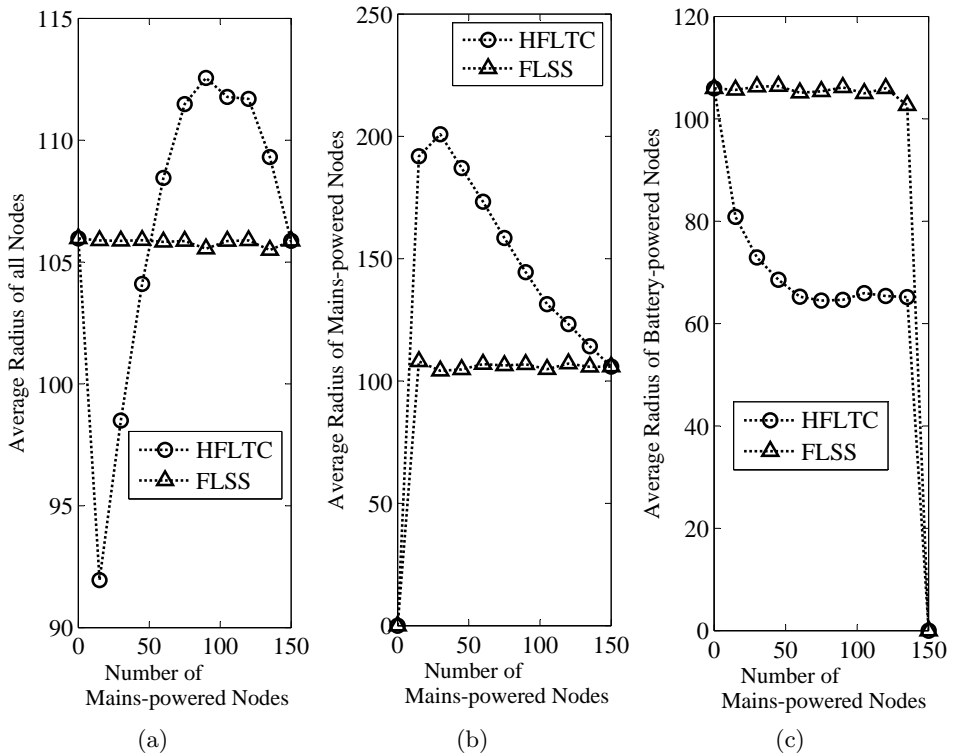
Figure 7.7 – (a) Average radius of all nodes, (b) average radius of mains-powered nodes, and (c) average radius of battery-powered nodes for the HFLTC and FLSS algorithms as a function of the number of mains-powered nodes in the network (out of a total of 150 nodes).

deviates more from that of FLSS (see Figure 7.7(c)). On the other hand, the average radius of MP nodes in HFLTC decreases to the value obtained by FLSS when the density of these nodes increases (see Figure 7.7(b)). When all nodes are MP, HFLTC again acts like FLSS. Thus, the decreasing trend for the average radius of BP nodes may not hold for all nodes. The superposition of increasing and decreasing trend of the average radius of BP and MP nodes coupled with the effect of the number of MP nodes results in a concave and convex plot for the average radius of all nodes (both MP and BP) in the HFLTC algorithm.

7.6.2   Network Lifetime

Can topology control harm the network lifetime? How does HFLTC perform with respect to the network lifetime? These are questions that we answer in this section. Here, we use the same simulation setup as we established to investigate the performance of battery-aware routing algorithm in the previous chapter. That is, nodes are uniformly distributed in a square area of size 750×750 [m^2], and the transmission range of each node is set to 150 [m]. Nodes are all equipped with the PRISM wireless chipset. After distributing nodes in the network and constructing the initial network topology G, HFLTC and FLSS are deployed to generate G_{HFLTC} and G_{FLSS} for $k = 2$ (2-connectivity). We choose routes with minimum accumulated ETX.

To collect simulation results, different algorithms are compared in a completely similar setting. We deploy a network randomly in each simulation run. Then, we create a replica of the network for each topology control algorithm to measure the network lifetime for that specific algorithm. The same sessions are generated in different replicas of the network. In other words, we have several samples of the same randomly deployed network which are completely the same (even the active sessions in these networks), but the deployed topology control algorithms are different. To increase the confidence of our results, we measure the lifetime of 100 randomly deployed networks and plot the average network lifetime over 100 simulation runs.

Results depicted in Figure 7.8 show that even though an optimized algorithm like FLSS can reduce the transmission power of devices, it reduced the network lifetime either. The reason lies in the fact that reducing the transmission power of nodes reduces the number of links that carry the traffic load between nodes. Thus, some nodes may be overused and fail quickly. This is also true for HFLTC when all nodes in the network are battery powered. Nevertheless, if there are some MP nodes in the network, HFLTC achieves a higher network lifetime compared to FLSS. HFLTC increases the network lifetime even compared to the case that topology control is not utilized. Forming a backbone of MP nodes and attaching

the BP nodes with the lowest required transmission power is the reason for the outstanding performance of HFLTC.

We have also investigated the impact of topology control on the network lifetime when the battery-aware routing algorithm RMLNR is used. As shown in Figure 7.8(b), HFLTC in conjunction with RMLNR profoundly increases the network lifetime when most nodes of the network are connected to the mains. The increasing trend for the network lifetime as the number of MP nodes of the network increases verifies this claim. This is while the network lifetime for the RMLNR algorithm without HFLTC has a decreasing trend (in general) even if the number of MP nodes increases in the network. Note that these simulation results have been achieved assuming overhearing is not being avoided. This means, we can consider topology control also as an effective scheme to reduce energy consumption of nodes due to overhearing of nodes in the network.

7.7   Summary

In this chapter, topology control in wireless multi-hop networks was studied. Topology control reduces the transmission range of nodes in such a way that the network remains connected (k-connected). Two new fault-tolerant topology control algorithms were proposed for networks with heterogeneous power supplies: HFLTC, which is a localized algorithm, and HFCTC which is a centralized algorithm. The proposed algorithms create a fault-tolerant backbone of mains-powered nodes of the network using the most energy-efficient links between them. Then, battery-powered nodes are attached to this backbone with the minimum required transmission power. We proved that these algorithms preserve k-connectivity of the network. That is, if the network is k-connected without topology control, it will be k-connected after reducing the transmission range of nodes either using HFCTC or using HFLTC. We also proved that HFLTC and HFCTC achieve min-max optimality for battery-powered nodes of the network. They minimize the maximum transmission power among battery-powered nodes of the network required to keep the network k-connected. The performance of these two algorithms was compared with the earlier scheme FLSS. We observed that while both FLSS and HFLTC algorithms can reduce the transmission range of nodes keeping the network k-connected, HFLTC further reduces the transmission power of battery-powered nodes especially at high node densities. Furthermore, the use of the topology control algorithm FLSS reduces the network lifetime, because the relay traffic per node increases. HFLTC, on the other hand, increases the network lifetime, because it creates a fault-tolerant backbone of mains-powered nodes and reduces the transmission range of battery-powered nodes considerably. As a result, energy consumption of battery-powered nodes for overhearing is also reduced. Consequently, directing the
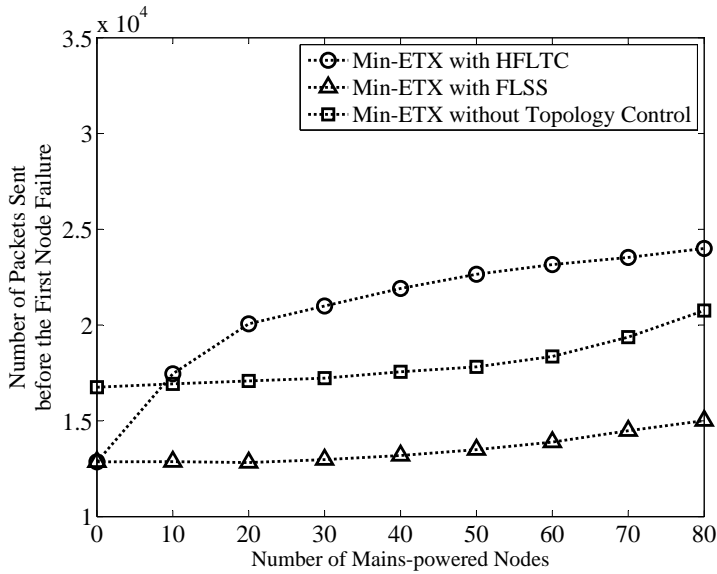
(a)
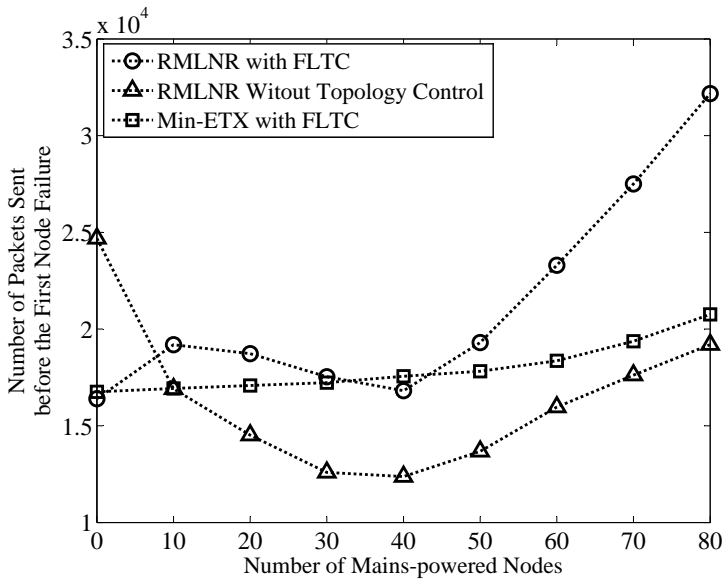
(b)

Figure 7.8 – Total number of packets sent by nodes before the first node failure happens in a network of size 750×750 [m²] consisting of 100 uniformly distributed static nodes. The horizontal axis shows the number of mains-powered nodes ((out of 100)). Different combinations of topology control and routing algorithms are considered.

traffic load to mains-powered nodes of the network using the battery-aware routing algorithm RMLNR –introduced in the previous chapter– increases the network lifetime, even if overhearing is not avoided using a sleep and wake up MAC protocol.

Chapter 8

Node-To-node Communication Lifetime

In previous chapters, we designed routing and topology control algorithms for wireless multi-hop networks. They are part of network and MAC layers of the communication stack. Topology control defines a neighbor discovery policy at the MAC layer which reduces the transmission power of nodes just enough to keep the network connected. Routing is handled at the network layer. These mechanisms together support energy-efficient communication between nodes in a wireless multi-hop network. The question remains is how long two nodes which are connected to each other in a multi-hop way can communicate with each other using the underlying MAC and routing protocols. Failure of intermediate nodes due to battery exhaustion interrupts communication between a source and a destination. However, even if communication between the source and the destination continues using other intermediate nodes, the source or the destination may themselves fail at some point. This will end their communication. Since nodes in a wireless multi-hop network may run on batteries, they have a limited supply of energy. Battery exhaustion is indeed a threat for communication in wireless multi-hop networks.

In this chapter, we analyze the node-to-node communication lifetime from the point of view of the transport layer. We formulate the node-to-node communication lifetime problem in the following way: *in a network with an arbitrary topology (which could be the result of a topology control algorithm) where end-to-end communication between nodes is supported by a routing protocol (which could be an energy-aware protocol), how long can an arbitrary source node communicate with its respective destination node?* To better understand this problem, we should notice that node redundancy in wireless multi-hop networks provides a degree of fault-tolerance. That is, after the first route between two nodes fails, there might be other routes
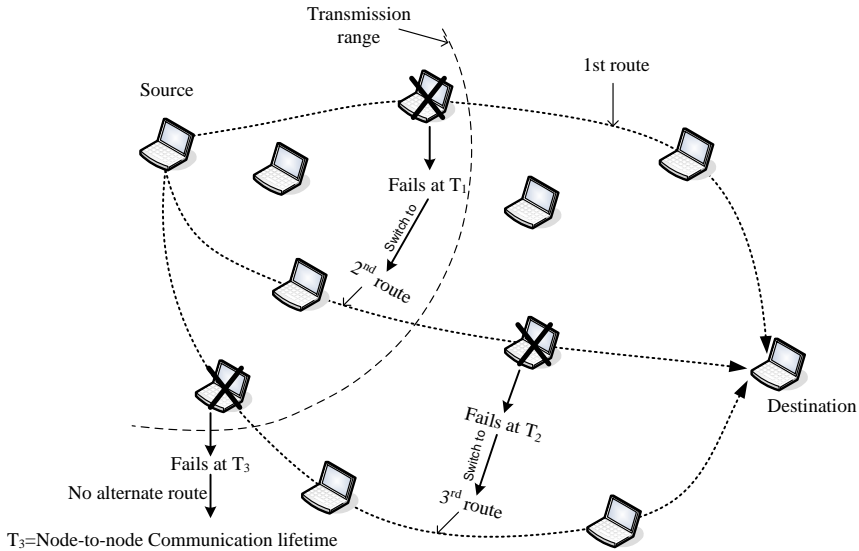
Figure 8.1 – Communication lifetime between a source and a destination node in a wireless multi-hop network.

through other intermediate nodes to keep the connectivity. Thus, a source node can transfer data to a destination node as long as they both are alive and there is at least one route to keep them connected (see Figure 8.1). The node-to-node communication lifetime determines the duration that any two arbitrary nodes in a wireless multi-hop network with a random topology can communicate with each other without interruption due to lack of routes before their own battery runs out. Analysis of this lifetime allows us to identify how and to what extent various factors such as node density, transmission range, network deployment area, packet transmission rate, packet size, and energy consumption characteristics of nodes affect the lifetime. This can help us to define configuration parameters such that the communication lifetime of nodes is maximized.

This chapter is organized as follows: In Section 8.1, we study related work. Assumptions we made in our analysis are presented in Section 8.2. In Section 8.3, we formulate the problem of node-to-node communication lifetime in multi-hop networks in terms of the energy consumption rate of nodes. An important factor which affects the energy consumption rate of nodes is overhearing. The impact of overhearing on the energy consumption rate of nodes is analyzed in Section 8.4, assuming MAC retransmissions are not supported, and in Section 8.5, assuming MAC retransmissions are supported. As a by-product of analyzing the energy consumption rate of nodes, we derive an upper and a lower bound on the lifetime of

node-disjoint routes in Section 8.6. In Section 8.7, we derive a closed-form expression for the expected communication lifetime of nodes in wireless multi-hop networks. We present simulation results in Section 8.8, and summarize the chapter in Section 8.9.

8.1   Related Work

Although many studies have addressed problems related to the problem of node-to-node communication lifetime in wireless multi-hop networks, a complete analysis considering all factors such as network connectivity and energy consumption characteristics of nodes is missing. The problem of connectivity of wireless multi-hop networks was studied extensively in [53, 55, 115–122]. As mentioned in Chapter 2, this problem deals with issues such as finding the minimum node density and the minimum transmission range required to keep the network k-connected. However, to determine node-to-node communication lifetime, we have to consider the energy consumption rate of nodes as well. Assuming the network is k-connected, the energy consumption rate of nodes determines when the first route, the second, and ultimately the kth route between two nodes fail due to the battery exhaustion of their intermediate nodes.

Analysis of the network lifetime is another problem related to the problem of node-to-node communication lifetime in wireless multi-hop networks. Many definitions of network lifetime have been proposed [123]. Some, for example, define network lifetime in terms of the time until the first node fails due to energy drain [124], the time until the first cluster head is drained of energy [125], or the time until only a fraction of the nodes have survived in the network [126]. Another perspective found in the literature defines the network lifetime in terms of coverage, e.g., the time until an area of interest is not covered anymore by a subset of nodes [127–130]. Studies which are more relevant to our work define network lifetime in terms of connectivity, e.g., the duration that the network remains k-connected [131, 132] or the duration that the size of the largest connected component of the network remains above a threshold [133] or the duration that a percentage of cluster heads remain alive and connected [134]. These connectivity-based definitions of network lifetime, however, are in terms of communication to a base station in wireless sensor networks. This is different from the ability of an arbitrary pair of nodes to communicate in a general purpose wireless multi-hop network.

Zhang et al, [135] and Tseng et al, [136] proposed algorithms to predict the lifetime of discovered routes between nodes. To this aim, they considered the duration that a route stays intact when the nodes are mobile. Nevertheless, we know that battery drain of nodes may also cause route failure. Furthermore,

communication between two nodes might be ended not only due to route failure but also due to depletion of their own batteries.

The node-to-node communication lifetime in wireless multi-hop networks also has some relation with the resilience of these networks. Najjar and Gaudiot [137] defined network resilience as the maximum number of node failures (say for example, due to battery exhaustion) which can be tolerated while the network remains connected with a certain probability. There are also some other definitions for the network resilience in the literature. Colboum [138] defined the network resilience as the expected number of node pairs that can communicate with each other when some nodes fail. Ganesan et al. [139] defined it as the likelihood that an alternative route is available between a source and a destination node when the shortest path between them fails. Dimitar et al. [140] defined the network resilience as the maximum number of nodes that can be removed from the network such that the probability of having a connection between a pair of nodes remains above a threshold. Considering the concept of resilience in wireless multi-hop networks, we may say that *the node-to-node communication lifetime is the duration that a connection between two nodes remains resilient.* This is a new definition of network resilience. To analyze this, we need to know when two nodes disconnect from each other due to failure of intermediate nodes. Among the various studies that addressed network resilience, only Xing and Wang [141] analyzed the expected duration that a node is connected to the rest of the network. Nevertheless, they modeled node failure as a Markov chain to analyze the connectivity of a mobile node to its neighboring nodes. They analyzed the problem in the steady state without considering the energy consumption of nodes and failure of routes due to failure of their intermediate nodes.

Our novelty in this chapter is the analysis of node-to-node communication lifetime considering both energy consumption of nodes and the network connectivity. The analysis is provided for networks in which the MAC layer supports retransmissions to recover lost packet, and networks in which MAC retransmissions are not supported. Our main contributions are as follows:

1. We propose numerical algorithms which can calculate the communication lifetime of two specific nodes in networks with and without MAC retransmission. To this end, we model energy consumption rate and remaining battery energy of nodes. The presented algorithms can predict at any moment the maximum duration that two arbitrary nodes can still communicate with each other.

2. We derive a closed-form expression for the expected value of maximum node-to-node communication lifetime. The expression that we derive can predict the expected maximum duration that two arbitrary nodes in a static network with a random topology can communicate with each other.

3. We derive upper and lower bounds for the lifetime of alternate node-disjoint routes between nodes.

Particular is that our treatment is comprehensive in its approach. A strong aspect of our analysis is that we consider the impact of overhearing, which increases the practical usefulness of our analysis.

8.2   Assumptions

In this section, we mention the assumptions we made in our analysis. We also recapitulate some notations from Chapter 2. This helps the reader to better understand the material of this chapter.

8.2.1   Network Model

Same as before, we represent the network topology by a graph $G(\mathbb{V}, \mathbb{E})$, where $\mathbb{V}$ and $\mathbb{E}$ are the set of nodes and links, respectively. We assume $N = |\mathbb{V}|$ static nodes are uniformly distributed in the network area. Thus, the network topology could be random. in our analysis, we consider a general case without making any assumption about the connectivity of the network. The network may not necessarily be a connected graph. It may consist of a number of disconnected subgraphs.

Nodes are all battery powered. We define $\mathbb{B}(t) = \{B_u(t)\}_{u=1}^N$ as the set of battery energy of nodes at time t, where $B_u(t)$ [J] denotes the battery energy of node $u \in \mathbb{V}$ at time t.

Definition 16. ***Node Failure:*** *If the residual battery energy of a node falls bellow a threshold B_{th}, the node is considered to have failed. Without loss of generality, we assume $B_{th} = 0$.*

As we assumed nodes fail due to battery exhaustion, other types of failure of nodes such as malicious attacks are excluded from our analysis. Communication failure between nodes is only due to battery exhaustion of nodes. Furthermore, since we study static networks, communication failure due to the mobility of nodes is not considered either.

The set $\mathbb{P} = \{p(u, v)\}$ is defined as the set of the PDR of links, where $p(u, v)$ is the PDR of (u, v) for packets of size L [bit][1]. If MAC retransmission is supported, we also define $\mathbb{Q} = \{q(u, v)\}$, in which $q(u, v)$ is the PDR of acknowledgments of size L_a [bit] acknowledging the reception of the data packet which has been transmitted over (u, v). We emphasize that the effect of transmission error due to fading, shadowing, and collision are considered in $p(u, v)$ and $q(u, v)$.

---

[1] To ease the presentations, we have changed the notation compared to what introduced in Chapter 3 for the PDR of a link.

8.2.2   Node-disjoint Routes

Alternative routes which are used to keep nodes connected are assumed to be node-disjoint.

Definition 17. *Node-disjoint Routes:* *Two routes between a source and a destination node are node-disjoint, if they do not have any intermediate nodes in common.*

We prefer the use of multiple node-disjoint routes for keeping nodes connected to each other in wireless multi-hop networks, because failure of a node in such routes results in failure of only one of the routes. The use of node-disjoint routes can also reduce the frequency of route discovery, because such routes could be discovered once before the communication between two nodes starts. In non-disjoint routes with common intermediate nodes, a new route discovery must be performed whenever a node in these routes fails[1]. This indeed generates a high overhead and increases energy consumption of nodes for route discovery. For this reason, many multi-path routing protocols try to discover node-disjoint routes [139, 142, 143]. How such routing protocols discover node-disjoint routes is out of the scope of this chapter. Interested readers are referred to [143] for details about multi-path routing in wireless multi-hop networks. In this chapter, we only analyze the duration that two nodes can communicate with each other using nodes-disjoint routes between them.

We denote $P_k = < n_{1,k}, n_{2,k}, ..., n_{h_k,k}, n_{h_k+1,k} >$ as the kth node-disjoint route between the source and the destination, in which $n_{l,k}$ is the lth node in P_k and h_k is the number of hops of P_k. In each route, $n_{1,k}$ is the source node, $n_{h_k+1,k}$ is the destination node, and $n_{2,k}, ..., n_{h_k,k}$ are intermediate (relay) nodes which forward packets hop by hop from the source to the destination. The number of node-disjoint routes between the source node i and the destination node j is denoted by $K_{i,j}$. Note that we use different notations for the same source and destination in different node-disjoint routes. That is, $n_{1,1}$, $n_{1,2}$,..., $n_{1,K_{i,j}}$ all refer to the source node i. Similarly, $n_{h_1+1,1}$, $n_{h_2+1,2}$,..., $n_{h_{K_{i,j}}+1,K_{i,j}}$ all refer to the destination node j (see Figure 8.2). We use this notation to ease our presentation in next sections. Here, we also define $S_{i,j} = \bigcup_{k=1}^{K_{i,j}} P_k$ as the set of constituent nodes of all $K_{i,j}$ node-disjoint routes between the source node i and the destination node j.

Without loss of generality, we assume the criterion for finding routes is minimizing the hop-count. Accordingly, the kth node-disjoint route between two nodes (i.e., P_k) is the route whose rank is k with regard to the hop count. Here, we do not consider any preference in ranking of routes with the same number of hops.

---

[1]Here, we basically assumed that a reactive route discovery mechanism is deployed in the multi-hop network. As mentioned in Chapter 2, reactive protocols are shown to be more effective in these networks.
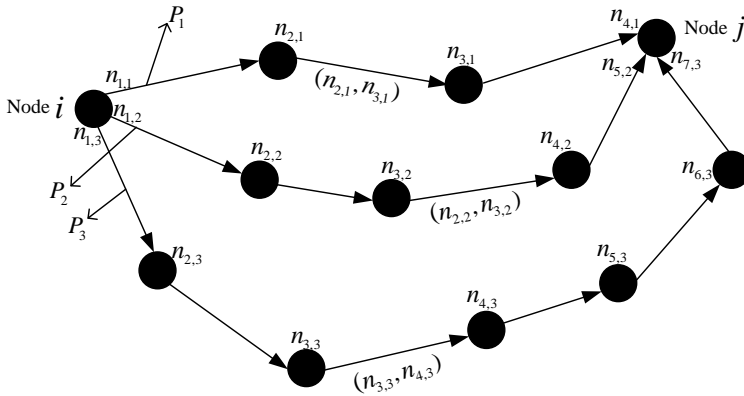
Figure 8.2 – Node-disjoint routes between a source node i, and a destination node, j. In this figure, there are three routes between the source and the destination, (i.e., $K_{i,j} = 3$). Depending on the route, different notations are considered for the source and the destination.

That is, if two routes have the same number of hops, one of them is ranked after the other one. It is also worthwhile to mention that if the source and the destination are neighbors, then the first ranked route P_1 will be the direct link between the two nodes (single-hop route). In such a case, no alternative route is required for communication, because the two nodes will communicate through the direct link between them until one of them fails. Failure of the source or destination will end their communication. In our analysis in this chapter, we distinguish between single-hop and multi-hop routes (connections).

8.2.3 Medium Access Control Mechanism

The analysis we provide here is independent of the type of medium access control mechanism. Nevertheless, since wireless multi-hop networks are autonomous systems without a central controller, usually carrier sense multiple access (CSMA) mechanisms are deployed at the MAC layer (see Chapter 2). We only make the following assumptions with regard to the medium access control mechanism to reduce complexity of calculating the energy consumption rate of intermediate nodes when they forward packets.

1. The transmission time of data packets over wireless links is assumed to be negligible compared to the inter-arrival time of data packets –belonging to the same session– from the application layer. The transmission time includes the waiting time at the MAC layer to access the channel as well as the duration

required to transmit all bits of the packet on the physical link. In fact, we assume the MAC mechanism is efficient enough to achieve a relatively small channel access waiting time. Furthermore, we assume the wireless technology supports a relatively high data rate such that the transmission time becomes sufficiently negligible compare to the inter-arrival time of packets from the application layer.

2. When an intermediate node relays a packet, the time required to receive and forward the packet is negligible compared to the inter-arrival time of data packets –belonging to the same session– to that intermediate node. Thus, in addition to having a negligible transmission time, the processing time of a packet at an intermediate node is also negligible compared to the inter-arrival time of packets.

3. When MAC retransmission is supported, we assume that the total time required to deliver a packet over a physical link is negligible compared to the inter-arrival of packets of a specific session to the MAC layer of the source node (from the application layer) or the MAC layer of relay nodes (from the physical layer).

8.3   Problem Statement and Formulation

We model and analyze the node-to-node communication lifetime as explained in the sequel. Assume an arbitrary source node $i \in \mathbb{V}$ transmits packets to an arbitrary destination node $j \in \mathbb{V}$ with a rate of λ [packet/s]. The packet transmission is started at the network startup (without loss of generality). At first, P_1, the first node-disjoint route between the source node and the destination, is used to transfer packets. If P_1 fails due to failure of its intermediate nodes, P_2 is used provided that the source and the destination both are still alive. This continues until either the source or the destination or the last available route between them, $P_{K_{i,j}}$ fails.

Our goal is to analyze the maximum duration that two nodes in a wireless ad hoc network can communicate with each other. To this end, nodes belonging to $\mathcal{S}_{i,j}$ must only carry and be affected by the generated traffic by node i destined to node j. To clarify this, assume that some nodes of $\mathcal{S}_{i,j}$ carry traffic other than the traffic generated by i. They may act as intermediate nodes or even source or destination in other traffic. However, even if these nodes are not directly involved in other traffic, they may overhear packets belonging to other traffic. In any case, their energy consumption will increase compared to the case where they are not involved with or affected by other traffic in the network. If the energy consumption rate of such nodes belonging to $\mathcal{S}_{i,j}$ increases, they live for a shorter time. This, in turn, may reduce the duration that i can communicate to j via nodes in $\mathcal{S}_{i,j}$. The

duration that i can transfer packets to j, denoted by $T_{i,j}$, is maximized if nodes in $S_{i,j}$ do not carry other traffic or are not affected by other traffic in the nerwork. $T_{i,j}$ as defined here is the *maximum* duration that i can transfer packets to j.

As we assumed, the network might be a disconnected network. Thus, there may not be a route between two nodes which are outside each other's transmission range. In such a case, their communication lifetime is zero. However, if there is at least one route between two nodes or the two nodes are neighbors, their communication lifetime is either the lifetime of the source node, the destination node, or the last available route between them.

We first assume that nodes are not neighbors. Let T_k be the time (with respect to the network start-up $t = 0$) at which P_k fails, and the use of the next route, P_{k+1}, starts for packet transfer. Furthermore, let $c(n_{l,k})$ [J/s] be the energy consumption rate of $n_{l,k} \in P_k$ when P_k is in-use for packet transfer. We also denote $B_{n_{l,k}}(T_{k-1})$ as the residual battery energy of $n_{l,k} \in P_k$ at the time of failure of P_{k-1}. Given these notations, we can determine T_1 as follows:

$$T_1 = \min(t_{1,1}, t_{2,1}, ..., t_{l,1}, ..., t_{h_1,1}, t_{h_1+1,1}),$$

in which $t_{l,1}$ is defined as

$$t_{l,1} = \frac{B_{n_{l,1}}(0)}{c(n_{l,1})}, \qquad \forall l = 1..h_1 + 1.$$

Here, there could be several possibilities. If $T_1 = t_{1,1}$, failure of the source node ends the communication between the source and the destination. If $T_1 = t_{h_1+1,1}$, failure of the destination ends the communication. If neither $T_1 = t_{1,1}$ nor $T_1 = t_{h_1+1,1}$, but there is only one route between the source and the destination (i.e., $K_{i,j} = 1$), then communication ends due to lack of alternative routes. Nevertheless, if there is a second route to continue the communication after failure of the first route, we can calculate the lifetime of the second route as follows:

$$T_2 = \min(t_{1,2}, t_{2,2}, ..., t_{l,2}, ..., t_{h_2,2}, t_{h_2+1,2}),$$

where $t_{l,2}$ is defined as

$$t_{l,2} = T_1 + \frac{B_{n_{l,2}}(T_1)}{c(n_{l,2})}, \qquad \forall l = 1..h_2 + 1.$$

We check again whether the source node or the destination node has failed, or they are still alive, but the second route has failed. According to our notation, in either case $T_{i,j} = T_2$. If the source and the destination are still alive, and there is another route to continue the communication, this procedure is repeated until the communication fails (see Figure 8.3).
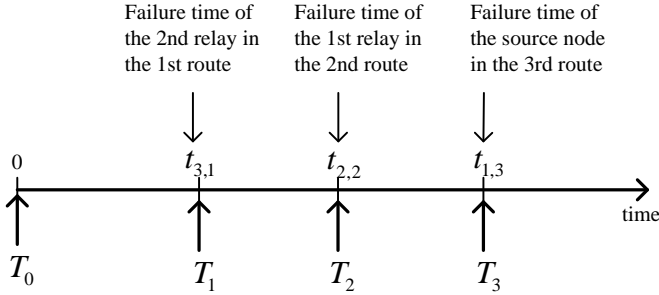
Figure 8.3 – Communication lifetime of two nodes for the example shown in Figure 8.2. Failure of the first route happens at the time that the second relay fails (i.e., $t_{3,1}$), and failure of the second route happens at the time that the first relay fails (i.e., $t_{2,2}$). Nevertheless, failure of the third route happens at the time that the source node fails (i.e., $t_{1,3}$).

In general, we have

$$T_k = \min(t_{1,k}, t_{2,k}, ..., t_{l,k}, ..., t_{h_k,k}, t_{h_k+1,k}), \qquad (8.1)$$

in which

$$t_{l,k} = T_{k-1} + \frac{B_{n_{l,k}}(T_{k-1})}{c(n_{l,k})}, \qquad \forall l = 1..h_k + 1, \ k = 1...K_{i,j}. \qquad (8.2)$$

Now, assume that the two nodes i and j are neighbors. That is, the single-hop route $P_1 = \{n_{1,1} = i, n_{h_1+1,1} = j\}$ is used for communication between them. In such a case, we obviously have

$$T_{i,j} = T_1 = \min(t_{1,1}, t_{h_1+1,1}).$$

As we see, to calculate the communication lifetime of two nodes, we generally need to determine the energy consumption rate of nodes, $c(n_{l,k})$, and their remaining battery energy $B_{n_{l,k}}(T_{k-1})$. In the next two sections, we model these values in networks with and without MAC retransmissions. On the basis of this modeling and the problem formulation presented in this section, we will also present in the next two sections numerical algorithms to calculate the communication lifetime between two specific nodes in the network.

8.4 Energy Consumption Rate of Nodes without MAC Retransmission

Energy consumption rate of nodes involved in an ongoing communication between two nodes depends on the consumed energy for transmission and/or reception of

data packets. As mentioned in Chapter 3, if TPC and MAC retransmission are not
supported, the energy consumed to transmit and receive a packet of length L [bit]
over a physical link is respectively as follows:

$$e_t = \epsilon_t L, \quad \forall (u, v) \in \mathbb{E}$$
$$e_r = \epsilon_r L, \quad \forall (u, v) \in \mathbb{E}$$

(8.3)

where, ϵ_t and ϵ_r [J/bit] are the energy consumed to transmit and receive a single
bit of the packet, respectively.

When it comes to the energy consumption rate, we also need to consider
other sources of energy consumption of nodes. For instance, in wireless multi-hop
networks, nodes consume energy for transmission and reception of control packets
for routing and neighbor discovery (this we call background traffic) and for channel
sensing. They may also consume energy for non-communication purposes such as
application execution (housekeeping). To take into account these sources of energy
consumption in our analysis, we abstract them for each node u by a parameter $g(u)$
[J/s]. The set of these values for all nodes are denoted by $\mathbb{G} = \{g(u)\}_{u=1}^{N}$. For several
reasons, the amount of $g(u)$ could be different for different nodes. One reason is that
different nodes might have a different number of neighboring nodes broadcasting
beacons and other control messages. Another reason is that nodes might be
heterogeneous and consume different amounts of energy for non-communication
purposes. Defining $g(u)$ in this general form makes our analysis also generic and
independent of the type of the networking protocols deployed. We refer to $g(u)$
as *idle-mode energy consumption rate* of node u. Here, we say a node is in *idle
mode* when it does not transmit or receive any data packet which belongs to an
active connection between a source and a destination. This should not be mistaken
for energy consumption of transceivers when they are idle and do not transmit or
receive any packets (data or control).

We consider two cases separately: when the route between the source and the
destination is single hop and when it is multi-hop. A single hop route is always
the only route which is used for packet transfer, because failure of the source or the
destination will end the communication. If the source node i transmits data packets
to the destination node j with the rate λ [packets/s], their energy consumption rate
in a single-hop route is as follows:

$$c(i) = \lambda e_t + g(i)$$
$$c(j) = \lambda e_r + g(j).$$

(8.4)

The following remark is the result of (8.4):

Remark 1. *Assuming $g(i) = g(j)$, the energy consumption rate of the source node
in a single-hop route when MAC retransmission is not supported is greater than the*
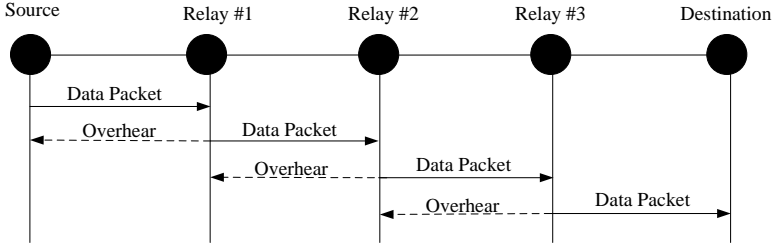
Figure 8.4 – Each node in a multi-hop connection overhears packets transmitted by its downstream node.

energy consumption rate of the destination node, if $\epsilon_t > \epsilon_r$. Otherwise, the energy consumption rate of the destination node is higher.

In a multi-hop route, each relay node forwards data packets that it receives from the previous relay node. There are two issues which must be considered for computing the energy consumption rate of nodes in multi-hop routes. First, the packet forwarding rate in each hop depends on the reliability of the upstream links. When $P_k =< n_{1,k}, n_{2,k}, ..., n_{h_k,k}, n_{h_k+1,k} >$ is used for packet transfer, $n_{l,k} \in P_k$ forwards packets with the rate $\lambda(n_{l,k})$, where

$$\lambda(n_{l,k}) = \begin{cases} \lambda, \ l = 1 \\ \lambda \prod_{m=1}^{l-1} p(n_{m,k}, n_{m+1,k}), \ \forall l = 2..h_k. \end{cases}$$

Here, λ is the packet transmission rate of the source node.

Remark 2. *Due to packet loss over physical links, the packet forwarding rate of each relay node is lower than or equal to the packet forwarding rate of its upstream nodes. That is, $\lambda(n_{l,k}) \leq \lambda(n_{l-1,k}) \leq ... \leq \lambda(n_{1,k})$.*

The second issue that we must consider is that each node overhears packets transmitted by its downstream node as shown in Figure 8.4. The figure shows that, for example, the second relay overhears packets transmitted by the third relay. Nevertheless, the third relay (in general the last relay) –which is next to the destination– does not overhear any packet. Taking into account these two issues and assumptions made in Section 8.2.3, the energy consumption rates of nodes in a multi-hop route are computed as follows:

$$\begin{aligned} c(n_{1,k}) &= \lambda(n_{1,k})e_t + \lambda(n_{2,k})e_r + g(n_{1,k}), \\ c(n_{l,k}) &= \lambda(n_{l-1,k})e_r + \lambda(n_{l,k})e_t + \lambda(n_{l+1,k})e_r + g(n_{l,k}), \quad \forall l = 2..h_k - 1, \\ c(n_{h_k,k}) &= \lambda(n_{h_k-1,k})e_r + \lambda(n_{h_k,k})e_t + g(n_{h_k,k}), \\ c(n_{h_k+1,k}) &= \lambda(n_{h_k,k})e_r + g(n_{h_k,k}). \end{aligned} \tag{8.5}$$

Remark 2 implies that $\lambda(n_{1,k}) \geq \lambda(n_{h_k,k})$. This means, if $g(n_{1,k}) \geq g(n_{h_k,k})$, then $c(n_{1,k}) > c(n_{h_k+1,k})$. Furthermore, we have $\lambda(n_{l,k}) \geq \lambda(n_{l+1,k})$, $\forall l = 2..h_k$. Thus, according to (8.5), if $g(n_{l,k}) \geq g(n_{l+1,k})$, then $c(n_{l_k}) > c(n_{l+1,k})$, $\forall l = 2..h_k$. Therefore, we can have the following two remarks:

Remark 3. *Assuming $g(n_{1,k}) \geq g(n_{h_k,k})$, the energy consumption rate of the source node in a multi-hop route when MAC retransmission is not supported is always greater than the energy consumption rate of the destination node.*

Remark 4. *Assuming $g(n_{l,k}) \geq g(n_{l+1,k})$, $\forall l = 2..h_k$, the energy consumption rate of each relay node in a multi-hop route when MAC retransmission is not supported is always greater than the energy consumption rate of its downstream relay node.*

Knowing the energy consumption rate of nodes, we can determine their remaining battery energy at a given time instance. Based on our problem formulation, we need to calculate the remaining battery energy of nodes in P_k at the time that this route is used for packet transfer to the destination node. When previous routes, $P_1, P_2, ..., P_{k-1}$ have been in use, the source node has continuously transmitted packets and the destination node has continuously received packets. Hence, their remaining battery energy at the time that P_k is used for packet transfer is computed as

$$
\begin{aligned}
B_{n_{1,k}}(T_{k-1}) &= B_{n_{1,k}}(0) - \sum_{d=1}^{k-1} c(n_{1,d})(T_d - T_{d-1}), \\
B_{n_{h_k+1,k}}(T_{k-1}) &= B_{n_{h_k+1,k}}(0) - \sum_{d=1}^{k-1} c(n_{h_k+1,d})(T_d - T_{d-1}).
\end{aligned} \tag{8.6}
$$

To determine the remaining battery energy of relay nodes in a multi-hop route, we notice that the relay nodes in this route may overhear packets transmitted by nodes in the previously in-use routes. That is, while $P_1, P_2, ..., P_{k-1}$ have been used, relay nodes in P_k may overhear packets transmitted along these routes (see Figure 8.5). To consider this phenomenon in our analysis, we assume $\gamma_{l,k}(d)$ is the number of nodes in P_d, $\forall d = 1..k-1$ –including the source and the destination nodes– which are neighboring nodes of $n_{l,k} \in P_k$. We define $\Phi_{l,k}(d) = \{\varphi_1, .., \varphi_{\gamma_{l,k}(d)}\}$ as the set of such nodes. With this definition, we have

$$
\begin{aligned}
B_{n_{l,k}}(T_{k-1}) =& B_{n_{l,k}}(0) - g(n_{l,k})T_{k-1} \\
& - \sum_{d=1}^{k-1} \sum_{\varphi_i \in \Phi_{l,k}(d)} (T_d - T_{d-1})\lambda(\varphi_i)e_r, \ \forall l = 2..h_k, k = 1..K_{i,j},
\end{aligned} \tag{8.7}
$$

where, $\lambda(\varphi_i)$ is the rate that φ_i forwards packets when it is part of a route. The following theorem specifies the maximum value of $\gamma_{l,k}(d)$.
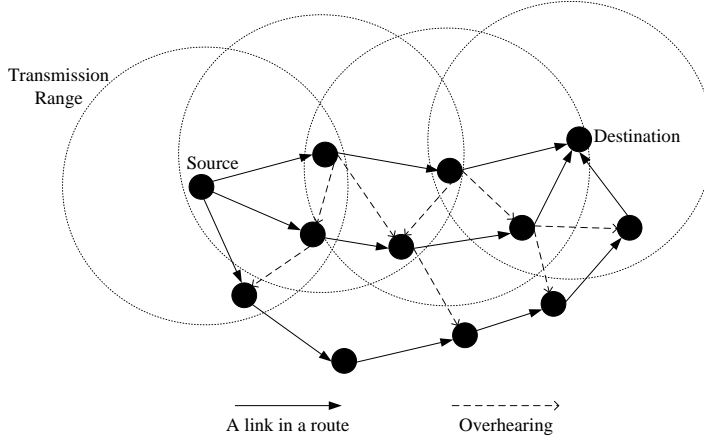
Figure 8.5 – Relay nodes in other routes may overhear packets transmitted along an in-use route.

Theorem 10. *Let* $\{P_k\}_{k=1}^{K}$ *be the ordered set of node-disjoint routes between two nodes with regard to the hop-count. Each relay node in* P_k *can have a physical link with at most three nodes in* P_d *–including the source and the destination nodes–* $\forall l = 2..h_k$ *and* $\forall k, d < k$.

Proof. Let $< A, B, C, D >$ in Figure 8.6 be the minimum-hop route between nodes A and D, and E is an arbitrary node. As figure shows, E could have links with three nodes A, B, and C without violating the assumption that $< A, B, C, D >$ is the minimum-hop path. Nevertheless, if there is a link between E and D (the fourth node), then the minimum-hop route from A to D will be $< A, E, D >$. This violates the initial assumption. $\qquad\square$

Corollary 1. *If the discovered routes are minimum-hop routes, then* $0 \leq \gamma_{l,k}(d) \leq 3$, $\forall l = 2..h_k$ *and* $\forall k, d < k$.

Corollary 2. *Since the first relay node is a neighboring node of the source node and the last relay node is a neighboring node of the destination node, we have* $1 \leq \gamma_{l,k}(d) \leq 3$, *for* $l \in \{2, h_k\}$ *and* $\forall k, d < k$.

So far, we calculated the energy consumption rate of nodes and their remaining battery energy in single-hop and multi-hop routes when MAC retransmission is not supported. We can use (8.4) to calculate the energy consumption rate of the source and the destination node in a single-hop route, and (8.5) to calculate the energy consumption rate of the source node, the destination node, and relay nodes in a multi-hop route. On the basis of the formulation provided in this section and in the previous section, we can derive an algorithm to calculate the communication lifetime
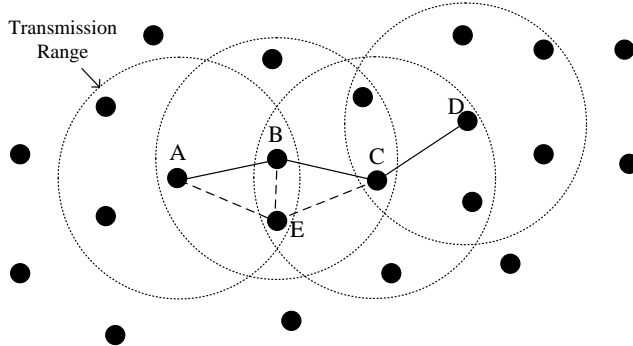
Figure 8.6 – Illustration of Theorem 10.

of two specific nodes i and j in the network. The algorithm has been presented in Algorithm 9 and its related procedure is presented in Algorithm 10. In Appendix A, we have shown that the time complexity of Algorithm 9 is $O(K_{max}|\mathbb{V}|^2)$ in dense networks and $O(K_{max}|\mathbb{V}|\log(|\mathbb{V}|) + K_{max}|\mathbb{E}|)$ in sparse networks. Here, K_{max} is the maximum number of node-disjoint routes that exist between two nodes of the network. That is, $K_{max} = \max(K_{i,j})\ \forall(i,j) \in \mathbb{V} \times \mathbb{V}$.

8.5 Energy Consumption Rate of Nodes with MAC Retransmission

If TPC is not supported but MAC retransmission is supported, the expected energy consumed by u and v when u tries to deliver a data packet of length L bits to v is (see Chapter 3):

$$
\begin{aligned}
e_t(u,v) &= \bar{\mathcal{X}}_{u,v}\epsilon_t L + \bar{\mathcal{Y}}_{v,u}\epsilon_r L_a \\
e_r(u,v) &= \bar{\mathcal{X}}_{u,v}\epsilon_r L + \bar{\mathcal{Y}}_{v,u}\epsilon_t L_a.
\end{aligned}
\tag{8.8}
$$

Here, $\bar{\mathcal{X}}_{u,v}(L)$ is the expected number of transmission attempts of node u to deliver a packet to node v, and $\bar{\mathcal{Y}}_{v,u}(L_a)$ is the expected number of acknowledgments of length L_a [bit] sent by v to u for a data packet. As a matter of fact, $L \geq L_a$, because L includes headers of higher layers and user data, while L_a only includes headers of MAC and physical layer. We can also state that $\bar{\mathcal{X}}_{u,v}(L) \geq \bar{\mathcal{Y}}_{v,u}(L_a)$, $\forall\,(u,v)$, because an acknowledgment is sent when a data packet is received correctly, possibly after several attempts. Thus, from (8.8), we can conclude the following:

Remark 5. *When MAC retransmission is supported, the energy consumed by a transmitting node to deliver a packet over a physical link is greater than the energy*

Algorithm 9 A numerical algorithm to calculate the communication lifetime of two nodes i and j in a wireless multi-hop network.

INPUT $G(\mathbb{V}, \mathbb{E})$, $\mathbb{B}(0)$, $\mathbb{G}$, $\mathbb{P}$, ϵ_r, ϵ_t, λ, $\mathbb{Q}$ (when MAC retransmission is supported)

if $(i, j) \in \mathbb{E}$ **then**
    Calculate $c_s(i)$ & $c_s(j)$
    $T_{i_s} \leftarrow \frac{B_i(0)}{c_s(i)}$, $T_{j_s} \leftarrow \frac{B_j(0)}{c_s(j)}$
    return $\min(T_{i_s}, T_{j_s})$
end if
$k = 1$
$T_{k-1} \leftarrow 0$
loop
    Find P_k
    if $P_k = \emptyset$ **then**
        return T_{k-1}
    end if
    Calculate $c(n_{l,k})$, $\forall l = 1...h_k + 1$
    $t_{l,k} \leftarrow T_{k-1} + \frac{B_{n_{l,k}}(T_{k-1})}{c(n_{l,k})}$
    $T_k \leftarrow \min(t_{1,k}, t_{2,k}, ..., t_{h_k,k}, t_{h_k+1,k})$
    if $T_k = \min(t_{1,k}, t_{h_k+1,k})$ **then**
        return T_k
    end if
    Update $\mathbb{B}$ and G
    $k \leftarrow k + 1$
end loop

---

consumed by the receiving node, if $\epsilon_t \geq \epsilon_r$. Otherwise, if $\epsilon_t < \epsilon_r$, the energy consumed by the receiving node will be higher.

The value of $\bar{\mathfrak{X}}_{u,v}(L)$ and $\bar{\mathfrak{y}}_{v,u}(L_a)$ depend on the quality of the forward link (u, v) and the reverse link (v, u). The significance of Remark 5 is that the energy consumed by a transmitting node is always greater than the energy consumed by the receiving node, regardless of the quality of the link between them.

Knowing the consumed energy for a packet exchange over a physical link, we can determine the energy consumption rate of nodes in single-hop and multi-top routes. Considering the assumptions in Section 8.2, the energy consumption rates of the source node i and the destination node j in a single-hop route are as follows:

$$c(i) = \lambda e_t(i, j) + g(i)$$
$$c(j) = \lambda e_r(i, j) + g(j),$$

$$(8.9)$$

where $e_t(i, j)$ and $e_r(i, j)$ are as expressed in (8.8).

Algorithm 10 Updating $\mathbb{B}$ and G when MAC retransmission is not supported.

$B_{n_{1,k}} \leftarrow B_{n_{1,k}} - c_{n_{1,k}}(T_k - T_{k-1})$
$B_{n_{h_k+1,k}} \leftarrow B_{n_{h_k+1,k}} - c_{n_{h_k+1,k}}(T_k - T_{k-1})$
for $u = 1$ to $|\mathbb{V}|$ & $u \notin P_k$ **do**
   $B_u \leftarrow B_u - g(u)(T_k - T_{k-1})$
   for $l = 1$ to h_k **do**
     if $(u, n_{l,k}) \in \mathbb{E}$ **then**
       $B_u \leftarrow B_u - \lambda(n_{l,k})\epsilon_r L(T_k - T_{k-1})$
     end if
   end for
end for
if $B_u < 0$ **then**
   Remove u from G
end if
Remove $P_k - \{n_{1,k}, n_{h_k+1,k}\}$ from G

To determine the energy consumption rate of nodes in multi-hop routes, we first determine the packet forwarding rate of nodes when MAC retransmission is supported. When $P_k = < n_{1,k}, n_{2,k}, ..., n_{h_k,k}, n_{h_k+1,k} >$ is used to transfer data packets, $n_{l,k}$ will forward packets at a rate

$$\lambda(n_{l,k}) = \begin{cases} \lambda, & l = 1 \\ \lambda \prod_{m=1}^{l-1} R(n_{m,k}, n_{m+1,k}), & \forall l = 2..h_k. \end{cases} \tag{8.10}$$

Here, $R(n_{m,k}, n_{m+1,k})$ is the reliability of the link $(n_{m,k}, n_{m+1,k})$ in P_k defined as

$$R(n_{m,k}, n_{m+1,k}) = 1 - [1 - p(n_{m,k}, n_{m+1,k})]^M,$$

and M is the maximum number of transmission attempts of a packet over a link.

When MAC retransmission is supported, nodes along a route may overhear not only data packets transmitted by their downstream nodes, but also acknowledgments transmitted by their upstream nodes (see Figure 8.7). In the example shown in Figure 8.7, the second relay overhears packets transmitted by the third relay to the destination, and acknowledgments sent by the first relay to the source. In general, depending on the number of relay nodes in a route and their position, a relay node may overhear nothing or it may overhear either data packets, acknowledgments, or both of them. In a route with only one relay node, the relay overhears nothing. In a route with two relays, the first relay overhears data packets transmitted by the second relay to the destination, and the second relay overhears acknowledgments sent by the first relay to the source. In a route with more than two relays the first relay overhears only data packets, the last relay
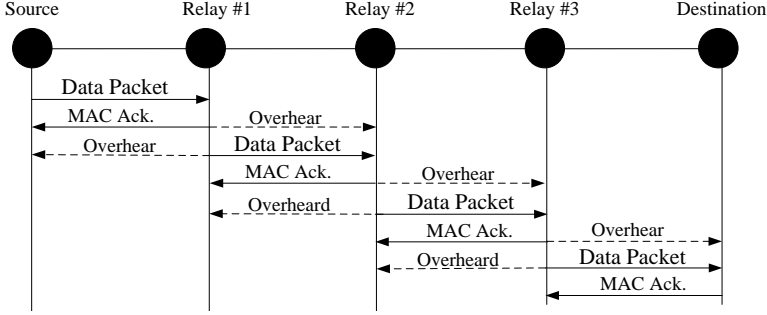
Figure 8.7 – When MAC retransmission is supported nodes along a route may overhear data packets transmitted by their downstream nodes and acknowledgments transmitted by their upstream nodes.

overhears only acknowledgments, and other relays overhear both acknowledgments and data packets.

Considering the above explanation, the energy consumption rate of the source and the destination in a multi-hop route P_k is as follows:

$$c(n_{1,k}) = \lambda(n_{1,k})e_t(n_{1,k}, n_{2,k}) + \lambda(n_{2,k})\mathcal{X}_{n_{2,k},n_{3,k}}\epsilon_r L + g(n_{1,k}),$$
$$c(n_{h_k+1,k}) = \lambda(n_{h_k,k})e_r(n_{h_k,k}, n_{h_k+1,k}) + \lambda(n_{h_k-1,k})\mathcal{Y}_{n_{h_k,k},n_{h_k-1,k}}\epsilon_r L_a + g(n_{h_k+1}).$$
$$(8.11)$$

Remark 6. *Even if $g(n_{1,k}) > g(n_{h_k+1})$, due to the effect of the quality of links, the energy consumption rate of the source node $n_{1,k}$ in a multi-hop route could be smaller than the energy consumption rate of the destination node n_{h_k+1}.*

As mentioned before, the energy consumption rate of a relay node in a multi-hop route depends on the hop-count of the route and the position of the relay in the route. In a route with two hops, $P_k =< n_{1,k}, n_{2,k}, n_{3,k} >$, the energy consumption rate of the relay node is

$$c(n_{2,k}) = \lambda(n_{1,k})e_r(n_{1,k}, n_{2,k}) + \lambda(n_{2,k})e_t(n_{2,k}, n_{3,k}) + g(n_{2,k}). \qquad (8.12)$$

In a route with three hops, $P_k =< n_{1,k}, n_{2,k}, n_{3,k}, n_{4,k} >$, the energy consumption rate of relay nodes $n_{2,k}$ and $n_{3,k}$ is

$$c(n_{2,k}) = \lambda(n_{1,k})e_r(n_{1,k}, n_{2,k}) + \lambda(n_{2,k})e_t(n_{2,k}, n_{3,k}) + \lambda(n_{3,k})\mathcal{X}_{n_{3,k},n_{4,k}}\epsilon_r L + g(n_{2,k})$$
$$c(n_{3,k}) = \lambda(n_{2,k})\mathcal{Y}_{n_{2,k},n_{1,k}}\epsilon_r L_a + \lambda(n_{2,k})e_r(n_{2,k}, n_{3,k}) + \lambda(n_{3,k})e_t(n_{3,k}, n_{4,k}) + g(n_{3,k}).$$
$$(8.13)$$

In a route with more than three hops, $P_k =< n_{1,k}, ..., n_{l,k}, ..., n_{h_k+1,k} >$, the energy consumption rate of the first relay, $n_{2,k}$, and the last relay, $n_{h_k,k}$, is the same as

the energy consumption rate of the first and the second relay in a route with three hops, respectively. The energy consumption rate of other relays is as follows:

$$
\begin{aligned}
c(n_{l,k}) =& \lambda(n_{l-2,k})_{n_{l-1,k},n_{l-2,k}}\epsilon_r L_a \\
&+ \lambda(n_{l-1,k})e_r(n_{l-1,k},n_{l,k}) + \lambda(n_{l,k})e_t(n_{l,k},n_{l+1,k}) \\
&+ \lambda(n_{l+1,k})\mathfrak{X}_{n_{l+1,k},n_{l+2,k}}\epsilon_r L \\
&+ g(n_{l,k}), \qquad \forall l = 3..h_k - 1.
\end{aligned}
\tag{8.14}
$$

Now, let us define the remaining battery energy of nodes when a route is used for packet transfer, i.e., $B_{n_{l,k}}(T_{k-1})$. Similar to the case that MAC retransmission is not supported, the remaining battery energy of the source and the destination when the source switches from P_{k-1} to P_k is defined by (8.6). The residual battery energy of relay nodes in P_k depends on overhearing of data and acknowledgment packets from other routes. Note that a relay node does not overhear acknowledgments from the source node, because the source never transmits an acknowledgment. On the other hand, the destination never transmits a data packet. Hence, we define $\Phi_{l,k}(d) = \{\varphi_1, .., \varphi_{\gamma_{l,k}(d)}\}$ as the set of nodes in $P_d - \{n_{h_d+1,d}\}$ ($n_{h_d+1,d}$ is the destination node), which are neighboring nodes of $n_{l,k} \in P_k$, where $\gamma_{l,k}(d)$ is the size of this set. The transmitted data packets by nodes of $\Phi_l(k,d)$ will be overheard by $n_{l,k} \in P_k$. We also define $\Delta_{l,k}(d) = \{\delta_1, .., \delta_{\gamma'_{l,k}(d)}\}$ as the set of nodes in $P_d - \{n_{1,d}\}$ ($n_{1,d}$ is the source node), which are neighboring nodes of $n_{l,k} \in P_k$, where $\gamma'_{l,k}(d)$ is the size of this set. The transmitted acknowledgments by these nodes will be overheard by $n_{l,k} \in P_k$. Given these two sets, $B_{n_{l,k}}(T_{k-1})$ is obtained as

$$
\begin{aligned}
B_{n_{l,k}}(T_{k-1}) =& B_{n_{l,k}}(0) - g(n_{l,k})T_{k-1} \\
&- \sum_{d=1}^{k-1} \sum_{\varphi_i \in \Phi_{l,k}(d)} (T_d - T_{d-1})\lambda(\varphi_i)a(\varphi_i, \varphi_{i+1})\epsilon_r L \\
&- \sum_{d=1}^{k-1} \sum_{\delta_i \in \Delta_{l,k}(d)} (T_d - T_{d-1})\lambda(\delta_i)b(\delta_i, \delta_{i+1})\epsilon_r L_a, \qquad \forall l = 2..h_k.
\end{aligned}
\tag{8.15}
$$

Lemma 5. *When discovered routes are minimum-hop routes and MAC retransmission is supported, $0 \leq \gamma_{l,k}(d) \leq 3$ and $0 \leq \gamma'_{l,k}(d) \leq 3$ $\forall l = 2..h_k$ and $\forall k, d < k$.*

Proof. The proof follows directly from Theorem 10. $\qquad \square$

To summarize, we can use the expressions provided in this section to determine the energy consumption rate of nodes and their remaining battery energy, when MAC retransmission is supported. On the basis of the formulations provided in this section, we can determine the communication lifetime between two specific nodes i and j using Algorithm 9 and its related procedure in Algorithm 11.

Algorithm 11 Updating $\mathbb{B}$ and G when MAC retransmission is supported.

$B_{n_{1,k}} \leftarrow B_{n_{1,k}} - c_{n_{1,k}}(T_k - T_{k-1})$
$B_{n_{h_k+1,k}} \leftarrow B_{n_{h_k+1,k}} - c_{n_{h_k+1,k}}(T_k - T_{k-1})$
for $u = 1$ to $|\mathbb{V}|$ & $u \notin P_k$ **do**
    $B_u \leftarrow B_u - g(u)(T_k - T_{k-1})$
    for $l = 1$ to h_k **do**
        if $(u, n_{l,k}) \in \mathbb{E}$ **then**
            $B_u \leftarrow B_u - \lambda(n_{l,k})\mathcal{X}_{u,n_{l,k}}\epsilon_r L(T_k - T_{k-1})$
        end if
    end for
    for $l = 2$ to $h_k + 1$ **do**
        if $(u, n_{l,k}) \in \mathbb{E}$ **then**
            $B_u \leftarrow B_u - \lambda(n_{l,k})\mathcal{Y}_{n_{l,k},u}\epsilon_r L_a(T_k - T_{k-1})$
        end if
    end for
end for
if $B_u < 0$ **then**
    Remove u from G
end if
Remove $P_k - \{n_{1,k}, n_{h_k+1,k}\}$ from G

8.6   Bounds on the Lifetime of Node-disjoint Routes

The lifetime of a route is defined as the time until one of its relay nodes fails (not the source or the destination node). To determine the route lifetime, we represent the expression given for T_k in (8.1) as follows:

$$T_k = T_{k-1} + D_k, \tag{8.16}$$

in which $D_k = \min\left(\frac{B_{n_{2,k}}(T_{k-1})}{c(n_{2,k})}, ..., \frac{B_{n_{h_k,k}}(T_{k-1})}{c(n_{h_k,k})}\right)$ is the duration that the kth route could be used for packet transfer from the source to the destination given that the source and the destination do not fail at all. Note that the remaining battery energy and the energy consumption rate of relay nodes in the kth route between different pairs of source-destination nodes could be different. This means, D_k (and hence T_k) may take different values for different pairs of source-destination nodes in the network. The strong point of our analysis in this section is that we determine lower and upper bounds of T_k for any pair of source-destination nodes.

To this end, let us define $B_{low}(T_{k-1})$ and $B_{up}(T_{k-1})$ as the lower and upper bounds for the remaining battery energy of a node in the kth node-disjoint route between a pair of source-destination nodes at time T_{k-1}, respectively. Furthermore,

we define c_{low} and c_{up} to be the lower and upper bounds for the energy consumption rate of a relay node in a multi-hop route, respectively. The following inequalities follow from the definition of D_k:

$$\frac{B_{low}(T_{k-1})}{c_{up}} \leq D_k \leq \frac{B_{up}(T_{k-1})}{c_{low}}. \tag{8.17}$$

If we replace (8.17) in (8.16), we have

$$T_{k-1} + \frac{B_{low}(T_{k-1})}{c_{up}} \leq T_k \leq T_{k-1} + \frac{B_{up}(T_{k-1})}{c_{low}}. \tag{8.18}$$

Now, we determine $B_{low}(T_{k-1})$, $B_{up}(T_{k-1})$, c_{low}, and c_{up} as well as the lower and the upper bounds of T_k in networks with and without MAC retransmissions.

8.6.1 Networks without MAC Retransmission

When MAC retransmission is not supported, the energy consumption rate of a relay nodes, $c(n_{l,k})$, was specified in (8.5). An upper bound for $c(n_{l,k})$ is achieved when a relay receives and transmits packets with the highest rate, and overhears packets transmitted by its downstream relay with the highest rate too. The highest packet forwarding rate for a relay is the rate at which the source transmits packets (i.e., λ). Let us define $g_{max} = \max\{g(u)\}_{u=1}^N$ as the largest energy consumption rate among nodes of the network for running networking protocols. Using (8.5), we can show that

$$c(n_{l,k}) < \begin{cases} \lambda L(2\epsilon_r + \epsilon_t) + g_{max}, & \forall l = 2..h_k - 1, \\ \lambda L(\epsilon_r + \epsilon_t) + g_{max}, & l = h_k. \end{cases} \tag{8.19}$$

From (8.19), we can conclude that the upper bound of $c(n_{l,k})$ is

$$c_{up} = \lambda L(2\epsilon_r + \epsilon_t) + g_{max}.$$

In theory, a lower bound for $c(n_{l,k})$ is achieved when a relay node receives packets with the lowest possible rate. According to Remark 2, the lowest rate that a relay node in a multi-hop route can receive packets belongs to the last relay in the route. However, in practice, the route lifetime will be dominated by the lifetime of a node which has the highest energy consumption rate in that route. Thus, c_{low} is the lowest energy consumption rate of a relay node whose death fails the route. According to (8.5), the lowest energy consumption rate for such a relay node belongs to the relay in a route with two hops. Let us define $g_{min} = \min\{g(u)\}_{u=1}^N$ as the lowest energy consumption rate among nodes for running networking protocols. Furthermore, let $p_{min} = \min\{p(u,v)\}, \forall (u,v) \in \mathbb{E}$. A lower bound for $c(n_{l,k})$ is

$$c_{low} = \lambda L(\epsilon_r + p_{min}\epsilon_t) + g_{min}.$$

To determine lower and upper bounds of the remaining battery energy of a relay node in a route, $B_{low}(T_{k-1})$ and $B_{up}(T_{k-1})$, we use Corollary 1. This corollary indicates that a relay node can at most overhear three nodes from other routes. Thus, $B_{low}(T_{k-1})$ is achieved for $\gamma_{l,k}(d) = 3$, $\forall d = 1...k-1$ in (8.7). Furthermore, all three overheard nodes in each route must transmit with the highest packet forwarding rate (i.e., λ). Therefore, $B_{low}(T_{k-1})$ is obtained as

$$B_{low}(T_{k-1}) = B - (g_{max} + 3\lambda\epsilon_r L)\, T_{k-1}.$$

The upper bound, $B_{up}(T_{k-1})$, is achieved if no node from the other routes is overheard. In other words, we must consider $\gamma_{l,k}(d) = 0$, $\forall d = 1...k-1$, in (8.7). Thus,

$$B_{up}(T_{k-1}) = B - g_{min}T_{k-1}.$$

By replacing the expressions found for $B_{low}(T_{k-1})$, $B_{up}(T_{k-1})$, c_{low}, and c_{up}, in (8.18), we arrive at the following expression:

$$A_1 + (1 - A_2)T_{k-1} \le T_k \le A_3 + (1 - A_4)T_{k-1}, \tag{8.20}$$

where

$$A_1 = \frac{B}{\lambda L(2\epsilon_r + \epsilon_t) + g_{max}}$$

$$A_2 = \frac{g_{max} + 3\lambda L\epsilon_r}{\lambda L(2\epsilon_r + \epsilon_t) + g_{max}}$$

$$A_3 = \frac{B}{\lambda L(\epsilon_r + p_{min}\epsilon_t) + g_{min}}$$

$$A_4 = \frac{g_{min}}{\lambda L(\epsilon_r + p_{min}\epsilon_t) + g_{min}}.$$

If we look at the definition of A_4, we realize that $0 < A_4 < 1$, which means $0 < 1 - A_4 < 1$. We can also show that if $\epsilon_t > \epsilon_r$, $A_2 < 1$ (hence, $0 < 1 - A_2 < 1$).

The resulting inequalities in (8.20) are recursive. To resolve the recursive dependency in (8.20), we can replace T_{k-1} in the left hand side of (8.20) by the lower bound of T_{k-1}, and T_{k-1} in the right hand side of (8.20) by the upper bound of T_{k-1}. This can widen the bounds, because both $1 - A_2$ and $1 - A_4$ are positive values (assuming $\epsilon_t > \epsilon_r$). Thus, the recursive inequalities in (8.20) could be represented as follows:

$$A_1\left(1 + (1 - A_2) + ... + (1 - A_2)^{k-1}\right) \le T_k \le A_3\left(1 + (1 - A_4) + ... + (1 - A_4)^{k-1}\right). \tag{8.21}$$

We can simplify the geometric series in (8.21) to arrive at the upper and lower bounds of T_k as follows:

$$T_{k_{low}} = A_1 \frac{1 - (1 - A_2)^k}{A_2}, \quad \forall k = 1, 2, ...$$

$$T_{k_{up}} = A_3 \frac{1 - (1 - A_4)^k}{A_4}, \quad \forall k = 1, 2, ...$$

The following theorem follows from the derivations in this section:

Theorem 11. *Let* $g_{min} = \min\{g(u)\}_{u=1}^N$, $g_{max} = \max\{g(u)\}_{u=1}^N$, *and* $p_{min} = \min\{p(u, v)\}$, $\forall (u, v) \in \mathbb{E}$. *If MAC retransmission is not supported, then* $T_{k_{low}} \leq T_k \leq T_{k_{up}}$ *in which* $T_{k_{low}} = A_1 \frac{1-(1-A_2)^k}{A_2}$ *and* $T_{k_{up}} = A_3 \frac{1-(1-A_4)^k}{A_4}$ *and* A_1 *to* A_4 *are defined as*

$$A_1 = \frac{B}{\lambda L(2\epsilon_r + \epsilon_t) + g_{max}}, \quad A_2 = \frac{g_{max} + 3\lambda L \epsilon_r}{\lambda L(2\epsilon_r + \epsilon_t) + g_{max}}$$

$$A_3 = \frac{B}{\lambda L(\epsilon_r + p_{min}\epsilon_t) + g_{min}}, \quad A_4 = \frac{f_{min}}{\lambda L(\epsilon_r + p_{min}\epsilon_t) + g_{min}}.$$

8.6.2 Networks with MAC Retransmission

When MAC retransmission is supported, the energy consumption rate of a relay nodes $c(n_{l,k})$ was specified in (8.12) for routes with two hops, in (8.13) for routes with three hops, and in (8.14) for routes with more than three hops. An upper bound for $c(n_{l,k})$ is achieved when a relay node receives and transmits packets with the highest rate, and overhears both data packets and acknowledgments transmitted by its downstream and upstream relay nodes. This situation happens in a route with more than three hops. Thus, from (8.14), we have

$$c_{up} = \lambda(a_{max}L + b_{max}L_a)(\epsilon_t + 2\epsilon_r) + g_{max},$$

in which $a_{max} = \max\{\bar{\mathcal{X}}_{u,v}\}$, $\forall (u, v) \in \mathbb{E}$, and $b_{max} = \max\{\bar{\mathcal{Y}}_{v,u}\}$, $\forall (u, v) \in \mathbb{E}$.

A lower bound for $c(n_{l,k})$ is achieved when a relay node receives packets with the lowest possible rate. According to Remark 2, the lowest rate at which a relay node in a multi-hop route can receive packets belongs to the last relay in the route[1]. However, in practice, the route lifetime will be dominated by the lifetime of a node which has the highest energy consumption rate in the route. When MAC retransmission is supported, the lowest energy consumption rate for a relay node whose death can cause route failure happens in a route with two hops, when each

---

[1]This remark was mentioned for the case in which MAC retransmission is not supported. However, it is also true, even if MAC retransmission is supported

data packet and its acknowledgment are transmitted only once. Using (8.12), we have

$$c_{low} = \lambda(L + L_a)(\epsilon_r + \epsilon_t) + g_{min}.$$

To determine the lower bound for the remaining battery energy of a relay node in a route $B_{low}(T_{k-1})$, we use Lemma 5. This lemma indicates a relay node can overhear data packets and acknowledgments at most from three nodes in the other routes. Therefore, $B_{low}(T_{k-1})$ is achieved as follows for $\gamma_{l,k}(d) = 3$ and $\gamma'_{l,k}(d) = 3$, $\forall d = 1...k - 1$ in (8.15):

$$B_{low}(T_{k-1}) = B - (g_{max} + 3\lambda(a_{max}L + b_{max}L_a)\epsilon_r) T_{k-1}.$$

The upper bound $B_{up}(T_{k-1})$, is achieved if no node from the other routes are overheard. Thus, $B_{up}(T_{k-1})$ is as follows, if we consider $\gamma_{l,k}(d) = 0$ and $\gamma'_{l,k}(d) = 0$ $\forall d = 1...k - 1$ in (8.15):

$$B_{up}(T_{k-1}) = B - g_{min}T_{k-1}.$$

By replacing the expressions found for $B_{low}(T_{k-1})$, $B_{up}(T_{k-1})$, c_{low}, and c_{up}, in (8.18), we arrive at the following inequalities:

$$H_1 + (1 - H_2)T_{k-1} \leq T_k \leq H_3 + (1 - H_4)T_{k-1}, \tag{8.22}$$

where

$$H_1 = \frac{B}{\lambda(a_{max}L + b_{max}L_a)(\epsilon_t + 2\epsilon_r) + g_{max}}$$

$$H_2 = \frac{g_{max} + 3\lambda(a_{max}L + b_{max}L_a)\epsilon_r}{\lambda(a_{max}L + b_{max}L_a)(\epsilon_t + 2\epsilon_r) + g_{max}}$$

$$H_3 = \frac{B}{\lambda(L + L_a)(\epsilon_r + \epsilon_t) + g_{min}}$$

$$H_4 = \frac{g_{min}}{\lambda(L + L_a)(\epsilon_r + \epsilon_t) + g_{min}}.$$

If we look at the definition of H_4, we realize that $0 < H_4 < 1$, which means $0 < 1 - H_4 < 1$. Assuming $\epsilon_t > \epsilon_r$, we can also show that $H_2 < 1$ ($0 < 1 - H_2 < 1$). Since both $1 - H_2$ and $1 - H_4$ are positive values, we can replace T_{k-1} in the left hand side of (8.22) by the lower bound of T_{k-1} and T_{k-1} in the right hand side of (8.20) by the upper bound of T_{k-1} to widen the bounds. Thus, we arrive at the following expression:

$$H_1 \left(1 + (1 - H_2) + ... + (1 - H_2)^{k-1}\right) \leq T_k \leq H_3 \left(1 + (1 - H_4) + ... + (1 - H_4)^{k-1}\right).$$
$$\tag{8.23}$$

We can simplify the geometric series in (8.23) to arrive at the upper and lower bound of T_k as follows:

$$T_{k_{low}} = H_1 \frac{1 - (1 - H_2)^k}{H_2}, \quad \forall k = 1, 2, \ldots$$

$$T_{k_{up}} = H_3 \frac{1 - (1 - H_4)^k}{H_4}, \quad \forall k = 1, 2, \ldots$$

The following theorem summarizes the derivations in this section:

Theorem 12. *Let* $g_{min} = \min\{g(u)\}_{u=1}^N$ *and* $g_{max} = \max\{g(u)\}_{u=1}^N$. *Let* $a_{max} = \max\{\bar{\mathcal{X}}_{u,v}\}$, $\forall (u,v) \in \mathbb{E}$, *and* $b_{max} = \max\{\bar{\mathcal{Y}}_{v,u}\}$, $\forall (u,v) \in \mathbb{E}$. *If MAC retransmission is, then* $T_{k_{low}} \leq T_k \leq T_{k_{up}}$ *in which* $T_{k_{low}} = H_1 \frac{1-(1-H_2)^k}{H_2}$ *and* $T_{k_{up}} = H_3 \frac{1-(1-H_4)^k}{H_4}$ *and* H_1 *to* H_4 *are defined as*

$$H_1 = \frac{B}{\lambda(a_{max}L + b_{max}L_a)(\epsilon_t + 2\epsilon_r) + g_{max}},$$

$$H_2 = \frac{g_{max} + 3\lambda(a_{max}L + b_{max}L_a)\epsilon_r}{\lambda(a_{max}L + b_{max}L_a)(\epsilon_t + 2\epsilon_r) + g_{max}},$$

$$H_3 = \frac{B}{\lambda(L + L_a)(\epsilon_r + \epsilon_t) + g_{min}}, \quad H_4 = \frac{g_{min}}{\lambda(L + L_a)(\epsilon_r + \epsilon_t) + g_{min}}.$$

8.7 Expected Node-to-node Communication Lifetime

In Section 8.4 and Section 8.5, we determined the communication lifetime between two specific nodes in the network. In this section, we determine the expected value of this lifetime. To this end, we need to know the PDF of the node-to-node communication lifetime in the network. We saw in Section 8.4 and Section 8.5 that the node-to-node communication lifetime depends on the reliability of the links. Thus, its PDF is also dependent on the PDF of the reliability of links in the network. The reliability of the links in turn depends on the modulation and channel coding schemes deployed at the physical layer as well as the model of the channel fading (e.g., Rayleigh or Rician). These dependencies complicate the calculation of the expected node-to-node communication lifetime in multi-hop networks with random topology. Furthermore, any analysis will be dependent on the assumed modulation and channel coding schemes. Considering the effect of overhearing and assuming different initial battery energy and idle-mode energy consumption rates for different nodes adds to the complexity of the problem.

In this section, however, we provide an analysis to approximate the expected value of the maximum lifetime between any two nodes in the network under some

assumptions. The importance of this approximation is that it gives a closed-form expression for the maximum duration that two nodes can communicate with each other in a multi-hop network with a random topology. In the next section, we will use simulation results to show that this approximate expression is of good accuracy even if we relax some of the assumptions. The following are our assumptions:

1. All nodes have the same idle-mode energy consumption rate, i.e., $g(u) = g$, $\forall u \in \mathbb{V}$.

2. The packet delivery ratio of all the links is 1 (perfect link), i.e., $p(u, v) = 1$ and $q(u, v) = 1$, $\forall(u, v) \in \mathbb{E}$.

3. All nodes have the maximum battery energy at network start up, i.e., $B_u(0) = B$, $\forall u \in \mathbb{V}$.

With these assumptions, we present the analysis for networks with MAC retransmission. The same analysis is valid for networks without MAC retransmission only if we set $L_a = 0$ in the equations presented in this section.

To calculate the expected communication lifetime in the network, we choose two nodes randomly. They might be either neighbors or several hops away from each other. If they are neighbors, the direct link between them will be used for communication. Otherwise, alternative node-disjoint min-hop routes will be used to keep them connected. The probability that the two nodes are neighbors is the probability that the destination node (which is chosen randomly) is within the transmission range of the source node. Since nodes are assumed to be uniformly distributed, we have $\Pr\{\text{connection is single hop}\} = \pi D_{max}^2 / A$, where D_{max} is the transmission range and A is the network area.

Let $\bar{T}$ be the expected value of the communication lifetime of two nodes. Furthermore, let $\bar{T}_{sh}$ be the expected communication lifetime if the two nodes are neighbors, and $\bar{T}_{mh}$ be the expected communication lifetime if they are not neighbors. We have

$$\bar{T} = \frac{\pi D_{max}^2}{A}\bar{T}_{sh} + \left(1 - \frac{\pi D_{max}^2}{A}\right)\bar{T}_{mh}. \tag{8.24}$$

8.7.1 Expected Communication Lifetime of Neighboring Nodes

Under the assumption of $p(u, v) = 1$ and $q(u, v) = 1$, we have $\bar{\mathcal{X}}_{u,v} = 1$ and $\bar{\mathcal{Y}}_{v,u} = 1$, $\forall(u, v) \in \mathbb{E}$. Considering (8.9) and (8.8), the energy consumption rate of the source node and the destination node, when they are neighbors, is respectively

$$c_{s_s} = \lambda\left(L\epsilon_t + L_a\epsilon_r\right) + g$$
$$c_{d_s} = \lambda\left(L\epsilon_r + L_a\epsilon_t\right) + g.$$

As a result, the lifetime of the source and the destination will be as follows:

$$T_{s_s} = \frac{B}{c_{s_s}} = \frac{B}{\lambda\left(L\epsilon_t + L_a\epsilon_r\right) + g}$$

$$T_{d_s} = \frac{B}{c_{d_s}} = \frac{B}{\lambda\left(L\epsilon_r + L_a\epsilon_t\right) + g}.$$

Assuming $\epsilon_t > \epsilon_r$ and $L > L_a$, the communication lifetime of two neighboring nodes is

$$T_{sh} = \min(T_{s_s}, T_{d_s}) = \frac{B}{\lambda\left(L\epsilon_t + L_a\epsilon_r\right) + g}. \tag{8.25}$$

Since there is no random variable associated with T_{sh}, we have

$$\bar{T}_{sh} = \frac{B}{\lambda\left(L\epsilon_t + L_a\epsilon_r\right) + g}. \tag{8.26}$$

8.7.2 Expected Communication Lifetime of Non-neighboring Nodes

We first assume that the number of available node-disjoint routes between the source and the destination is known. Then, we take into account the effect of randomness of the number of available routes between two arbitrary nodes.

Assuming $p(u,v) = 1$ and $q(u,v) = 1$, $\forall(u,v) \in \mathbb{E}$ and considering (8.11), we can express the energy consumption rate of the source node and the destination node as

$$c_{s_m} = \lambda(L\epsilon_t + L_a\epsilon_r) + \lambda\epsilon_r L + g$$

$$c_{d_m} = \lambda(L\epsilon_r + L_a\epsilon_t) + \lambda\epsilon_r L_a + g. \tag{8.27}$$

The first term in the expression given for c_{s_m} in (8.27) is the energy consumed by the source node to transmit λ packets per second. The second term is the energy consumed during overhearing of the packets forwarded by the first relay node. Similarly, the first term in c_{d_m} is the energy consumed by the destination to receive a packet, and the second term is the energy consumed to overhear acknowledgments sent by the last relay. Thus, the lifetime of the source and the destination in a multi-hop connection will be as follows:

$$T_{s_m} = \frac{B}{\lambda\left(L\epsilon_t + (L_a + L)\epsilon_r\right) + g}$$

$$T_{d_m} = \frac{B}{\lambda\left((L + L_a)\epsilon_r + L_a\epsilon_t\right) + g}. \tag{8.28}$$

We recall that the energy consumption rate of relay nodes depends on the hop-count of the route they are part of. Nevertheless, if we assume the probability

that two arbitrary nodes in the network are more than three hops away from each other[1] is much higher than the probability that they are less than three hops away from each other, we can calculate the energy consumption rate of a relay node using (8.14) as

$$c_r = \lambda \left((L + L_a) \left(2\epsilon_r + \epsilon_t \right) \right) + g. \tag{8.29}$$

Now, we can compute the lifetime of the first route as

$$\bar{T}_1 = \frac{B}{\bar{c}_r}. \tag{8.30}$$

To compute the lifetime of other node-disjoint routes, we need to determine the amount of energy remaining for a relay node in these routes at the time that the route previously used fails. For this, we define $\bar{\gamma}_k$ as the expected number of nodes in P_k which have physical links with a node from the previous routes $P_d, \forall d = 1..k-1$. In the worst case, a relay node whose death causes route failure, overhears both acknowledgments and data packets transmitted by a node in the route that is in use. Therefore, using (8.15), we can calculate the amount of battery energy remaining for such a relay node in P_k as

$$B_k = B - T_{k-1} \left[\bar{\gamma}_k \lambda \epsilon_r (L + L_a) + g \right], \qquad \forall k = 1, 2, ..K,$$

where K is the number of node-disjoint routes between the source and the destination. Thus, the expected lifetime of the kth route between a source and a destination is as follows:

$$T_k = T_{k-1} + \frac{B_k}{c_r}, \qquad \forall k = 1, 2, ..K, \tag{8.31}$$

in which $T_0 = 0$. The recursive equation in (8.31) could be simplified to

$$T_k = \frac{B}{c_r} \sum_{i=0}^{k-1} \rho^i, \qquad \forall k = 1, 2, ..K, \tag{8.32}$$

where

$$\rho = 1 - \frac{\bar{\gamma}_k \lambda \epsilon_r (L + L_a) + g}{c_r}. \tag{8.33}$$

From Theorem 10, we have $\max\{\bar{\gamma}_k\} = 3$. Considering this fact, we can show that if $\epsilon_t > \epsilon_r$, then $\rho < 1$. Therefore, the geometric series in (8.32) could be further simplified as

$$T_k = \left(\frac{B}{c_r} \right) \left(\frac{1 - \rho^k}{1 - \rho} \right), \qquad \forall k = 1, 2, ...K. \tag{8.34}$$

---

[1]more than two hops, in case of no MAC retransmission

Knowing T_k, T_{s_m}, and T_{d_m}, we can calculate the communication lifetime of non-neighboring nodes as follows:

$$T_{mh} = \min(T_{s_m}, T_K, T_{d_m}), \tag{8.35}$$

in which T_K is the lifetime of the last available route between a source and a destination node, which is obtained using (8.34) for $k = K$. Assuming $\epsilon_t > \epsilon_r$, we can show that

$$\min(T_{s_m}, T_{d_m}) = T_{s_m} = \frac{B}{\lambda(L\epsilon_t + (L_a + L)\epsilon_r) + f}.$$

Therefore, from (8.35) we conclude that

$$T_{mh} = \begin{cases} T_K, & \text{if } \frac{1-\rho^K}{1-\rho} < \frac{c_r}{c_{s_m}} \\ T_{s_m}, & \text{if } \frac{1-\rho^K}{1-\rho} > \frac{c_r}{c_{s_m}} \end{cases} \tag{8.36}$$

The fact that whether $\frac{1-\rho^K}{1-\rho} < \frac{c_r}{c_{s_m}}$ or $\frac{1-\rho^K}{1-\rho} > \frac{c_r}{c_{s_m}}$ depends on the value of K. Since nodes are distributed randomly, K could be a random variable for an arbitrary pair of source-destination nodes. Therefore, depending on the value of K, T_{mh} may take a value from the set $\{0, T_{s_m}, T_1, T_2, T_3, T_4, ...\}$. To determine the probability that T_{mh} takes one of these values, we first need to determine the minimum value of K which meets the inequality of $\frac{1-\rho^K}{1-\rho} > \frac{c_r}{c_{s_m}}$. Let this minimum value of K be denoted by K^*. Since $\frac{1-\rho^K}{1-\rho}$ is the summation of a geometric series with $K-1$ positive elements, if $\frac{1-\rho^K}{1-\rho} > \frac{c_r}{c_{s_m}}$ is true for $K = K^*$, it will be true for $K > K^*$ as well. Thus, we can state that

$$T_{mh} = \begin{cases} T_{s_m}, & \text{with } \Pr\{K \geq K^*\} \\ T_k, & \text{with } \Pr\{K = k\}, \; \forall k = 0...K^* - 1. \end{cases} \tag{8.37}$$

In (8.37), $\Pr\{K \geq K^*\}$ is the probability that there are at least K^* node-disjoint routes between the source and the destination, while $\Pr\{K = k\}$ is the probability that there are exactly k node-disjoint routes between them. Let us define

$$\sigma(k) = \Pr\{K \geq k\}. \tag{8.38}$$

Then, we have

$$\Pr\{K = k\} = \sigma(k) - \sigma(k+1). \tag{8.39}$$

Therefore, the expected value of T_{mh} is obtained as follows:

$$\bar{T}_{mh} = T_{s_m}\sigma(K^*) + \sum_{k=0}^{K^*-1} T_k\left[\sigma(k) - \sigma(k+1)\right]. \tag{8.40}$$

To find an expression for $\sigma(k)$, we define $\theta(k)$ as the probability that there are at least k node-disjoint routes between *every* two nodes in the network. Note that $\sigma(k)$ is the probability that there are at least k node-disjoint routes between two *arbitrary* nodes. The former event is stricter than the latter event. As a result, we have

$$\sigma(k) \geq \theta(k). \tag{8.41}$$

Considering (8.40) and the inequality in (8.41), we have shown in Appendix B that

$$\bar{T}_{mh} \geq T_{s_m}\theta(K^*) + \sum_{k=0}^{K^*-1} T_k\left[\theta(k) - \theta(k+1)\right]. \tag{8.42}$$

Since $\epsilon_t > \epsilon_r$, if we replace $\bar{T}_{mh}$ from (8.42) and $\bar{T}_{sh}$ from (8.26) in (8.24), we arrive at the following expression for the expected communication lifetime of two nodes:

$$
\begin{aligned}
\bar{T} \geq \frac{\pi D_{max}^2}{A} T_{s_s} + \\
\left(1 - \frac{\pi D_{max}^2}{A}\right)\left[T_{s_m}\theta(K^*) + \sum_{k=1}^{K^*-1} T_k\left[\theta(k) - \theta(k+1)\right]\right].
\end{aligned}
\tag{8.43}
$$

We can approximate $\theta(k)$ using the theory of connectivity of wireless ad-hoc networks. As mentioned in Chapter 2, if nodes in an ad-hoc network are uniformly distributed in a square area, $\theta(k)$ is approximated as follows [53]:

$$\theta(k) = \left(1 - e^{-\tau}\sum_{i=0}^{k-1} \frac{\tau^i}{i!}\right)^N,$$

where $\tau = N\pi D_{max}^2/A$. Here, N is the number of nodes, D_{max} is the transmission range, and A is the area of the square field.

Equation (8.43) is *our closed-form expression for the expected node-to-node communication lifetime in wireless multi-hop networks with random topology.* Although, (8.43) gives a lower bound, we show in the next section using simulation results that it is a very tight bound and could be considered as an approximate expression for the expected communication lifetime of two nodes.

8.8   Simulation Studies

In this section, we present simulation results to verify our analysis.

Table 8.1 – Default Values of Simulation Parameters

Parameter	Value
Initial battery energy of each node (B)	10 [J]
Source packet transmission rate (λ)	1 [packet/s]
Energy consumed for transmission of a single bit (ϵ_t)	160 [nJ/bit]
Energy consumed for reception of a single bit (ϵ_r)	85 [nJ]
Data packet size (L)	1088 [bit]
Acknowledgment packet size (L_a)	240 [bit]
Transmission range (D_{max})	70 [m]
Battery death threshold (B_{th})	0
Maximum transmission tries on each link (M)	7
Minimum delivery probability of data packets ($p_{d_{min}}$)	0.6
Minimum energy consumption rate g_{min}	$0.1\epsilon_t L$ [J/s]
Maximum energy consumption rate g_{max}	$2\epsilon_t L$ [J/s]

8.8.1 Simulation Setup

We distribute nodes uniformly in a square area of size $8D_{max} \times 8D_{max}$, where D_{max} is the transmission range of nodes. In our simulations, the quality of different links could be different from each other. The PDR of a link for data packets is chosen randomly from the interval $[p_{d_{min}}, 1]$. When MAC retransmission is supported, the PDR of acknowledgments is computed accordingly considering the ratio between the length of acknowledgments and data packets. We also assume that the idle-mode energy consumption rate of different nodes could be different. The idle-mode energy consumption rate of each node $g(u)$ is chosen randomly from the interval $[g_{min}, g_{max}]$ [J/s]. Note that in practice the PDR of links and the idle-mode energy consumption rate of nodes may not have a uniform distribution. We chose them randomly from a given interval only to ensure that different links have different qualities and different nodes have different idle-mode energy consumption rates.

Upon transmission (reception) of a packet of length L bits by a node, $\epsilon_t L$ ($\epsilon_r L$) [J] is deducted from its remaining battery energy. If the remaining battery energy of a node falls bellow a threshold B_{th}, the node is considered to be dead. When a node fails, we remove the failed links and update the network topology. To measure the communication lifetime of two specific nodes, we transmit packets from the source node to the destination node until the source, the destination, or the last available route between them fails. *Nevertheless, instead of measuring the time duration, we measure the communication lifetime in terms of the total number of data packets transmitted by the source before the communication between the source and the destination fails.*

Table 8.1 shows the default value of various parameters that we use in our simulations. Considering $\epsilon_t = 160$ [nJ/bit] and $\epsilon_r = 80$ [nJ/bit] in the table means that 0.174 [mJ] is consumed for transmission of a packet of size $L = 1088$ [bit] and 0.087 [mJ] is consumed for reception of the packet. Since we assumed $B = 10$, each node has enough energy to transmit 57471 packets or receive 114942 packets of length 1088 [bit]. Values of g_{min} and g_{max} in the table are chosen in such a way that the idle-mode energy consumption rate of each node is in the same order of the consumed energy for transmission of a data packet (i.e., $\epsilon_t L$). With the proliferation of energy-efficient networking protocols and low power devices (e.g., in wireless sensor networks), the idle-mode energy consumption of nodes could be a small value in practice.

8.8.2 Estimating Node-to-node Communication Lifetime using Numerical Algorithms

In this experiment, we generate a network randomly in each simulation run. Then, we choose a pair of nodes as source and destination randomly. The communication lifetime of these two nodes is determined using simulation. We also determine their communication lifetime using Algorithm 9 and its related procedures for networks with and without MAC retransmissions (i.e., Algorithm 10 and Algorithm 11, respectively). This procedure is repeated 1000 times to compute the average communication lifetime between two nodes in the network with a confidence level of 98%. The experiment is conducted separately for networks with and without MAC retransmissions.

8.8.2.1 Effect of the Number of Nodes

Figure 8.8 shows the average node-to-node communication lifetime as a function of the total number of nodes in the network. The figure shows that there is a good match between the simulation results and the results predicted by Algorithm 9 in both types of networks. We also observe that the communication lifetime of nodes increases as the number of nodes increases. The reason lies in the fact that when the number of nodes increases, the probability of communication failure between two nodes due to lack of routes decreases. In such a case, the communication lifetime of two nodes can reach its maximum value, which is the time that one of the two nodes fails. Comparison of Figure 8.8(a) with Figure 8.8(b) reveals that the average node-to-node communication lifetime in networks with MAC retransmissions is smaller than that of networks without MAC retransmissions. This is due to the fact that when MAC retransmission is supported, the energy consumption rate of nodes increases due to retransmissions of data and acknowledgment packets.
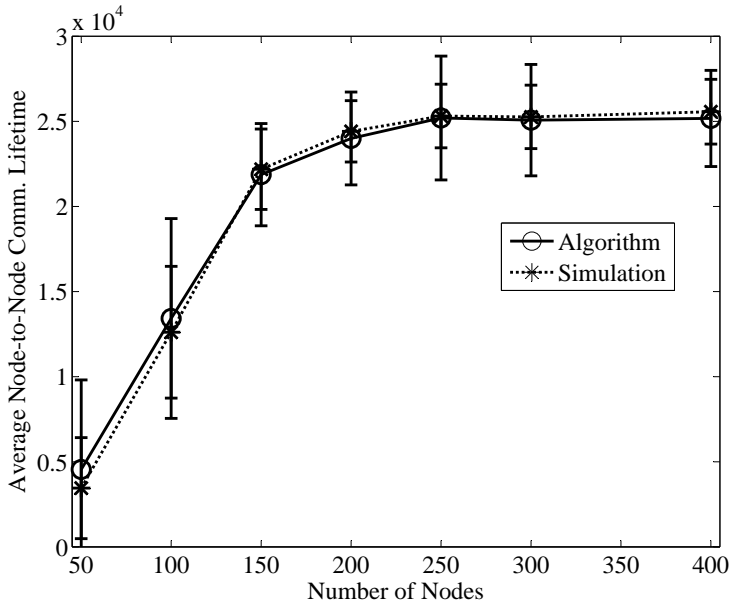
(a) Without MAC retransmission
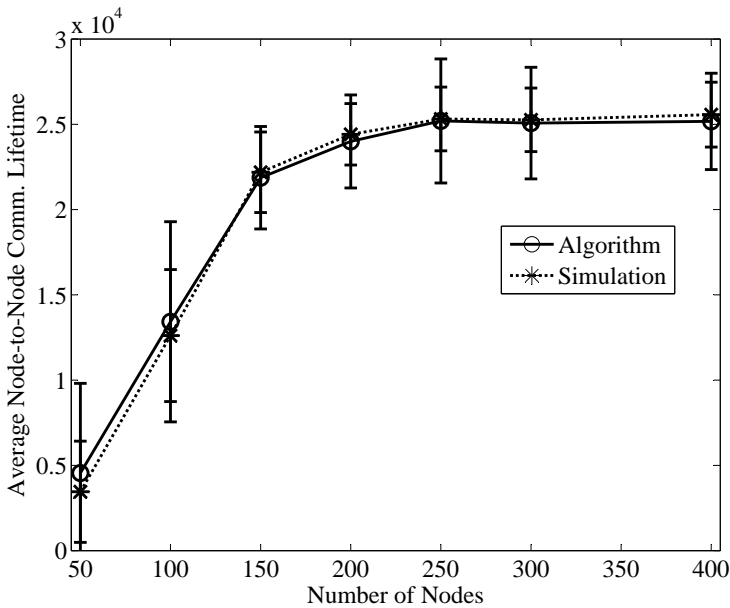
(b) With MAC retransmission

Figure 8.8 – Average node-to-node communication lifetime as predicted by Algorithm 9 and simulations for different number of nodes.

8.8.2.2   Effect of the Idle-mode Energy Consumption Rate of Nodes

In this experiment, we set g_{min} to $0.1\epsilon_t L$ and we increase the value of g_{max}. By increasing g_{max}, the idle-mode energy consumption rate of nodes increases on an average. We change g_{max} from $0.1\epsilon_t L$ to $10\epsilon_t L$. Here, $g_{max} = 0.1\epsilon_t L$ represents a situation in which the idle-mode energy consumption rate of nodes is much smaller than the energy consumed for transmission of a data packet. On the other hand, $g_{max} = 10\epsilon_t L$ represents a situation in which the idle-mode energy consumption rate of a node could be several times greater than the energy consumed for transmission of a data packet. This may happen, for instance, when many control packets are overheard by nodes or their energy is highly consumed for non-communication purposes (e.g, gaming on a laptop).

Figure 8.9 shows the average node-to-node communication lifetime for networks with and without MAC retransmissions as a function of the ratio of $\frac{g_{max}}{\epsilon_t L}$. As we expect, when $\frac{g_{max}}{\epsilon_t L}$ increases, the average node-to-node communication lifetime decreases, because the energy consumption rate of nodes increases on the average. When there are 300 nodes in the network and MAC retransmission is not supported, the average node-to-node communication lifetime drops from 21701 to 4178, if g_{max} changes from $0.1\epsilon_t L$ to $10\epsilon_t L$ (i.e., 80% decrease). In the network with MAC retransmissions, it drops by around 70%. When there are 100 (50) nodes, it drops 81% (85%) in networks without MAC retransmissions and 68% (67%) in networks with MAC retransmissions. This highlights the importance of minimizing the idle-mode energy consumption rate of nodes compared to the energy they consume for data communication in order to maximize the node-to-node communication lifetime.

8.8.3   Expected Node-to-node Communication Lifetime

In this section, we present results verifying the accuracy of the closed-form expression derived for the expected communication lifetime of nodes in (8.43). In each simulation run, we generate a network randomly, and choose two nodes randomly. Then we measure their communication lifetime using the simulation model. The expected value of the communication lifetime of nodes is computed by averaging over 1000 simulation runs. We also calculate the expected communication lifetime of nodes using the expression given in (8.43).

8.8.3.1   Accuracy of Analytical Results in the Ideal Case

We recall that the closed form expression in (8.43) derived under the assumption that $g(u) = g, \forall u \in \mathbb{V}$, and the PDR of each link is 1 (i.e., $p(u, v) = 1 \ \forall (u, v) \in \mathbb{E}$). Here, we first present results for this ideal case. Then, we study the accuracy of
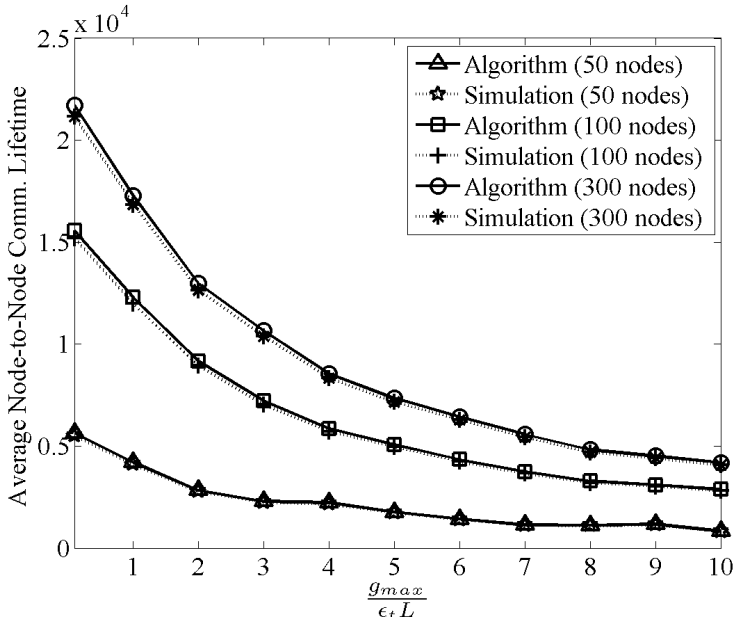
(a) Without MAC Retransmission
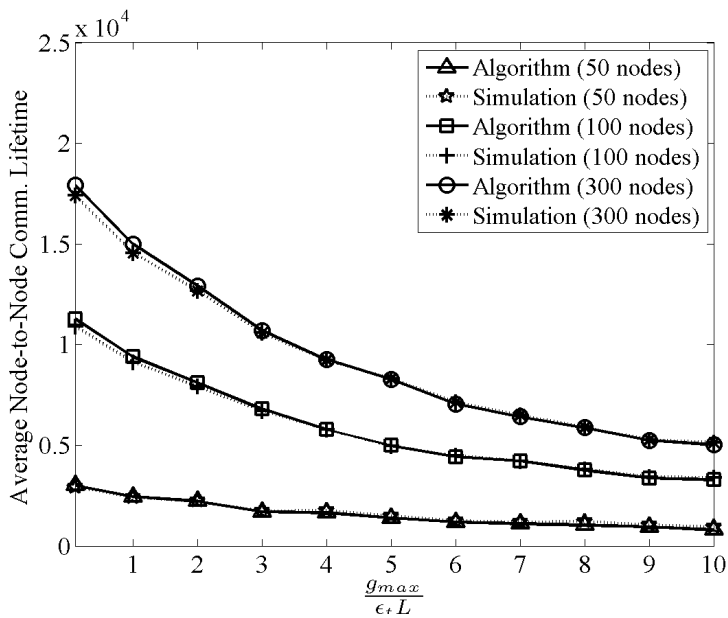
(b) With MAC Retransmission

Figure 8.9 – Average node-to-node communication lifetime as predicted by Algorithm 9 and the simulation results for different values of g_{max}.

(8.43) when we deviate from this ideal case. That is, when $g(u)$ is not the same for all nodes and the PDRs of various links are different.

Figure 8.10 shows the simulation and the analytical results for $g = \epsilon_t L$. Results have been shown for networks with and without MAC retransmissions separately. We observe a good match between simulation and analytical results in both types of networks. Analytical and simulation results follow the same trend when the number of nodes increases in the network. An important point is that the expression given in (8.43) for the expected node-to-node communication lifetime is in fact a lower bound. However, since the lower bound is relatively tight as shown in Figure 8.10, it could even be considered as an approximation for the expected node-to-node communication lifetime. That is, we can represent (8.43) as

$$
\begin{aligned}
\bar{T} \approx{} & \frac{\pi D_{max}^2}{A} T_{s_s} + \\
& \left(1 - \frac{\pi D_{max}^2}{A}\right) \left[T_{s_m} \theta(K^*) + \sum_{k=1}^{K^*-1} T_k \left[\theta(k) - \theta(k+1)\right] \right].
\end{aligned}
\tag{8.44}
$$

To study the accuracy of (8.44) when we deviate from the ideal case that it was derived for, we first assume $g(u)$ for all nodes is the same, but $p(u,v)$ can take different values for different links. Then, we assume $p(u,v)$ is the same for all links, but $g(u)$ can take different values for different nodes. Finally, we assume both $g(u)$ and $p(u,v)$ can take different values for different nodes and links.

8.8.3.2   Effect of the PDR of Links

Here, we set $g(u) = \epsilon_t L$, $\forall u \in \mathbb{V}$, and we choose the value of $p(u,v)$ for each link randomly from the interval $[p_{d_{min}}, 1]$. Note that if we decrease the value of $p_{d_{min}}$, the PDR of links decreases on the average. Furthermore, the PDRs vary more from one link to another link. In other words, as $p_{d_{min}}$ decreases, we deviate more from the ideal case of having the perfect quality for all links. As Figure 8.11 shows, there are different trends for the node-to-node communication lifetime in networks with and without MAC retransmissions. In networks without MAC retransmission, the analytical results become less accurate as $p_{d_{min}}$ decreases. This is true regardless of the number of nodes in the network. Furthermore, the node-to-node communication lifetime increases if the PDR of links decreases. The reason lies in the fact that nodes consume less energy for packet forwarding, because they receive less packets which they have to forward. This increased lifetime comes at the cost of having less packets delivered to their destinations. On the other hand, in networks with MAC retransmissions, the node-to-node communication lifetime decreases if the PDR of links decreases. When MAC retransmission is supported, nodes have to consume more energy to forward packets on low quality links, because they have to
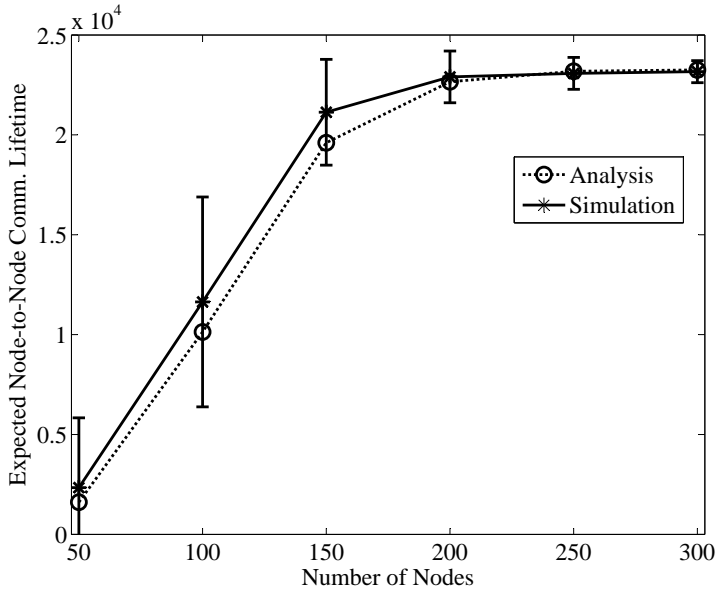
(a) Without MAC Retransmission
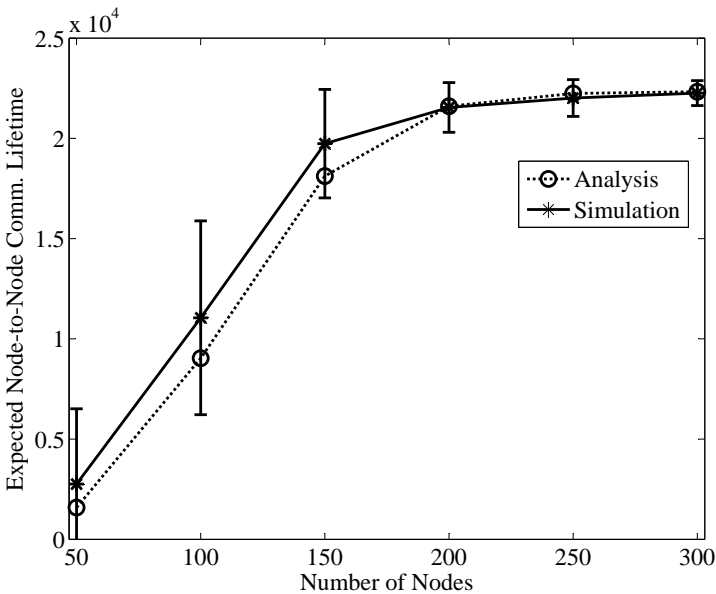
(b) With MAC Retransmission

Figure 8.10 – Analytical and simulation results for the expected node-to-node communication lifetime in terms of the total number of nodes in the network. The idle-mode energy consumption rate is the same for all nodes and the PDR is 1 for all links.

(a) Without MAC Retransmission

(b) With MAC Retransmission

Figure 8.11 – The impact of the PDR of links on the analytical and simulation values of the expected node-to-node communication lifetime in the network.

retransmit the same packet more times. Moreover, the accuracy of the analytical results might even become better if $p_{d_{min}}$ decreases. This, however, depends on the number of nodes in the network. For $N = 100$, the most accurate results belong to the case of $p_{d_{min}} = 0.6$. For $N = 150$, this happens at $p_{d_{min}} = 0.7$. For $N = 200$, it happens at $p_{d_{min}} = 1$.

8.8.3.3   Effect of the Idle-mode Energy Consumption Rate of Nodes

Here, we set $p(u, v) = 1$ for all links and we choose $g(u)$ for each node randomly from the interval $[g_{min}, g_{max}]$. We fix g_{min} to $\epsilon_t L$ and change g_{max} from $\epsilon_t L$ to $19\epsilon_t L$. Recall that (8.44) was derived assuming $g(u)$ is the same for all nodes. However, in this experiment $g(u)$ is different for different nodes. The question is, if we want to use (8.44) when $g(u)$ is not the same for all the nodes, what should be the value of g in the expressions given for c_{s_s}, c_{d_s}, c_{s_m}, c_{d_m}, and c_r in Section 8.7? One may say that since $g(u)$ is assumed to have a uniform distribution between g_{min} and g_{max}, we might be able to derive another expression for the expected node-to-node communication lifetime assuming $g(u)$ is uniformly distributed. This, however, may not be useful in practice, because $g(u)$ may not have a uniform distribution in practice. We only made this assumption for the sake of simulations. Furthermore, even if we use a realistic distribution for $g(u)$ in the network, it would depend on many factors such as the wireless technology and the routing and MAC protocols. This harms our generic analysis.

To resolve the problem, we *conjecture* that if we replace g with the average idle-mode energy consumption rate of all nodes, we still might be able to use (8.44) as an approximation for the expected node-to-node communication lifetime. That is, we assume $g = \frac{1}{N} \sum_{\forall u \in \mathbb{V}} g(u)$. With this assumption, we have plotted simulation and analytical values of the lifetime in Figure 8.12 as a function of g_{max}. Figure 8.12(a) and Figure 8.12(b) show that even if the value of $g(u)$ varies from one node to another node, (8.44) is still accurate enough. The accuracy of the analytical results increases as the number of nodes increases in the network.

8.8.3.4   Joint Effect of the PDR of Links and the Idle-mode Energy Consumption Rate of Nodes

Here, we choose $p(u, v)$ for each link randomly from the interval $[0.6, 1]$, and $g(u)$ for each node randomly from the interval $[0.1\epsilon_t L, 2\epsilon_t L]$. Figure 8.13(a) and Figure 8.13(b) show the simulation and the analytical results as a function of the number of nodes in network. The figures show that even if we deviate from the ideal case that (8.44) was derived for, this expression is able to follow the increasing trend of the expected node-to-node communication lifetime as the number of nodes increases. More specifically, when MAC retransmission is not supported, analytical results
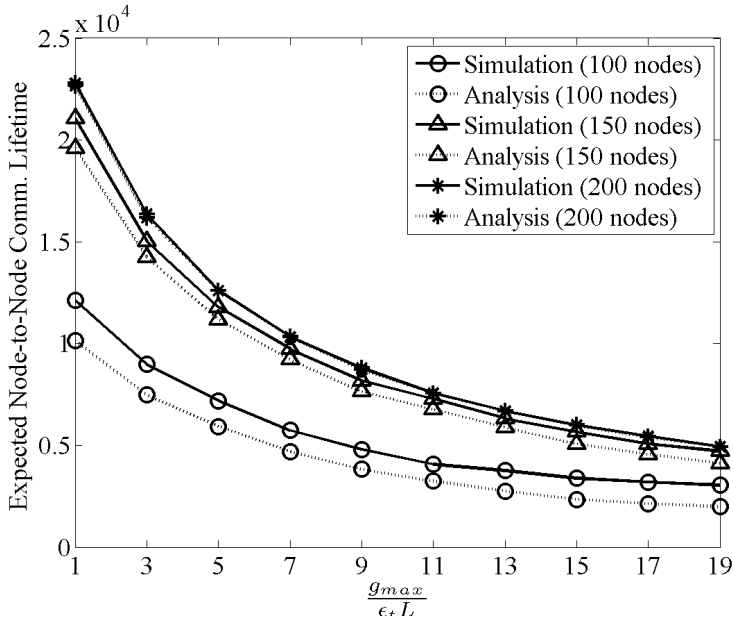
(a) Without MAC Retransmission
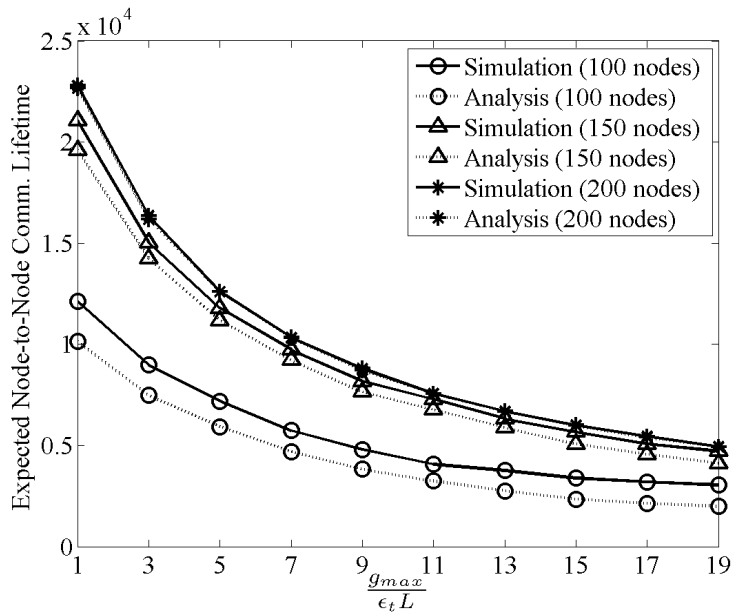
(b) With MAC Retransmission

Figure 8.12 – The impact of the idle-mode energy consumption of nodes on analytical and simulation values of the expected node-to-node communication lifetime in the network.
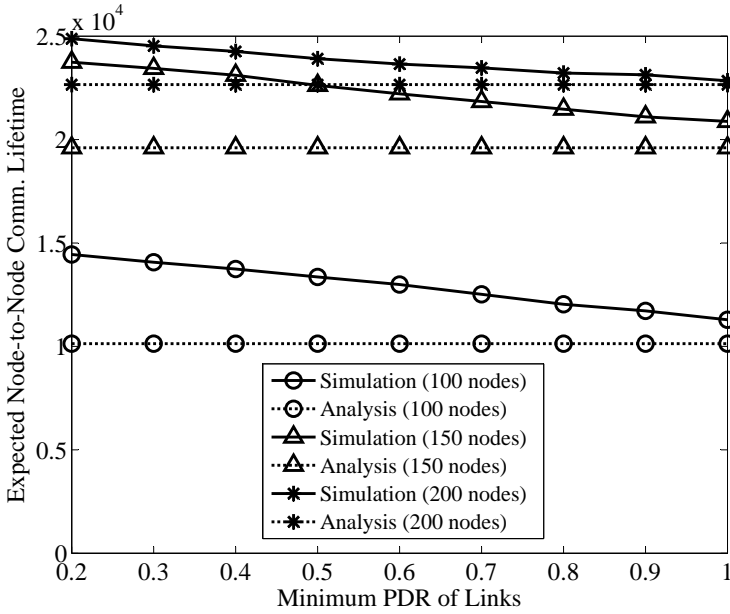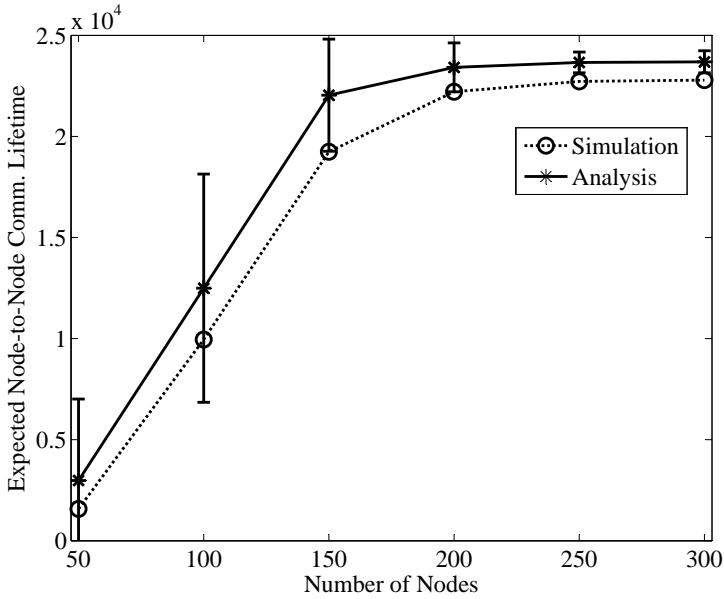
(a) Without MAC Retransmission
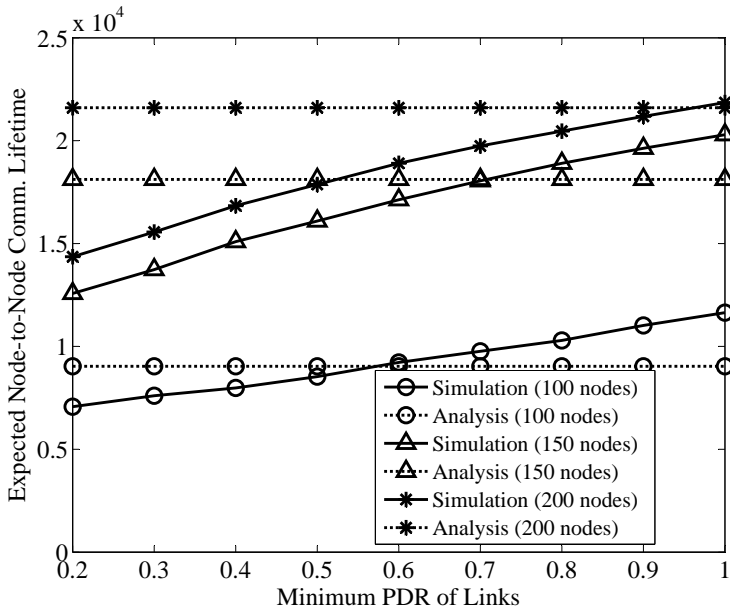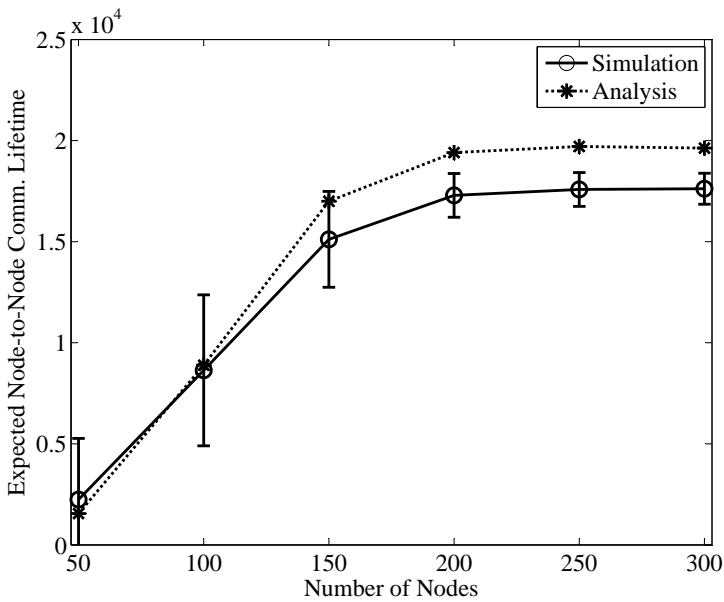

(b) With MAC Retransmission

Figure 8.13 – Analytical and simulations results for the expected node-to-node communication lifetime. The idle-mode energy consumption rate is different for different nodes and the PDR is different for different links.

are of higher accuracy at higher numbers of nodes. When MAC retransmission is supported, analytical results are of higher accuracy at lower numbers of nodes.

8.8.4 Lifetime of Node-to-node Communication for Concurrent Connections

So far, we studied the node-to-node communication lifetime when there is no concurrent communication in the network. We made this assumption in order to find the maximum node-to-node communication lifetime. In this section, we examine the node-to-node communication lifetime when there are concurrent communications between different pairs of source-destination nodes. To this aim, at network start up, we establish several connections between different pairs of source-destination nodes which are chosen randomly. Packets are transmitted between each pair of nodes until their connection fails due to battery exhaustion of the source or the destination or due to lack of alternative routes between them. We repeat this experiment for $n \in \{1, 2, 3, 4, 8, 12, 20, 40, 80\}$ concurrent connections and for $N \in \{50, 100, 150, 200, 250\}$ nodes in the network. For each pair of values (n, N), the average value of the lifetime of all the established connections during 700 simulation runs is recorded as the average node-to-node communication lifetime.

Results in Figure 8.14 show that when the number of connections increases, the average node-to-node communication lifetime converges to a constant value for each value of the number of nodes. These constant values for different values of N seem to be close to each other. Figure 8.14 also shows that with increasing number of nodes, the node-to-node communication lifetime decreases faster. Let us explain the reason behind this behavior. Since the network area is fixed in this experiment, the average node degree increases if the number of nodes increases. This, in turn, improves network connectivity [53]. If the number of connections increases in a network with a higher degree of connectivity, the energy consumption rate of nodes increases more. The reason lies in the fact that intermediate nodes in node-disjoint routes between a pair of source-destination nodes overhear more packets belonging to different connections. On the other hand, at lower densities, the probability that a node overhears packets belonging to different connections decreases. This also explains why the slope of the average communication lifetime is lower at lower densities.

8.8.5 Bounds on the Lifetime of Node-disjoint Routes

In this section, we verify the accuracy of the upper and lower bounds of the lifetime of node-disjoint routes. We set the number of nodes in the network to 500 at which we observed that the network is likely to be 3-connected. We chose two nodes randomly in a randomly generated network. The time at which the first
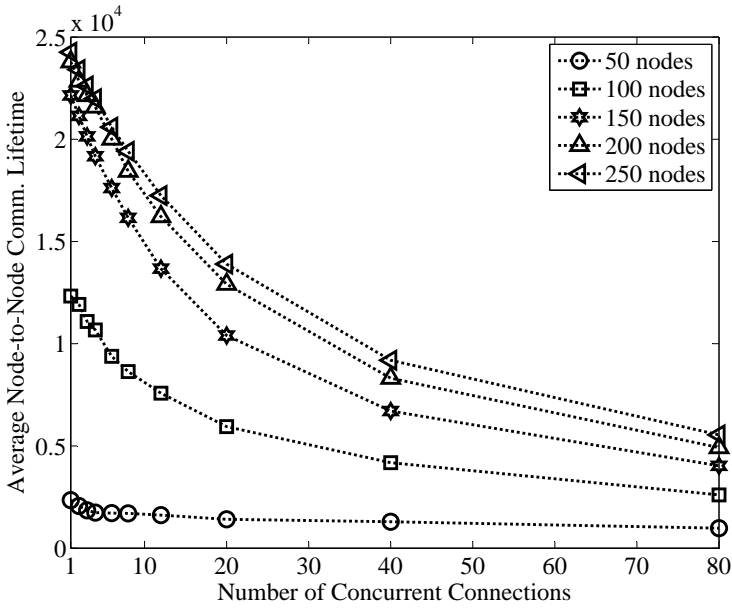
(a) Without MAC Retransmission
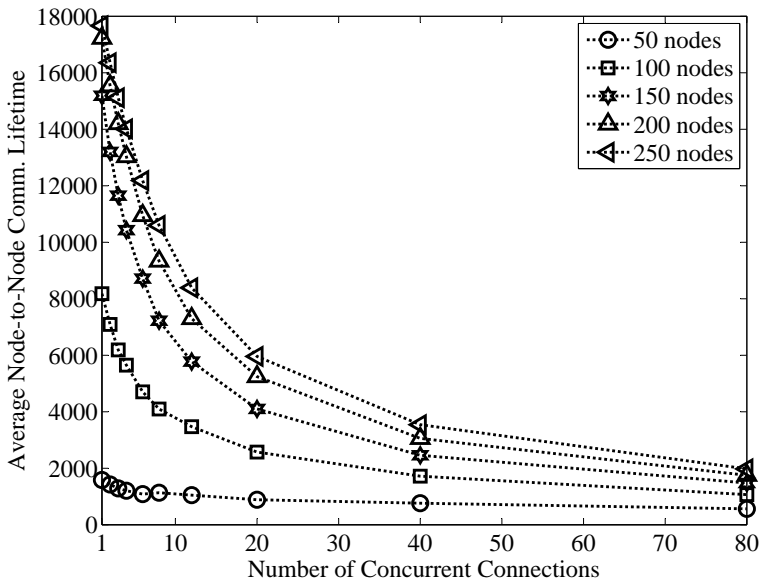
(b) With MAC Retransmission

Figure 8.14 – Average node-to-node communication lifetime in networks with and without MAC retransmissions when there are concurrent connections in the network.

route between the selected nodes fails is recorded as the lifetime of the first route. After failure of the first route, the second route is used which is disjoint from the first route. Similarly, the time at which the second route fails is recorded as its lifetime and similarly for the third route. To guarantee that the source and the destination do not fail before routes, we set their initial battery energy to infinity. This procedure is repeated for 1000 source-destination pairs of nodes to measure the lifetime of the first, the second, and the third node-disjoint route between them.

We also computed the lower and the upper bounds using the expressions derived for them in Section 8.6. Results are shown in Figure 8.15 for networks without MAC retransmissions and Figure 8.16 for networks with MAC retransmissions. The obtained value for each pair of nodes is shown by a dot in each figure (1000 dots for each point of the horizontal axis). We have plotted the route lifetime as a function of the ratio between the energy consumed by the wireless interface to transmit a single bit to the energy consumed to receive a single bit, i.e., $\frac{\epsilon_t}{\epsilon_r}$. The figures show that the derived bounds can accurately bind various values obtained for the lifetime of the first node-disjoint route between different pairs of source-destination nodes in both types of network (with and without MAC retransmission). For the second and third routes, the lower bound is still accurate in both types of networks. The upper bound, however, is not very accurate when $\frac{\epsilon_t}{\epsilon_r}$ is low. Nevertheless, as $\frac{\epsilon_t}{\epsilon_r}$ increases, the upper bounds become accurate as well.

8.9 Summary

In this chapter, the lifetime of node-to-node communication was analyzed in static wireless multi-hop networks. The analysis was provided for two types of multi-hop networks: networks which support MAC retransmissions to recover lost packets, and networks which do not support MAC retransmissions. We observed that MAC retransmission reduces the node-to-node communication lifetime. Numerical algorithms were presented for predicting the maximum duration that two nodes can still communicate with each other at a given moment. We also derived a closed-form expression for the expected value of the maximum node-to-node communication lifetime in static wireless multi-hop networks with random topology. Upper and lower bounds on the lifetime of node-disjoint routes between two arbitrary nodes in networks with random topology were derived. Extensive simulation studies were used to verify the accuracy of the analysis.

(a) 1st Route

(b) 2nd Route

(c) 3rd Route
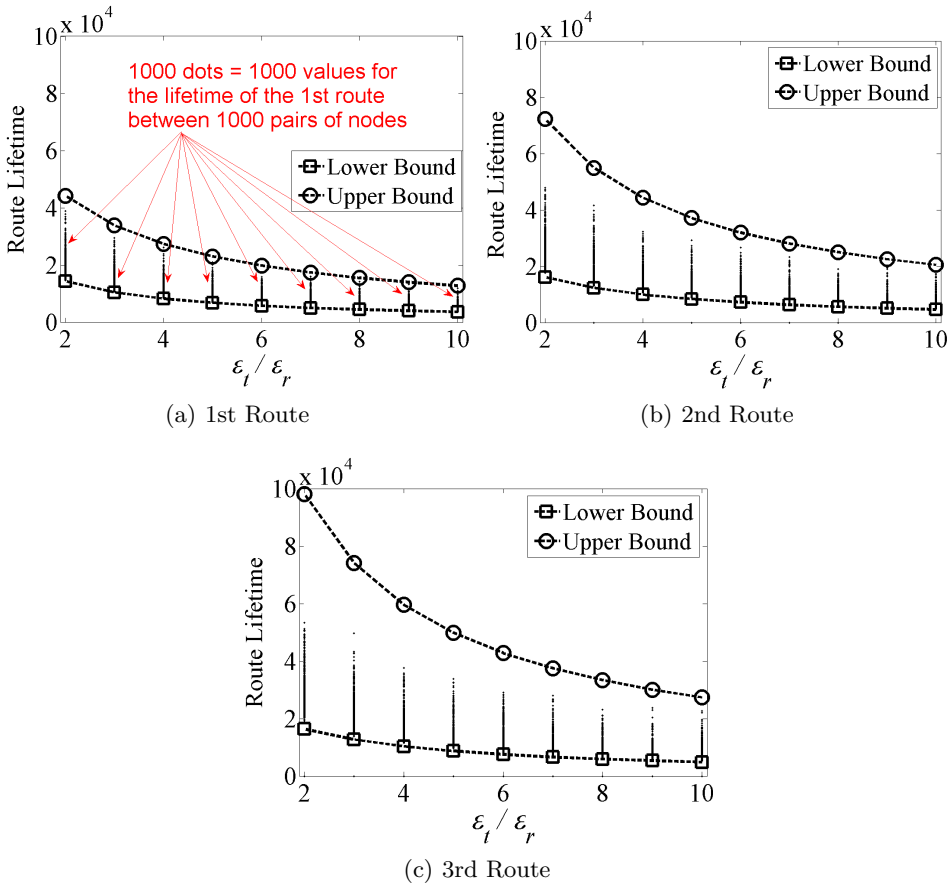
Figure 8.15 – Upper and lower bound of the lifetime of the first, the second, and the third node-disjoint routes between a pair of source-destination nodes in networks without MAC retransmissions. Each dot between the two lines is a value obtained for one pair of source-destination nodes. In this experiment, $g(u)$ for each node is chosen randomly from the interval $[0.1\epsilon_t L_d, 2\epsilon_t L_d]$.

(a) 1st Route

(b) 2nd Route

(c) 3rd Route
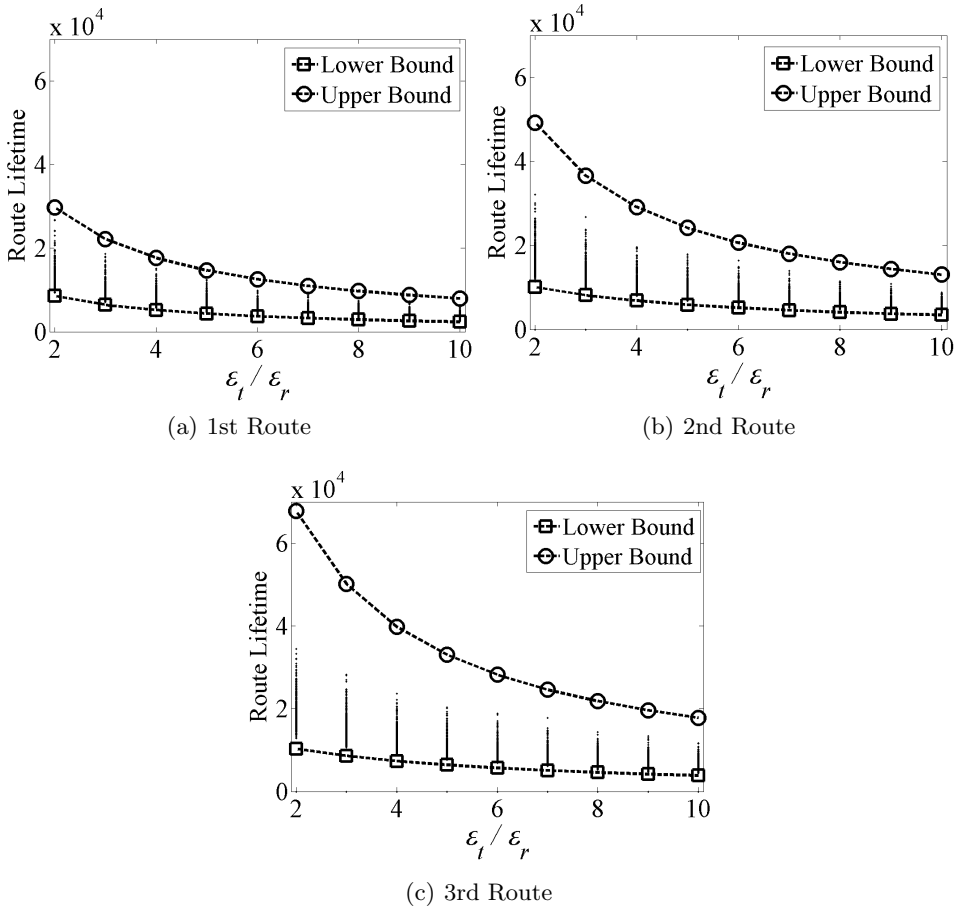
Figure 8.16 – Upper and lower bound of the lifetime of the first, the second, and the third node-disjoint routes between a pair of source-destination nodes in networks with MAC retransmissions. Each dot between the two lines is a value obtained for one pair of source-destination nodes. In this experiment, $g(u)$ for each node is chosen randomly from the interval $[0.1\epsilon_t L_d, 2\epsilon_t L_d]$.

Chapter 9

Cooperative Signal Transmission Techniques

So far in this dissertation, we have studied the design of energy-efficient techniques for routing and topology construction in wireless multi-hop networks. We also analyzed the duration that nodes can stay connected to each other in these networks. Our study has covered MAC, network (routing), and transport layers of the communication stack. We observed that the proposed mechanisms for these layers can substantially reduce the energy consumption of nodes for communicating with each other. Nevertheless, we can still reduce the energy consumption of nodes in wireless multi-hop networks by bringing energy-efficiency into the physical layer of the communication stack. In this chapter, we study a novel technique for reducing the transmission power of nodes for reliable wireless signal transmission[1]. This technique is called *cooperative signal transmission (CST)*, in which nodes cooperate with each other to transmit signals to their respective receiving nodes. We address CST in single-antenna and multi-antenna wireless networks. Our novelty in this chapter is two-fold: 1) we propose a multi-antenna CST system based on block space-time codes and we analyze its performance. 2) We propose a multi-hop CST system, and we analyze it performance.

The rest of this chapter is organized as follows: we first provide the background on CST in Section 9.1. Then, the multi-antenna cooperative system is presented in Section 9.2, and the multi-hop cooperative system is presented in Section 9.3. We summarize the chapter in Section 9.4.

---

[1]Another possible way for bringing the energy-efficiency into the physical layer is to design very low power circuits to reduce the energy consumption of processing elements of transceivers during packet transmission and reception. This research line, however, is beyond the scope of this thesis.
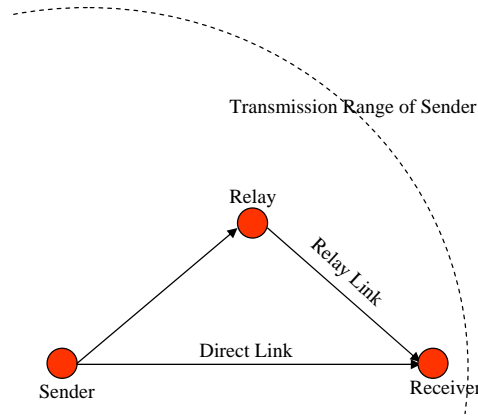
Figure 9.1 – A simple schematic of a CST system with one relaying node.

9.1   Background

An inherent characteristic of wireless networks is that signals are propagated over a shared medium. Thus, neighboring nodes of a transmitting node can overhear transmitted signals over the shared medium. This provides an opportunity to create diversity gain by retransmission of the overheard signals by the neighbors, and combining the retransmitted signals with the original signal at the receiving node. A receiving node receives signals not only directly from the transmitting node but also indirectly from its common neighbors with the transmitting node (referred to as relay nodes). An example is shown in Figure 9.1, where one relay node which is a common neighbor of the transmitting node (the sender) and the receiving node (the receiver) forwards the overheard signals from the sender. To detect information originally transmitted by the sender, the receiver combines signals received through the direct link with those received through the relay link(s) A Maximal Ratio Combiner (Rake Receiver) [50] could be used to combine these signals in such a way that the detection error is minimized at the receiver. A degree of transmission diversity is created in this way, which can reduce the symbol error rate (SER) at the receiver. Compared to other types of diversity in communication networks such as time diversity and spatial diversity, the diversity in the CST systems is called *cooperative diversity* [144–146]. However, the sender and the relay nodes need to use orthogonal channels (e.g., using different time slots in a TDMA-based MAC) in order to achieve the cooperative diversity. In such a case, the maximum diversity order equal to the number of transmitted and retransmitted signals can be achieved [144]. An important goal in the design of a CST system is to achieve the maximum diversity gain through cooperation between wireless nodes.

CST systems were proposed and studied for the first time in [144–146]. Sandonaris et al. [145, 146] studied the capacity gain of a CST system consisting of two senders cooperating with each other to transmit their signals to their respective receivers. In another perspective, Laneman et al. [144] proposed two types of CST systems, namely amplify-and-forward (AF) and detect-and-forward (DF) systems. They analyzed the outage probability in these two CST systems, i.e., the probability that the received instantaneous SNR is below a threshold. Laneman's work is considered as fundamental in this area.

In an AF system, the relay node amplifies the signals received from the sender. Thus, retransmitted signals by the relay are a faded and noisy version of the original signals of the sender. On the other hand, in a DF system, the relay node detects signals transmitted by the sender. The detected signals are modulated again and retransmitted to the receiver via a different channel. Since the retransmitted signals in a DF system are subjected to a decision error in the relay node, a DF system may not provide a cooperative diversity gain [144]. AF systems, on the other hand, can achieve a diversity gain, because relaying nodes retransmit an amplified version of the signals. Ribeiro et al. [147] have shown that at high SNRs the symbol error rate (SER) at the receiver in a single antenna AF system with Q relaying nodes is approximated as

$$SER_{AF} \approx \frac{\prod_{i=1}^{Q+1} 2i - 1}{2k_{mod}^{Q+1}(Q+1)!} \frac{1}{\bar{\gamma}_{sd}} \prod_{i=1}^{Q} \frac{1}{\bar{\gamma}_{s_i}} + \frac{1}{\bar{\gamma}_{d_i}} \tag{9.1}$$

in which $\bar{\gamma}_{sd}$ is the average received SNR in the direct channel between the sender and the receiver. Furthermore, $\bar{\gamma}_{s_i}$ is the average received SNR in the wireless channel between the sender and the ith relay, and $\bar{\gamma}_{d_i}$ is the average received SNR in the wireless channel between the ith relay and the receiver. Parameter k_{mod} is a constant which depends on the modulation scheme (e.g., $k_{mod} = 2$ for BPSK).

The question that arises here is how CST could provide energy-efficiency in wireless networks. The key point is, since CST reduces the transmission error probability at the receiver (due to diversity gain), the sender can transmit signals with a lower transmission power while the same target BER requirement is satisfied. However, since relay nodes also consume energy for retransmission of signals, one may think that the overall energy consumption in the CST system may even be higher compared to a system without CST. In several studies [144, 145, 147], it has been shown that this is not true. Cooperation between the sender and the relay nodes can reduce the overall energy consumption for signal transmission to the receiver. To give some insight into this issue, we have plotted the SER of several single-antenna transmission systems in Figure 9.2. AF systems with 1, 2, and 3 relays have been compared to a DF system with 1 relay and a system without cooperation. To have a fair comparison between various systems, the
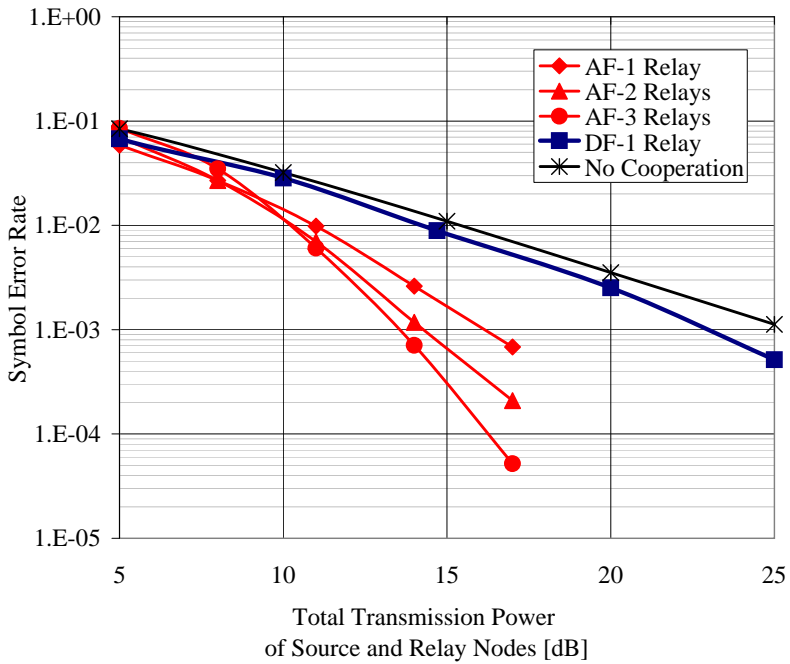
Figure 9.2 – Symbol error rate of several single-antenna transmission systems as a function of the total transmission power of the transmitting nodes. The wireless channel is assumed to be slowly flat Rayleigh, and the modulation scheme is BPSK. The channel power and the noise power are normalized to one.

total transmission power of transmitting nodes in various systems is kept the same. The figure shows that CST systems (both AF and DF systems) outperform signal transmission without cooperation, and the AF systems outperform the DF system. Furthermore, increasing the number of relays in the AF system increases the energy-efficiency of the system in terms of the required power of nodes for reliable signal transmission to the receiver.

9.2 Multi-antenna Cooperative Systems

If nodes are equipped with multiple antennas, a cooperative strategy could improve the performance of the communication system by providing additional diversity gain. The question we answer in this section is how to design an efficient CST system when nodes are equipped with multiple transmitting and receiving antennas. Such a system is called a *multi-antenna CST* system. Here, we present a generalized multi-antenna CST system, and analyze its performance. In this system, the sender, the receiver, and each relay node can have multiple antennas. Nodes use orthogonal space-time block codes (OSTBCs) to code symbols transmitted over their multiple antennas. Space-time block codes are effective channel codes for signal transmission in multi-antenna systems [148–150].

9.2.1 Space-Time Coding and Decoding

In OSTBCs, modulated symbols are transmitted block-by-block. Each block of transmitted symbols is represented by a matrix known as *code matrix*. Every transmitted space-time code matrix in node u is a matrix of size $N_u \times T_u$, [148], where T_u is the number of the required time slots for transmission of the elements of the code matrix over N_u transmitting antennas. The particular OSTBC designed for the system determines the way a code matrix is generated from the original information symbols, and the way the coded symbols are transmitted over multiple antennas. Variants of OSTBCs have been proposed in the literature. A simple and early-proposal of these codes is the Alamouti code [151] which has been designed for two transmitting antennas. If two information symbols s_1 and s_2 are about to be transmitted by the node, the code matrix in the Alamouti code is as follows:

$$\begin{pmatrix} s_1 & s_2 \\ -s_2^* & -s_1^* \end{pmatrix}$$

where, x^* is the complex conjugate of x. In the Alamouti code, elements of the first row of the matrix code are transmitted over the two antennas in the first time-slot. Elements of the second row are transmitted in the second time-slot. Here, s_1 and s_2 are symbols generated by a digital modulation such as BPSK.

An important criterion in the design of block space time codes is the efficiency of these codes. The efficiency of a code is determined by the number of information symbols transmitted during the time slots required for transmitting elements of a code matrix. In this regard, we observe that the efficiency of the Alamouti code is one, because two information symbols are transmitted in two time slots[1].

In general, for transmission of a block of W modulated symbols (henceforth information symbols) from u to v (u and v are neighbors), they are divided into $\mathcal{M}_u = W/\mathcal{K}_u$ vectors of information symbols of length $\mathcal{K}_u$, where $\mathcal{K}_u$ is the number of information symbols per code matrix. Each vector of information symbols is represented by $\mathbf{s}_u^{(m)}$, $m = 1...\mathcal{M}_u$, and its kth element is shown by $s_u^{(m,k)}$, $k = 1...\mathcal{K}_u$. The generated code matrix corresponding to the information vector $\mathbf{s}_u^{(m)}$ is denoted by $\mathbf{S}_u^{(m)}$. Under the assumption of having a flat fading wireless channel, after transmission of elements of $\mathbf{S}_u^{(m)}$ from u, v receives $\mathbf{U}_{uv}^{(m)}$ as follows:

$$\mathbf{U}_{uv}^{(m)} = \mathbf{H}_{uv}^{(m)}\mathbf{S}_u^{(m)} + \mathbf{Z}_{uv}^{(m)}, \qquad m = 1...\mathcal{M}_u, \tag{9.2}$$

where $\mathbf{U}_{uv}^{(m)}$ is a complex valued matrix of size $N_v \times T_u$, and its (i,j) element is received by the ith antenna of node v at the jth time slot. Here, $\mathbf{H}_{uv}^{(m)}$ is the channel coefficient matrix of the (u,v) link for the mth transmitted code matrix. The (i,j) elements of $\mathbf{H}_{uv}^{(m)}$ represents the channel coefficient between the ith antenna of u and the jth antenna of v. These elements are i.i.d. complex Gaussian random variables with variance Ω_{uv}. Since the channel is flat, these coefficients, which are assumed to be known at the receiver, remain fixed during transmission of one code matrix, but may vary independently from one code matrix to another. In (9.2), $\mathbf{Z}_{uv}^{(m)}$ is the noise matrix whose elements are also assumed to be i.i.d. zero mean complex Gaussian random variables with variance $\mathcal{N}$.

The information symbols of the code matrix $\mathbf{S}_u^{(m)}$ can be detected separately after linear processing of the elements of $\mathbf{U}_{uv}^{(m)}$ [148]. The details of the decoding procedure and the linear processing procedure can be found in [149]. Following the outlined method in [149], we can show that by linear processing of the elements of $\mathbf{U}_{uv}^{(m)}$, $\mathcal{K}_u$ decision statistics are generated, each of which is a noisy version of just one information symbol. The decision statistics for detecting $s_u^{(m,k)}$ is obtained as follows:

$$\tilde{u}_{uv}^{(m,k)} = \|\mathbf{H}_{uv}^{(m)}\|_F^2 s_u^{(m,k)} + \tilde{w}_{uv}^{(m,k)}, \qquad m = 1...\mathcal{M}_u \, k = 1...\mathcal{K}_u, \tag{9.3}$$

where $\|\mathbf{H}_{uv}^{(m)}\|_F^2$ is the square Frobenius norm of $\mathbf{H}_{uv}^{(m)}$ and $\tilde{w}_{uv}^{(m,k)}$ is a white zero mean Gaussian noise sample with variance $\|\mathbf{H}_{uv}^{(m)}\|_F^2 \mathcal{N}$. Using these decision statistics, we can detect each transmitted symbol separately using a maximum likelihood detector [50].

---

[1] Interested readers are referred to [149, 150] to see other variants of OSTBCs designed for more complex multi-antenna systems.
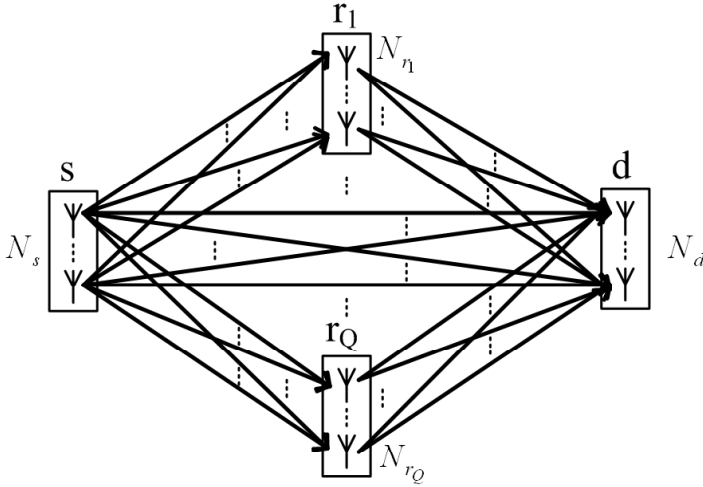
Figure 9.3 – A schematic model of a multi-antenna CTS system.

9.2.2 Signal Transmission in the Multi-antenna Cooperative System

The strong point of the MIMO (multi-input multi-output) cooperative system that we propose is that it is a generalized system. There could be an arbitrary number of relay nodes each of which have an arbitrary number of antennas. The sender and the receiver have also an arbitrary number of antennas. Nodes use OSTBCs for information transmission over their multiple antennas. We also propose a new model of cooperation in MIMO systems called *process-and-forward (PF)*. In this mode, the retransmitted signals from the relay nodes are obtained by linear processing of the received space-time coded signals from the sender and not by just amplifying these signals or detecting them. In the sequel, we explain how relay nodes construct forwarded signals, and how the receiver combines signals received from the sender and the relay nodes.

Figure 9.3 shows a generic model of the multi-antenna cooperative system in which Q relay nodes are present. Sender, receiver and relay nodes are denoted as s, d, r_q, $q = 1...Q$, respectively, and N_p, $p \in \{s, r_1, ..., r_Q, d\}$, represents the number of antennas of the corresponding node. In this system, the sender transmits a block of W information symbols to the receiver and each of the relay nodes (in the same way as described in the previous subsection). The number of corresponding code matrices generated at the sender is $\mathcal{M}_s = W/\mathcal{K}_s$, where $\mathcal{K}_s$ is the number of information symbols per code matrix of the sender (we assume that W is an integer multiple of $\mathcal{K}_s$.) Upon transmission of a generated code matrix from the sender,

Table 9.1 – Received signals and the generated decision statistics at relays and the receiver.

Received Signals	Generated Decision Statistics
$\mathbf{U}_{sd}^{(m)} = \mathbf{H}_{sd}^{(m)}\mathbf{S}_s^{(m)} + \mathbf{Z}_{sd}^{(m)}$, $m = 1...\mathcal{M}_s$	$\tilde{u}_{sd}^{(m,k)} = \|\mathbf{H}_{sd}^{(m)}\|_F^2 s_s^{(m,k)} + \tilde{w}_{sd}^{(m,k)}$ $k = 1...\mathcal{K}_s$
$\mathbf{U}_{sr_q}^{(m)} = \mathbf{H}_{sr_q}^{(m)}\mathbf{S}_s^{(m)} + \mathbf{Z}_{sr_q}^{(m)}$, $m = 1...\mathcal{M}_s$	$\tilde{u}_{sr_q}^{(m,k)} = \|\mathbf{H}_{sr_q}^{(m)}\|_F^2 \, s_s^{(m,k)} + \tilde{w}_{sr_q}^{(m,k)}$ $k = 1...\mathcal{K}_s$
$\mathbf{U}_{r_q d}^{(l_q)} = \mathbf{H}_{r_q d}^{(l_q)}\mathbf{S}_{r_q}^{(l_q)} + \mathbf{Z}_{r_q d}^{(l_q)}$, $l_q = 1...\mathcal{M}_{r_q}$	$\tilde{u}_{r_q d}^{(l_q,t_q)} = \|\mathbf{H}_{r_q d}^{(l_q)}\|_F^2 \zeta_{r_q}^{(i)} \tilde{u}_{sr_q}^{(i,j)} + \tilde{w}_{r_q d}^{(l_q,t_q)}$, $t_q = 1...\mathcal{K}_{r_q}$

denoted by $\mathbf{S}_s^{(m)}$, $m = 1...\mathcal{M}_s$, the receiver receives $\mathbf{U}_{sd}^{(m)}$, and the relay node r_q receives $\mathbf{U}_{sr_q}^{(m)}$ as shown in Table 9.1. After the so-called linear processing of the elements of $\mathbf{U}_{sd}^{(m)}$, the receiver generates $\mathcal{K}_s$ decision statistics. They are denoted a $\tilde{u}_{sd}^{(m,k)}$ in Table 9.1. Similarly, the relay node r_q generates $\mathcal{K}_s$ decision statistics after the linear processing of the elements of $\mathbf{U}_{sr_q}^{(m)}$ which are represented by $\tilde{u}_{sr_q}^{(m,k)}$ in the table.

When all $\mathcal{M}_s$ code matrices are transmitted from the sender, the receiver and each of the relay nodes generate $\mathcal{M}_s \times \mathcal{K}_s = W$ decision statistics. Each of these decision statistics is a noisy version of one of the originally transmitted symbols from the sender. The receiver retains these decision statistics until it receives the retransmitted information from the relay nodes. Each relay nodes transmits its W generated samples to the receiver in the next phase after encoding them using an OSTBC designed for its number of antennas. But before encoding, each decision statistics is multiplied by an appropriate coefficient. This coefficient is used to equalize the power of the noisy sample with the average transmission power of the sender (denoted by P_s). In fact, the statistics $\tilde{u}_{sr_q}^{(m,k)}$ is multiplied by the coefficient

$$\zeta_{r_q}^{(m)} = \sqrt{\frac{P_s}{\|\mathbf{H}_{sr_q}^{(m)}\|_F^2 \left(\|\mathbf{H}_{sr_q}^{(m)}\|_F^2 P_s + \mathcal{N}\right)}}. \tag{9.4}$$

As a result, the set of samples which are transmitted from r_q to d is specified by $S_{r_q} = \{\{\zeta_{r_q}^{(m)} \tilde{u}_{sr_q}^{(m,k)}\}_{k=1}^{\mathcal{K}_s}\}_{m=1}^{\mathcal{M}_s}$. The members of S_{r_q} act as information symbols for r_q. They are encoded by $\mathcal{M}_{r_q} = W/\mathcal{K}_{r_q}$ code matrices where $\mathcal{K}_{r_q}$ is the number of information symbols per code matrix generated by r_q. We assume that W is also an integer multiple of $\mathcal{K}_{r_q}$. The relay nodes transmit the generated code matrices to the receiver through orthogonal channels. After transmission of the l_qth code matrix from r_q, denoted by $\mathbf{S}_{r_q}^{(l_q)}$, $l_q = 1...\mathcal{M}_{r_q}$, the receiver receives $\mathbf{U}_{r_q d}^{(l_q)}$ as shown

in Table 9.1 and generates $\mathcal{K}_{r_q}$ decision statistics denoted by $\tilde{u}_{r_q d}^{(l_q, t_q)}$ in the table, each of which is actually a noisy version of one member of S_{r_q}. The mapping between pairs (i, j) and (l_q, t_q) in the expression given for $\tilde{u}_{r_q d}^{(l_q, t_q)}$ in the table is specified by $i = \lceil \frac{(l_q - 1)\mathcal{K}_{r_q} + t_q}{\mathcal{K}_s} \rceil$ and $j = (l_q - 1)\mathcal{K}_{r_q} + t_q - (i - 1)\mathcal{K}_s$ in which $\lceil x \rceil$ is equal to the smallest integer not less than x. According to this mapping, we can easily show that when l_q varies between 1 and $\mathcal{M}_{r_q}$, and t_q varies between 1 and $\mathcal{K}_{r_q}$, i varies between 1 and $\mathcal{M}_s$ and j varies between 1 and $\mathcal{K}_s$. This verifies that there is a one-to-one mapping between the generated statistics $\tilde{u}_{r_q d}^{(l_q, t_q)}$, $l_q = 1 ... \mathcal{M}_{r_q}$, $t_q = 1 ... \mathcal{K}_{r_q}$, and the members of set S_{r_q}.

If we substitute $\tilde{u}_{sr_q}^{(i,j)}$ in the expression given for $\tilde{u}_{r_q d}^{(l_q, t_q)}$ in Table 9.1, from the given expression for $\tilde{u}_{sr_q}^{(m,k)}$ in the table (after replacing (i, j) with (m, k)), an alternative formula for $\tilde{u}_{r_q d}^{(l_q, t_q)}$ can be obtained as follows:

$$\tilde{u}_{r_q d}^{(l_q, t_q)} = \|\mathbf{H}_{sr_q}^{(i)}\|_F^2 \|\mathbf{H}_{r_q d}^{(l_q)}\| F^2 \zeta_{r_q}^{(i)} s_s^{(i,j)} + \breve{w}_{r_q d}^{(l_q, t_q)}, \tag{9.5}$$

where, $\breve{w}_{r_q d}^{(l_q, t_q)}$ is a white zero-mean Gaussian noise sample with variance

$$\|\mathbf{H}_{r_q d}^{(l_q)}\|_F^2 \|\mathbf{H}_{sr_q}^{(i)}\|_F^2 \|\mathbf{H}_{r_q d}^{(l_q)}\|_F^2 ((\zeta_{r_q}^{(i)})^2 + 1)\mathcal{N}.$$

Equation (9.5) shows that $\tilde{u}_{r_q d}^{(l_q, t_q)}$ contains information about $s_s^{(i,j)}$, i.e., an information symbol transmitted by the sender. Therefore, according to (9.5) and the expression given for $\tilde{u}_{sd}^{(m,k)}$ in Table 9.1, we can observe that for every transmitted symbol from the sender, the receiver generates Q decision statistics from the relays and 1 decision statistics from the sender. By a maximal ratio combination of these $Q + 1$ decision statistics, each information symbol of the sender can be estimated at the receiver as follows:

$$\hat{s}_s^{(m,k)} = \underset{\alpha \in \mathbb{S}}{\arg \max} \ \text{Real}\{\Lambda_{m,k} \times \alpha^*\}, \qquad m = 1 ... \mathcal{M}_s, \ k = 1 ... \mathcal{K}_s, \tag{9.6}$$

where $\hat{s}_s^{(m,k)}$ is an estimation of $s_s^{(m,k)}$, and $\mathbb{S}$ is the signal constellation of the used modulation. In (9.6), $\Lambda_{m,k}$ is defined as

$$\Lambda_{m,k} = \tilde{u}_{sd}^{(m,k)} + \sum_{q=1}^{Q} \frac{\|\mathbf{H}_{sr_q}^{(m)}\|_F^2 \zeta_{r_q}^{(m)} \tilde{u}_{r_q d}^{(f_q, g_q)}}{\|\mathbf{H}_{sr_q}^{(m)}\|_F^2 \|\mathbf{H}_{r_q d}^{(f_q)}\|_F^2 (\zeta_{r_q}^{(m)})^2 + 1}. \tag{9.7}$$

Here, the superscripts f_q and g_q are obtained as $f_q = \lceil \frac{(m-1)\mathcal{K}_s + k}{\mathcal{K}_{r_q}} \rceil$ and $g_q = (m - 1)\mathcal{K}_s + k - (f_q - 1)\mathcal{K}_{r_q}$.

9.2.3   Symbol Error Rate Analysis

The error rate performance of the described multi-antenna cooperative system depends on the distribution of SNR in the decision variable $\Lambda_{m,k}$. This SNR is referred to as the *post-detection SNR*. To find an expression for the post-detection SNR, we substitute $\tilde{u}_{sd}^{(m,k)}$ from its definition in Table 9.1, and $\tilde{u}_{r_q d}^{(f_q, g_q)}$ from (9.5), (after replacing (l_q, t_q) with (f_q, g_q)), into (9.7). We arrive at an alternative expression for $\Lambda_{m,k}$ as follows:

$$\Lambda_{m,k} = \left(A_m + \sum_{q=1}^{Q} \frac{B_m^2 C_{l_q} (\zeta_{r_q}^{(m)})^2}{B_m C_{l_q} (\zeta_{r_q}^{(m)})^2 + 1} \right) s_{m,k} + \tilde{w}_{sd}^{(m,k)} + \sum_{q=1}^{Q} \frac{B_m \zeta_{r_q}^{(m)} \check{w}_{r_q d}^{(f_q, g_q)}}{B_m C_{l_q} (\zeta_{r_q}^{(m)})^2 + 1},$$

where

$$A_m = \|\mathbf{H}_{sd}^{(m)}\|_F^2$$
$$B_m = \|\mathbf{H}_{sr_q}^{(m)}\|_F^2$$
$$C_{l_q} = \|\mathbf{H}_{r_q d}^{(f_q)}\|_F^2.$$

The post-detection SNR is defined as the ratio of the power of the signal component to the power of the noise component in the decision variable $\Lambda_{m,k}$. After some calculations, the post-detection SNR is obtained as

$$\lambda_{m,k} = \left(A_m + \sum_{q=1}^{Q} \frac{B_m^2 C_{l_q} (\zeta_{r_q}^{(m)})^2}{B_m C_{l_q} (\zeta_{r_q}^{(m)})^2 + 1} \right) \frac{P_s}{\mathcal{N}}. \tag{9.8}$$

If we substitute $\zeta_{r_q}^{(m)}$ from (9.4) into (9.8), we have

$$\lambda_{m,k} = \gamma_{sd}^{(m)} + \sum_{q=1}^{Q} \frac{\gamma_{sr_q}^{(m)} \gamma_{r_q d}^{(l_q)}}{\gamma_{sr_q}^{(m)} + \gamma_{r_q d}^{(l_q)} + 1}. \tag{9.9}$$

Parameters $\gamma_{sd}^{(m)}$, $\gamma_{sr_q}^{(m)}$, and $\gamma_{r_q d}^{(l_q)}$ are defined as

$$\gamma_{sd}^{(m)} = A_m \frac{P_s}{\mathcal{N}}$$
$$\gamma_{sr_q}^{(m)} = B_m \frac{P_s}{\mathcal{N}}$$
$$\gamma_{r_q d}^{(l_q)} = C_{l_q} \frac{P_s}{\mathcal{N}}.$$

Since these parameters are dependent on the realization of the channel matrices, the post-detection SNR for each information symbol is represented as a random

variable. According to (9.9), this random variable can be represented as follows:

$$\chi = \chi_{sd} + \sum_{q=1}^{Q} \frac{\chi_{sr_q} \chi_{r_q d}}{\chi_{sr_q} + \chi_{r_q d} + 1}. \tag{9.10}$$

Here, χ_{sd}, χ_{sr_q} and $\chi_{r_q d}$ are random variables corresponding to the parameters $\gamma_{sd}^{(m)}$, $\gamma_{sr_q}^{(m)}$ and $\gamma_{r_q d}^{(l_q)}$, respectively. It can be verified that $\chi_{uv} \sim g(\Delta_{uv}, \bar{\gamma}_{uv})$ in which $\Delta_{uv} = N_u N_v$ and $\bar{\gamma}_{uv} = \Omega_{uv} P_s / \mathcal{N}$, for $u \in \{s, r_q\}$ and $v \in \{r_q, d\}$. The notation $X \sim g(a, b)$ means that the random variable X has a gamma distribution with parameters a and b (see [152] for further information about the gamma distribution).

The SER of the MIMO cooperative system can then be expressed using Marcum's Q-function as

$$SER = \int_0^{\infty} Q\left(\sqrt{k_{mod} x}\right) f_\chi(x) dx, \tag{9.11}$$

where $f_\chi(x)$ is the PDF of the random variable χ and k_{mod} is a constant which depends on the modulation type. As shown in [153], if the derivatives of $f_\chi(x)$ up to order $n-1$ are null, at high SNRs (9.11) can be approximated using the McLaurin series of $f_\chi(x)$ as follows:

$$SER \approx \frac{\prod_{i=1}^{n+1} (2i-1)}{2(n+1)! k_{mod}^{n+1}} \frac{\partial^n f_\chi}{\partial x^n}(0). \tag{9.12}$$

Therefore, in order to calculate the SER, we need to determine the value of n so that $\frac{\partial^j f_\chi}{\partial x^j}(0) = 0$ for $j < n$, but $\frac{\partial^n f_\chi}{\partial x^n}(0) \neq 0$, and also find the corresponding value of $\frac{\partial^n f_\chi}{\partial x^n}(0)$. To this end, we first approximate χ at high SNRs as

$$\chi \approx \chi_{sd} + \sum_{q=1}^{Q} \frac{\chi_{sr_q} \chi_{r_q d}}{\chi_{sr_q} + \chi_{r_q d}}. \tag{9.13}$$

Then, we use the following proposition.

Proposition 1. *Let $1_{(\pi)}$ be equal to 1 if π is a true statement and equal to 0 if π is a false statement. Let us define a random variable A as $A = X + \sum_{q=1}^{Q} Y_q Z_q / (Y_q + Z_q)$ in which the mutually independent random variables X, Y_q and Z_q ,$q = 1...Q$, have a gamma distribution so that $X \sim g(a, \bar{x})$, $Y_q \sim g(b_q, \bar{y}_q)$, and $Z_q \sim g(c_q, \bar{z}_q)$ (a, b_q, and c_q are integers). If we represent the PDF of the random variable A by $f_A(w)$, then all derivatives of $f_A(w)$ up to order $n-1$ are null, where $n = a - 1 + \sum_{q=1}^{Q} \min(b_q, c_q)$, and $\frac{\partial^n f_A}{\partial w^n}(0) = \frac{1}{\bar{x}^a} \prod_{q=1}^{Q} \left[\frac{1}{\bar{y}_q^{b_q}} \cdot 1_{(b_q \leq c_q)} + \frac{1}{\bar{z}_q^{c_q}} \cdot 1_{(c_q \leq b_q)} \right]$.*

Proof. See Appendix C. $\qquad \square$

Using the above proposition, we can establish that:

$$\frac{\partial^n f_\chi}{\partial x^n}(0) = \frac{1}{\bar{\gamma}_{sd}^{\Delta_{sd}}} \prod_{q=1}^{Q} \frac{1}{\bar{\gamma}_{sr_q}^{\Delta_{sr_q}}} \cdot 1_{\left(\Delta_{sr_q} \leq \Delta_{r_q d}\right)} + \frac{1}{\bar{\gamma}_{r_q d}^{\Delta_{r_q d}}} \cdot 1_{\left(\Delta_{r_q d} \leq \Delta_{sr_q}\right)}, \qquad (9.14)$$

where $n = \Delta_{sd} - 1 + \sum_{q=1}^{Q} \min(\Delta_{sr_q}, \Delta_{r_q d})$. After substituting $\frac{\partial^n f_\chi}{\partial x^n}(0)$ from (9.14) into (9.12), and replacing the parameters $\bar{\gamma}_{sd}$, $\bar{\gamma}_{sr_q}$, $\bar{\gamma}_{r_q d}$ with their definitions given earlier, we arrive at the following expression for the SER of the multi-antenna cooperative system:

$$SER \approx \frac{\prod_{i=1}^{g_d}(2i-1)}{2g_d! k_{mod}^{g_d}} \frac{1}{\Omega_{sd}^{N_s N_d}}$$

$$\times \prod_{q=1}^{Q} \left[\frac{1}{\Omega_{sr_q}^{N_s N_{r_q}}} \cdot 1_{\left(N_s N_{r_q} \leq N_{r_q} N_d\right)} + \frac{1}{\Omega_{r_q d}^{N_{r_q} N_d}} \cdot 1_{\left(N_{r_q} N_d \leq N_s N_{r_q}\right)} \right] \left(\frac{P_s}{\mathcal{N}}\right)^{-g_d} \qquad (9.15)$$

in which

$$g_d = n + 1 = N_s N_d + \sum_{q=1}^{Q} \min(N_s N_{r_q}, N_{r_q} N_d).$$

All this complex calculations show us that the *proposed multi-antenna cooperative system can achieve a diversity gain of order g_d*, because the SER decays with power g_d when SNR increases. If we look at the expression given for g_d, we can see that g_d is equal to the summation of $Q + 1$ terms, each of which represents the achieved diversity order of one of the existing links between s and d (direct or relayed). The term $N_s N_d$ in this summation represents the diversity order of the direct MIMO link between s and d, which according to [148] is the maximum achievable spatial diversity order of such a MIMO link. Similarly, the term $\min(N_s N_{r_q}, N_{r_q} N_d)$ represents the diversity order of the relayed link $s \rightarrow r_q \rightarrow d$, which is the minimum value of the maximum achievable diversity orders of $s \rightarrow r_q$ and $r_q \rightarrow d$ MIMO links. Intuitively, we can say that this is the maximum achievable diversity order of the two hop link $s \rightarrow r_q \rightarrow d$. *Thus, the proposed multi-antenna cooperative system can provide the maximum achievable diversity order.*

9.2.4   Simulation Studies

We present simulation results to give a hint about the SER performance of the proposed multi-antenna cooperative system. In our simulations, we assume that each of the sender and relay nodes has two transmitting antennas and uses the Alamouti code. The receiver has a single receiving antenna. For comparison, we also consider a similar configuration but with single antenna relay nodes. The modulation scheme is QPSK, and the channel power is normalized to one for

all links. The channels are slowly flat Rayleigh. For a fair comparison between various systems, we again keep the total transmission power of all transmitting nodes (sender and relays) constant in various systems. That is, in each system $RP_s = cte$, in which R is the summation of the number of antennas of the sender and all relay nodes in that system.

Figure 9.4 shows the SER for the various cooperative systems. The figure shows that when the number of relay nodes or the number of antennas of each node increases, the performance of the cooperative system improves. For instance, to achieve an SER of 10^{-5}, increasing the number of single antenna relay nodes from 1 to 2 or from 2 to 4 provides approximately 3 and 2.5 dB gain, respectively. Hence, we can decrease the total transmission power of nodes to half keeping the same SER for the system. We can also observe that shifting from one double antenna relay node to two double antenna relays provides a 2.5 dB gain of transmission power.

At high SNRs, the SER performance of the cooperative system with two single antenna relays is the same as that of the cooperative system with one double-antenna relay. The same is true for the system with 4 single-antenna relays and the system with 2 double-antenna relays. Therefore, we can replace two single-antenna relays with one double-antenna relay (or vice versa) and still have the same SER performance. We can also replace 4 single-antenna relays with 2 double-antenna relays while the SER remains unchanged. *As a general rule and based on (9.15), we can say that cooperative systems with different antenna configurations can have the same SER performance provided that g_d is the same for all of them.* Thus, for example, the systems with 4 single-antenna or 2 double-antenna relays can also be replaced with a system in which the sender has 3 antennas, the receiver has one antenna and one relay with 3 antennas used ($g_d = 6$ for all of them).

9.3 Multi-hop Cooperative Systems

The cooperative systems introduced in the previous sections are primarily designed for creating diversity gain. In these systems, the relay node blindly retransmits the overheard signals either after detecting (the DF model), amplifying (the AF model), or processing (the PF model) the received signals. This inspires us to think about a new way of multi-hop communication in which nodes blindly relay a signal until it is received by the destination. This eliminates the need for a routing protocol in wireless multi-hop networks. However, it can create a high overhead, since every node forwards blindly any signal that it receives. Nevertheless, we can think of applications in which such a multi-hop communication strategy could still be efficient. For instance, we can think of a *linear wireless multi-hop network* in which sensors are deployed along a narrow corridor for measuring the temperature.
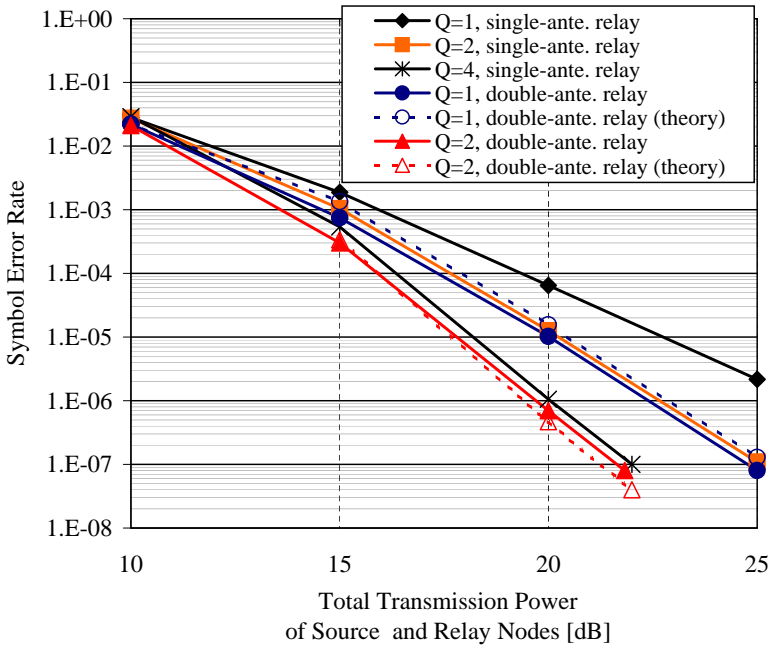
Figure 9.4 – Symbol error rate of multi-antenna cooperative systems with the Alamouti code.

Figure 9.5 – A simple schematic of a multi-hop CST system.

In such an application, we can line up sensor nodes each of which cover part of the corridor (see Figure 9.5). At the end of the corridor, there could be a sink node which collects the values measured by all sensors. Since each sensor node knows that whatever it receives has to be forwarded, there will be no need for a routing protocol. The only issue is that if nodes can not distinguish the direction from where the signal has received, they may forward some packets unnecessarily. For instance, in Figure 9.5, n_1 should not forward signals that it receives from n_2. Similarly n_2 should not forward what it receives from n_3 and so on. To resolve this problem, we need to either use directional antennas, where the angle of arrival specifies the direction that the signal has been received from. In such a case, both AF and DF models could be utilized for signal forwarding. Nonetheless, if nodes use omni-directional antennas, then we need to find another solution to increase the energy-efficiency of the system. One possible way is to assign each node an identifier which shows the position of the node in the line. Each transmitted packet by a sensor should have the sender identifier in its PHY header. Only if the sender identifier in the received packet is smaller than the identifier of the receiving node, the packet must be forwarded. This scheme could be easily deployed using the DF model. It is not suitable for the AF model, because in the AF model signals are forwarded without being detected. Thus, the sender identifier could not be known. To know the sender identifier, we need to detect the signals and re-construct at least the PHY header. Nevertheless, we show in this section that AF and DF multi-hop cooperative systems have the same SER at high SNRs and quite comparable performance at other SNRs.

9.3.1 Signal Transmission in Multi-hop Cooperative Systems

Figure 9.6 depicts a multi-hop communication system with h hops in which n_0 and n_h are considered as the source and destination nodes, respectively. Nodes labeled $n_1, n_2, \ldots n_{n-1}$ are relay nodes. In this model, $u_i \in \mathbb{S}$ represents the transmitted symbol from the node n_i, $i = 0...h - 1$. Here, $\mathbb{S}$ is the signal constellation of an $\mathcal{M}$-ary modulation scheme, which its elements denoted as s_m, $m = 1...\mathcal{M}$. In the figure, y_i, $i = 1...h$, is the symbol received by n_i. Without loss of generality, we assume a flat-fading model for wireless channels between nodes. Thus,

$$y_i = c_i u_{i-1} + z_i, \qquad i = 1...h, \qquad (9.16)$$

Figure 9.6 – System model of a multi-hop cooperative system.

where c_i is the channel coefficient of the (n_{i-1}, n_i), which is a zero mean Gaussian random variable with variance Ω_i. Furthermore, z_i is an additive white Gaussian noise sample with variance $\mathcal{N}$. The transmitted symbol from the sender u_0 is achieved after modulating $\log_2 \mathcal{M}$ binary digit(s). The method for generating the transmitted symbols by the relay nodes depends on the type of forwarding protocol.

9.3.1.1   Multi-hop AF Cooperative System

For the AF system, we have

$$u_i = \zeta_i y_i, \qquad i = 1...h - 1, \tag{9.17}$$

where ζ_i is a coefficient required to equalize the power of the transmitted symbol u_i with the transmission power of the sender. If we assume that the elements of the signal constellation have equal energy, then

$$\zeta_i = \sqrt{\frac{P_s}{|c_i|^2 P s + \mathcal{N}}}, \qquad i = 1...h - 1.$$

Here, P_s is the transmission power of the source node. After replacing u_{h-1} from (9.17) into the expression given for y_h in (9.16), and repeating this for u_{h-2} and so on, we arrive at the following expression for y_h:

$$y_h = \left(\prod_{k=1}^{h} c_k \zeta_{k-1} \right) u_0 + \sum_{k=1}^{h-1} \left(\prod_{l=k+1}^{h} h_l \zeta_{l-1} \right) z_k + z_n, \tag{9.18}$$

with the convention $\zeta_0 = 1$.

From (9.18), the symbol transmitted by the source node u_0 can be estimated at the destination node using a maximum likelihood detector as follows:

$$u_h = \arg \max_{\alpha \in \mathbb{S}} \text{Real}\{A_h^* y_h \times \alpha^*\},$$

where, $A_h = \prod_{k=1}^{h} c_k \alpha_{k-1}$ and * stands for the complex conjugate. Here, u_h denotes the detected symbol at the destination node.

9.3.1.2 Multi-hop DF Cooperative System

For the DF system, we have

$$u_i = \hat{u}_{i-1}, \qquad i = 1...h-1, \tag{9.19}$$

where $\hat{u}_{i-1}$ is an estimation for u_{i-1}, i.e., the transmitted symbol from n_{i-1}, obtained at n_i as follows:

$$\hat{u}_{i-1} = \arg\max_{\alpha \in \mathbb{S}} \text{Real}\{d_i^* y_i \times \alpha^*\}, \qquad i = 1...h-1. \tag{9.20}$$

The detected symbol at the next hop can be the same as the transmitted symbol from the previous hop. However, due to a detection error, they might be different, but still belong to the same signal constellation. Based on the convention introduced in (9.19), for the DF model the detected symbol at the destination node, i.e., u_h, can be obtained using (9.20) for $i = n$.

9.3.2 Symbol Error Rate Analysis

The SER of the multi-hop cooperative system depends on whether the AF or the DF model is used. We consider these two cases separately.

9.3.2.1 Multi-hop AF Cooperative System

For the prescribed multi-hop AF system, the SER can be approximated at high SNRs as follows [147]:

$$SER_{AF}(h) \approx \sum_{i=1}^{h} \frac{1}{2k_{mod}} \bar{\gamma}_i, \tag{9.21}$$

in which, $\bar{\gamma}_i$ is the average received SNR of the ith hop defined as $\bar{\gamma}_i = \Omega_i P_s / \mathcal{N}$.

9.3.2.2 Multi-hop DF Cooperative System

For the multi-hop DF system, we define the SER as the probability that the detected symbol at the destination is different from the symbol transmitted by the source. However, a detection error at each hop may compensate the decision errors made in the previous hops. As a result, even if there are some detection errors at the relay nodes, the detected symbol at the destination node could be the same as the transmitted symbol from the source node. This adds to the complexity of the problem.

In order to find an expression for the SER of the multi-hop DF system, we model the system as a Markov chain (see Figure 9.7). As shown in the figure, the detected symbol at each hop is dependent on the transmitted symbol from the previous hop
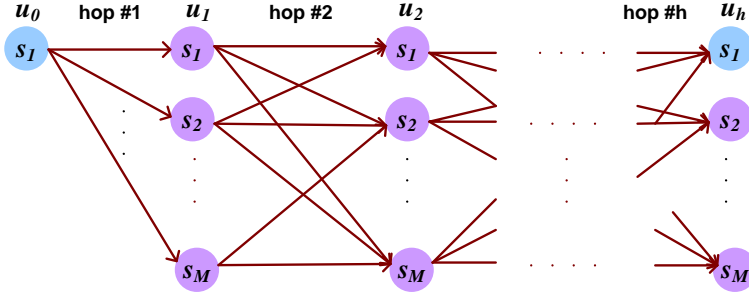
Figure 9.7 – Markov model of a multi-hop DF system.

and the error probability in the current hop. In Figure 9.7, we have assumed that the transmitted symbol from the source node is s_1. The transmitted symbol from the source node could be estimated at n_1 as another symbol, and after transmission of the estimated symbol from n_1, it might be detected again as another symbol at n_2, and so on. We denote the probability that $u_i = s_k$ subject to having $u_{i-1} = s_j$, by $p_{i_{jk}}$ (a transition probability). Considering the model shown in Figure 9.7, the end-to-end symbol error probability of the multi-hop DF system can be calculated as

$$SER_{DF}(h) = \Pr\{u_h \neq u_0\} = \sum_{j=1}^{\mathcal{M}} \sum_{\substack{k=1 \\ k \neq j}}^{\mathcal{M}} \frac{1}{\mathcal{M}} a_{n_{jk}}, \tag{9.22}$$

where $a_{n_{jk}} = \Pr\{u_h = s_k | u_0 = s_j\}$. In (9.22), we assumed that the members of the signal constellation are equally probable, i.e., $\Pr\{u_0 = s_j\} = 1/\mathcal{M}$. To find an expression for $a_{n_{jk}}$, we use the fact that

$$\Pr\{u_h = s_k\} = \sum_{l=1}^{\mathcal{M}} \Pr\{u_{h-1} = s_l\} p_{h_{lk}}, \qquad k = 1...\mathcal{M}. \tag{9.23}$$

By introducing a $1 \times \mathcal{M}$ vector as $\mathbf{s}[h] = [\Pr\{u_h = s_1\}, ..., \Pr\{u_h = s_{\mathcal{M}}\}]$, (9.23) can be represented in a vector form as follows:

$$\mathbf{s}[h] = \mathbf{s}[h-1]\mathbf{P}_h, \tag{9.24}$$

where $\mathbf{P}_h$ is defined as

$$\mathbf{P}_h = \begin{bmatrix} p_{h_{11}} & p_{h_{12}} & \cdots & p_{h_{1\mathcal{M}}} \\ \vdots & \vdots & \ddots & \vdots \\ p_{h_{\mathcal{M}1}} & p_{h_{\mathcal{M}2}} & \cdots & p_{h_{\mathcal{M}\mathcal{M}}} \end{bmatrix}.$$

Equation (9.24) verifies that the multi-hop DF system can be modeled as a Markov chain [154]. The recursive expression in (9.24) could also be represented in this form:

$$\mathbf{s}[h] = \mathbf{s}[0]\mathbf{P}_1 \times \mathbf{P}_2 \times ... \times \mathbf{P}_h, \tag{9.25}$$

where $\mathbf{s}[0]$ is an initial value vector.

Our goal is to find an expression for $a_{n_{jk}} = \Pr\{u_h = s_k | u_0 = s_j\}$. Note that the kth element of $\mathbf{s}[h]$ is equal to $\Pr\{u_h = s_k\}$. However, we already have taken into account the probability of u_0 being equal to s_j for calculating $SER_{DF}(h)$ in (9.22). Thus, the kth element of $\mathbf{s}[h]$ will be equal to $a_{h_{jk}}$, if we assume that $\mathbf{s}[0]$ in (9.25) is equal to $\mathbf{w}_j$, where $\mathbf{w}_j$ is a $1 \times \mathcal{M}$ vector whose elements are all zero except the jth element, which is one. This assumption means that $u_0 = s_j$, and the kth element of $\mathbf{s}[h]$ is actually $a_{h_{jk}}$.

To find the kth element of $\mathbf{s}[h]$, we start with $h = 1$ in (9.25). We have

$$\mathbf{s}[1] = \mathbf{w}_j\mathbf{P}_1 = [p_{1_{j1}}, p_{1_{j2}}, ..., p_{1_{jj}}, ...p_{1_{j\mathcal{M}}}].$$

For $h = 2$, we have

$$\mathbf{s}[2] = \left[\sum_{m=1}^{\mathcal{M}} p_{1_{jm}}p_{2_{m1}}, ..., \sum_{m=1}^{\mathcal{M}} p_{1_{jm}}p_{2_{m\mathcal{M}}}\right].$$

Note tha $p_{i_{ll}} = 1 - \sum_{\substack{m=1 \\ m \neq l}}^{\mathcal{M}} p_{i_{lm}}$. Thus, after some calculations we can show that the kth, $k \neq j$, element of $\mathbf{s}[2]$, denoted by $\mathbf{s}_k[2]$, can be represented as follows:

$$\mathbf{s}_k[2] = p_{1_{jk}} + p_{2_{jk}} + C_{k,2}, \qquad k \neq j, \tag{9.26}$$

where,

$$C_{k,2} = \sum_{\substack{m=1 \\ m \neq j,k}}^{\mathcal{M}} p_{1_{jm}}p_{2_{mk}} - p_{1_{jk}}\sum_{\substack{m=1 \\ m \neq k}}^{\mathcal{M}} p_{2_{km}} - p_{2_{jk}}\sum_{\substack{m=1 \\ m \neq j}}^{\mathcal{M}} p_{1_{jm}}.$$

Equation (9.26) shows that $\mathbf{s}_k[2]$, for $k \neq j$, is equal to the summation of the two first order terms $p_{1_{jk}}$ and $p_{2_{jk}}$, and a number of second order terms whose effects have been captured by $C_{k,2}$. By deduction we can show that the kth element of $\mathbf{s}[h]$, can be expressed as follows:

$$\mathbf{s}_k[h] = \sum_{i=1}^{h} p_{i_{jk}} + C_{k,h}, \qquad k \neq j, \tag{9.27}$$

in which the term $C_{k,h}$ captures the effect of the higher order terms from order 2 to order h. In general, a term with order q is proportional to the multiplication

of q transition error probabilities chosen from the set $\{p_{i_{jk}}|j,k = 1...\mathcal{M}, j \neq k, i = 1...h\}$.

By substituting $\mathbf{s}_k[n]$ from (9.27) with $a_{n_{jk}}$ in (9.22), we can arrive at the following expression:

$$SER_{DF}(h) = \sum_{j=1}^{\mathcal{M}} \sum_{\substack{k=1 \\ k \neq j}}^{\mathcal{M}} \sum_{i=1}^{h} \frac{1}{\mathcal{M}} p_{i_{jk}} + C_h, \qquad (9.28)$$

where,

$$C_h = \frac{1}{\mathcal{M}} \sum_{\substack{k=1 \\ k \neq j}}^{\mathcal{M}} C_{k,h}.$$

If we assume that the transition error probability $p_{i_{jk}}$ for $k \neq j$ is a very small value, then we expect $C_{k,n}$, $(k \neq j, n \geq 2)$ to take a relatively small value compared to the first order terms in (9.27). Consequently, C_h is likely to be negligible compared to the first order terms in (9.28). Therefore, the following approximation can be obtained:

$$SER_{DF}(h) \approx \sum_{i=1}^{h} \sum_{j=1}^{\mathcal{M}} \sum_{\substack{k=1 \\ k \neq j}}^{\mathcal{M}} \frac{1}{\mathcal{M}} p_{i_{jk}}. \qquad (9.29)$$

Equation (9.29) can be represented in terms of the individual error probabilities of the h hops. We denote the individual error probability of the ith hop by δ_i, which is calculated as

$$\delta_i = \sum_{j=1}^{\mathcal{M}} \sum_{\substack{k=1 \\ k \neq j}}^{\mathcal{M}} \frac{1}{\mathcal{M}} p_{i_{jk}}, \qquad i = 1...h.$$

Thus, we can write (9.29) alternatively as

$$SER_{DF}(h) \approx \sum_{i=1}^{h} \delta_i. \qquad (9.30)$$

Equation (9.30) shows that the end-to-end SER of the multi-hop DF system is approximately equal to the summation of the SERs of the individual hops subject to $p_{i_{jk}}$, $\forall j, k \in [1, \mathcal{M}]$, $j \neq k$, $\forall i$ are sufficiently small values. Such a condition can be true at high SNRs, especially when the two symbols are not adjacent symbols in the signal constellation. However, as $\mathcal{M}$ and h increase, the number of higher order terms in (9.28) increases exponentially. Thus, it is possible that in some situations C_h is not negligible compared to the summation of the first order terms. But our

experiments show that at high SNRs, e.g., greater than 10 dB, the approximation in (9.30) is a good approximation[1].

Although the model of the multi-hop DF system was expressed for slow-varying flat fading Rayleigh channels with coherent detection, but to arrive at (9.29), we just considered the equivalent model in Figure 9.7. This model is valid for **any** multi-hop DF system regardless of the modulation scheme, the channel model (it is even valid for wired links), the detection scheme, the accuracy of the channel state information, and even the number of transmitting and receiving antennas. We can even consider different communication systems for each hop. The effects of all these assumptions can be captured by the corresponding values of $\delta_1...\delta_h$. *This means that the obtained result for the SER of the multi-hop DF system is surprisingly general and applicable to any type of multi-hop DF communication system.*

Let us consider single antenna nodes and Rayleigh channels with coherent detection. For this case, δ_i at high SNRs for MPSK modulation is approximated as [50]:

$$\delta_i \approx \frac{1}{2k_{mod}}\bar{\gamma}_i, \qquad i = 1...h.$$

Thus, at high SNRs, the SER of the multi-hop DF system is given by

$$SER_{DF}(h) \approx \sum_{i=1}^{h} \frac{1}{2k_{mod}}\bar{\gamma}_i. \tag{9.31}$$

If we compare the expressions given for the SER of the multi-hop DF system in (9.31) and the expression given for the SER of the multi-hop AF system in (9.21), interestingly we can find out that for the case of slow-varying flat-fading Rayleigh channels and coherent detection and single antenna nodes, these two systems have the same SER performance at high SNRs. This means that whether the relay nodes detect the received signals and transmit the detected symbols or they just retransmit the amplified signals, the end-to-end SER will be the same at high SNRs.

9.3.3   Simulation Studies

In this section, we present simulation results to compare the performance of the multi-hop DF and AF systems. We assume the modulation scheme is QPSK, and the channel power is normalized to one in all hops. Figure 9.8 shows the SER of the multi-hop DF system with 6 hops as a function of the transmission power of the source node. Both analytical and simulation results are presented. Analytical results are obtained using (9.31). Plots in Figure 9.8 show that there is a good agreement between analytical and simulation results at high SNRs. Similar

---

[1]We assume that δ_i is a small value for all $i = 1...h$, and hence the $\sum_{i=1}^{h} \delta_i$ never exceeds 1 which is the maximum feasible value for the error probability.

observation can be made through plots in Figure 9.9. This figure shows the SER of a multi-hop DF system with different number of hops. As Figure 9.9 reveals, when the number of hops in a multi-hop DF system increases, the SER at the destination node increases. For instance, when the transmission power is 20 dB, the error rate is increased by approximately a factor of 10 as the number of hops increases from 2 to 16. We can also observe that at an SER of 10^{-2}, shifting from two to four hops (or from four to eight hops) causes 3 dB degradation in the SER performance. That is, the transmission power of each node must be doubled if we want to have a SER similar to the case of two hops (or four hops).

Figure 9.9 compares the SER of the multi-hop DF and AF systems. The plots in this figure show that the SER of these two systems are comparable not only at high SNRs – as (9.21) and (9.31) predict – but also at low and moderate SNRs.

9.4   Summary

In this chapter, cooperative signal transmission techniques in wireless multi-hop networks were studied. A cooperative model for multi-antenna wireless networks was proposed on the basis of Orthogonal Space-time Block Codes. An approximate formula for the symbol error rate of the proposed system was derived. We proved mathematically that the proposed multi-antenna cooperative system can provide maximum diversity order. Furthermore, various multi-antenna cooperative systems with different structures could have the same symbol error performance. Simulation studies showed that if nodes cooperate with each other in signal transmission, a smaller transmission power can provide the same symbol error rate. We also studied multi-hop forwarding schemes based on amplify-and-forward and detect-and-forward cooperative signal transmission. Their performance was analyzed and closed-form expressions were derived to approximate the symbol error rate of these systems. We showed that the performances of multi-hop cooperative signal transmission schemes based on amplify-and-forward and detect-and-forward models are close.
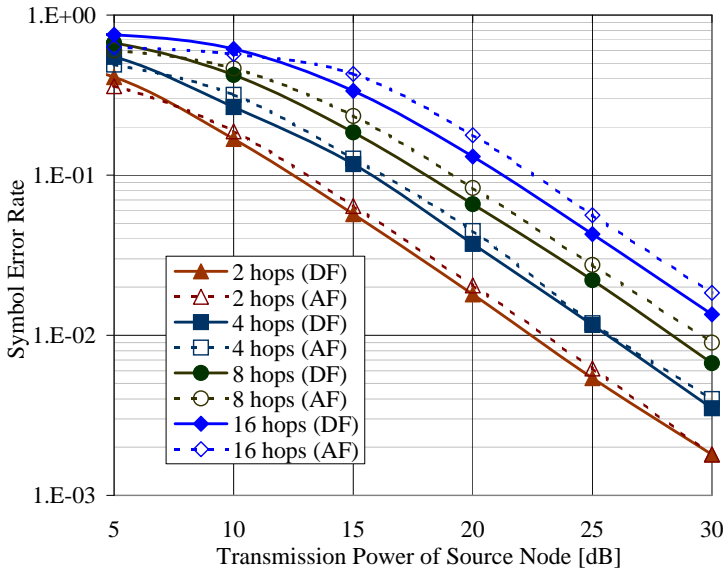
Figure 9.8 – Symbol error rate of the multi-hop DF and AF systems for QPSK modulation. Only simulation results have been presented.
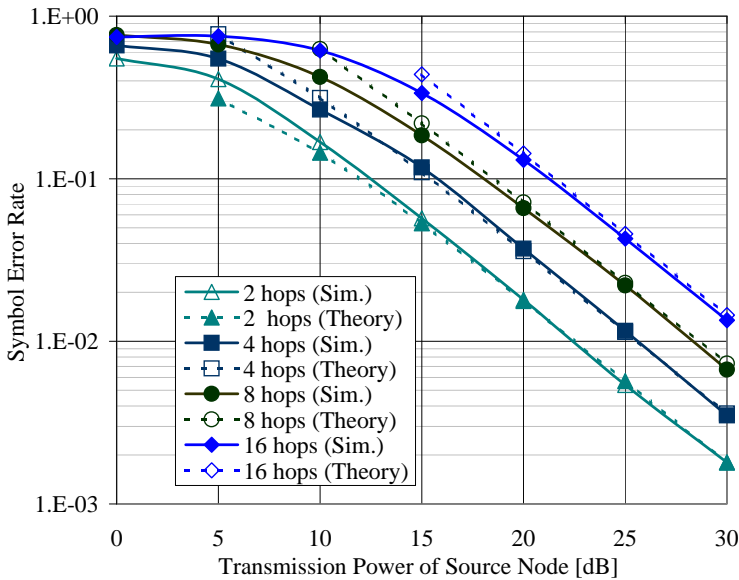
Figure 9.9 – Simulation and analytical values of the symbol error rate of the multi-hop DF system with varying number of relaying nodes when QPSK modulation is used.
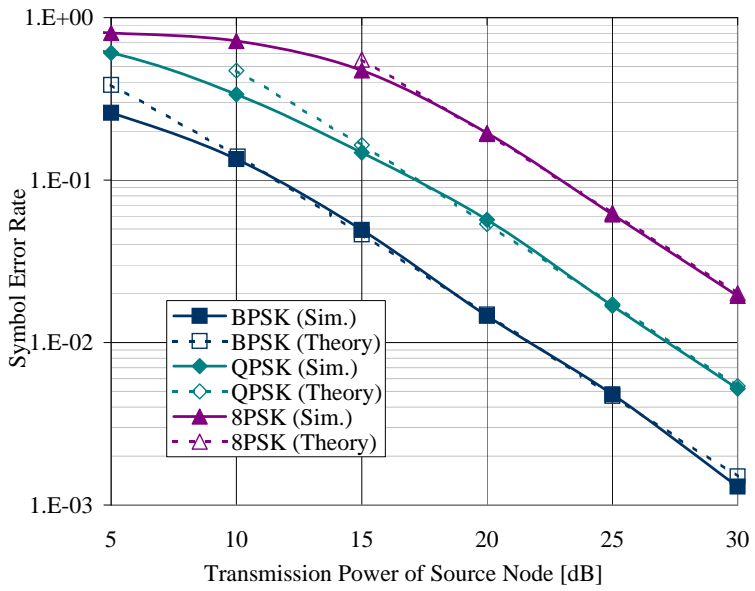
Figure 9.10 – Symbol error rate of a multi-hop DF system with 6 relay nodes for various modulations.

Chapter 10

Conclusion and Outlook

Multi-hop wireless communication enables personal networking, sensor networking, and mobile ad hoc networking. Wireless devices could be easily networked in a self-organized way to expand infrastructure networks or to provide local services. Limited energy budget of wireless devices and vast deployment of wireless multi-hop networks around the world necessitate the use of energy-efficient communication schemes in these networks. This not only can save a considerable amount of energy world-wide, but also can increase the operational lifetime of battery-powered wireless devices in a network environment.

In this dissertation, we provided an in-depth study of energy-aware and energy-efficient design and analysis of wireless multi-hop networks. A suite of optimized communication schemes were designed considering energy as the key parameter. These schemes together form a platform to bring energy-efficiency across various layers of the communication stack accompanied by load balancing and reliability. Effectiveness of the proposed schemes was studied extensively.

10.1 Recapitulation of our Contributions

We briefly review the challenges and novelty of our contributions in this dissertation.

10.1.1 Modeling Link Level Energy Consumption

At first, we developed a detailed mathematical model for energy consumption during packet exchange over wireless links. Many existing models are not accurate, since they neglect minute details such as the energy consumption of processing elements of transceivers, impact of packet retransmission and the reliability of links

and the packet size on the energy consumption. To develop a realistic and an accurate model, we considered the structure of commercial transceivers. We also used experimental results to show that most of the time, lost packets are actually detected completely by receivers but discarded due to erroneous bits. This implies that energy consumed for receiving lost packets can be the same as the energy consumed to receive packets correctly. Our investigations also showed that energy consumption of transceivers for packet processing during transmission or reception is quite considerable compared to the energy consumed by them to generate the required power for signal transmission over the air. Thus, to be able to design optimal energy-efficient communication schemes for wireless multi-hop networks, these sources of energy consumption must be considered.

10.1.2   Energy Cost for End-to-end Packet Traversal

After modeling the energy consumption across wireless links, we analyzed the total energy required to transfer a packet between two nodes of the network in a multi-hop way. The impact of packet retransmissions triggered by the data link and transport layers was discussed in detail. Energy consumption in four types of packet transfer in wireless multi-hop networks was analyzed. These four types of packet transfer are: 1) without link layer and transport layer (end-to-end) retransmissions, 2) with only link layer retransmissions, 3) with only transport layer retransmissions, and 4) with both link and transport layer retransmissions. Investigations showed that when links are of low quality, transport layer retransmissions increase energy consumption of devices dramatically in large networks. Link layer retransmissions are more energy-efficient and allow scalable expansion of wireless multi-hop networks.

10.1.3   Energy-efficient Routing

To reduce energy consumption of nodes, it is important to find energy-efficient routes which minimize the required energy for end-to-end packet traversal between nodes. This issue was tackled next. We designed routing algorithms to find energy-efficient routes in wireless multi-hop networks. We observed that the required energy depends on whether link and transport layer retransmissions are supported. Thus, we designed energy-efficient routing algorithms for each of the four types of packet transfer in wireless multi-hop networks. However, to reduce the complexity of routing due to cross-layer dependency on physical, data link, and transport layers, we unified the four algorithms into one algorithm. We showed that the unified algorithm can still find energy-efficient and reliable routes in all the four cases. The proposed routing algorithms link between energy efficiency and reliability of links in wireless multi-hop networks. They not only find energy-efficient

routes but also are able to find reliable routes. This in fact is the result of the use of a realistic energy consumption model in the design of our proposed energy-efficient routing algorithms. Investigations showed that the use of inaccurate energy consumption models (those neglecting energy cost of processing elements and the effect of link quality) in the design of an energy-efficient routing algorithm harms both energy-efficiency and reliability of the network.

10.1.4 Battery-aware Routing

The use of energy-efficient routes, however, may result in node overuse, because some nodes might be frequently selected as part of energy-efficient routes between nodes. It is important to consider the remaining battery energy of nodes in route selection to balance the traffic load between nodes. Nevertheless, this should not result in a lack of energy-efficiency and reliability. How to achieve these goals was the next issue that we addressed in this dissertation. We proposed enhanced battery-aware routing algorithms for wireless multi-hop networks. The proposed algorithms consider the remaining battery energy of nodes, the reliability of links, and the energy consumption characteristics of transceivers altogether to find energy-efficient and reliable routes that balance the traffic load in the network.

In some applications of wireless multi-hop networks (e.g., personal networks), some nodes of the network can be connected to the mains (grid network). This fact was used to develop battery-aware routing algorithms which consider the type of power supply of nodes and avoid relaying packets over battery-powered nodes. An issue, here, is the increased latency since long routes consisting of many mains-powered nodes could be favored to short routes consisting of few battery-powered nodes. To mitigate the problem, we proposed bi-objective battery-aware routing algorithms that consider minimizing a battery-cost and the latency as two objectives in route selection. This can effectively reduce latency of the end-to-end packet traversal while the traffic is effectively directed to the mains-powered nodes of the network. However, we observed that directing the traffic load to mains-powered nodes can increase the lifetime of nodes only if overhearing of neighboring nodes is avoided. Overhearing reduces the lifetime of nodes profoundly and neutralizes the gain which could be achieved by relaying packets over mains-powered nodes of the network. If relay traffic is directed towards mains-powered nodes, battery-powered nodes around these nodes overhear many packets and fail quickly. The network lifetime increases only if overhearing is eliminated using sleep and wake up MAC protocols, or is reduced using topology control algorithms. Next, we studied topology control in wireless multi-hop networks.

10.1.5   Topology Control

Topology control reduces the transmission range of nodes in such a way that the network remains connected (or k-connected) with a fewer number of links. In fact, topology control determines the neighbor discovery policy at the data link layer of the communication stack. A new localized fault-tolerant topology control algorithm was proposed for networks with heterogeneous power supplies (e.g., personal networks). The proposed algorithm creates a fault-tolerant backbone of mains-powered nodes using the most energy-efficient links. Then, battery-powered nodes are attached to this backbone with the minimum required transmission power. We proved that this algorithm preserves k-connectivity of the network. That is, if the network is k-connected without topology control, it will be k-connected after reducing the transmission range of nodes using our proposed algorithm. We also proved that our proposed algorithm minimizes the maximum transmission power among battery-powered nodes of the network for keeping the network k-connected. Simulation studies showed that the proposed algorithm can substantially reduce the transmission range of all the nodes and in particular the battery-powered nodes of the network. Reducing the transmission range of battery-powered nodes reduces the energy consumption of these nodes for overhearing. Thus, directing the relay traffic to mains-powered nodes can still provide a gain even if overhearing is not eliminated using energy-efficient MAC protocols.

10.1.6   Analysis of Node-to-node Communication Lifetime

We analyzed the duration that two arbitrary nodes in a wireless multi-hop network with a random topology could communicate with each other from the transport layer viewpoint. A closed-form expression for the lifetime of a connection between two nodes was derived in static networks with random topology. This expression specifies the expected duration that two arbitrary nodes of the network can communicate with each other via intermediate nodes between them. It also specifies how and to what extent various factors such as node density, transmission range, network deployment area, packet transmission rate, and energy consumption characteristics of nodes affect the lifetime.

10.1.7   Cooperative Signal Transmission

Finally, we studied cooperative signal transmission at the physical layer for reducing the energy consumption of nodes for signal transmission over the air. A cooperative model for multi-antenna wireless networks was proposed and its performance was analyzed. The proposed scheme used Orthogonal Space-time Block Codes and

a novel process-and-forward technique for cooperation in signal transmission in networks with MIMO devices. We proved mathematically that the proposed multi-antenna cooperative system can provide the maximum achievable diversity gain for such systems. Furthermore, we showed that when nodes cooperate with each other during signal transmission over the wireless medium, even with a smaller transmission power the same symbol error rate could be achieved. We also proposed a novel cooperative signal transmission technique for multi-hop packet forwarding at the physical layer, namely multi-hop detect-and-forward cooperative communication. The performance of the proposed scheme was analyzed mathematically.

10.2 Our Results in a Nutshell

In this section, we list some of findings in this research, and relate them with research issues mentioned in Chapter 1. Our main findings with regard to Research Issue R_1 are as follows:

- Energy consumption of processing circuits of transceivers is quite considerable compared to the energy consumed for signal transmission over the air. As a result, the traditional belief that in wireless networks multi-hop communication is more energy-efficient than single-hop communication is not always true.

- Adjusting the transmission power of nodes according to the distance results in energy-efficiency only if reliability of links is not harmed due to reducing the transmission power.

- Energy consumption in wireless multi-hop network increases exponentially with the size of these networks if end-to-end retransmissions are used. It increases linearly if link level retransmissions are used instead.

With regard to Research Issue R_2, we found that:

- Neglecting the energy consumption of processing circuits of transceivers in the design of energy-efficient routing algorithms not only harms energy-efficiency in wireless multi-hop network but also reduces the reliability of these networks.

- Reliability and energy-efficiency are linked together in wireless multi-hop networks. The use of less reliable routes is not energy-efficient either.

- Energy consumption for reception of broadcast messages used by routing protocols is the dominant source of energy consumption of nodes in the network. Reducing this source of energy consumption can significantly increase the operational lifetime of the network.

With regard to Research Issues R_3 and R_4, we found that:

- Load balancing in wireless multi-hop networks must be accompanied by energy-efficiency. The use of non-energy-efficient routes neutralizes the gain achieved by a load balancing scheme.

- Directing the relay traffic to mains-powered nodes in a wireless multi-hop network can increase the operational lifetime of the network only if overhearing is reduced. This could be achieved using a topology control algorithm to keep the number of neighboring nodes of battery-powered nodes as small as required to keep the network connected (or fault-tolerant).

With regard to Research Issues R_5 and R_6, we found that:

- Overhearing neighboring nodes can substantially reduce node-to-node communication lifetime in wireless multi-hop networks.

- Cooperative signal transmission can reduce the transmission power of cooperative nodes for reliable signal transmission over wireless channels.

10.3   Vistas for Future

We can highlight four main research areas to follow up this work. First, one can study the minimum amount of energy required for communication in various types of networks including infrastructure wireless networks. Given the transmission power of nodes, we in this dissertation specified the minimum energy required for multi-hop communication from the transport layer viewpoint. In a follow up work, one could focus more the physical layer. To this end, one can determine the minimum required energy for reliable communication over various types of wireless channels, i.e., flat and frequency-selective channels with Rayleigh, Rician, or Nakagami-m fading models. Considering various types of channel codes (block and convolutional codes) and various digital modulation schemes would also be an interesting dimension of the follow up research.

Another interesting area is the use of energy-efficient multi-hop networks that we designed here to provide energy efficiency to our daily lives by creating a distributed intelligence for monitoring our activities and surroundings. Here, one can think of middleware solutions to reduce energy consumption at buildings. The role of

personal networks could be important to achieve this goal. Personal networks can provide a distributed intelligence around people to monitor their activities to collect required context for saving energy in buildings. On top of energy-efficient personal networks that we designed in this dissertation, we can also support many types of other applications and services as well. For instance, one can investigate middleware solutions to support health-care and telepresence in personal networks.

As another research area, one can implement the proposed energy-efficient and energy-aware routing schemes to verify their effectiveness using experimental studies as well. Experimental studies could also be used to investigate the impact of link quality variation in wireless channels on the performance of these schemes. In practice, many factors such as interference from other networks, signal blockage by people, and time-varying fading may cause link quality variation in wireless networks. How such factors affect energy-efficiency in wireless multi-hop networks is another interesting research topic.

Last but not least, one can investigate MAC protocols for the multi-hop detect-and -forward cooperative system proposed in this dissertation. Such a multi-hop transmission system can eliminate the need for a routing protocol in many applications of wireless multi-hop networking (e.g., wireless sensor networks). To this end, however, an efficient MAC protocol is required to coordinate communication between nodes in such a way that overhearing is minimized. This results in a new way of communication in wireless multi-hop networks different from what is popularly known for these networks.

Appendix A

Complexity of the Numerical Algorithm for Estimating Node-to-node Communication Lifetime

The time complexity of Algorithm 9 depends on the complexity of its main loop, where the lifetime of node-disjoint routes is determined. Within the main loop, the instruction "Find P_k" finds the next node-disjoint route between the source and the destination. By the time we find the next route, the previous routes would have been removed from $G(\mathbb{V}, \mathbb{E})$ by the procedure "Update $\mathbb{B}$ and G". Thus, finding the next route corresponds to finding the shortest path between the two nodes. This could be done using the Dijkstra's algorithm. Hence, the complexity of "Find P_k" will be $O(|\mathbb{V}|^2)$ in dense networks and $O(|\mathbb{V}| \log(|\mathbb{V}|) + |\mathbb{E}|)$ in sparse networks.

Another time-consuming procedure in Algorithm 9 is "Update $\mathbb{B}$ and G". If MAC retransmission is not supported, the procedure "Update $\mathbb{B}$ and G" is specified by Algorithm 10. The main loop of Algorithm 10 has to be repeated $(|\mathbb{V}| - h_k - 1) \times h_k$ times. Removing u from G may need up to $|\mathbb{V}| - 1$ comparisons to determine which links have to be removed from G. Similarly, removing $P_k - \{n_{1,k}, n_{h_k+1,k}\}$ may need up to $(|\mathbb{V}| - 2) \times (h_k - 1)$ comparisons. In practice, we can assume that the number of nodes in the network is much greater than the hop count of the shortest path, i.e., $|\mathbb{V}| >> h_k$. Thus, the complexity of Algorithm 10 would be $O(|\mathbb{V}|)$. Therefore, the complexity of one loop of Algorithm 9 will be $O(|\mathbb{V}|^2)$ in dense networks and $O(|\mathbb{V}| \log(|\mathbb{V}|) + |\mathbb{E}|)$ in sparse networks. Note that the main loop of Algorithm 9 could be repeated up to the number of available node-disjoint routes between the two nodes, i.e., $K_{i,j}$. Thus, the worst case complexity of Algorithm 9 is $O(K_{max}|\mathbb{V}|^2)$

Table A.1 – Complexity of Algorithm 9 and its related procedure "Update $\mathbb{B}$ and G". Support of the MAC retransmission does not change the complexity order.

Algorithm/Procedure	Sparse networks	Dense networks
Update $\mathbb{B}$ and G	$O(|\mathbb{V}|)$	$O(|\mathbb{V}|)$
Algorithm 9	$O(K_{max}|\mathbb{V}|\log(|\mathbb{V}|) + K_{max}|\mathbb{E}|)$	$O(K_{max}|\mathbb{V}|^2)$

in dense networks and $O(K_{max}|\mathbb{V}|\log(|\mathbb{V}|) + K_{max}|\mathbb{E}|)$ in sparse networks. Here, K_{max} is the maximum number of node-disjoint routes that exist between two nodes of the network. That is, $K_{max} = \max(K_{i,j}) \ \forall (i,j) \in \mathbb{V} \times \mathbb{V}$.

If MAC retransmission is supported, the procedure "Update $\mathbb{B}$ and G" is specified by Algorithm 11. This algorithm is almost similar to Algorithm 10 except that the main loop in Algorithm 11 is repeated $(|\mathbb{V}| - h_k - 1) \times 2h_k$ times. This, however, does not change the order of the complexity of this algorithm. As a result, the complexity of Algorithm,9 also remains unchanged. Table A.1 summarizes the discussion.

Appendix B

Lower Bound on Expected Node-to-node Communication Lifetime

In this appendix, we prove (8.42). To this end, we need to show that

$$T_{s_m}\sigma(K^*) + \sum_{k=0}^{K^*-1} T_k\left[\sigma(k) - \sigma(k+1)\right] \geq T_{s_m}\theta(K^*) + \sum_{k=0}^{K^*-1} T_k\left[\theta(k) - \theta(k+1)\right].$$

(B.1)

We can expand (B.1) as

$$T_{s_m}\left[\sigma(K^*) - \theta(K^*)\right] + \sum_{k=0}^{K^*-1} T_k\left[\sigma(k) - \theta(k)\right]$$

$$- \sum_{k=0}^{K^*-2} T_k\left[\sigma(k+1) - \theta(k+1)\right] \geq T_{K^*-1}\left[\sigma(K^*) - \theta(K^*)\right],$$

which can also be expressed as

$$\sum_{k=0}^{K^*-1} T_k\frac{\sigma(k) - \theta(k)}{\sigma(K^*) - \theta(K^*)} - \sum_{k=0}^{K^*-2} T_k\frac{\sigma(k+1) - \theta(k+1)}{\sigma(K^*) - \theta(K^*)} \geq T_{K^*-1} - T_{s_m}. \quad \text{(B.2)}$$

Now, we replace k by $k+1$ in the second summation of (B.2), and merge the resulting summation with the first summation. Since $T_0 = 0$, (B.2) can equivalently be expressed as

$$\sum_{k=1}^{K^*-1} (T_k - T_{k-1})\frac{\sigma(k) - \theta(k)}{\sigma(K^*) - \theta(K^*)} \geq T_{K^*-1} - T_{s_m}. \quad \text{(B.3)}$$

Therefore, if we show that (B.3) is true, recursively we can show that (B.1) is true as well. To this end, we notice that T_k is always greater than T_{k-1}. We also know that $\sigma(k) \geq \theta(k)$. Thus, the right side of (B.3) is a positive value. Note that K^* is the minimum number of routes required to prevent communication failure due to lack of routes. Hence, the source node dies after the nodes in the K^*th route. As a result, $T_{K^*-1} < T_{s_m}$. This means $T_{K^*-1} - T_{s_m} \leq 0$, which implies that (B.3) is always true.

Appendix C

Proof of Proposition 1

Using the initial value theorem of the Laplace transfer, we can establish that

$$\frac{\partial^n f_A}{\partial w^n}(0) = \lim_{s \to \infty} (-s)^{n+1} \Psi_A(s), \tag{C.1}$$

in which $\Psi_A(s)$ is the moment generation function (MGF) of the random variable A. Since all random variables X, Y_q and Z_q, $q = 1...Q$, are mutually independent, $\Psi_A(s)$ can be expressed as

$$\Psi_A(s) = \Psi_X(s) \prod_{q=1}^{Q} \Psi_{V_q}(s),$$

where $\Psi_X(s)$ is the MGF of the random variable X and $\Psi_{V_q}(s)$ is the MGF of the random variable V_q, in which V_q is defined as $V_q = Y_q Z_q / (Y_q + Z_q)$. After substituting this equivalent expression for $\Psi_A(s)$ into (C.1), and writing the limit as the product of $Q + 1$ limits, we have

$$\frac{\partial^n f_A}{\partial w^n}(0) = \lim_{s \to \infty} (-s)^{\eta_x + 1} \Psi_X(s)$$

$$\times \prod_{q=1}^{Q} \lim_{s \to \infty} (-s)^{\eta_{v_q} + 1} \Psi_{V_q}(s),$$

where the variables η_x, η_{v_q}, $q = 1...Q$, are defined so that $n = \eta_x + Q + \sum_{q=1}^{Q} \eta_{v_q}$. If we consider the initial value theorem of the Laplace transform, (C.2) can be expressed alternatively as

$$\frac{\partial^n f_A}{\partial w^n}(0) = \frac{\partial^{\eta_x} f_X}{\partial x^{\eta_x}}(0) \times \prod_{q=1}^{Q} \frac{\partial^{\eta_{v_q}} p_{V_q}}{\partial v_q^{\eta_{v_q}}}(0), \tag{C.2}$$

259

in which $f_X(x)$ represents the PDF of the random variable X and $f_{V_q}(v_q)$ is the PDF of the random variable V_q. Since X has a Gamma distribution with parameters a and $\bar{x}$, $f_X(x)$ is defined as [152]

$$f_X(x) = \frac{x^{a-1}}{\Gamma(a)\bar{x}^a} e^{-x/\bar{x}} \qquad x \geq 0, \tag{C.3}$$

where $\Gamma(a)$ is the Gamma function. Based on (C.3), it is obvious that $\frac{\partial^{\eta_x} f_X}{\partial x^{\eta_x}}(0)$ is zero for $\eta_x < a - 1$, and is equal to $1/\bar{x}^a$ for $\eta_x = a - 1$.

In order to find the value of $\frac{\partial^{\eta_{v_q}} f_{V_q}}{\partial v_q^{\eta_{v_q}}}(0)$, we first calculate the cumulative density function (CDF) of the random variable V_q, denoted by $F_{V_q}(x)$, as follows:

$$F_{V_q}(x) = \int \int_{D=\{u,v|\frac{uv}{u+v} \leq x \ \& \ u \geq 0 \ \& \ v \geq 0\}} f_{Y_q}(u) f_{Z_q}(v) \ du \ dv, \tag{C.4}$$

where $f_{Y_q}(u)$ is the PDF of the random variable Y_q and $f_{Z_q}(v)$ is the PDF of the random variable Z_q. In (C.4), we used the assumption that Y_q and Z_q are mutually independent.

The first derivative of $F_{V_q}(x)$ is actually equal to $f_{V_q}(x)$. Thus, to determine $\frac{\partial^{\eta_{v_q}} f_{V_q}}{\partial v_q^{\eta_{v_q}}}(0)$, we need to calculate the $(\eta_{v_q} + 1)^{th}$ derivative of $F_{V_q}(x)$ evaluated at $x = 0$. To this aim, we can divide the region D in (C.4) into five region and write $F_{V_q}(x)$ as

$$F_{V_q}(x) = I_1 + I_2 + I_3 + I_4 + I_5,$$

in which

$$I_1 = \int_0^{2x} \int_0^{2x} f_{Y_q}(u) f_{Z_q}(v) du dv$$

$$I_2 = \int_0^{\infty} \int_0^{x} f_{Y_q}(u) f_{Z_q}(v) du dv$$

$$I_3 = \int_0^{\infty} \int_0^{x} f_{Y_q}(u) f_{Z_q}(v) dv du$$

$$I_4 = \int_{2x}^{\infty} \int_x^{\frac{vx}{v-x}} f_{Y_q}(u) f_{Z_q}(v) du dv$$

$$I_5 = \int_{2x}^{\infty} \int_x^{\frac{ux}{u-x}} f_{Y_q}(u) f_{Z_q}(v) dv du.$$

To calculate the value of the $(\eta_{v_q} + 1)^{th}$ derivative of $F_{V_q}(x)$ at $x = 0$, we need to find the value of the corresponding derivative of each of these five integrals at $x = 0$, and add these values together. Following these steps, we can show that

$$\frac{\partial^{\eta_{v_q}} f_{V_q}}{\partial x^{\eta_{v_q}}}(0) = \frac{\partial^{\eta_{v_q}} f_{Y_q}}{\partial u^{\eta_{v_q}}}(0) + \frac{\partial^{\eta_{v_q}} f_{Z_q}}{\partial v^{\eta_{v_q}}}(0). \tag{C.5}$$

Since $Y_q \sim g(b_q, \bar{y}_q)$ and $Z_q \sim g(c_q, \bar{z}_q)$ and we assumed b_q and c_q are integers, $\frac{\partial^{\eta_{v_q}} f_{Y_q}}{\partial u^{\eta_{v_q}}}(0)$ is equal to 0 for $\eta_{v_q} < b_q - 1$ and is equal to $1/\bar{y}_q^{b_q}$ for $\eta_{v_q} = b_q - 1$. Moreover, $\frac{\partial^{\eta_{v_q}} f_{Z_q}}{\partial v^{\eta_{v_q}}}(0)$ is equal to 0 for $\eta_{v_q} < c_q - 1$ and is equal to $1/\bar{z}_q^{c_b}$ for $\eta_{v_q} = c_q - 1$. Taking into account these facts and the aforementioned fact that $\frac{\partial^{\eta_x} f_X}{\partial x^{\eta_x}}(0)$ is zero for $\eta_x < a - 1$ and is equal to $1/\bar{x}^a$ for $\eta_x = a - 1$, and considering (C.2), we can conclude that

$$
\frac{\partial^n f_A}{\partial w^n}(0) = \frac{1}{\bar{x}^a} + \prod_{q=1}^{Q} \left(\frac{1}{\bar{y}_q^{b_q}} \cdot 1_{b_q \leq c_q} + \frac{1}{\bar{z}_q^{c_b}} \cdot 1_{c_q \leq b_q} \right)
$$

(C.6a)

$$
n = a + -1 + \sum_{q=1}^{Q} \min(b_q, c_q).
$$

(C.6b)

Appendix D

List of Algorithms

Table D.1 – Energy-efficient routing algorithms and their characteristics in terms of information they consider in routing.

Algorithm	Energy Cost of Tx. and Rx Circuits	Link Reliability	MAC Retx.	E2E Retx.	Proposed in
RMER	+	+	+	+	This thesis
Unified RMER	+	+	+	-	This thesis
PAMAS	-	-	-	-	Literature
PARO	-	-	-	-	Literature
MTTPR	Only Rx.	-	-	-	Literature
MPR	-	+	+	-	Literature
BAMER	-	+	-	+	Literature

Table D.2 – Battery-aware routing algorithms and their characteristics in terms of information they consider in routing.

Algorithm	Battery Energy	Energy of Tx. and Rx.	Link Reliability	Type of Power Supply	Single or Bi Objective	Proposed in
RMECR	+	+	+	-	Single	This thesis
RMLNR	+	+	+	+	Single	This thesis
RMLNR-LM	+	+	+	+	Bi (LM)	This thesis
RMLNR-WSA	+	+	+	+	Bi (WSA)	This thesis
RLBNR	-	+	+	+	Single	This thesis
RLBNR-LM	-	+	+	+	Bi (LM)	This thesis
RMLNR-WSA	-	+	+	+	Bi (WSA)	This thesis
MBCR	+	-	-	-	Single	Literature
MMBCR	+	-	-	-	Single	Literature
CMMBCR	+	Partially	-	-	Single	Literature
MRPC	+	Partially	+	-	Single	Literature
CMRPC	+	Partially	+	-	Single	Literature

Table D.3 – Topology control algorithms and their characteristics.

Algorithm	Fault Tolerant	Localized or Centralized	Type of Power Supply	Min-Max Optimality	Proposed in
HFLTC	k-vertex	Localized	+	+	This thesis
HFCTC	k-vertex	Centralized	+	+	This thesis
FLSS	k-vertex	Localized	-	+	Literature
FGSS	k-vertex	Centralized	-	+	Literature
Yao	k-vertex	Localized	-	-	Literature
CBTC	k-vertex	Localized	-	-	Literature
LTRT	k-edge	Localized	-	-	Literature

Appendix E

Notations

$\mathbb{V}$	the set of nodes of the network
$\mathbb{E}$	the set of links of the network
$G(\mathbb{V}, \mathbb{E})$	a graph representing the network topology
N	the number of nodes in the network
$\mathbb{V}_b$	the set of BP nodes of the network
$\mathbb{E}_b$	the set of BP links of the network
$\mathbb{V}_m$	the set of MP nodes of the network
$\mathbb{E}_m$	the set of MP links of the network
(u, v)	the physical link from u to v
$w_{u,v}$	the weight of the link between u and v
$P_{u,v}$	the transmission power from u to v
$p_{u,v}(x)$	the PDR of (u, v) for packets of length x bits
$L_{u,v}(x)$	the reliability of (u, v) for packets of length x bits
$d_{u,v}$	the distance between u and v
P_u	the maximum transmission power of u
D_u	the maximum transmission range of u
B_u	the remaining battery energy of u
B	the maximum battery energy of nodes
$id(u)$	the identifier of u
$g(u)$	the idle-mode energy consumption rate of u
$\mathbb{N}_u^{\mathbb{V}}$	the set of neighbors of u
f_u	a ligic-wise variable specifying the type of power supply of u
D_{max}	the common transmission range of nodes in homogenous networks
η	the path-loss exponent
α	an energy consumption parameter of the transmitter

β	an energy consumption parameter of the transmitter
ϵ_r	an energy consumption parameter of the receiver
κ	the power efficiency of transmitting power amplifier
r	the data rate of the physical link
$\bar{\mathfrak{X}}_{u,v}(L_d)$	the ETX of data packets of size L_d bits sent over (u,v)
$\bar{\mathfrak{Y}}_{u,v}(L_a)$	the ETX of MAC acknowledgements of size L_a bits sent over (u,v)
$\bar{\mathfrak{X}}_{u,v}(L_e)$	the ETX of E2E acknowledgements of size L_e bits sent over (u,v)
$\mathcal{P}(s,v)$	a path between s and v in the network
$\mathcal{C}(\mathcal{P}(s,v))$	the energy cost of the path between s and v
$\bar{\mathfrak{X}}(\mathcal{P}(s,v))$	the accumulated ETX of the path between s and v
$K_{s,v}$	the number of node-disjoint paths between s and v
$T_{s,v}$	the lifetime of node-to-node communication between s and v
$\mathcal{N}$	the noise power
$\mathbf{S}_u^{(m)}$	the mth a transmitted OSTBC matrix by u
$\mathbf{U}_{uv}^{(m)}$	the mth a received signal matrix of the MIMO link between u and v
$\mathbf{H}_{uv}^{(m)}$	the mth a channel coefficient matrix of the MIMO link between u and v

Appendix F

Abbreviations

AF	Amplify and Forward
AODV	Ad Hoc On-Demand Distance Vector
ARQ	Automatic Repeat-reQuest
BAMER	Basic Algorithm for Minimum Energy Routing
BER	Bit Error Rate
BP	Battery-Powered
BPSK	Binary Phase Shift Keying
CBTC	Cone-Based distributed Topology Control
CCK	Complementary Code Keying
CMDR	Conditional Minimum battery Drain Routing
CMMBCR	Conditional Max-Min Battery Cost Routing
CMRPC	Conditional Maximum Residual Packet Capacity
CRC	Cyclical Redundancy Check
CSMA/CA	Carrier Sense Multiple Access with Collision Avoidance
CST	Cooperative Signal Transmission
DF	Decode and Forward
E2E	End to End
EPP	Expected energy Per Packet
ETX	Expected Transmission Count
FCS	Frame Check Sequence
FGSS	Fault-tolerate Global Spanning Subgraph
FLSS	Fault-tolerate Local Spanning Subgraph
HFCTC	Heterogeneous Fault-Tolerant Centralized Topology Control
HFLTC	Heterogeneous Fault-Tolerant Localized Topology Control
ICT	Information and Communication Technology

IEEE	Institute of Electrical and Electronics Engineers
IF	Intermediate Frequency
IP	Internet Protocol
ITU	International Telecommunication Union
LM	Lexicographic Method
LNA	Low-Noise Amplifier
LTRT	Local Tree-based Reliable Topology
MAC	Medium Access Control
MANET	Mobile Ad Hoc Network
MBCR	Minimum Battery Cost Routing
MCP	Maximum Collision Probability
MDR	Minimum battery Drain Routing
MEP	Minimum Energy Path
MIMO	Multi-Input Multi-Output
MMBCR	Max-Min Battery Cost Routing
MP	Mains-Powered
MPR	Minimum Power Routing
MRPC	Maximum Residual Packet Capacity
MTTPR	Minimum Total Transmission Power Routing
OLSR	Optimized Link State Routing
OQPSK	Offset Quaternary Phase Shift Keying
OSI	Open Systems Interconnection
OSTBC	Orthogonal Space Time Block Code
PA	Power Amplifier
PAMAS	Power-Aware Multi-Access Protocol with Signaling
PARO	Power-Aware Routing Optimization
PDF	Probability Density Function
PDR	Packet Delivery Ratio
PF	Process and Forward
PHY	Physical Layer
PN	Personal Network
PNC	Pico-Net Controller
QoS	Quality of Service
QPSK	Quaternary Phase Shift Keying
RF	Radio Frequency
RLBNR	Reliable Least BP Nodes Routing
RMECR	Reliable Minimum Energy Cost Routing
RMER	Reliable Minimum Energy Routing
RMLNR	Reliable Minimum battery cost with Least BP Nodes Routing
RREP	Route Reply

RREQ	Route Request
RSSI	Received Signal Strength Indicator
SER	Symbol Error Rate
SNR	Signal to Noise Ratio
TCP	Transmission Control Protocol
TDMA	Time Division Multiple Access
TNO	Nederlandse Organisatie voor Toegepast Natuurwetenschappelijk Onderzoek (Netherlands Organization for Applied Scientific Research)
TPC	Transmission Power Control
TRANS	Trans sector Research Academy for Complex Networks and Services
UDP	User Datagram Protocol
UHF	Ultra High Frequency
UMTS	Universal Mobile Telephony System
UWB	Ultra-Wideband
WiFi	Wireless Fidelity
WiMax	Worldwide Interoperability for Microwave Access
WLAN	Wireless Local Area Network
WMAN	Wireless Metropolitan Area Network
WPAN	Wireless Personal Area Network
WSA	Weighted Sum Approach
WWRF	Wireless World Research Forum

Bibliography

[1] N. Baken, N. van Belleghem, E. van Boven, and A. de Korte., "Unravelling 21st century riddles -universal network visions from a human perspective," *The Journal of The Communication Network*, vol. 5, no. 5, pp. 11–20, 2007. 1

[2] C. K. Toh, *Ad Hoc Mobile Wireless Networks: Protocols and Systems.* Prentice Hall, 2002. 2

[3] S. Basagni, M. Conti, S. Giordano, and I. Stojmenovic, *Mobile Ad Hoc Networking.* Wiley-IEEE Press, 2004. 2

[4] A. Hac, *Wireless Sensor Network Designs.* John Wiley and Sons, 2003. 4

[5] J. Zheng and A. Jamalipour, *Wireless Sensor Networks: A Networking Perspective.* Wiley, 2009. 4

[6] V. Lesser, C. L. Ortiz, and M. Tambe, *Distributed Sensor Networks: A Multiagent Perspective.* Kluwer, 2003. 4

[7] I. G. M. M. Niemegeers and S. M. Heemstra De Groot, "Research issues in ad-hoc distributed personal networking," *Wireless Personal Communications*, vol. 26, no. 2-3, pp. 149–167, 2003. 5, 107

[8] M. Jacobsson, I. Niemegeers, and S. H. de Groot, *Personal Networks: Wireless Networking for Personal Devices.* Wiley, 2010. 5

[9] E. Aarts and J. Encarnao, *True Visions: The Emergence of Ambient Intelligence.* Springer, 2006. 6

[10] W. Mohr et al., *The Book of Visions 2000 - Visions of the Wireless World.* Wireless Strategic Initiative, November 2000. 7

271

[11] J. Vazifehdan, M. G. Hawas, R. Hekmat, and I. Niemegeers, "Design of dependable personal networks," in *3rd international workshop on adaptive and dependable mobile ubiquitous systems (ADAMUS '09)*, pp. 1–6, 2009. 8

[12] M. Jacobsson, *Personal Networks -An architecture for self-organized personal wireless communications*. PhD thesis, Delft University of Technology, 2008. 8

[13] Y. Gu, *Personal Networks: Mobility and Clustering.* PhD thesis, Delft University of Technology, 2010. 8, 9

[14] J. Zhou, *Impact of Wirelsss Link Quality across Communication Layers*. PhD thesis, Delft University of Technology, 2010. 8

[15] M. Ghader, *Service Discovery and Use in Personal Networks.* PhD thesis, University of Surrey, 2008. 8

[16] R. Hekmat, *Fundamental properties of wireless mobile ad-hoc networks*. PhD thesis, Delft University of Technology, 2005. 8

[17] X. Shi and G. Stromberg, "Syncwuf: An ultra low-power mac protocol for wireless sensor networks," *IEEE Transactions on Mobile Computing*, vol. 6, no. 1, pp. 115 –125, January 2007. 9

[18] C.-M. Chao, J.-P. Sheu, and I.-C. Chou, "An adaptive quorum-based energy conserving protocol for ieee 802.11 ad hoc networks," *IEEE Transactions on Mobile Computing*, vol. 5, no. 5, pp. 560 – 570, May 2006. 9

[19] R. Jurdak, A. Ruzzelli, and G. O'Hare, "Radio sleep mode optimization in wireless sensor networks," *IEEE Transactions on Mobile Computing*, vol. 9, no. 7, pp. 955 –968, July 2010. 9

[20] Y. Wu, X.-Y. Li, Y. Liu, and W. Lou, "Energy-efficient wake-up scheduling for data collection and aggregation," *IEEE Transactions on Parallel and Distributed Systems*, vol. 21, no. 2, pp. 275 –287, February 2010. 9

[21] O. Younis and S. Fahmy, "Heed: a hybrid, energy-efficient, distributed clustering approach for ad hoc sensor networks," *IEEE Transactions on Mobile Computing*, vol. 3, no. 4, pp. 366 – 379, October-December 2004. 9

[22] S. Basagni, M. Mastrogiovanni, A. Panconesi, and C. Petrioli, "Localized protocols for ad hoc clustering and backbone formation: a performance comparison," *IEEE Transactions on Parallel and Distributed Systems*, vol. 17, no. 4, pp. 292 – 306, April 2006. 9

[23] *IEEE 802.15.4: Wireless Medium Access Control (MAC) and Physical Layer (PHY) Specifications for Low-Rate Wireless Personal Area Networks (LR-WPANs).* IEEE Computer Society, 2003. 13

[24] *IEEE 802.15.3: Wireless Medium Access Control (MAC) and Physical Layer (PHY) Specifications for High Rate Wireless Personal Area Networks (WPAN).* IEEE Computer Society, 2003. 13

[25] X. An, J. Vazifehdan, R. Prasad, R. Hekmat, H. Harada, and I. Niemegeers, "Extending wpans to support multi-hop communication with qos provisioning," in *7th IEEE Consumer Communications and Networking Conference (CCNC)*, January 2010. 14

[26] *IEEE 802.11b: Wireless LAN Medium Access Control (MAC) and Physical Layer (PHY) specifications: Higher-Speed Physical Layer Extension in the 2.4 GHz Band.* IEEE Computer Society, 1999. 14

[27] *IEEE 802.1lg: Wireless LAN Medium Access Control (MAC) and Physical Layer (PHY) specifications Amendment 4: Further Higher Data Rate Extension in the 2.4 GHz Band.* IEEE Computer Society, 2003. 14

[28] *IEEE 802.1ln: Wireless LAN Medium Access Control (MAC) and Physical Layer (PHY) specifications Amendment 5: Enhancements for Higher Throughput.* IEEE Computer Society, 2009. 14

[29] *IEEE 802.16: Air Interface for Broadband Wireless Access Systems.* IEEE Computer Society, 2009. 14, 15

[30] J. Eriksson, M. Faloutsos, and S. V. Krishnamurthy, "Dart: Dynamic address routing for scalable ad hoc and mesh networks," *IEEE/ACM Transactions on Networking*, vol. 15, pp. 119 –132, Frb. 2007. 17

[31] J. Kuruvila, A. Nayak, and I. Stojmenovic, "Hop count optimal position-based packet routing algorithms for ad hoc wireless networks with a realistic physical layer," *IEEE Journal on Selected Areas in Communications*, vol. 23, pp. 1267 – 1275, June 2005. 17

[32] K. Sanzgiri, D. LaFlamme, B. Dahill, B. Levine, C. Shields, and E. Belding-Royer, "Authenticated routing for ad hoc networks," *IEEE Journal on Selected Areas in Communications*, vol. 23, pp. 598 – 610, March 2005. 17

[33] J.-H. Song, V. Wong, and V. Leung, "Efficient on-demand routing for mobile ad hoc wireless access networks," *IEEE Journal on Selected Areas in Communications*, vol. 22, pp. 1374 – 1383, Sept. 2004. 17

[34] L. Abusalah, A. Khokhar, and M. Guizani, "A survey of secure mobile ad hoc routing protocols," *IEEE Communications Surveys Tutorials*, vol. 10, no. 4, pp. 78 –93, 2008. 17

[35] A. Abdrabou and W. Zhuang, "Statistical qos routing for ieee 802.11 multihop ad hoc networks," *IEEE Transactions on Wireless Communications*, vol. 8, pp. 1542 –1552, March 2009. 17

[36] P. Jacquet, B. Mans, P. Muhlethaler, and G. Rodolakis, "Opportunistic routing in wireless ad hoc networks: upper bounds for the packet propagation speed," *IEEE Journal on Selected Areas in Communications*, vol. 27, pp. 1192 –1202, Sept. 2009. 17, 18

[37] Z. Haas, J. Halpern, and L. Li, "Gossip-based ad hoc routing," *IEEE/ACM Transactions on Networking*, vol. 14, pp. 479 –491, June 2006. 17

[38] X. Hong, K. Xu, and M. Gerla, "Scalable routing protocols for mobile ad hoc networks," *IEEE Network*, vol. 16, pp. 11 –21, July/August 2002. 17

[39] F. Kuhn, R. Wattenhofer, and A. Zollinger, "An algorithmic approach to geographic routing in ad hoc and sensor networks," *IEEE/ACM Transactions on Networking*, vol. 16, pp. 51 –62, Feb. 2008. 17

[40] T. Clausen and P. Jacquet, "Rfc-3626 optimized link state routing protocol (olsr)," 2003. available online: www.ietf.org/rfc/rfc3626.txt. 17

[41] D. B. Johnson and D. A. Maltz, "Dynamic source routing in ad hoc wireless networks," in *Mobile Computing*, pp. 153–181, Kluwer Academic Publishers, 1996. 17, 18

[42] C. E. Perkins, E. M. Royer, and S. R. Das, "Ad-hoc on-demand distance venctor (aodv) protocol," in *RFC 3561*, 2001. 17, 18

[43] F. Li and Y. Wang, "Routing in vehicular ad hoc networks: A survey," *IEEE Vehicular Technology Magazine*, vol. 2, pp. 12 –22, June 2007. 17

[44] H. Yih-Chun and A. Perrig, "A survey of secure wireless ad hoc routing," *IEEE Security Privacy*, vol. 2, pp. 28 –39, May-June 2004. 17

[45] D. B. Johnson, D. A. Maltz, and Y. C. Hu, "The dynamic source routing protocol (dsr) for mobile ad hoc networks for ipv4," *IETF MANET Working Group (Technical Report)*, February 2007. 18, 124, 125

[46] A. Kumar, L. C. Reddy., and P. S. Hiremath, "Performance comparison of wireless mobile ad-hoc network routing protocols," *International Journal of Computer Science and Network Security*, vol. 8, pp. 433–459, June 2008. 18

[47] J. Broch, D. A. Maltz, D. B. Johnson, Y.-C. Hu, and J. Jetcheva, "A performance comparison of multi-hop wireless ad hoc network routing protocols," in *Proceedings of the 4th annual ACM/IEEE international conference on Mobile computing and networking (MobiCom '98)*, pp. 85–97, 1998. 18

[48] C. Perkins, E. Royer, S. Das, and M. Marina, "Performance comparison of two on-demand routing protocols for ad hoc networks," *IEEE Personal Communications,*, vol. 8, pp. 16–28, Feb. 2001. 18

[49] M. Abomasan, T. Wysoeki, and J. Lipman, "Performance investigation on three-classes of manet routing protocols," in *Proceedings of 2005 Asia-Pacific Conference on Communications*, pp. 774–778, Oct. 2005. 18

[50] J. Proakis, *Digital Communications.* McGraw-Hill, 4 ed., 2000. 22, 224, 228, 243

[51] H. Bertoni, *Radio Propagation for Modern Wireless Systems.* Upper Saddle River, NJ, USA: Prentice-Hall, Inc., 2000. 23

[52] R. Hekmat, *Ad-hoc networks: fundamental properties and network topologies.* Springer, 2006. 23, 24

[53] C. Bettstetter, "On the minimum node degree and connectivity of a wireless multihop network," in *Proceedings of the 3rd ACM International Symposium on Mobile Ad Hoc Networking and Computing (MobiHoc '02)*, pp. 80–91, June 2002. 23, 24, 25, 179, 206, 218

[54] R. Hekmat and P. Van Mieghem, "Degree distribution and hopcount in wireless ad-hoc networks," in *Proceedings on the 11th IEEE International Conference on Networks (ICON'03)*, pp. 603 – 609, September 2003. 23

[55] M. D. Penrose, "On k-connectivity for a geometric random graph," *Random Structures and Algorithms*, vol. 15, no. 2, pp. 145–164, 1999. 23, 24, 179

[56] Q. Wang, M. Hempstead, and W. Yang, "A realistic power consumption model for wireless sensor network devices," in *Proceedings of 3rd Annual IEEE Communications Society on Sensor and Ad Hoc Communications and Networks (SECON '06)*, pp. 286 –295, September 2006. 29, 30, 50

[57] P. Liaskovitis and C. Schurgers, "Energy consumption of multi-hop wireless networks under throughput constraints and range scaling," *Mobile Computing and Communications Review*, vol. 13, no. 3, pp. 1–13, 2009. 29, 30, 50

[58] W. R. Heinzelman, A. Chandrakasan, and H. Balakrishnan, "Energy-efficient communication protocol for wireless microsensor networks," in *Proc. of 33rd Hawaii International Conference on System Sciences (HICSS'00)*, p. 8020, 2000. 29, 30, 50

[59] R. Hekmat and X. An, "A framework for performance evaluation of wireless ad-hoc and sensor networks," in *Proc. of 15th IEEE International Conference on Networks*, pp. 412–418, November 2007. 29, 50

[60] J. Zhu, C. Qiao, and X. Wang, "On accurate energy consumption models for wireless ad hoc networks," *IEEE Transactions on Wireless Communications*, vol. 5, no. 11, pp. 3077–3086, November 2006. 29, 30, 59

[61] "Cc2420 data sheet." Texas Instruments, [available online] http://focus.ti.com/lit/ds/symlink/cc2420.pdf. 31, 35

[62] "Cc1000 data sheet." Texas Instruments, [available online] http://focus.ti.com/lit/ds/symlink/cc2420.pdf. 31, 35

[63] B. Burns and J.-P. Ebert, "Power consumption, throughput, and packet error measurements of an ieee 802.11 interface," *TKN Technical Report TKN-01-007, Telecommunication Networks Group, Technical University Berlin.* 31, 35

[64] J. Gomez and A. Campbell, "Variable-range transmission power control in wireless ad hoc networks," *IEEE Transactions on Mobile Computing*, vol. 6, no. 1, pp. 87–99, January 2007. 33

[65] S. Panichpapiboon, G. Ferrari, and O. Tonguz, "Optimal transmit power in wireless sensor networks," *IEEE Transactions on Mobile Computing*, vol. 5, no. 10, pp. 1432 –1447, October 2006. 33

[66] W. L. Huang and K. Letaief, "Cross-layer scheduling and power control combined with adaptive modulation for wireless ad hoc networks," *IEEE Transactions on Communications*, vol. 55, no. 4, pp. 728–739, April 2007. 33

[67] A. Muqattash and M. M. Krunz, "A distributed transmission power control protocol for mobile ad hoc networks," *IEEE Transactions on Mobile Computing*, vol. 3, no. 2, no. 2, pp. 113–128, 2004. 33

[68] W. Wang, V. Srinivasan, and K.-C. Chua, "Power control for distributed mac protocols in wireless ad hoc networks," *IEEE Transactions on Mobile Computing*, vol. 7, no. 10, pp. 1169–1183, 2008. 33

[69] P. Gupta and P. Kumar, "The capacity of wireless networks," *IEEE Transactions on Information Theory*, vol. 46, no. 2, pp. 388–404, March 2000. 33

[70] N. Li and J. C. Hou, "Localized fault-tolerant topology control in wireless ad hoc networks," *IEEE Transactions on Parallel and Distributed Systems*, vol. 17, pp. 307–320, 2006. 33, 154, 158, 160, 161, 164, 166

[71] P. Mahasukhon, M. Hempel, H. Sharif, T. Zhou, S. Ci, and H.-H. Chen, "Ber analysis of 802.11b networks under mobility," in *Proceedings of IEEE ICC '07*, pp. 4722 –4727, June 2007. 49

[72] B. Sklar, *Digital communications: fundamentals and applications*. Prentice-Hall, Inc., 1988. 49

[73] http://homepage.tudelft.nl/w5p50/E2Code.zip. 50

[74] S. Singh and C. Raghavendra, "Pamas - power aware multi-access protocol with signalling for ad hoc networks," *ACM Computer Communication Review*, vol. 28, pp. 5–26, 1999. 54, 63, 75, 88

[75] J. Gomez, A. T. Campbell, M. Naghshineh, and C. Bisdikian, "Paro: supporting dynamic power controlled routing in wireless ad hoc networks," *Wireless Networks*, vol. 9, no. 5, pp. 443–460, 2003. 54, 63, 75, 88

[76] S. Singh, M. Woo, and C. S. Raghavendra, "Power-aware routing in mobile ad hoc networks," in *Proc. of 4th annual ACM/IEEE international conference on Mobile computing and networking*, (Dallas, Texas, USA), October 1998. 54, 63, 75, 108

[77] S. Banerjee and A. Misra, "Minimum energy paths for reliable communication in multi-hop wireless networks," in *In Proceedings of Mobihoc*, pp. 146–156, 2002. 54, 59, 75, 88, 97, 102

[78] Q. Dong, S. Banerjee, M. Adler, and A. Misra, "Minimum energy reliable paths using unreliable wireless links," in *Proceedings of the 6th ACM international symposium on mobile ad hoc networking and computing*, pp. 449–459, 2005. 54, 59, 75, 88, 100

[79] A. Misra and S. Banerjee, "Mrpc: Maximizing network lifetime for reliable routing in wireless environments," in *Proceedings of IEEE Wireless Communications and Networking Conference*, pp. 800–806, 2002. 54, 59, 63, 75, 108, 112

[80] X.-Y. Li, Y. Wang, H. Chen, X. Chu, Y. Wu, and Y. Qi, "Reliable and energy-efficient routing for static wireless ad hoc networks with unreliable links," *IEEE Trans. Parallel Distrib. Syst.*, vol. 20, no. 10, pp. 1408–1421, 2009. 54, 59, 75

[81] X. yang Li, H. Chen, Y. Shu, X. Chu, and Y. wei Wu, "Energy efficient routing with unreliable links in wireless networks," in *IEEE International Conference on Mobile Adhoc and Sensor Systems Conference*, 2006. 54, 59, 75

[82] C. Toh, "Maximum battery life routing to support ubiquitous mobile computing in wireless ad hoc networks," *IEEE Communications Magazine*, vol. 39, no. 6, pp. 138–147, June 2001. 54, 75, 88, 97, 108, 110

[83] M. Mathis, J. Mahdavi, S. Floyd, and A. Romanow, "TCP Selective Acknowledgment Options." RFC 2018, October 1996. 59

[84] D. S. J. De Couto, D. Aguayo, J. Bicket, and R. Morris, "A high-throughput path metric for multi-hop wireless routing," in *the 9th annual international conference on Mobile computing and networking*, pp. 134–146, 2003. 75, 89, 96

[85] D. Kim, J. J. G. luna aceves, K. Obraczka, J. carlos Cano, and P. Manzoni, "Routing mechanisms for mobile ad hoc networks based on the energy drain rate," *IEEE Transactions on Mobile Computing*, vol. 2, no. 2, pp. 161–173, April-June 2003. 75, 108, 113

[86] J.-H. Chang and L. Tassiulas, "Maximum lifetime routing in wireless sensor networks," *IEEE/ACM Transactions on Networking*, vol. 12, no. 4, pp. 609–619, August 2004. 75, 108, 113

[87] A. Nagy, A. El-Kadi, and M. Mikhail, "Swarm congestion and power aware routing protocol for manets," in *Proc. of 6th Annual Communication Networks and Services Research Conference*, (Nova Scotia, Canada), May 2008. 75, 108, 113

[88] A. B. Mohanoor, S. Radhakrishnan, and V. Sarangan, "Online energy aware routing in wireless networks," *Ad Hoc Networks*, vol. 7, no. 5, pp. 918–931, July 2009. 75, 108, 113

[89] T. H. Cormen and C. S. Charles E. Leiserson, Ronald L. Rivets, *Introduction to Algorithms (Second Edition.* MIT Press, 2001. 77

[90] M. L. Fredman and R. E. Tarjan, "Fibonacci heaps and their uses in improved network optimization algorithms," *Journal of ACM*, vol. 34, no. 3, pp. 596–615, July 1987. 77, 78

[91] A. Paul and E. Wan, "Rssi-based indoor localization and tracking using sigma-point kalman smoothers," *IEEE Journal of Selected Topics in Signal Processing*, vol. 3, no. 5, pp. 860 –873, October 2009. 89

[92] H.-S. Ahn and W. Yu, "Environmental-adaptive rssi-based indoor localization," *IEEE Transactions on Automation Science and Engineering*, vol. 6, no. 4, pp. 626 –633, October 2009. 89

[93] C. Savarese and J. M. Rabaey, "Locationing in distributed ad-hoc wireless sensor networks," in *Proceedings of IEEE ICASSP*, pp. 2037–2040, 2001. 89

[94] T. He, C. Huang, B. M. Blum, J. A. Stankovic, and T. Abdelzaher, "Range-free localization schemes for large scale sensor networks," in *Proceedings of the 9th annual international conference on Mobile computing and networking (Mobicom'03)*, pp. 81–95, 2003. 89

[95] K.-H. Kim and K. G. Shin, "On accurate measurement of link quality in multi-hop wireless mesh networks," in *Proceedings of ACM MobiCom*, pp. 38–49, 2006. 89

[96] H. Zhang, A. Arora, and P. Sinha, "Link estimation and routing in sensor network backbones: Beacon-based or data-driven?," *IEEE Transactions on Mobile Computing*, vol. 8, no. 5, pp. 653 –667, May 2009. 89

[97] M. Senel, K. Chintalapudi, D. Lal, A. Keshavarzian, and E. Coyle, "A kalman filter based link quality estimation scheme for wireless sensor networks," pp. 875–880, November 2007. 89

[98] L. Verma, S. Kim, S. Choi, and S.-J. Lee, "Reliable, low overhead link quality estimation for 802.11 wireless mesh networks," June 2008. 89

[99] K. Wang, Y.-l. Xu, G.-l. Chen, and Y.-f. Wu, "Power-aware on-demand routing protocol for manet," in *Proc. of 24th International Conference on Distributed Computing Systems*, (Tokyo, Japan), March 2004. 108, 113

[100] V. Rishiwal, M. Yadav, and S. Verma, "Power aware routing to support real time traffic in mobile adhoc networks," in *Proc. of 1st International Conference on Emerging Trends in Engineering and Technology*, (Nagpur, India), July 2008. 108, 113

[101] J. Vazifehdan, R. Hekmat, R. V. Prasad, and I. Niemegeers, "Performance evaluation of power-aware routing algorithms in personal networks," in *The 28th IEEE International Performance Computing and Communications Conference (IPCCC '09)*, pp. 95–102, Dec. 2009. 115

[102] K. Deb, *Multi-Objective Optimization Using Evolutionary Algorithms*. Wiley, June 2002. 118

[103] M. . Henig, "The shortest path problem with two objective functions," *European Journal of Operational Research*, vol. 25, no. 2, pp. 281–291, 1986. 118

[104] B.-S. J. and D. Shier, "An empirical investigation of some bicriterion shortest path algorithms," *European Journal of Operational Research*, vol. 43, no. 2, pp. 216–224, 1989. 118

[105] H. Corley and I. Moon, "Shortest paths in networks with vector weights," *Journal of Optimization Theory and Applications*, vol. 46, no. 1, pp. 79–86, 1989. 118

[106] P. Hansen, "Bicriterion path problems," *Lecture Notes in Economics and Mathematical Systems*, pp. 109–127, 1980. 118

[107] E. Q. V. Martins, "On a multicriteria shortest path problem," *European Journal of Operational Research*, vol. 16, no. 2, pp. 236–245, 1984. 118, 119

[108] A. Raith and M. Ehrgott, "A comparison of solution strategies for biobjective shortest path problems," *Computers and Operations Research*, vol. 36, pp. 1299–1331, April 2009. 119

[109] C. Bettstetter and C. Wagner, "The node distribution of the random waypoint mobility model for wireless ad hoc networks," *IEEE Transactions on Mobile Computing*, vol. 2, no. 3, pp. 257–269, July-September 2003. 141

[110] M. Bahramgiri, M. Hajiaghayi, and V. S. Mirrokni, "Fault-tolerant and 3-dimensional distributed topology control algorithms in wireless multi-hop networks," *Wireless Networks*, vol. 12, no. 2, no. 2, pp. 179–188, 2006. 154

[111] X.-Y. Li, P.-J. Wan, Y. Wang, and C.-W. Yi, "Fault tolerant deployment and topology control in wireless ad hoc networks," *Wireless Communications and Mobile Computing*, vol. 4, no. 1, no. 1, pp. 109–125, 2004. 154

[112] K. Miyao, H. Nakayama, N. Ansari, and N. Kato, "Ltrt: An efficient and reliable topology control algorithm for ad-hoc networks," *IEEE Transactions on Wireless Communications*, vol. 8, no.12, pp. 6050–6058, December 2009. 154

[113] E. Dinic, "Analgorithm for the solution of the max-flow problem with the polynomial estimation," *Doklaya Akademii Nauk SSSR (in Russian)*, vol. 194, no. 4, pp. 1277–264, 1970. 157

[114] Y. Dinitz, "Dinitz' algorithm: The original version and even's version," *In Oded Goldreich, Arnold L. Rosenberg, and Alan L. Selman; Theoritical Computer Science: Essays in Memory of Shimon Even*, pp. 218–240, Springer, 2006. 157

[115] T. Philips, S. Panwar, and A. Tantawi, "Connectivity properties of a packet radio network model," *IEEE Transactions on Information Theory*, vol. 35, pp. 1044–1047, September 1989. 179

[116] P. Piret, "On the connectivity of radio networks," *IEEE Transactions on Information Theory*, vol. 37, pp. 1490–1492, September 1991. 179

[117] M. Desai and D. Manjunath, "On the connectivity in finite ad hoc networks," *IEEE Communications Letters*, vol. 6, pp. 437–439, October 2002. 179

[118] A. Ghasemi and S. Nader-Esfahani, "Exact probability of connectivity one-dimensional ad hoc wireless networks," *IEEE Communications Letters*, vol. 10, pp. 251–253, April 2006. 179

[119] A. Misra, G. Teltia, and A. Chaturvedi, "On the connectivity of circularly distributed nodes in ad hoc wireless networks," *IEEE Communications Letters*, vol. 12, pp. 717–719, October 2008. 179

[120] P. Santi and D. M. Blough, "The critical transmitting range for connectivity in sparse wireless ad hoc networks," *IEEE Transactions on Mobile Computing*, vol. 2, no. 1, pp. 25–39, 2003. 179

[121] P. Santi, "The critical transmitting range for connectivity in mobile ad hoc networks," *IEEE Transactions on Mobile Computing*, vol. 4, no. 3, pp. 310–317, 2005. 179

[122] J. Diaz, D. Mitsche, and X. Perez-Gimenez, "Large connectivity for dynamic random geometric graphs," *IEEE Transactions on Mobile Computing*, vol. 8, no. 6, pp. 821–835, 2009. 179

[123] I. Dietrich and F. Dressler, "On the lifetime of wireless sensor networks," *ACM Transactions on Sensor Networks*, vol. 5, no. 1, pp. 1–39, February 2009. 179

[124] R. Madan, S. Cui, S. Lall, and A. Goldsmith, "Cross-layer design for lifetime maximization in interference-limited wireless sensor networks," in *Proceedings of INFOCOM 2005*, vol. 3, pp. 1964 – 1975 vol. 3, March 2005. 179

[125] S. Soro and W. Heinzelman, "Prolonging the lifetime of wireless sensor networks via unequal clustering," in *Proceedings of 19th IEEE International Parallel and Distributed Processing Symposium*, April 2005. 179

[126] A. Cerpa and D. Estrin, "Ascent: adaptive self-configuring sensor networks topologies," *IEEE Transactions on Mobile Computing*, vol. 3, pp. 272 – 285, July-August 2004. 179

[127] M. Cardei, M. Thai, Y. Li, and W. Wu, "Energy-efficient target coverage in wireless sensor networks," in *Proceedings of INFOCOM 2005*, vol. 3, pp. 1976 – 1984 vol. 3, March 2005. 179

[128] M. Bhardwaj and A. Chandrakasan, "Bounding the lifetime of sensor networks via optimal role assignments," in *Proceedings of INFOCOM 2002*, vol. 3, pp. 1587 – 1596 vol.3, 2002. 179

[129] B. Carbunar, A. Grama, J. Vitek, and O. Carbunar, "Redundancy and coverage detection in sensor networks," *ACM Transactions on Sensor Networks*, vol. 2, pp. 94–128, February 2006. 179

[130] H. Zhang and J. C. Hou, "On the upper bound of alpha-lifetime for large sensor networks," *ACM Transactions on Sensor Networks*, vol. 1, no. 2, pp. 272–300, 2005. 179

[131] V. Mhatre, C. Rosenberg, D. Kofman, R. Mazumdar, and N. Shroff, "A minimum cost heterogeneous sensor network with a lifetime constraint," *IEEE Transactions on Mobile Computing*, vol. 4, no. 1, pp. 4 – 15, January-February 2005. 179

[132] K. Sha and W. Shi, "Modeling the lifetime of wireless sensor networks," 2004. 179

[133] D. M. Blough and P. Santi, "Investigating upper bounds on network lifetime extension for cell-based energy conservation techniques in stationary ad hoc networks," in *Proceedings of the 8th ACM International Conference on Mobile Computing and Networking (MOBICOM*, pp. 183–192, 2002. 179

[134] F. Al-Turjman, H. Hassanein, and M. Ibnkahla, "Connectivity optimization with realistic lifetime constraints for node placement in environmental monitoring," in *Proceedings of the 34th IEEE Conference on Local Computer Networks (LCN 2009)*, pp. 617 –624, October 2009. 179

[135] X. M. Zhang, F. F. Zou, E. B. Wang, and D. K. Sung, "Exploring the dynamic nature of mobile nodes for predicting route lifetime in mobile ad hoc networks," *IEEE Transactions on Vehicular Technology*, vol. 59, pp. 1567–1572, march 2010. 179

[136] Y.-C. Tseng, Y.-F. Li, and Y.-C. Chang, "On route lifetime in multihop mobile ad hoc networks," *IEEE Transactions on Mobile Computing,*, vol. 2, pp. 366–376, oct.-dec. 2003. 179

[137] W. Najjar and J.-L. Gaudiot, "Network resilience: A measure of network fault tolerance," *IEEE Transactions on Computers*, vol. 39, no. 2, pp. 174–181, 1990. 180

[138] C. J. Colboum, "Network resilience," *SIAM Journal on Algebraic and Discrete Methods*, vol. 8, pp. 404–409, 1987. 180

[139] D. Ganesan, R. Govindan, S. Shenker, and D. Estrin, "Highly-resilient, energy-efficient multipath routing in wireless sensor networks," in *Proc. of 2nd ACM international symposium on mobile ad hoc networking and computing*, pp. 251–254, October 2001. 180, 182

[140] T. Dimitar, F. Sonja, M. Jani, and G. Aksenti, "Connection resilience to nodes failures in ad hoc networks," in *Proceedings of the 12th IEEE Mediterranean Electrotechnical Conference*, vol. 2, pp. 579–582, May 2004. 180

[141] F. Xing and W. Wang, "On the expected connection lifetime and stochastic resilience of wireless multi-hop networks," in *Proceedings of 2007 IEEE Global Telecommunications Conference*, pp. 1263–1267, November 2007. 180

[142] A. Valera, W. Seah, and S. Rao, "Improving protocol robustness in ad hoc networks through cooperative packet caching and shortest multipath routing," *IEEE Transactions on Mobile Computing*, vol. 4, no. 5, no. 5, pp. 443–457, 2005. 182

[143] S. Mueller, R. Tsang, and D. Ghosal, "Multipath routing in mobile ad hoc networks: Issues and challenges," *Lecture Notes in Computer Science (LNCS)*, vol. 2965, pp. 209–234, 2004. 182

[144] J. Laneman, D. Tse, and G. Wornell, "Cooperative diversity in wireless networks: Efficient protocols and outage behavior," *IEEE Transactions on Information Theory*, vol. 50, no. 12, pp. 3062–3080, 2004. 224, 225

[145] A. Sendonaris, E. Erkip, and B. Aazhang, "User cooperation diversity. part i. system description," *IEEE Transactions on Communications*, vol. 51, pp. 1927–1938, November 2003. 224, 225

[146] A. Sendonaris, E. Erkip, and B. Aazhang, "User cooperation diversity. part ii. implementation aspects and performance analysis," *IEEE Transactions on Communications*, vol. 51, pp. 1939 – 1948, November 2003. 224, 225

[147] A. Ribeiro, X. Cai, and G. Giannakis, "Symbol error probabilities for general cooperative links," *IEEE Transactions on Wireless Communications*, vol. 4, pp. 1264 – 1273, May 2005. 225, 239

[148] V. Tarokh, H. Jafarkhani, and A. Calderbank, "Space-time block codes from orthogonal designs," *IEEE Transactions on Information Theory*, vol. 45, pp. 1456 –1467, July 1999. 227, 228, 234

[149] G. B. Giannakis, Z. Liu, X. Ma, and S. Zhou, *Space Time Coding for Broadband Wireless Communications*. Wiley-Interscience, 2003. 227, 228

[150] H. Jafarkhani, *Space Time Coding: Theory and Practice*. Cambridge University Press, 2005. 227, 228

[151] S. Alamouti, "A simple transmit diversity technique for wireless communications," *IEEE Journal on Selected Areas in Communications*, vol. 16, pp. 1451 –1458, October 1998. 227

[152] S. U. P. A. Papoulis, *Probability, Random Variables, and Stochastic Processes*. New York, USA: McGraw-Hill Higher Education, fourth edition ed., 2001. 233, 260

[153] Z. Wang and G. Giannakis, "A simple and general parameterization quantifying performance in fading channels," *IEEE Transactions on Communications*, vol. 51, pp. 1389 – 1398, August 2003. 233

[154] P. V. Mieghem, *Performance Alalysis of Communications Networks and Systems*. Cambridge University Press, 2006. 241

Samenvatting
(Summary in Dutch)

Moderne draadloze netwerken bieden veel diensten die de communicatie tussen mensen en machines wereldwijd mogelijk maken. Mobiele telefonie, mobiel internet en HD video zijn voorbeelden van diensten die worden ondersteund door draadloze netwerken. De vooruitgang in draadloze communicatietechnologie, in combinatie met verbeteringen in de processortechnologie, heeft geresulteerd in elektronisch apparaten met zeer hoge communicatie- en dataverwerkingsmogelijkheden. Zowel kleine draagbare apparaten als geminiaturiseerde apparaten, ingebed in onze omgeving, zijn in staat geavanceerde communicatieprotocollen uit te voeren. Dit maakt het mogelijk om gedistribueerde draadloze netwerken te vormen die diensten aanbieden zonder de noodzaak voor vaste en dure infrastructuur. Dergelijke netwerken zijn bekend als draadloze multi-hop netwerken. In plaats van een infrastructuur bestaande uit krachtige basisstations wordt multi-hop communicatie gebruikt om apparaten te verbinden die buiten elkaars zend- en ontvangbereik vallen. Elk apparaat gedraagt zich als een router die datapakketjes namens andere apparaten doorstuurt. Voorbeelden hiervan zijn: ad-hoc communicatie tussen laptops in een conferentiezaal, multi-hop communicatie tussen persoonlijke apparaten thuis, en collaboratieve communicatie tussen sensoren verdeeld over een groot gebied.

Dit proefschrift richt zich op de studie van energiebewuste draadloze multi-hop netwerken, waarin energie een belangrijke factor is in het ontwerp. Draadloze multi-hop netwerken moeten energiebewust worden om twee redenen. Ten eerste, deze apparaten werken meestal met batterijen. Door het verminderen van het energieverbruik, kan op de schaarse batterij energie bespaard worden, waardoor bijvoorbeeld de autonomie van een systeem vergroot wordt. Ten tweede, door de enorme toename van deze netwerken stijgt het energieverbruik van de ICT-sector exponentieel. Energie-efficinte en energiebewuste communicatie protocollen en mechanismen worden heel belangrijk niet alleen uit het oogpunt van de operationele

levensduur van systemen, maar ook uit het oogpunt van duurzaamheid. Een reeks van nieuwe protocollen vormen het hart van dit proefschrift. Deze protocollen maken energiebewuste en energie-efficinte communicatie platformen mogelijk. Een dergelijk platform betreft verschillende lagen van de communicatiearchitectuur en houdt rekening met de onderlinge afhankelijkheid van de lagen (cross-layer) uit het oogpunt van energiebesparing. De energie-efficintie van de onderste vier lagen van de OSI Referentie Architectuur lagen, van de fysieke laag (Laag 1) tot de transport laag (Laag 4), wordt in zijn geheel beschouwd. Voor de fysieke laag, stellen wij coperatieve signaaloverdracht voor op basis van MIMO (Multi-Input Multi-Output) technologie om het zendvermogen van knooppunten te beperken zonder concessies te doen voor de link betrouwbaarheid. Voor de data link laag richten we ons op de controle van de netwerk topologie. Deze is gebaseerd op een techniek voor het ontdekken van netwerkknooppunten, die ertoe leidt dat het maximaal zendvermogen van knooppunten zo laag mogelijk gehouden wordt bij het tot stand brengen van de netwerkverbindingen. Voor de netwerklaag, stellen wij routeringalgoritmen voor die de meest energie-efficinte routes tussen twee knooppunten van het netwerk ontdekken, rekening houdend met de impact van de transmissie controle van de transport laag. Bovendien bieden deze algoritmen de mogelijkheid om het verkeer optimaal te routeren op basis van de beschikbare energie in de batterij van de knooppunten. We analyseren eveneens de verwachte levensduur van de communicatie tussen twee knooppunten in een draadloos multi-hop netwerk met een willekeurige topologie. De in dit proefschrift voorgestelde oplossingen zullen leiden tot significant energie-efficintere draadloze multi-hop netwerken. Dit proefschrift heeft een fundamenteel en theoretisch karakter en wordt onderbouwd door simulatieresultaten. Het ligt voor de hand dat een verdere onderbouwing en verfijning nodig is aan de hand van experimenteel onderzoek d.m.v. een testbed.

Acknowledgments

This dissertation would not have been possible without the guidance and the help of several individuals. They provided me their valuable assistance in the preparation and completion of this study. It is a pleasure to thank my promoter Prof. Ignas Niemegeers for his support. He gave me the freedom to choose my research topic, and supported my ideas. I greatly appreciate my co-promoter Dr. Venkatesha Prasad for his untiring effort, commitment, and the encouragement that helped me in completing this thesis. His advice improved the quality of my work and his effort played a major role in publishing the results of this study. I also thank his wife Vasanthi for reading and editing my papers. I acknowledge Prof. Nico Baken for initiating and funding this project under Dutch Research Delta and TRANS. I also thank Dr. Hamza Ouibrahim, director operations of TRANS, for supporting my work, for the cheerful talks which inspired me a lot, and for his help in translating the thesis summary to Dutch. I am also grateful to my friend, Dr. Ramin Hekmat whose advice and support helped me get through all the problems that I faced during my Ph.D research and life as well. It is my duty to thank Prof. Catholijn Jonker for her help and support during my PhD.

I acknowledge Dr. Martin Jacobsson for his help in setting up the testbeds for experimental measurements that support this study. I also enjoyed working with him as well as Dr. Ertan Onur and Dr. Jos Weber as co-authors of some of my papers. I also thank the secretaries of the Telecommunications department of TU Delft, namely Wendy, Marjon and Stefanie for their help. I am grateful to all the colleagues at 19th floor of the Faculty of Electrical Engineering, Mathematics, and Computer Science of TU Delft who provided me joyful and cheerful moments namely VP, Antonio, Anteneh, Xuile, Yue, Siyu, Javier, Wynand, Jos, Martin, Norbert, Edgar, Huijuan, Malohat, Yanying, Jinglong, and all others. My special thanks goes to my Iranian friends for making my life colorful and full of happiness: Hojat, Mohsen, Amir, Alireza, Arash, Mohamad Reza, Mehdi, Nima, Hamed, Mahmoud, Mehdi, Rahim, Saeed and other friends.

And finally, I owe my deepest gratitude to my family for all the love and the support that they gave me: my loving parents from whom I received everything,

my sister Zahra and my brother-in-law Ali for continued support during my stay in The Netherlands, and Mahin, Sahar and Nima for the happiness they shared with me.

Javad Vazifehdan
Delft, July 2011

Curriculum Vitae

Javad Vazifehdan was born in Ferdos, Iran in 1980. He finished primary and high school educations in his hometown as a top student, and received his B.Sc. from Iran University of Science and Technology, Tehran, Iran in Electrical Engineering (electronics) in 2002. He achieved the 1st rank in GPA for two semesters (1997-1998 and 1999-2000) amongst all students of the faculty of Electrical Engineering of Iran University of Science and Technology. He achieved the 85th rank in Iranian Graduate Entrance Exam in Electrical Engineering in 2002. This permitted him to start his M.Sc. in University of Tehran (the national university of Iran) focusing on Communication Systems. In the second year of his M.Sc. and while he was doing his master project, he started working as a part time engineer in Frineh company in Tehran. The focus of his work in the company was software development of the Fieldbus protocol, a real time communication protocol for process control. He received his M.Sc. degree in 2005 with honor. After graduation, he continued his job as a full time employee in Farineh, and he and his colleagues succeed to get certificate for the developed protocol from Fraunhofer IITB in Karlsruhe, Germany. In January 2007, he started his work as a PhD candidate in the Wireless and Mobile Communications (WMC) group at Delft University of Technology. In October 2010, he received the second prize in the Netelcom competition for the most scientific and innovative PhD student under Dutch Research Delta.

Publications

Journals

J.1 J. Vazifehdan, R.V. Prasad, E. Onur, and I. Niemegeers, "Energy-aware routing algorithms for ad hoc networks with heterogeneous power supplies," *Elsevier Computer Networks*, Vol. 55, Issue 15, October 2011, pp 3256-3274.

J.2 J. Vazifehdan, R.V. Prasad, M. Jacobsson, and I. Niemegeers, "An analytical energy consumption model for packet transfer over wireless links," *IEEE Communications Letters. Resubmitted after minor revision.*

J.3 J. Vazifehdan, R.V. Prasad, and I. Niemegeers, "Energy-efficient reliable routing with load balancing in wireless ad hoc networks," *IEEE Transactions on Mobile Computing. Under review.*

J.4 J. Vazifehdan, R.V. Prasad, and I. Niemegeers, "Exploiting heterogeneity of power supplies of nodes for topology control in wireless multi-hop networks," *IEEE Transactions on Wireless Communications. Under review.*

J.5 J. Vazifehdan, R.V. Prasad, and I. Niemegeers, "On the lifetime of node-to-node communication in wireless ad hoc networks," *Elsevier Computer Networks. Under review.*

J.6 J. Vazifehdan, R.V. Prasad, and I. Niemegeers, "Battery-aware routing in personal networks," *Springer Wireless Personal Communications. Under review.*

Conferences

C.1 J. Vazifehdan, R.V. Prasad, and I. Niemegeers, "Minimum battery cost reliable routing in ad hoc wireless networks," proceedings of *8th IEEE Consumer Communications and Networking Conference (CCNC)*, January 2011.

C.2 J. Vazifehdan, R.V. Prasad, E. Onur, and I. Niemegeers, "Energy-aware routing in wireless ad hoc networks with mains-powered nodes," proceedings of *Future Networks and Mobile Summit 2010*, June 2010.

C.3 J. Vazifehdan, E. Onur, and I. Niemegeers, "On the resilience of personal networks," proceedings of *5th IEEE International Symposium on Wireless Pervasive Computing (ISWPC)*, May 2010.

C.4 J. Vazifehdan, R. Hekmat, R. V. Prasad, and I. Niemegeers, "Performance evaluation of power-aware routing algorithms in personal networks," proceedings of *28th IEEE International Performance Computing and Communications Conference (IPCCC)*, pp. 95–102, December 2009.

C.5 J. Vazifehdan, R. Hekmat, R. V. Prasad, and I. Niemegeers, "A bi-objective power-aware routing algorithm for personal networks," proceedings of *3rd IEEE International Conference on New Technologies, Mobility and Security (NTMS)*, December 2009.

C.6 J. Vazifehdan, M. G. Hawas, R. Hekmat, and I. Niemegeers, "Design of dependable personal networks," proceedings of *3rd International Workshop on Adaptive and Dependable Mobile Ubiquitous Systems (ADAMUS) in Conjunction with the ACM International Conference on Pervasive Services (ICPS)*, July 2009.

C.7 J. Vazifehdan, M. Jacobsson, and I. Niemegeers, "A framework for gateway and access network selection in ad-hoc distributed personal networks," proceedings of *6th IEEE Consumer Communications and Networking Conference (CCNC)*, January 2009.

C.8 J. Vazifehdan and R. Hekmat, "Performance evaluation of multi-hop detect-and-forward and amplify-and-forward wireless transmission systems," proceedings of *19th IEEE International Symposium on Personal, Indoor and Mobile Radio Communications (PIMRC)*, September 2008.

C.9 J. Vazifehdan and J. Weber, "Symbol error rate of space-time coded multi-antenna wireless cooperative networks," proceedings of *2008 IEEE Vehicular Technology Conference (VTC Spring)*, April 2008.

C.10 J. Vazifehdan and H. Shafiee, "Efficient configuration of multi-branch wireless cooperative networks," proceedings of *4th International Symposium on Wireless Communication Systems (ISWCS)*, October 2007.

C.11 J. Vazifehdan and H. Shafiee, "Multi-branch configuration of dynamic wireless cooperative networks," proceedings of *IEEE International Conference on Signal Processing and Communications (ICSPC)*, November 2007.

C.12 X. An, J. Vazifehdan, R. Prasad, R. Hekmat, H. Harada, and I. Niemegeers, "Extending wpans to support multi-hop communication with qos provisioning," proceedings of *7th IEEE Consumer Communications and Networking Conference (CCNC)*, January 2010.

Table – Relation between chapters of the thesis and the list of publications by the author; •: Major relation ○:Minor relation

Publication	Ch.2	Ch. 3	Ch. 4	Ch. 5	Ch. 6	Ch. 7	Ch. 8	Ch. 9
J.1				•	•			
J.2		•	○	○	○		○	
J.3		○	•	•	○			
J.4						•		
J.5							•	
J.6					•			
C.1		○	○	•	○			
C.2				○	•			
C.3						•		
C.4					•			
C.5						•		
C.6	○							
C.7	○							
C.8								•
C.9								•
C.10								○
C.11								○
C.12	○							